Hypoxic Blackwater Events - Identifying High Risk Catchments in Estuaries Now and Under Future Climate Scenarios

Katrina Waddington[1], Alice Harrison[2], Duncan Rayner[3], Toby Tucker[2], and William Glamore[4]

[1]University Of NSW Sydney
[2]University of NSW, Sydney
[3]Water Research Laboratory, UNSW Sydney
[4]University of New South Wales

April 16, 2023

Abstract

Hypoxic blackwater events occur worldwide, affecting inland and coastal waters. These events have been exacerbated by man-made floodplain drainage, leading to large-scale fish kills and ecological degradation. This paper presents a new method to identify estuarine catchment areas that are most likely to generate hypoxic conditions. The method uses established blackwater risk factors, including vegetation type, inundation extent and duration, ground-truthed in eastern Australia. A catchment is at higher risk of blackwater generation if (i) it is located where floodwaters are high and/or drainage is impeded, (ii) the site topography includes an extensive, low-lying floodplain; and/or (iii) the land-use and environmental characteristics have a high deoxygenation potential. Blackwater impacts in an estuary are determined by the floodplain connectivity with the estuary, and the discharge characteristics of the catchment drainage system. Where multiple, proximate catchments have similar drainage conditions, compounding blackwater plumes can overwhelm the assimilation capacity of the estuary. Climate change may significantly increase the volume and frequency of blackwater events in estuarine environments as a result of reduced drainage due to sea level rise, higher temperatures, and more intense and sporadic rainfall events. It is recommended that management measures be introduced to mitigate the effects of climate change and avoid further widespread hypoxic blackwater events.

Hypoxic Blackwater Events - Identifying High Risk Catchments in Estuaries Now and Under Future Climate Scenarios

K. Waddington[1], A. Harrison[1], D. Rayner[1], T. Tucker[1] and W. Glamore[1]

[1] Water Research Laboratory, School of Civil and Environmental Engineering, UNSW Sydney, NSW 2093, Australia.

Corresponding author: Katrina Waddington (k.waddington@unsw.edu.au)

Key Points:

- A methodology is presented to differentiate estuarine catchments by their potential to generate hypoxic blackwater.
- Local topographic and hydrodynamic conditions strongly influence the potential volume of blackwater generated over a catchment.
- Climate change may increase the frequency and severity and change the distribution of blackwater risk throughout an estuary.

Abstract

Hypoxic blackwater events occur worldwide, affecting inland and coastal waters. These events have been exacerbated by man-made floodplain drainage, leading to large-scale fish kills and ecological degradation. This paper presents a new method to identify estuarine catchment areas that are most likely to generate hypoxic conditions. The method uses established blackwater risk factors, including vegetation type, inundation extent and duration, ground-truthed in eastern Australia. A catchment is at higher risk of blackwater generation if (i) it is located where floodwaters are high and/or drainage is impeded, (ii) the site topography includes an extensive, low-lying floodplain; and/or (iii) the land-use and environmental characteristics have a high deoxygenation potential. Blackwater impacts in an estuary are determined by the floodplain connectivity with the estuary, and the discharge characteristics of the catchment drainage system. Where multiple, proximate catchments have similar drainage conditions, compounding blackwater plumes can overwhelm the assimilation capacity of the estuary. Climate change may significantly increase the volume and frequency of blackwater events in estuarine environments as a result of reduced drainage due to sea level rise, higher temperatures, and more intense and sporadic rainfall events. It is recommended that management measures be introduced to mitigate the effects of climate change and avoid further widespread hypoxic blackwater events.

1 Introduction

Blackwater is the common name for dark coloured water characterised by low levels of dissolved oxygen (DO) (Howitt, Baldwin, Rees, & Williams, 2007; Moore, 2006). Blackwaters are typically associated with the presence of humic substances leached from decaying vegetation (Coble, Koenig, Potter, Parham, & McDowell, 2019) or floodplain sediments (Meyer, 1990; Rixen et al., 2008). This transfer of dissolved organic matter and nutrients from riparian zones and floodplains to adjacent waterways is a natural part of the nutrient cycle. However, excessive stimulation of microbial respiration, particularly via elevated levels of organic matter and higher temperatures, can lead to hypoxic conditions, whereby DO concentrations are reduced below 2mg/L (Rabalais, Turner, & Wiseman Jr., 2002; Vithana, Sullivan, & Shepherd, 2019). Indeed, hypoxic blackwater plumes have been linked to decreased aquatic ecosystem health, including mass fish kills, and detrimental impacts on sessile flora and fauna (Hladyz, Watkins, Whitworth, & Baldwin, 2011; Pahor & Newton, 2013; Vaquer-Sunyer & Duarte, 2008). Blackwater may also affect the broader estuarine environment through disrupted trophic levels, interrupted life cycles, reductions in suitable habitat, overcrowding, and forced migration (Rabalais et al., 2002; Vaquer-Sunyer & Duarte, 2008).

Globally, hypoxia is frequently associated with the decomposition of autochthonous algal blooms fuelled by the eutrophication of inland and coastal waterways, as exemplified by the infamous dead zones of the Gulf of Mexico (Diaz, 2001; Górniak, 2017), the Baltic (Conley et al., 2011) and Black Seas (Rabalais et al., 2002). However, hypoxic conditions can also develop following direct, precipitous carbon loading of lakes, rivers or estuaries as a result of extended catchment inundation, in what are commonly known as blackwater events (Moore, 2006). Globally, flood-induced blackwater events are widespread, having been reported on the Paraguay River, Brazil (Hamilton, Sippel, Calheiros, & Melack, 1997), the Atchafalaya River, USA (Bonvillain et al., 2011; Pasco et al., 2016) and in Lake FilsØ, Denmark (Kragh, Martinsen, Kristensen, & Sand-Jensen, 2020). In Australia, blackwater events have affected inland rivers in arid and temperate regions of the Murray-Darling Basin (King, Tonkin, & Lieshcke, 2012; Whitworth, Baldwin, & Kerr, 2012) and the Edward-Wakool River system (Hladyz et al., 2011); tropical waters in the Katherine (Townsend, Boland, & Wrigley, 1992) and Mary (Townsend & Edwards, 2003) Rivers of the Northern Territory; and coastal estuaries, including the Hunter (Carney et al., 2015; Hitchcock, Westhorpe, Glamore, & Mitrovic, 2021), Clarence (Johnston, Kroon, Slavich, Cibilic, & Bruce, 2003) and Richmond (Walsh, Copeland, & Westlake, 2004) Rivers in northern New South Wales (NSW).

While eutrophic and blackwater hypoxic events may occur naturally, anthropogenic activities appear to have escalated their frequency and magnitude (Carstensen, Andersen, Gustafsson, & Conley, 2014; Kerr, Baldwin, & Whitworth, 2013; Paerl, 2006; Rabalais et al., 2002; Wong et al., 2010). Dead zones have spread exponentially since the 1960s (Diaz & Rosenberg, 2008), with scientifically confirmed accounts of hypoxia affecting over 500 catchments globally (Breitburg et al., 2018; Díaz & Rosenberg, 2011). This increase has been attributed to anthropogenic impacts, including wastewater discharges (Breitburg et al., 2018), modifications to floodplain hydrology following river regulation and water extraction (Whitworth et al., 2013), and the construction of drainage and flood mitigation works

(Moore, 2006), with changes to vegetation and land-use contributing to increased nutrient loads (Arellano et al., 2019; Conley et al., 2007; Godinho et al., 2019).

Efforts to mitigate the impacts of hypoxia have included nutrient reduction schemes, primarily aimed at improving the quality of industrial and municipal wastewater discharges (Conley, 2012), reducing the impacts of agricultural land-use practices (Tallis et al., 2019), changes to river regulation procedures (Kerr et al., 2013; King et al., 2012; Watts et al., 2018), and dilution/aeration techniques (Whitworth et al., 2013). However, effective mitigation requires a thorough understanding of the mechanisms that contribute to the formation and persistence of blackwater. To this aim, conceptual models have been developed to improve blackwater management for the Atchafalaya River (Pasco et al., 2016), Gulf of Mexico (Scavia et al., 2017) and San Francisco Bay (Cloern, Schraga, Nejad, & Martin, 2020) in the United States, and the Murray-Darling River system in Australia (Whitworth and Baldwin (2016)). For example, the Blackwater Risk Assessment Tool (BRAT) developed by Howitt (2007) and Hladyz (2011) describes the carbon load generated over the Murray-Darling floodplain via litter accumulation and decomposition rates, carbon leaching, microbial degradation and respiration. The carbon load is then converted to a volumetric biochemical oxygen demand (BOD) by considering the area, depth and duration of inundation (Howitt et al., 2007; Whitworth & Baldwin, 2016). Other key variables are temperature, re-aeration and dilution potential (Howitt et al., 2007). The Dissolved Oxygen-Dissolved Organic Carbon (DODOC) model developed by Mosley, Wallace, Rahman, Roberts, and Gibbs (2021) has subsequently integrated hydrologic capability with the BRAT ecological assessment to better represent the complex interactions between catchment hydrology and floodplain inundation (Gibbs, Wallace, & Mosley, 2022; Mosley et al., 2021). Consequently, environmental flow releases in the regulated, lowland inland rivers of Australia are now managed to avoid periods of high carbon production on floodplains (Saintilan, Kelleway, Mazumder, Kobayashi, & Wen, 2021).

Many of the same risk factors that apply to the generation of blackwater over the floodplains of inland rivers also apply to coastal floodplains. However, tidal flows present a different hydrodynamic regime to that experienced in riverine environments, and within many estuarine environments the retention and release of floodplain waters has been heavily modified by extensive flood mitigation and drainage schemes. Over the course of the 20th century, meandering channels with low hydraulic gradients and limited outlets have been replaced by extensive networks of drainage channels that have breached the natural hydraulic separation between an estuary and the adjacent coastal floodplains (Tulau, 2011). Blackwaters that were once predominately retained within extensive tracts of freshwater and tidal wetlands, allowing the carbon cycle to complete and the water column to become re-aerated, are now discharged swiftly to the estuary (Johnston, Slavich, Sullivan, & Hirst, 2003).

These floodplain drainage schemes have been directly linked to blackwater events that resulted in major fish kills throughout the northern estuaries of NSW (Walsh et al., 2004). Such events closed the Macleay River to fishing for 3 months in 2001 (Walsh et al., 2004), and the Richmond River for 4.5 months in 2001 (Steffe, Macbeth, & Murphy, 2007) and 2 months in 2008 (Wong et al., 2010). Consequently, analyses of blackwater events in the Clarence (Johnston et al., 2003) and Richmond (Wong et al., 2010) Rivers of Australia have identified three characteristic stages of an estuarine blackwater event (Figure 1):

1. Initially low-lying floodplain areas are inundated as floodwaters rise. The concentration of dissolved organic carbon (DOC) in the water column starts to increase and microbial metabolization of DOC rapidly reduces the DO concentration (Stage 1).
2. Floodplain waters become anoxic and the deoxygenation potential (DOP) increases as the BOD continues to rise (Stage 2).
3. The assimilation capacity of the river decreases as the floodwaters recede and the high oxygen demand of the blackwaters discharged from the floodplain drainage systems has a substantial impact on the adjacent waterway (Stage 3). This stage may be exacerbated by the drainage of acidic groundwaters from behind the flood mitigation structures.

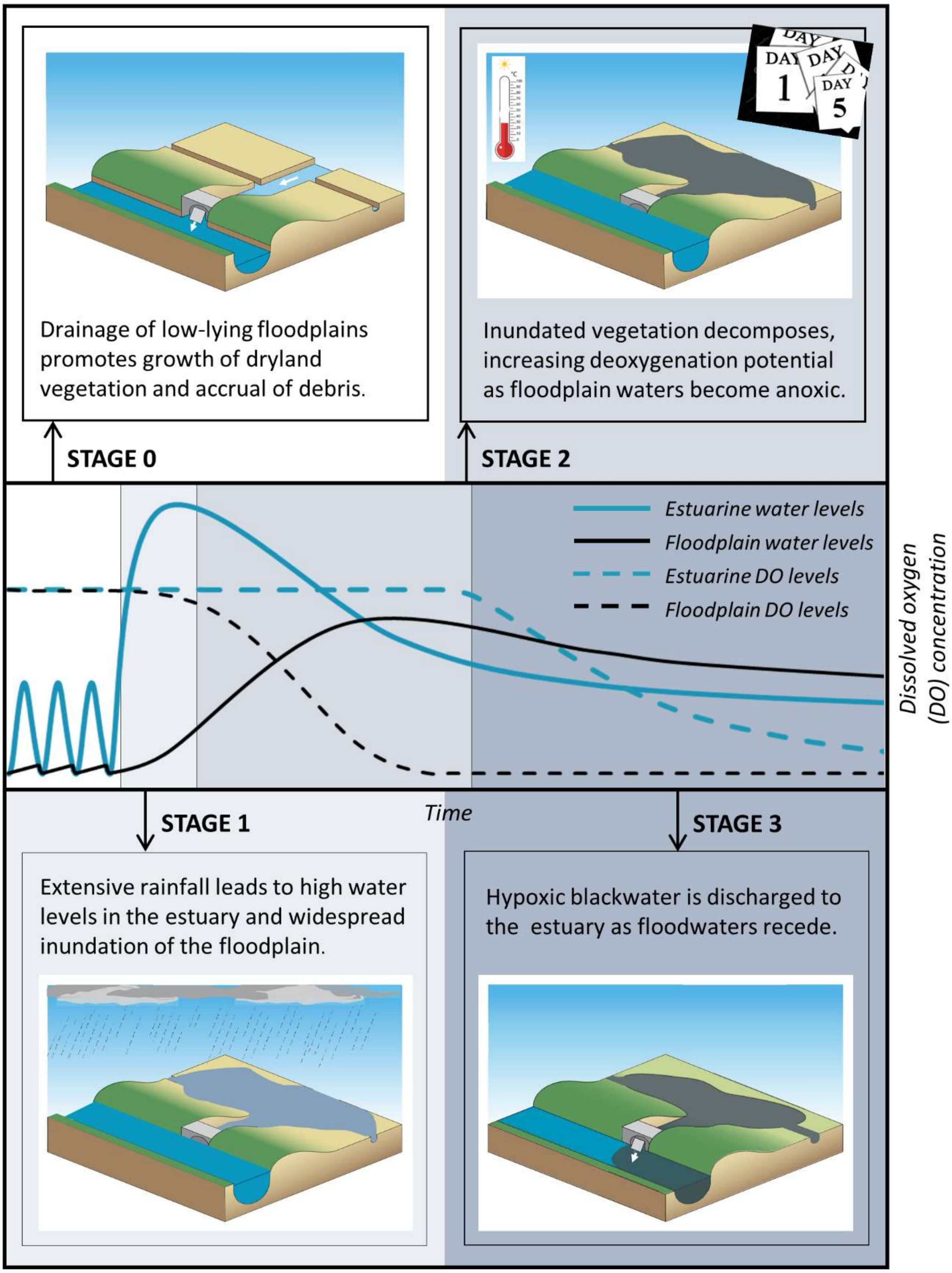

Figure 1. Conceptual stages of a blackwater event in an estuary (graph adapted from (Johnston et al., 2003))

The influence of constructed drainage systems and tidal floodgates on the magnitude and frequency of hypoxic blackwater events is evident in each of the three stages identified in Figure 1. Indeed, the construction of drainage schemes on estuarine floodplains has increased the potential for blackwater generation for a number of reasons. First, enhanced drainage promotes dry-land pastural grasses and agricultural crops in favour of water-tolerant vegetation species. These dry-land species are more susceptible to inundation and can provide a highly labile source of carbon for microbial metabolisation (Eyre, Kerr, & Sullivan, 2006; Johnston et al., 2003). Second, the reduced frequency of floodplain inundation increases the availability of carbon as organic debris accumulates between flood events (Ning, Petrie, Gawne, Nielsen, & Rees, 2015; Pahor & Newton, 2013). Finally, enhanced drainage intensifies the impact of blackwater by promoting the rapid discharge of anoxic floodwaters with high DOP directly to the estuary and by increasing the volume of blackwater that is transferred to the estuary (Wong et al., 2010).

Studies to date have focussed on the first two impacts of constructed drainage schemes; developing a detailed understanding of the local mechanisms by which blackwater is generated over estuarine floodplains. However, there have been limited investigations into the hydrodynamic interactions between the estuary and floodplain. Indeed, variability of rainfall and inundation across various drainage catchments within the floodplain has been identified as a primary difficulty in prioritising areas for blackwater management (Moore, 2006). Estuarine water levels are fundamental to the retention of water on the floodplains and the release of impounded water to the estuary. The former presents a limitation to the volume of blackwater that may be generated on the floodplain, while the latter is a determining factor regarding blackwater impacts upon the estuarine environment.

This paper presents a methodology to address this knowledge gap by incorporating the hydrodynamic regime and the topographic constraints underlying the generation of hypoxic blackwater in estuarine floodplains. The methodology quantifies the relative potential for blackwater contribution from each drainage catchment within an estuary. Water quality surveys from historic blackwater events in south-eastern Australia are used to explore the validity of the blackwater risk assessment. The results provide insights into the susceptibility of various catchments within an estuary to blackwater under current and future climate conditions. It is anticipated that this approach may be used to optimise strategic monitoring programmes and future management options.

2 Methodology

2.1 Blackwater risk factors

Differentiating the potential for blackwater generation between various catchments within an estuary requires the identification and quantification of risk factors that may contribute to a blackwater event. These include biological (carbon availability and microbial metabolization), chemical (for example, inorganic reactions, acidity and salinity) and physical (primarily temperature and pressure) mechanisms affecting the DOP of the floodwaters. Further, the extent and duration of inundation over the catchment is critical to the volume of blackwater that may be generated. An overview and the assessment of these risk factors is presented in the following sections.

2.1.2 BOD and carbon availability

BOD is a critical factor contributing to changes in DO levels within a water column, with the rate of oxidation assumed to be directly proportional to the BOD (Cox, 2003). BOD accounts for both the chemical oxidation of inorganic cations such as Fe^{2+}, Mn^{2+} and S^{2-} (Johnston, Slavich, & Hirst, 2005; Vithana et al., 2019; Wong et al., 2010), and the microbial decomposition of biodegradable organic matter (Hladyz et al., 2011).

In coastal estuaries of southeast Australia, the impacts of chemical oxidation are associated with acid sulfate soils (ASS) (Johnston et al., 2003). ASS are chemically stable when undisturbed, however constructed drainage systems have exposed large floodplain areas to oxygen, producing sulphuric acid and, via dissolution, metallic cations. Secondary oxidation of these ions can create a significant oxygen demand within the water column (Johnston et al., 2003; Lin, Wood, Haskins, Ryffel, & Lin, 2004) and the associated acidity has been independently attributed to fish kills (Walsh et al., 2004). Analysis of the geochemical signature of floodwaters in the main channel of the Clarence (Johnston et al., 2003) and Richmond Rivers (Wong et al., 2010) identified the anaerobic decomposition of floodplain vegetation as the primary process leading to generation of hypoxic blackwater conditions. Further, mesocosm experiments in the Richmond (Eyre et al., 2006) and Edward-

Wakool (Hladyz et al., 2011) Rivers determined the BOD of a variety of vegetation types and confirmed the potential for microbial decomposition of inundated floodplain vegetation to be sufficient to trigger a blackwater event.

The rate at which vegetation decays and deoxygenates water during periods of prolonged inundation differs depending on the vegetation type (Eyre et al., 2006; Johnston et al., 2005; Whitworth & Baldwin, 2016), with DOP being a factor of, *inter alia*, the labile carbon concentration (often measured as dissolved organic carbon) and temperature (Wong et al., 2011). Labile carbon is the organic component that is readily bio-available, with a higher lability associated with faster decomposition rates (Zhang et al., 2019). For example, when examining the impacts of flooding observed in the Clarence River, Johnston et al. (2003) attributed the relatively high oxygen demand from one catchment to the dominance of labile dryland pasture species compared to another that was vegetated predominately by recalcitrant *Melaleuca quinquenervia* forest. Thus, floodplains dominated by endemic wetland plant species would be less likely to generate blackwater than those that have been drained and revegetated with pasture grasses or crops that are less tolerant of inundation (Vithana et al., 2019; Wong et al., 2011). Research determining the oxygen demand of various vegetation, litter and soil types has subsequently been used to hypothesise the relative risk and potential contribution of different land-uses to blackwater events (Liu, Watts, Howitt, & McCasker, 2019).

2.1.2.1 Quantifying the DOP risk factor

It is difficult to establish strong links between land-use (for which spatial data is readily available) and BOD (Amiri & Nakane, 2008). However, a review of Australian literature identified five vegetation types typical of coastal floodplains for which experimental data regarding DOP has been established. Experimental methods differ between the various studies, making direct comparison difficult and there is limited data available regarding the spatial distribution of vegetation on coastal floodplains. Consequently, a risk-based approach linking vegetation types with comparative DOP was devised for this study, as detailed in Table 1. The vegetation types and corresponding risk factors were then assigned to each land-use identified in the 2017 (released in June 2020) Australian Land Use and Management (ALUM) classification (DPIE, 2020). Full details are presented in the Supplementary Material.

Table 1. Blackwater generation risk factors for typical vegetation types in coastal NSW

Vegetation Type	Water Tolerance		Comparative Deoxygenation Potential		Risk Factor**
	Rating	Score	Rating	Score	
Dryland grasses (e.g. pasture)	Low	3	High [a, c, e] Medium [b]	3	**3**
Forestry (other than tea tree) *	Low	3	High [b, c]	3	**3**
Tea tree leaves*	Low	3	Low [d] Low – Medium [a] Medium [e]	2	**2**
Sugar cane[+]	Medium	2	Low – Medium [a]	2	**2**
Freshwater wetland grasses (e.g. Grey rush)	High	1	Low [a] Medium [d]	1	**1**

[a] Eyre et al. (2006)

[b] Whitworth and Baldwin (2016)

[c] Liu et al. (2019)

[d] Johnston et al. (2005)

[e] Southern Cross GeoScience (2019)

* Low water tolerance is attributed to the presence of readily available leaf litter, rather than the likelihood of plants dying.

[+] Sugar cane is relatively tolerant to water, but the presence of waste after harvest increases the DOP.

** The risk factor is the average of the scores for water tolerance and comparative DOP.

2.1.3 Floodplain inundation characteristics

Flood mitigation and drainage systems have been implemented to increase floodplain productivity by limiting floodplain inundation and increasing drainage efficiency. This reduces the risk of blackwater generation during smaller, localised rainfall events, as inundated catchments can drain freely when downstream waterways are not in flood. However, regardless of the efficiency and scale of drainage infrastructure, floodplain drainage is limited by the receiving (downstream) water level. Consequently, widespread blackwater generation is more commonly associated with extensive flooding when floodplain drainage is restricted by the rate of floodwater recession in the estuary.

2.1.3.1 Inundation duration

To determine the potential for blackwater generation in a floodplain, it is important to quantify the inundation duration required to generate and sustain a blackwater event. This will vary depending on catchment characteristics, seasonal and antecedent conditions, and the unique hydrologic and hydraulic profile of each flood event.

The microbial metabolisation of highly labile carbon sources can rapidly deoxygenate a water column. Organic compounds on the floodplains will start to decompose within hours of inundation (Vithana et al., 2019; Wallace, Ganf, & Brookes, 2008), with the most labile fractions leached of carbon within the first 24 hours. In-situ mesocosm experiments on the floodplain of the Richmond River by Eyre et al. (2006) indicated that microbial metabolisation of harvested sugar cane and dropped tea tree leaves can reduce the dissolved oxygen levels in a 300 mm deep water column to 3 – 4 mg/L within 10 hours, while slashed pasture grass can deoxygenate the same volume of river water almost completely (DO < 1 mg/L) under the same conditions. Similar experiments have shown that DO was reduced to near 0 mg/L over a period of two to three days for a variety of vegetation types (Johnston et al., 2005; Liu et al., 2019; Vithana et al., 2019).

After prolonged immersion, living plants may start to die and more recalcitrant plants decompose, contributing new carbon sources to the water column (Hladyz et al., 2011). Additionally, experiments by Vithana et al. (2019) and Liu et al. (2019) suggest that both DOC and BOD can continue to rise for more than two weeks after initial inundation. Similarly, Wong et al. (2011) showed that chemical oxygen demand (COD) peaked approximately 15 to 20 days after the flood peak in a backswamp on the Clarence River, NSW. This suggests that the DOP is likely to persist for floodplain inundation durations of at least two weeks.

During the 2001 floods in the Richmond, Clarence and Macleay Rivers, it was reported that river water started to deoxygenate as floodplains began to drain, becoming completely deoxygenated within 1 to 3 days, depending on site conditions (Walsh et al., 2004). Mass deoxygenation of coastal estuaries in NSW is typically observed 4 to 6 days after the peak of a flood event (Johnston et al., 2003; Southern Cross GeoScience, 2019; Wong et al., 2010). In part, this reflects the recession of the flood hydrograph and the limited drainage from the floodplain to the estuary during prolonged floods. However, similar observations were made by Bonvillain et al. (2011) following flooding of the Atchafalaya River Basin (USA) in September 2008, where hypoxic conditions were recorded within 3 days and extensive fish kills occurred within 5 days.

Both experimental evidence and recorded observations indicate that floodplain inundation of less than 24 hours can generate blackwater during flood events. However, the limited volume of blackwater generated during this short period is unlikely to have a significant impact on receiving waters. Conversely, the longer that floodwaters are retained on a floodplain, the greater the volume of water that can be deoxygenated (Hladyz et al., 2011), the higher the DOP of the floodwaters (Eyre et al., 2006), and the greater the risk of a blackwater event when those waters are discharged to the receiving estuary (Howitt et al., 2007).

2.1.3.2 Inundation depth and extent

While there are no known long-term records of floodplain inundation within estuaries of NSW, the Department of Planning and Environment maintains a network of water level gauges throughout the estuarine channels (MHL, 2023). These gauges provide continuous long-term, historic water level records which were adopted to represent the depth and duration of floodplain inundation as onsite drainage is controlled by the downstream water levels. The spatial extent of inundation across the floodplain was determined by extrapolating these historic estuarine water levels using ground-truthed digital elevation models (DEMs) with a 5 metre grid resolution (Geoscience Australia, 2018).

2.1.3.3 Inundation depth and duration matrices

Flood hydrographs are highly variable. The influence of the hydrograph shape on the potential for blackwater generation is illustrated in Figure 2. For example, flood events 1 and 2 generate approximately the same volume of flow within the estuary, whereas the higher peak water levels generated during event 2 have a shorter duration. Despite the higher peak flood levels, for floodplain areas below 1m AHD (Australian Height Datum, which equates approximately to mean sea level), the inundation conditions presented by flood event 1 (Figure 2) are likely to generate more hypoxic blackwater than those of event 2, as inundation would be maintained over a longer period of time. Floodplain areas above 2m AHD would only generate blackwater during flood event 3 as they would not be inundated during event 1 and there would be insufficient inundation duration during event 2.

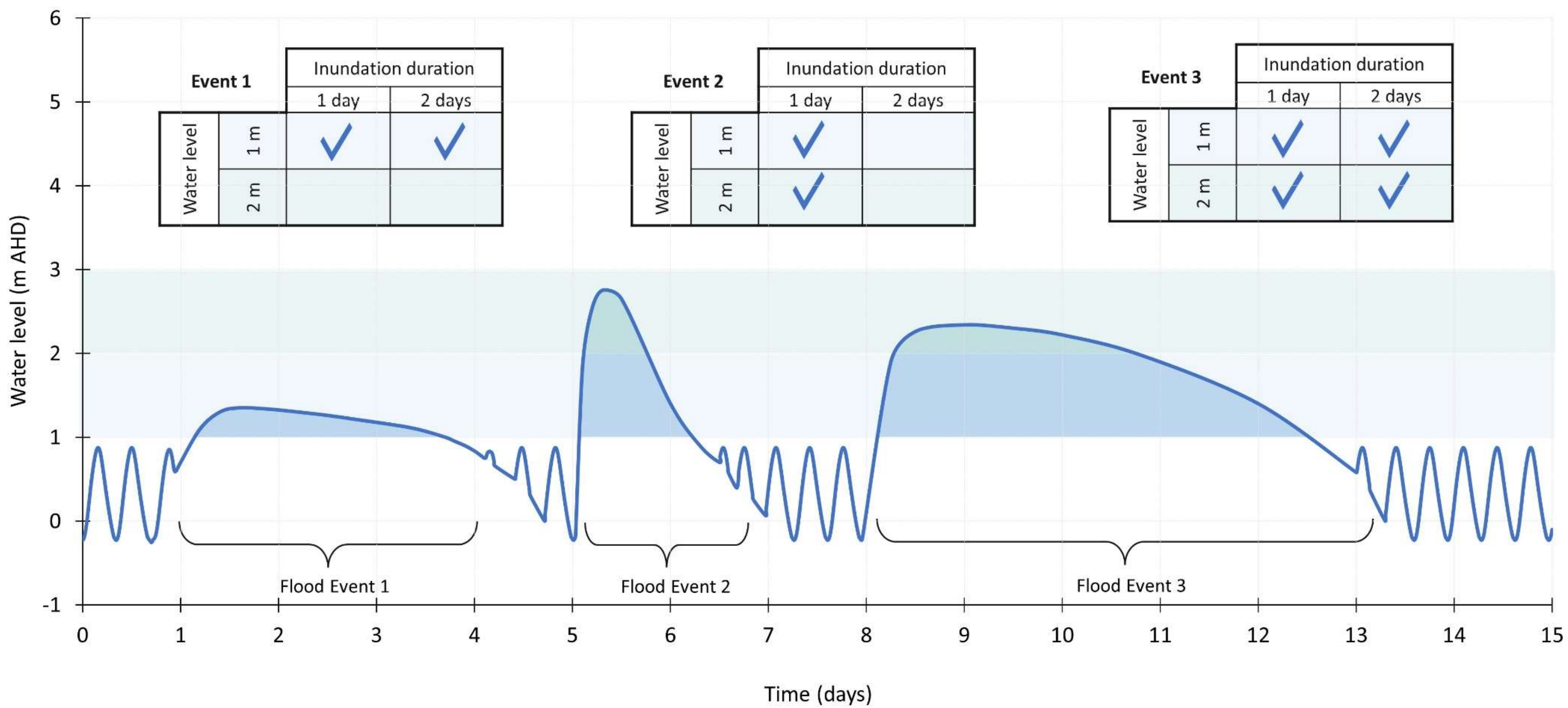

Figure 2. A conceptual hydrograph depicts three different flood events to highlight the blackwater potential risks for each event. At a floodplain elevation of 1m AHD, all floods contribute to the blackwater risk but for different inundation periods. At an elevation of 2m AHD, only flood events 2 and 3 would contribute blackwater. Flooding that persists over a broader area and a longer period (Flood Event 3) has a higher likelihood of producing larger volumes of blackwater.

Based on the conceptual model depicted in Figure 2, inundation risk matrices can be established at each water level gauge by identifying the historic frequency at which various combinations of inundation depth and duration have been exceeded. As such, the inundation duration was calculated at 0.1m increments in water level between 0.1m and 5.0m AHD. This covers the range of water levels and topographic elevations typical of estuarine floodplains. Additionally, as the tidal cycle will restrict discharges from the floodplain drainage systems during flood events, the long-term average mean high water (MHW) level (as documented by Fitzhenry, Alley, Hesse, and Couriel (2012)) was adopted as the minimum floodplain inundation level at each gauge location.

Within the estuaries of NSW, recorded flooding events rarely exceed five days. As the critical duration of inundation for the generation of blackwater may be achieved during floods with a duration of less than one day, event durations between one and five days were adopted for the inundation matrices. For each day a flood event exceeded any particular water level, it was assumed to contribute to the blackwater risk for that duration. This ensured that longer duration events contributed more blackwater risk than events of short duration, although the matrix could be extended to incorporate additional flood durations for estuaries regularly subject to longer floods.

To maximise the available data and account for any differences in the data record at each gauge, the full data record was analysed for each water level monitoring station. These results were then normalised by the length of the data record to calculate the average recurrence interval of each incremental inundation level at each gauge location.

2.2 Aggregated blackwater risk assessment

For each catchment, a blackwater contribution factor was calculated using spatial analysis tools within Geographic Information System (GIS) over a 5m square grid. This information was used to determine the area inundated and the land-use risk factor associated with that area for every 0.1m increment in water level (as illustrated in Figure 3). The blackwater contribution factor corresponding to the water level was then calculated for all combinations of inundation duration and frequency. A statistical mean of the factors calculated from the matrix of inundation levels affecting each catchment was adopted as the aggregated blackwater risk factor for that catchment. This factor was then used to rank the catchments according to their relative potential to generate blackwater.

2.3 Study area

The methodology described in Section 2 was applied to seven major estuaries within NSW, including (from north to south, as indicated in Figure 4):

- Tweed River;
- Richmond River;
- Clarence River;
- Macleay River;
- Hastings River;
- Manning River; and
- Shoalhaven River.

Each selected estuary has been previously identified as blackwater pollution sites resulting from the clearing and drainage of coastal wetlands (Fletcher and Fisk, 2017). In particular, the Richmond River has been the focus of detailed investigations into the causes of blackwater events that resulted in mass fish kills.

Details of government water level gauges used in this assessment are identified in the Supplementary Material, including gauge locations and historic flow distribution curves.

3 Results

The calculated aggregated blackwater risk factors provide an objective, data-driven evidence base to identify which catchments present the highest potential risk of generating blackwater. The ranking of catchments based on blackwater risk can be used to inform and prioritise floodplain management options. Ongoing and future monitoring programs may be optimised and used to further validate and refine the assessment methodology.

The risk factors and catchment ranking within each estuary are tabulated with a statistical analysis of the corresponding historic water levels in the Supplementary Material. Maps indicating the distribution of blackwater risk are also provided, with sample results for the Richmond River presented in Figure 5. These maps incorporate the median extent of

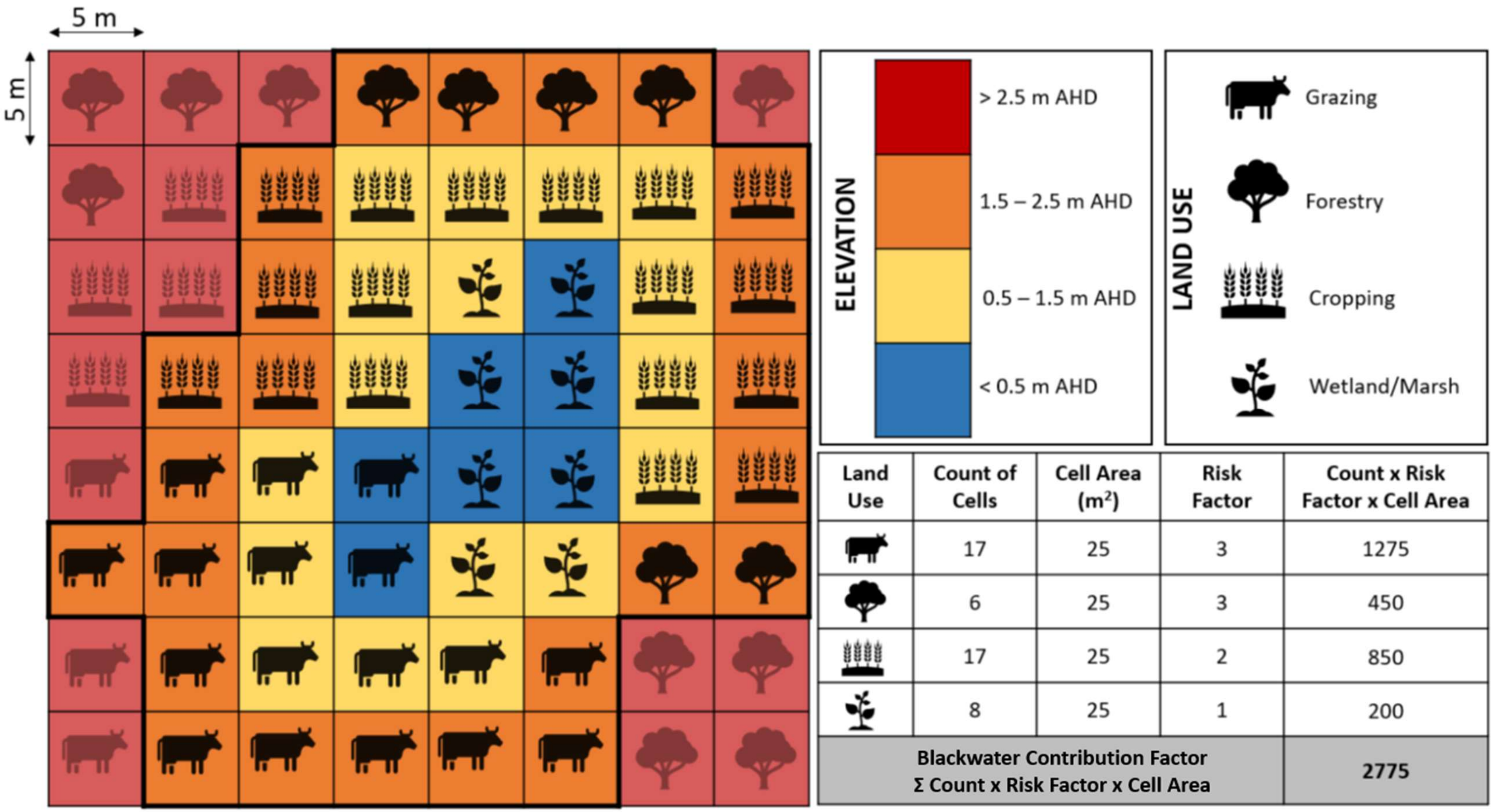

Figure 3. An example calculation of a catchment blackwater contribution factor for an inundation level of 2.5 m AHD. The coloured matrix depicts the land-use type and elevation. The number of each land-use cells multiplied by the area and risk factor summed for the catchment is the blackwater contribution factor for that catchment. Within an estuary, multiple catchments were calculated to rank priority risk areas.

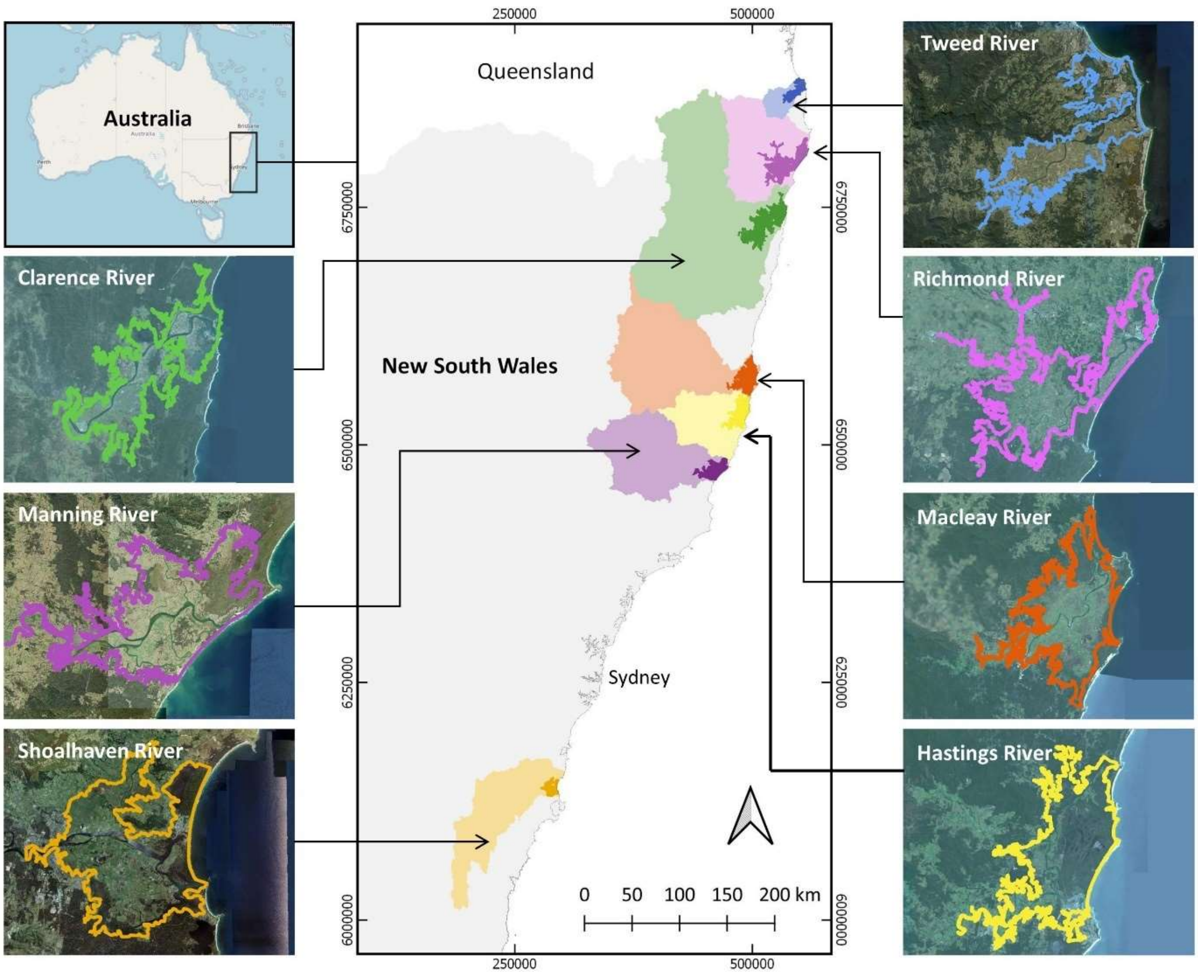

Figure 4. Selected estuaries (shaded) and estuarine floodplain areas below 5m AHD (outlined) defining the study area.

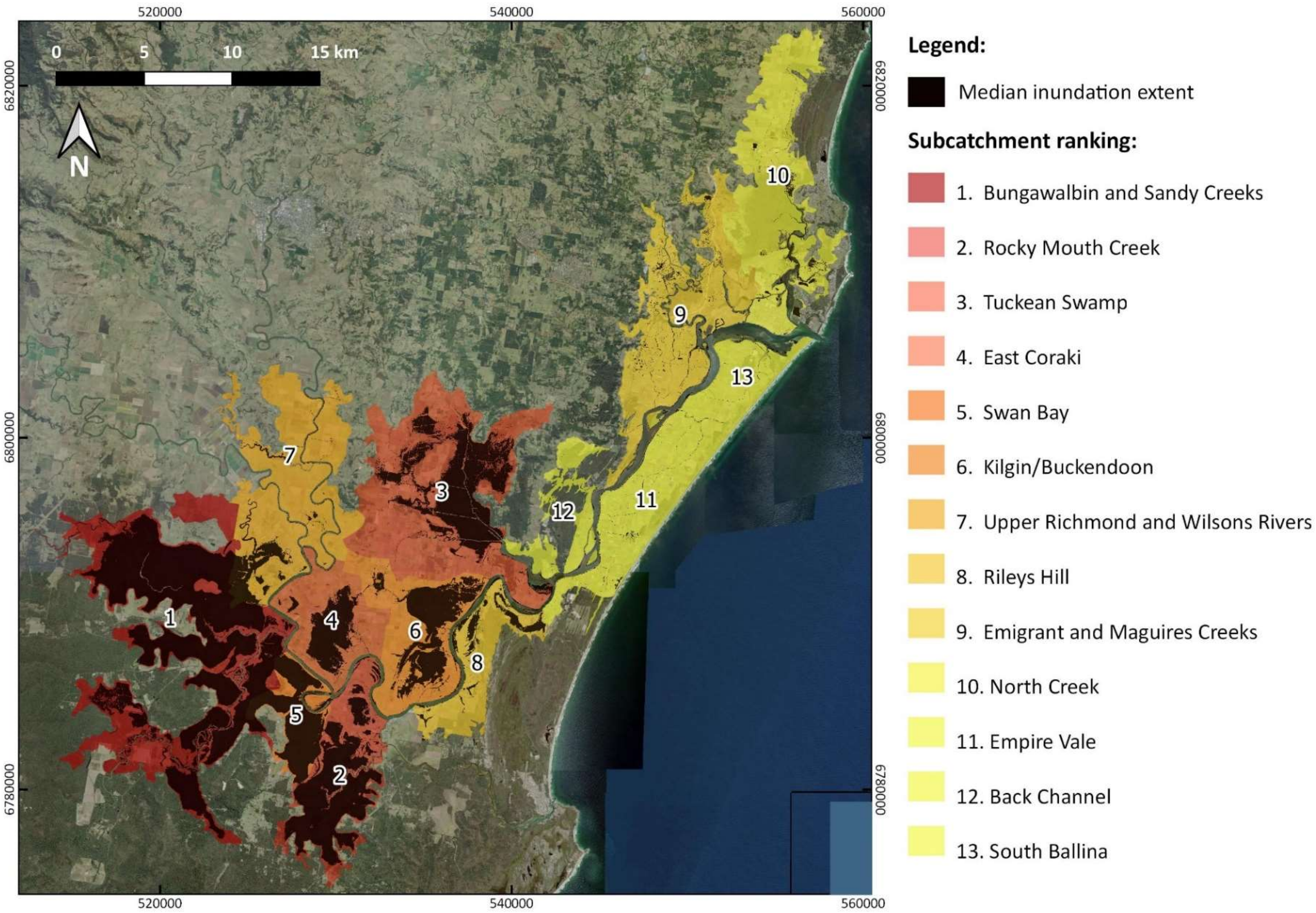

Figure 5. Ranking of catchments by aggregated blackwater risk factor and extent of inundation under median water levels for the Richmond River estuary (maps of results for all estuaries within the study area are included in the Supplementary Material).

inundation corresponding to the historic water levels in the estuary to provide an indication of the areal extent of potential blackwater generation within each catchment.

3.1 Validation of results

In the Richmond River the highest risk catchments were identified as Bungawalbyn and Sandy Creeks (ranked 1), Rocky Mouth Creek (ranked 2), and the Tuckean Swamp (ranked 3). These results correlate well with several previous scientific investigations and help to validate the assessment outcomes. Exceptionally low oxygen levels were previously recorded at Bungawalbyn and Rocky Mouth Creeks following the February 2001 flood (Eyre et al., 2006). Similarly, Wong et al. (2010) identified the Tuckean, Bungawalbyn, Sandy and Rocky Mouth Creek catchments as primary sources of DOP following the January 2008 flood. The same three catchments were attributed the highest risk of blackwater generation and impact by an expert panel under the Richmond Estuary Ecosystem Health Monitoring Strategy (Moore, 2006) and identified as the three top priority areas for blackwater management within the Richmond River floodplain by a collaborative Australian Research Council project (Southern Cross GeoScience, 2019). The latter study prioritised lower Bungawalbyn Creek as the largest blackwater generator on the floodplain.

The validity of the blackwater risk methodology is strengthened by a review of water quality, fish and crustacean mortality data undertaken by Walsh et al. (2004) following major flooding in February and March 2001. This investigation also identified blackwater risk areas within the Richmond River as Rocky Mouth Creek, Bungawalbyn Creek and Tuckean Swamp. Additionally, Walsh et al. (2004) prioritised the Coldstream River (ranked 1 under this study's methodology) and Everlasting Swamp (in the Sportsmans Creek catchment, ranked 2) in the Clarence River, and Belmore Swamp (ranked 2), the Swan Pool (Kinchela Creek, ranked 1) and Seven Oaks wetland (Collombatti-Clybucca, ranked 3) in the Macleay River, further supporting this study's methodology.

3.2 Limitations of methodology

3.2.1 Land use, ambient and antecedent conditions

Due to the relative homogeneity of land-use across the study area, the catchment rankings presented herein are highly influenced by the catchment size and inundation extent. The

Spearman's rank correlation between the aggregated blackwater risk factor and the area flooded at the median inundation level varied from 0.82 to 0.97 throughout each estuary, with the exception of the Shoalhaven River, where it was 0.55. Within the Shoalhaven River, the largest discrepancy was within the Comerong Island catchment, where over 12% of the land area is below the median inundation level but does not contribute to the blackwater risk factor as it is a tidal wetland. Further refinement of the weighting of blackwater risk factors may therefore be required in landscapes with more diverse land uses.

Where land-use is more critical in the assessment of blackwater risk, a weighting factor scaled to BOD may provide greater differentiation than the direct rank-order weighting adopted in this study. Scaled weightings may vary with time of inundation, as indicated by the results of the mesocosm and inundation experiments on which the rank-order weightings were based, (e.g. Liu et al. (2019) and Vithana et al. (2019)). The depth of inundation may also influence the rate of deoxygenation as shallow waters are likely to be warmer (increasing microbial metabolisation rates and reducing oxygen saturation levels) and subject to photochemical deoxygenation processes (Southern Cross GeoScience, 2019).

Indeed, decomposition rates are strongly affected by environmental factors such as temperature, solar radiation, salinity and acidity (Voß, Fernández, & Schäfer, 2015) and BOD has been shown to respond to plant density, shadowing, soil mineralogy and light transmission (Cox, 2003; Voß et al., 2015). Conversely, the bioavailability of organic matter has generally been found to respond more directly to land management practices, such as chemical and nutrient application, harvesting practices and stocking rates (Voß et al., 2015). Thus the potential for blackwater generation over various catchment areas may alternatively be differentiated by assessing variations in land management (both historic and current) and intensity of use (Barlow, Christy, & Weeks, 2009; Buck, Niyogi, & Townsend, 2004) rather than vegetation types or land-use categories, as the accumulation of surface litter is likely to drive the majority of oxygen demand in many environments (Mehring et al., 2014).

Similarly, seasonal changes and antecedent conditions will also impact the potential BOD. By reviewing antecedent weather conditions in the Richmond River, Wong, Walsh, and Morris (2018) found that fish kills were more common when the previous six months had been drier than usual prior to the blackwater flooding event. Conversely, wetter than average conditions are likely to reduce the amount of DOC that is available, thereby lowering the risk of blackwater generation (Hladyz et al., 2011). Antecedent conditions will influence the accumulation of organic matter and the bioavailability of carbon on the floodplain. Vegetation stress due to drought, for example, may increase litterfall (Whitworth et al., 2012), with the accumulation of organic debris increasing as the time between flood events is extended (Wong et al., 2018; Xiong, 1997). The amount of carbon leached from organic matter also reduces when the litter has been previously inundated.

Nevertheless, the spatial and temporal variability of environmental influences on BOD is unlikely to affect the intrinsic risk across a catchment or estuary within the study area presented in this assessment (refer to Supplementary Material). Indeed, current literature suggests that various vegetation and land cover types all have the ability to deoxygenate a waterbody (Kobayashi et al., 2009; Liu et al., 2019; O'Connell, Baldwin, Robertson, & Rees, 2000). Under equivalent environmental conditions, it would therefore be the extent and duration of inundation throughout a catchment which provides the greatest risk differential for blackwater generation.

3.2.2 Water level data

The accuracy of the assessment with respect to inundation characteristics relies on the suitability of the water level data available. In this regard, the results for the Shoalhaven River may also have been adversely affected by the limited distribution of water level data within major tributaries of the estuary. No gauges are located within the estuarine reaches of Broughton Creek, while water levels on the Crookhaven River are only recorded at the downstream limits of the estuary (refer to Supplementary Material). As the inundation extents were estimated by a direct extrapolation of the estuarine water levels, it is important to obtain a representative distribution of flood conditions throughout the estuary. If the adopted water levels are lower than those typically experienced at any catchment (as may occur when upstream water levels are poorly represented), the inundated area, and corresponding aggregated blackwater risk factor, will be underestimated.

4 Discussion

4.1 Floodplain inundation characteristics

Results from the catchment rankings provide insights into the influence of estuarine hydrodynamics on the blackwater risk profiles. For example, in the Tweed River the median extent of inundation over the Stotts Creek catchment ($3.9km^2$) exceeds that experienced in the Condong catchment ($2.2km^2$), yet Condong presents a higher overall blackwater risk than Stotts Creek (Figure 5). This reflects the differences in catchment size and topography as well as the water surface elevations.

As illustrated in Figure 6, Stotts Creek presents a relatively flat, low-lying floodplain below the local median inundation level of 0.7m AHD. However, the topography rises steeply, with limited additional catchment area contributing to potential blackwater generation at higher water levels. Conversely, the Condong catchment would produce limited volumes of blackwater until the surface water levels exceed 0.5m AHD. Once inundation levels reach 1.2m AHD, the area contributing to blackwater generation in the Condong catchment would exceed the Stotts Creek catchment and the risk factor would increase accordingly. At higher inundation levels (experienced during more significant, but less frequent rainfall events), the large potential volumetric contribution of blackwater from the Condong catchment outweighs that of the Stotts Creek catchment. In general, both greater topographic exposure and higher inundation levels increase the overall blackwater risk presented by any particular catchment to the receiving estuary.

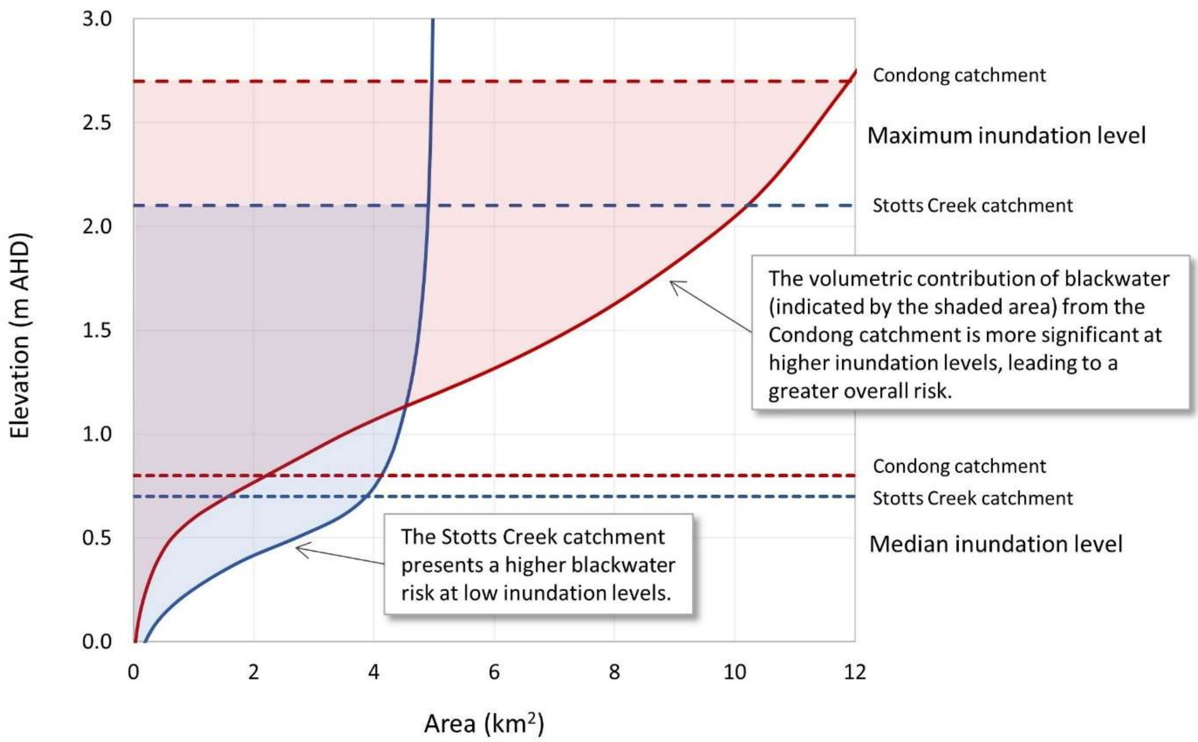

Figure 6. Hypsographic graph of the Stotts Creek (blue) and Condong (red) catchments in the Tweed River estuary, illustrating the changing risk profiles based on inundation levels.

Comparing the Stotts Creek and Condong catchments (Figure 6) also highlights the sensitivity of the method to the duration and frequency of flood events. This was further investigated by modifying the inundation matrix to assess the aggregated blackwater risk factor. Removing the 1 and 2 day inundation durations from the aggregated blackwater risk assessment matrix reduced the overall inundation levels, as lower water levels are experienced during the rising and falling limbs of a flood hydrograph. Conversely, limiting the analysis to flood events with a recurrence interval of 2 to 5 years or 3 to 5 years typically increased the median inundation levels as fewer minor events were included in the statistics. Importantly, the relative risk remained consistent throughout this sensitivity analysis, with Spearman's rank correlation remaining above 0.9 in all estuaries except the Shoalhaven River (detailed in the Supplementary Material). Notably, the ranking of catchments within the Shoalhaven River was more sensitive to the influence of shorter duration events, although the correlation between the top five ranked catchments remained above 0.9 in all analyses.

The robustness of the assessment to variations in the flood duration and recurrence interval reflects the consistency of the hydrodynamic response to flood events throughout each estuary. As illustrated in Figure 7, peak flood levels are typically highest in the upper estuary, where water levels rise rapidly and remain high due to restricted drainage from elevated tailwaters in the mid- and lower portions of the estuary. Flood profiles in the lower estuary are further moderated as the hydraulic energy and flow volumes are dispersed over the low-lying floodplains. Additionally, in the lower estuary water levels are less affected by flood flows as offshore waters can assimilate large flood volumes. These effects are exemplified in the comparison between the Condong (located in the upper estuary and subject to higher inundation levels) and Stotts Creek (mid-estuary) catchments (Figure 6).

Based on these spatial differences in drainage across an estuary, the free-draining lower reaches of an estuary typically have a lower risk of blackwater generation. The environmental impacts of blackwater discharged from these downstream catchments may also be mitigated by high tidal flushing and reduced residence times due to their proximity to the ocean (Johnston et al., 2003; Rabalais et al., 2002). To this aim, Eyre and Twigg (1997) indicated that dissolved oxygen levels were higher in parts of the estuary with higher salinity (or increased tidal flushing) for the first seven weeks after the flood event. In contrast, the upper estuary is likely to have a higher blackwater risk as residence times may be prolonged (i.e. any blackwater released would remain in the estuary for extended periods) and flood levels tend to remain elevated for longer periods (i.e. any blackwater generated may discharge into an estuary with less assimilation capacity).

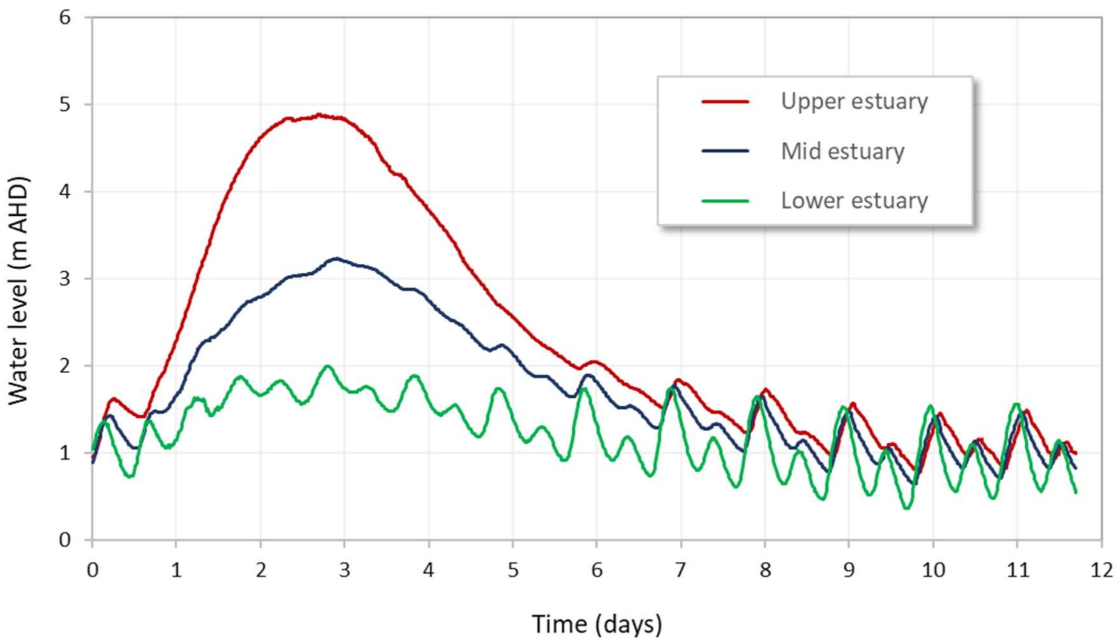

Figure 7. Spatial illustration of typical water level response to a flood in the lower, mid and upper reaches of an estuary from an event recorded in the Richmond River in June 2005. The upper estuary was measured at Coraki (refer to Supplementary Material for gauge locations) and represents conditions for the Upper Richmond and Wilsons River catchments (Figure 5). The mid estuary was measured at Woodburn (Rocky Mouth Creek catchment) and the lower estuary at Wardell (Empire Vale and Back Channel catchments.

As inundation levels and inundation durations are often spatially correlated within an estuary, the risk factors for blackwater generation and impact may be simplified to the estuarine water levels, floodplain geomorphology, and the potential for BOD generation. These primary factors are conceptualised in Figure 8 for an idealised system. Based on these factors, a catchment may present a higher risk of blackwater generation and impact if:

- it is located in a portion of the estuary where floodwaters are maintained at higher levels and/or for longer durations (Figure 8(a));
- the topography contains an extensive, low-lying floodplain that can accommodate large volumes of floodwater (Figure 8(b)); and/or
- the land use and environmental characteristics have a higher potential to generate BOD (Figure 8(c)).

The environmental impact of blackwater in an estuary is then determined by the floodplain connectivity with the estuary and the discharge characteristics of the catchment drainage system (Figure 8(d)). Modern drainage systems facilitate the rapid transfer of DOP to the estuary, with substantial volumes of blackwater discharged as the flood recedes (Figure 8(a)). These discharges can be particularly harmful when there is limited assimilative capacity in the estuary. The impact from any individual catchment discharge is also affected by discharges from nearby catchments as individual blackwater plumes can intermix. The dilution capacity and potential environmental impacts from these blackwater plumes are highlighted in Figure 9.

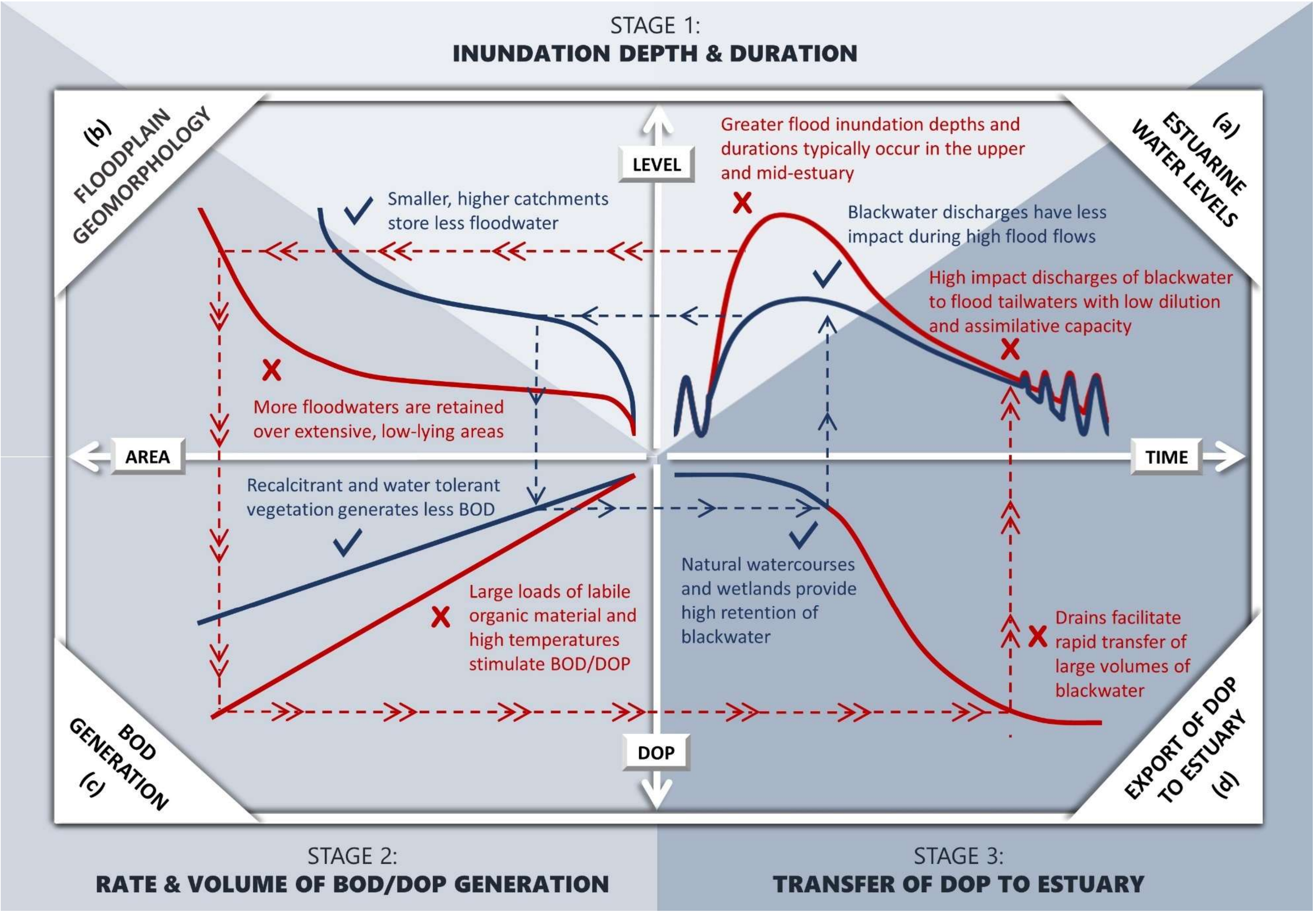
STAGE 1:
INUNDATION DEPTH & DURATION
(b) FLOODPLAIN GEOMORPHOLOGY
(a) ESTUARINE WATER LEVELS
LEVEL
Greater flood inundation depths and durations typically occur in the upper and mid-estuary
Smaller, higher catchments store less floodwater
Blackwater discharges have less impact during high flood flows
High impact discharges of blackwater to flood tailwaters with low dilution and assimilative capacity
More floodwaters are retained over extensive, low-lying areas
AREA
TIME
Recalcitrant and water tolerant vegetation generates less BOD
Natural watercourses and wetlands provide high retention of blackwater
Large loads of labile organic material and high temperatures stimulate BOD/DOP
Drains facilitate rapid transfer of large volumes of blackwater
BOD GENERATION (c)
DOP
EXPORT OF DOP TO ESTUARY (d)
STAGE 2:
RATE & VOLUME OF BOD/DOP GENERATION
STAGE 3:
TRANSFER OF DOP TO ESTUARY

551

Figure 8. Conceptual diagram of the key risk factors for blackwater generation on an estuarine floodplain. The diagram should be read counter clockwise from the top right corner. A high-risk scenario is realised by following the progression of a blackwater event via the red arrows from Stages 1 to 3. Commencing in quadrant (**a**), high flood levels in the estuary lead to extensive inundation (**b**) during Stage 1. Increased biochemical oxygen demand (BOD) generated at Stage 2 (**c**) will result in a high deoxygenation potential (DOP). The greatest impacts occur when the blackwater discharges at Stage 3 (**d**) overwhelm the assimilative capacity of the receiving waters (a). An alternative low risk scenario is proposed via the blue arrows.

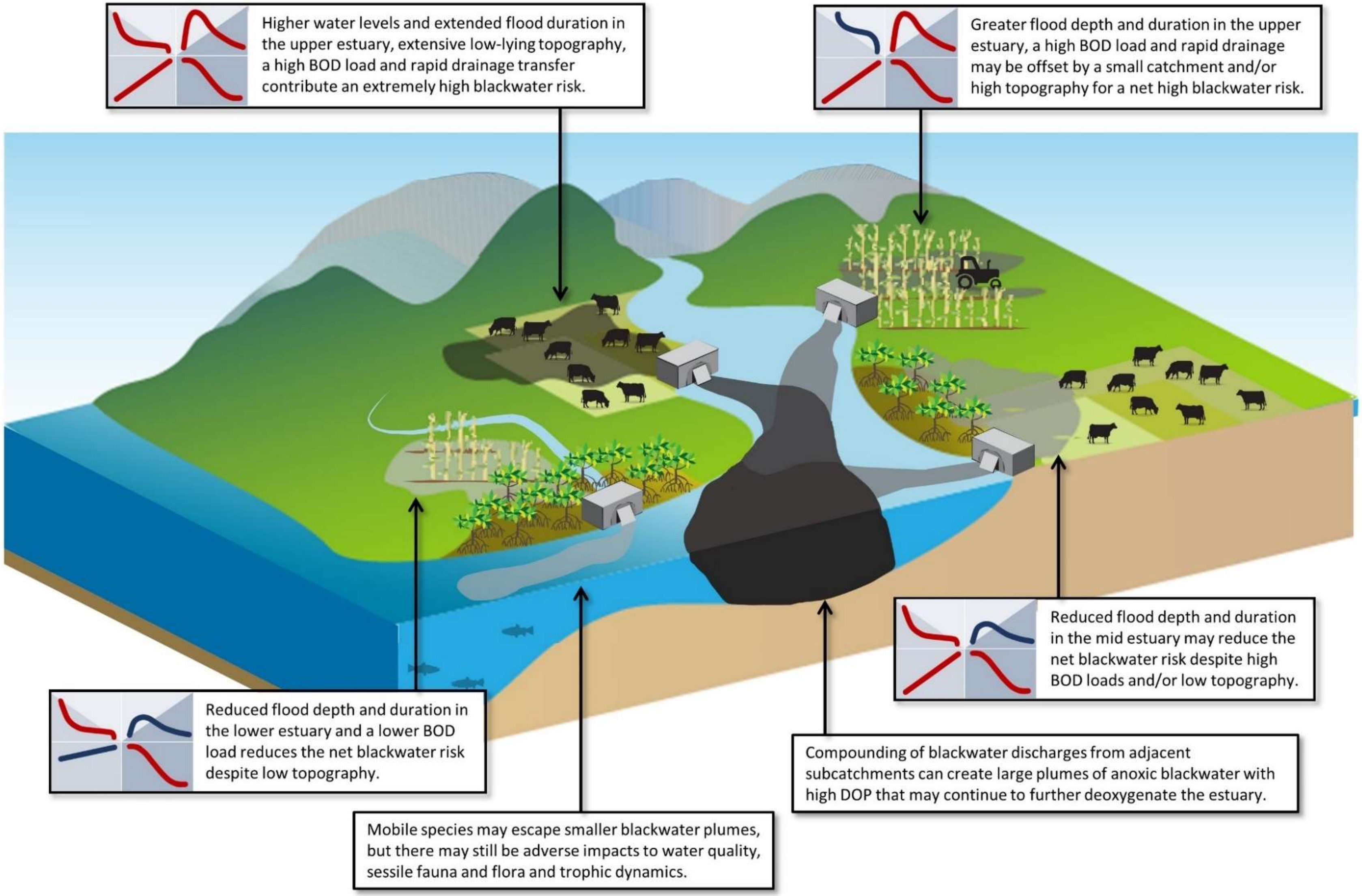
Higher water levels and extended flood duration in the upper estuary, extensive low-lying topography, a high BOD load and rapid drainage transfer contribute an extremely high blackwater risk.
Greater flood depth and duration in the upper estuary, a high BOD load and rapid drainage may be offset by a small catchment and/or high topography for a net high blackwater risk.
Reduced flood depth and duration in the mid estuary may reduce the net blackwater risk despite high BOD loads and/or low topography.
Reduced flood depth and duration in the lower estuary and a lower BOD load reduces the net blackwater risk despite low topography.
Compounding of blackwater discharges from adjacent subcatchments can create large plumes of anoxic blackwater with high DOP that may continue to further deoxygenate the estuary.
Mobile species may escape smaller blackwater plumes, but there may still be adverse impacts to water quality, sessile fauna and flora and trophic dynamics.

558

Figure 9. Conceptual diagram of common blackwater risk factors and compounding discharges within an estuary. The risk from each drainage catchment is described with reference to the four risk factors illustrated in Figure 8.

4.2 Spatial distribution of floodplain drainage

Impacts of compounding blackwater plumes are typified by the blackwater risk profiles of the Clarence and Richmond Rivers. The inundation extent at the median inundation level for the Clarence River (285 km^2) is more than twice the Richmond River (137 km^2). However, the impact of blackwater events in the Richmond River has been more severe, with extensive fish kills regularly reported after comparable flood events (Walsh et al., 2004). This has previously been attributed to the substantially larger river discharges and assimilation capacity of the Clarence River, which also provides opportunities for fish to seek refuge in the less affected parts of the estuary (Walsh et al., 2004).

Results from the aggregated blackwater risk analysis indicate that the highest ranked sub-catchments in the Clarence River discharge to different parts of the estuary. As such, blackwater discharges are likely to impact the estuary at different stages of a flood event. In comparison, the Richmond River has four of the five highest ranking sub-catchments discharging into the estuary within a 20km reach. With such close proximity, these individual plumes are likely to intermix, resulting in compounding impacts that are more likely to overwhelm the assimilation capacity of the estuary. These potential compounding impacts are illustrated in Figure 9.

4.3 Climate change impacts

Investigating the sensitivity of spatial and temporal factors on blackwater generation also provides insights into how climate change may influence future blackwater conditions. Climate change has been predicted to increase temperatures (Masson-Delmotte et al., 2021), and create more intense and sporadic rainfall conditions (Dey, Lewis, Arblaster, & Abram, 2019). These impacts are expected to exacerbate hypoxic blackwater events (Carstensen et al., 2014; Godinho et al., 2019; Koehn, 2022; Vaquer-Sunyer & Duarte, 2008), with larger floods increasing the spatial and temporal inundation patterns, while warmer conditions may increase the microbial reaction rates (Wong et al., 2010). Changes in flood frequency and meteorological conditions may also encourage the accumulation of organic matter between floods providing high BOD potential.

In estuarine environments these effects will be further compounded by sea level rise, which is expected to increase standing water levels and reduce drainage (Waddington et al., 2022).

Higher downstream water levels may lead to increased spatial inundation, while reduced drainage will extend the temporal inundation. Overall, both factors will likely increase blackwater generation risk.

The potential for blackwater generation from sea level rise was investigated by examining the projected increase in area inundated for incremental increases in water levels across the floodplain sub-catchments. Unsurprisingly, the larger Clarence, Richmond and Macleay River systems, which already suffer the highest rate of fish mortality from blackwater events, would experience the greatest increases under rising sea levels. Normalising the increase in area inundated by the total catchment area (Figure 10(a)) indicates that the future risk of blackwater creation in the Tweed River is likely to be substantially higher than in other estuaries. This is primarily attributable to the topography of the Tweed River floodplain, where there is a greater increase in the area inundated by higher water levels.

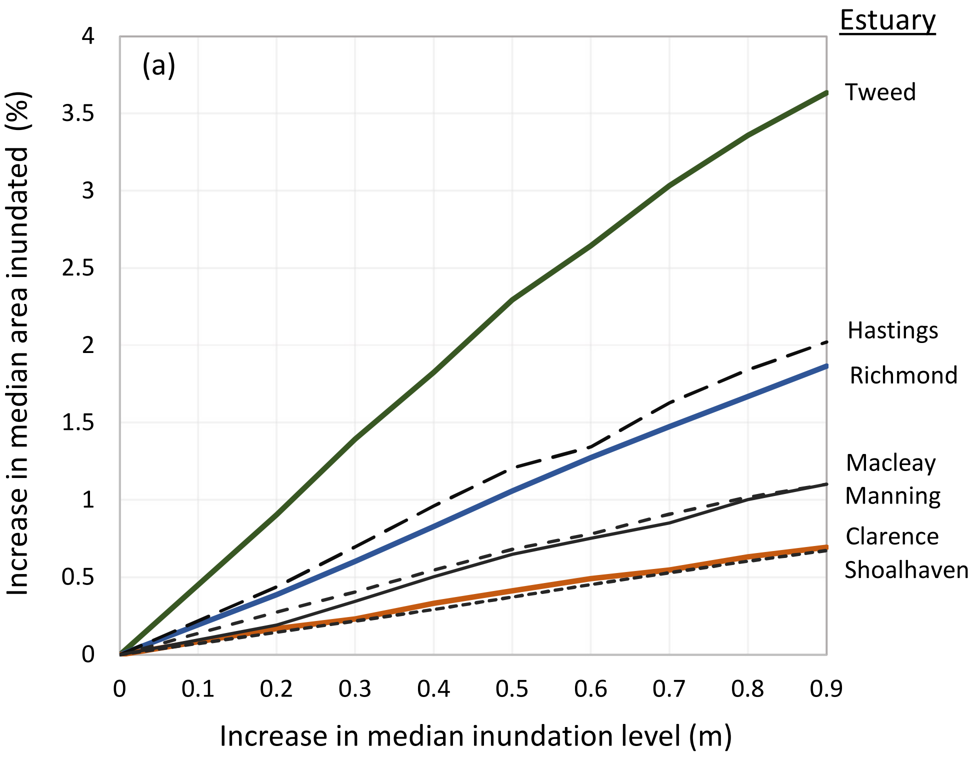

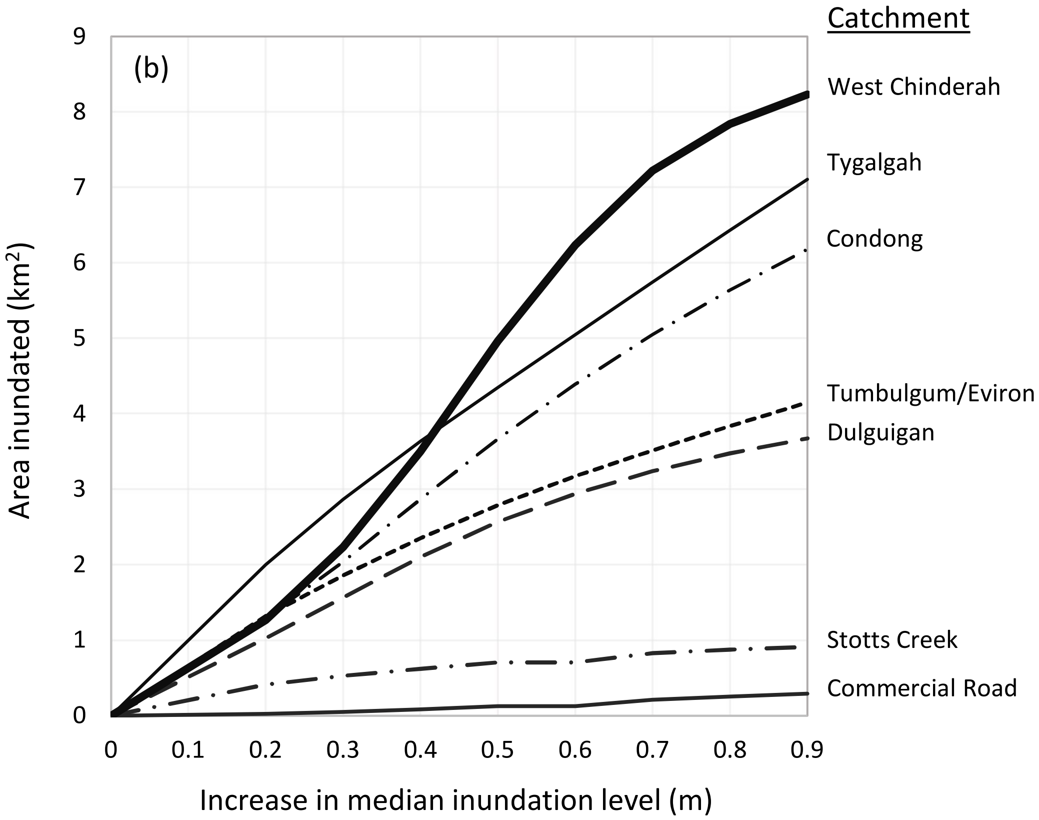

Figure 10. The (**a**) increase in median area inundated after an incremental rise in water level expressed as a percentage of the total catchment area. Within any given estuary (the Tweed River is used as an example here) the sub-catchments most extensively inundated and the locations discharging the most blackwater may change (**b**).

This analysis can be further extended to identify which catchments within a particular estuary present an increased risk of blackwater generation under existing or future conditions. For example, while the West Chinderah catchment of the Tweed River estuary currently presents a relatively moderate risk, the potential for blackwater generation may increase exponentially once the median inundation level rises by approximately 0.3m (Figure 10(c)).

4.4 Management and mitigation of blackwater risk

The improved understanding of estuarine blackwater events, as provided by this assessment, enables a nuanced assessment of potential mitigation measures. In areas identified as low risk for blackwater generation, minor changes to land management may mitigate blackwater generation by reducing the bioavailability of carbon. For example, the removal of cuttings from slashed pastures has been suggested as an effective means of reducing the DOP of grazing lands (Eyre et al., 2006). Alternatively, mechanical oxygenation has been employed to mitigate blackwater impacts in the Swan and Canning Rivers of Western Australia (Greenop, Lovatt, & Robb, 2001), although this is generally regarded as an emergency response measure as it is substantially limited by the area that can be serviced and operational costs (Baldwin, Boys, Rohlfs, Ellis, & Pera, 2022).

As the potential for blackwater generation increases, the impact of effective mitigation measures on current land uses is also likely to increase. Where the median inundation level is relatively shallow, the depth and density of floodplain drains may be reduced to encourage the growth of water-tolerant vegetation and facilitate reaeration of the water column (Hamilton et al., 1997; Rixen et al., 2008). However, in areas subject to prolonged, deep inundation, reaeration will be hampered by the lower ratio of the air-water interface to flood volume and there is likely to be greater plant morbidity and contribution to BOD. Such conditions are typified in the low energy backswamp environments, which may be best suited to reinstatement into natural wetland systems. Indeed, tidal restoration and the reinstatement of coastal and floodplain wetlands has been identified as the preferred management measure for the mitigation of blackwater events in the coastal estuaries of NSW (Moore, 2006).

Social and economic ramifications accompanying land-use change may be significant due to the level of development throughout the floodplains (Moore, 2006; Southern Cross GeoScience, 2019). Identification of areas at highest risk of backwater generation (as discussed in this paper) is recommended to support trials and further investigations into these options. This will ensure that decisions to reinstate wetland systems are evidence-based and transparent, optimising water quality benefits and ongoing floodplain productivity.

5 Conclusion

Hypoxic blackwater events occur worldwide and affect both inland and coastal waters. The mechanisms underpinning these events are associated with the microbial metabolisation of carbon and the accumulation/discharge of deoxygenated water during and post flood events. This paper presents a methodology developed to prioritise catchments within an estuarine floodplain based on their potential to generate hypoxic blackwater and to identify those catchments from which blackwater discharges are likely to have the most significant impact on the estuary. Local topography and changes to the flood hydrograph as it progresses along an estuary are shown to influence the extent and duration of inundation over the floodplain. In turn, inundation characteristics are identified as critical factors in determining the volume of blackwater generated and the DOP discharged to the receiving waters. Concerns related to increased blackwater generation from climate change, and sea level rise in particular, are highlighted.

It is anticipated that this research will be used to inform evidence-based decision making to manage catchment risks to water quality. This may enable a strategic approach to future investments in floodplain and estuarine research and management measures to optimise economic, social and environmental outcomes.

Acknowledgements

The blackwater risk assessment methodology presented herein was developed with funding from the New South Wales Marine Estate Management Strategy (MEMS). Katrina Waddington was supported by a scholarship jointly funded by UNSW Sydney and MEMS. The authors would like to thank Anna Blacka from UNSW Sydney for her assistance with the preparation of figures. We also thank Danial Khojasteh for his constructive comments which helped us to greatly improve this manuscript.

Declaration

The authors declare that they have no known competeing financial interests or personal relationships that could have appeared to influence the work reported in this paper.

Data availability statement

Water level data was sourced from the NSW Water Level Data Collection Program (MHL, 2023) available at https://mhl.nsw.gov.au/Data-Level. Land-use mapping was based on the Australian Land Use and Management (ALUM) classification (DPIE, 2020). Climate (monthly temperature) data presented in the Supplementary Material was downloaded from the Climate Data Online service of the Australia Bureau of Meteorology website Climate Data Online - Map search (bom.gov.au). Mapping was undertaken using the QGIS software, which can be freely downloaded from Discover QGIS. Digital elevation data (Geoscience Australia,

2018) was obtained from the National Elevation Data Framework spatial dataset Elvis (fsdf.org.au) managed by Geoscience Australia Digital Elevation Data | Geoscience Australia (ga.gov.au).

References

Amiri, B. J., & Nakane, K. (2008). Entire catchment and buffer zone approaches to modeling linkage between river water quality and land cover—A case study of Yamaguchi Prefecture, Japan. *Chinese Geographical Science, 18*(1), 85-92. doi:10.1007/s11769-008-0085-6

Arellano, A., Bianchi, T. S., Osburn, C., D'Sa, E., Ward, N. D., Oviedo-Vargas, D., . . . Kurian, G. (2019). Mechanisms of Organic Matter Export in Estuaries with Contrasting Carbon Sources. *Journal of Geophysical Research: Biogeosciences, 124*(10), 3168-3188.

Baldwin, D. S., Boys, C. A., Rohlfs, A.-M., Ellis, I., & Pera, J. (2022). Field trials to determine the efficacy of aerators to mitigate hypoxia in inland waterways. *Marine and Freshwater Research, 73*(2), 211-222. doi:https://doi.org/10.1071/MF20365

Barlow, K., Christy, B., & Weeks, A. (2009). *Nutrient generation and transport at the catchment scale.* Paper presented at the 18th World IMACS Congress and MODSIM09 International Congress on Modelling and Simulation.

Bonvillain, C. P., Halloran, B. T., Boswell, K. M., Kelso, W. E., Harlan, A. R., & Rutherford, D. A. (2011). Acute Physicochemical Effects in a Large River-Floodplain System Associated with the Passage of Hurricane Gustav. *Wetlands, 31*(5), 979. doi:10.1007/s13157-011-0213-4

Breitburg, D., Levin, L. A., Oschlies, A., Grégoire, M., Chavez, F. P., Conley, D. J., . . . Zhang, J. (2018). Declining oxygen in the global ocean and coastal waters. *Science, 359*(6371), eaam7240. doi:doi:10.1126/science.aam7240

Buck, O., Niyogi, D. K., & Townsend, C. R. (2004). Scale-dependence of land use effects on water quality of streams in agricultural catchments. *Environmental Pollution, 130*(2), 287-299. doi:https://doi.org/10.1016/j.envpol.2003.10.018

Carney, R. L., Mitrovic, S. M., Jeffries, T., Westhorpe, D., Curlevski, N., & Seymour, J. R. (2015). River bacterioplankton community responses to a high inflow event. *Aquatic Microbial Ecology, 75*(3), 187-205.

Carstensen, J., Andersen, J. H., Gustafsson, B. G., & Conley, D. J. (2014). Deoxygenation of the Baltic Sea during the last century. *Proceedings of the National Academy of Sciences, 111*(15), 5628-5633. doi:doi:10.1073/pnas.1323156111

Cloern, J. E., Schraga, T. S., Nejad, E., & Martin, C. (2020). Nutrient Status of San Francisco Bay and Its Management Implications. *Estuaries and Coasts, 43*(6), 1299-1317. doi:10.1007/s12237-020-00737-w

Coble, A. A., Koenig, L. E., Potter, J. D., Parham, L. M., & McDowell, W. H. (2019). Homogenization of dissolved organic matter within a river network occurs in the smallest headwaters. *Biogeochemistry, 143*(1), 85-104.

Conley, D. J. (2012). Save the Baltic Sea. *Nature, 486*(7404), 463-464. doi:10.1038/486463a

Conley, D. J., Carstensen, J., Ærtebjerg, G., Christensen, P. B., Dalsgaard, T., Hansen, J. L. S., & Josefson, A. B. (2007). LONG-TERM CHANGES AND IMPACTS OF HYPOXIA IN DANISH COASTAL WATERS. *Ecological Applications, 17*(sp5), S165-S184. doi:10.1890/05-0766.1

Conley, D. J., Carstensen, J., Aigars, J., Axe, P., Bonsdorff, E., Eremina, T., . . . Zillén, L. (2011). Hypoxia Is Increasing in the Coastal Zone of the Baltic Sea. *Environmental Science & Technology, 45*(16), 6777-6783. doi:10.1021/es201212r

Cox, B. A. (2003). A review of currently available in-stream water-quality models and their applicability for simulating dissolved oxygen in lowland rivers. *Science of The Total Environment, 314-316*, 335-377. doi:https://doi.org/10.1016/S0048-9697(03)00063-9

Dey, R., Lewis, S. C., Arblaster, J. M., & Abram, N. J. (2019). A review of past and projected changes in Australia's rainfall. *WIREs Climate Change, 10*(3), e577. doi:https://doi.org/10.1002/wcc.577

Diaz, R. J. (2001). Overview of Hypoxia around the World. *Journal of environmental quality, 30*(2), 275-281. doi:10.2134/jeq2001.302275x

Diaz, R. J., & Rosenberg, R. (2008). Spreading Dead Zones and Consequences for Marine Ecosystems. *Science, 321*(5891), 926-929. doi:doi:10.1126/science.1156401

Díaz, R. J., & Rosenberg, R. (2011). Introduction to Environmental and Economic Consequences of Hypoxia. *International Journal of Water Resources Development, 27*(1), 71-82. doi:10.1080/07900627.2010.531379

DPIE. (2020). NSW Landuse 2017 Version 1.2. Retrieved from https://datasets.seed.nsw.gov.au/dataset/nsw-landuse-2017-v1p2-f0ed

Eyre, B., & Twigg, C. (1997). Nutrient behaviour during post-flood recovery of the Richmond River Estuary, Northern NSW, Australia. *Estuarine, Coastal and Shelf Science, 44*(3), 311-326.

Eyre, B. D., Kerr, G., & Sullivan, L. A. (2006). Deoxygenation potential of the Richmond River Estuary floodplain, northern NSW, Australia. *River Research and Applications, 22*(9), 981-992. doi:10.1002/rra.950

Fitzhenry, M., Alley, K., Hesse, S., & Couriel, E. (2012). *OEH NSW Tidal Planes Analysis: 1990 - 2010 Harmonic Analysis*. Retrieved from

Geoscience Australia. (2018). Retrieved from https://elevation.fsdf.org.au/

Gibbs, M. S., Wallace, T., & Mosley, L. M. (2022). Constraining organic matter composition and dynamics as a dominant driver of hypoxic blackwater risk during river Murray floodplain inundation. *Hydrological processes, 36*(3), e14529. doi:https://doi.org/10.1002/hyp.14529

Godinho, F. N., Segurado, P., Franco, A., Pinheiro, P., Pádua, J., Rivaes, R., & Ramos, P. (2019). Factors related to fish kill events in Mediterranean reservoirs. *Water Research, 158*, 280-290. doi:https://doi.org/10.1016/j.watres.2019.04.027

Górniak, A. (2017). A new version of the Hydrochemical Dystrophy Index to evaluate dystrophy in lakes. *Ecological Indicators, 78*, 566-573. doi:https://doi.org/10.1016/j.ecolind.2017.03.030

Greenop, B., Lovatt, K., & Robb, M. (2001). The use of artificial oxygenation to reduce nutrient availability in the Canning River, Western Australia. *Water Sci Technol, 43*(9), 133-144.

Hamilton, S. K., Sippel, S. J., Calheiros, D. F., & Melack, J. M. (1997). An anoxic event and other biogeochemical effects of the Pantanal wetland on the Paraguay River. *Limnology and Oceanography, 42*(2), 257-272.

Hitchcock, J. N., Westhorpe, D., Glamore, W., & Mitrovic, S. (2021). Estuarine zooplankton responses to flood pulses and a hypoxic blackwater event.

Hladyz, S., Watkins, S. C., Whitworth, K. L., & Baldwin, D. S. (2011). Flows and hypoxic blackwater events in managed ephemeral river channels. *Journal of Hydrology, 401*(1), 117-125. doi:https://doi.org/10.1016/j.jhydrol.2011.02.014

Howitt, J. A., Baldwin, D. S., Rees, G. N., & Williams, J. L. (2007). Modelling blackwater: Predicting water quality during flooding of lowland river forests. *Ecological Modelling, 203*(3), 229-242. doi:https://doi.org/10.1016/j.ecolmodel.2006.11.017

Johnston, S., Kroon, F., Slavich, P., Cibilic, A., & Bruce, A. (2003). Restoring the balance-guidelines for managing floodgates and drainage systems on coastal floodplains.

Johnston, S. G., Slavich, P. G., & Hirst, P. (2005). Changes in surface water quality after inundation of acid sulfate soils of different vegetation cover. *Soil Research, 43*(1), 1-12. doi:https://doi.org/10.1071/SR04073

Johnston, S. G., Slavich, P. G., Sullivan, L. A., & Hirst, P. (2003). Artificial drainage of floodwaters from sulfidic backswamps: effects on deoxygenation in an Australian estuary. *Marine and Freshwater Research, 54*(6), 781-795. doi:https://doi.org/10.1071/MF02016

Kerr, J. L., Baldwin, D. S., & Whitworth, K. L. (2013). Options for managing hypoxic blackwater events in river systems: A review. *Journal of Environmental Management, 114*, 139-147. doi:https://doi.org/10.1016/j.jenvman.2012.10.013

King, A. J., Tonkin, Z., & Lieshcke, J. (2012). Short-term effects of a prolonged blackwater event on aquatic fauna in the Murray River, Australia: considerations for future events. *Marine and Freshwater Research, 63*(7), 576-586. doi:https://doi.org/10.1071/MF11275

Kobayashi, T., Ryder, D. S., Gordon, G., Shannon, I., Ingleton, T., Carpenter, M., & Jacobs, S. J. (2009). Short-term response of nutrients, carbon and planktonic microbial communities to floodplain wetland inundation. *Aquatic Ecology, 43*(4), 843-858. doi:10.1007/s10452-008-9219-2

Koehn, J. D. (2022). Key steps to improve the assessment, evaluation and management of fish kills: lessons from the Murray–Darling River system, Australia. *Marine and Freshwater Research, 73*(2), 269-281. doi:https://doi.org/10.1071/MF20375

Kragh, T., Martinsen, K. T., Kristensen, E., & Sand-Jensen, K. (2020). From drought to flood: Sudden carbon inflow causes whole-lake anoxia and massive fish kill in a large shallow lake. *Science of The Total Environment, 739*, 140072. doi:https://doi.org/10.1016/j.scitotenv.2020.140072

Lin, C., Wood, M., Haskins, P., Ryffel, T., & Lin, J. (2004). Controls on water acidification and de-oxygenation in an estuarine waterway, eastern Australia. *Estuarine, Coastal and Shelf Science, 61*(1), 55-63.

Liu, X., Watts, R. J., Howitt, J. A., & McCasker, N. (2019). Carbon and nutrient release from experimental inundation of agricultural and forested floodplain soil and vegetation: influence of floodplain land use on the development of hypoxic blackwater during floods. *Marine and Freshwater Research*. doi:10.1071/mf18452

Masson-Delmotte, V., Zhai, P., Priani, A., Connors, S. L., Pean, C., Berger, S., . . . Zhou, B. (2021). *IPCC: Climate Change 2021: The Physical Science Basis. Contribution of Working Group I to the Sixth Assessment Report of the Intergovernmental Panel on Climate Change.* Retrieved from

Mehring, A. S., Kuehn, K. A., Tant, C. J., Pringle, C. M., Lowrance, R. R., & Vellidis, G. (2014). Contribution of surface leaf-litter breakdown and forest composition to benthic oxygen demand and ecosystem respiration in a South Georgia blackwater river. *Freshwater Science, 33*(2), 377-389. doi:10.1086/675507

Meyer, J. L. (1990). A blackwater perspective on riverine ecosystems. *BioScience, 40*(9), 643-651.

MHL. (2023). New South Wales water level data collection program. Retrieved from https://mhl.nsw.gov.au/Data-Level

Moore, A. (2006). Blackwater and fish kills in the Richmond River estuary. Defining the issues - Assessing the risks - Providing management options. *Southern Cross University: Lismore, NSW, Australia*.

Mosley, L. M., Wallace, T., Rahman, J., Roberts, T., & Gibbs, M. (2021). An integrated model to predict and prevent hypoxia in floodplain-river systems. *Journal of Environmental Management, 286*, 112213. doi:https://doi.org/10.1016/j.jenvman.2021.112213

Ning, N. S. P., Petrie, R., Gawne, B., Nielsen, D. L., & Rees, G. N. (2015). Hypoxic blackwater events suppress the emergence of zooplankton from wetland sediments. *Aquatic Sciences, 77*(2), 221-230. doi:10.1007/s00027-014-0382-3

O'Connell, M., Baldwin, D. S., Robertson, A. I., & Rees, G. (2000). Release and bioavailability of dissolved organic matter from floodplain litter: influence of origin and oxygen levels. *Freshwater Biology, 45*(3), 333-342. doi:10.1111/j.1365-2427.2000.00627.x

Paerl, H. W. (2006). Assessing and managing nutrient-enhanced eutrophication in estuarine and coastal waters: Interactive effects of human and climatic perturbations. *Ecological Engineering, 26*(1), 40-54. doi:https://doi.org/10.1016/j.ecoleng.2005.09.006

Pahor, S., & Newton, G. (2013). *Understanding blackwater events in rivers* (Vol. 22): Australian Network for Plant Conservation Inc.

Pasco, T. E., Kaller, M. D., Harlan, R., Kelso, W. E., Rutherford, D. A., & Roberts, S. (2016). Predicting Floodplain Hypoxia in the Atchafalaya River, Louisiana, USA, a Large, Regulated Southern Floodplain River System. *River Research and Applications, 32*(5), 845-855. doi:https://doi.org/10.1002/rra.2903

Rabalais, N. N., Turner, R. E., & Wiseman Jr., W. J. (2002). Gulf of Mexico Hypoxia, A.K.A. “The Dead Zone”. *Annual Review of Ecology and Systematics, 33*(1), 235-263. doi:10.1146/annurev.ecolsys.33.010802.150513

Rixen, T., Baum, A., Pohlmann, T., Balzer, W., Samiaji, J., & Jose, C. (2008). The Siak, a tropical black water river in central Sumatra on the verge of anoxia. *Biogeochemistry, 90*(2), 129-140. doi:10.1007/s10533-008-9239-y

Saintilan, N., Kelleway, J. J., Mazumder, D., Kobayashi, T., & Wen, L. (2021). Incorporation of local dissolved organic carbon into floodplain aquatic ecosystems. *Aquatic Ecology, 55*(3), 779-790. doi:10.1007/s10452-021-09860-7

Scavia, D., Bertani, I., Obenour, D. R., Turner, R. E., Forrest, D. R., & Katin, A. (2017). Ensemble modeling informs hypoxia management in the northern Gulf of Mexico. *Proceedings of the National Academy of Sciences, 114*(33), 8823-8828. doi:doi:10.1073/pnas.1705293114

Southern Cross GeoScience. (2019). *Episodic estuarine hypoxia: resolving the geochemistry of coastal floodplain blackwaters – Summary of project findings* (Southern Cross GeoScience Technical Report No. 119). Retrieved from Southern Cross University, Lismore NSW 2480:

Steffe, A. S., Macbeth, W. G., & Murphy, J. J. (2007). Status of the recreational fisheries in two Australian coastal estuaries following large fish-kill events. *Fisheries Research, 85*(3), 258-269. doi:https://doi.org/10.1016/j.fishres.2007.02.003

Tallis, H., Polasky, S., Hellmann, J., Springer, N. P., Biske, R., DeGeus, D., . . . Weaver, S. K. (2019). Five financial incentives to revive the Gulf of Mexico dead zone and Mississippi basin soils. *Journal of Environmental Management, 233*, 30-38. doi:https://doi.org/10.1016/j.jenvman.2018.11.140

Townsend, S. A., Boland, K. T., & Wrigley, T. J. (1992). Factors contributing to a fish kill in the Australian wet/dry tropics. *Water Research, 26*(8), 1039-1044. doi:https://doi.org/10.1016/0043-1354(92)90139-U

Townsend, S. A., & Edwards, C. A. (2003). A fish kill event, hypoxia and other limnological impacts associated with early wet season flow into a lake on the Mary River floodplain, tropical northern Australia. *Lakes & Reservoirs: Research & Management, 8*(3-4), 169-176.

Tulau, M. J. (2011). Lands of the richest character: Agricultural drainage of backswamp wetlands on the north coast of New South Wales, Australia: Development, conservation and policy change: An environmental history.

Vaquer-Sunyer, R., & Duarte, C. M. (2008). Thresholds of hypoxia for marine biodiversity. *Proceedings of the National Academy of Sciences, 105*(40), 15452-15457. doi:doi:10.1073/pnas.0803833105

Vithana, C. L., Sullivan, L. A., & Shepherd, T. (2019). Role of temperature on the development of hypoxia in blackwater from grass. *Science of The Total Environment, 667*, 152-159. doi:https://doi.org/10.1016/j.scitotenv.2019.02.386

Voß, K., Fernández, D., & Schäfer, R. B. (2015). Organic matter breakdown in streams in a region of contrasting anthropogenic land use. *Science of The Total Environment, 527-528*, 179-184. doi:10.1016/j.scitotenv.2015.04.071

Wallace, T. A., Ganf, G. G., & Brookes, J. D. (2008). A comparison of phosphorus and DOC leachates from different types of leaf litter in an urban environment. *Freshwater Biology, 53*(9), 1902-1913. doi:10.1111/j.1365-2427.2008.02006.x

Walsh, S., Copeland, C., & Westlake, M. (2004). Major fish kills in the northern rivers of NSW in 2001: causes, impacts and responses. *NSW Department of Primary Industries. Fisheries final report series*(68), 55.

Watts, R. J., Kopf, R. K., McCasker, N., Howitt, J. A., Conallin, J., Wooden, I., & Baumgartner, L. (2018). Adaptive Management of Environmental Flows: Using Irrigation Infrastructure to Deliver Environmental Benefits During a Large Hypoxic Blackwater Event in the Southern Murray–Darling Basin, Australia. *Environmental Management, 61*(3), 469-480. doi:10.1007/s00267-017-0941-1

Whitworth, K. L., & Baldwin, D. S. (2016). Improving our capacity to manage hypoxic blackwater events in lowland rivers: the Blackwater risk assessment tool. *Ecological Modelling, 320*, 292-298.

Whitworth, K. L., Baldwin, D. S., & Kerr, J. L. (2012). Drought, floods and water quality: Drivers of a severe hypoxic blackwater event in a major river system (the southern Murray–Darling Basin, Australia). *Journal of Hydrology, 450-451*, 190-198. doi:https://doi.org/10.1016/j.jhydrol.2012.04.057

Whitworth, K. L., Kerr, J. L., Mosley, L. M., Conallin, J., Hardwick, L., & Baldwin, D. S. (2013). Options for managing hypoxic blackwater in river systems: case studies and framework. *Environmental Management, 52*(4), 837-850.

Wong, V., Walsh, S., & Morris, S. (2018). Climate affects fish-kill events in subtropical estuaries of eastern Australia. *Marine and Freshwater Research, 69*(11), 1641-1648.

Wong, V. N. L., Johnston, S. G., Burton, E. D., Bush, R. T., Sullivan, L. A., & Slavich, P. G. (2011). Anthropogenic forcing of estuarine hypoxic events in sub-tropical catchments: Landscape drivers and biogeochemical processes. *Science of The Total Environment, 409*(24), 5368-5375.

Wong, V. N. L., Johnston, S. G., Bush, R. T., Sullivan, L. A., Clay, C., Burton, E. D., & Slavich, P. G. (2010). Spatial and temporal changes in estuarine water quality during a post-flood hypoxic event. *Estuarine, Coastal and Shelf Science, 87*(1), 73-82. doi:https://doi.org/10.1016/j.ecss.2009.12.015

Xiong, S., Nilsson, C. (1997). Dynamics of leaf litter accumulation and its effects on riparian vegetation: A review. . *The Botanical Review, 69*. doi:10.1071/mf17307

Zhang, M., Cheng, X., Geng, Q., Shi, Z., Luo, Y., & Xu, X. (2019). Leaf litter traits predominantly control litter decomposition in streams worldwide. *Global Ecology and Biogeography, 28*(10), 1469-1486.

Hypoxic Blackwater Events - Identifying High Risk Catchments in Estuaries Now and Under Future Climate Scenarios

K. Waddington[1], A. Harrison[1], D. Rayner[1], T. Tucker[1] and W. Glamore[1]

[1] Water Research Laboratory, School of Civil and Environmental Engineering, UNSW Sydney, NSW 2093, Australia.

Corresponding author: Katrina Waddington (k.waddington@unsw.edu.au)

Key Points:

- A methodology is presented to differentiate estuarine catchments by their potential to generate hypoxic blackwater.
- Local topographic and hydrodynamic conditions strongly influence the potential volume of blackwater generated over a catchment.
- Climate change may increase the frequency and severity and change the distribution of blackwater risk throughout an estuary.

Abstract

Hypoxic blackwater events occur worldwide, affecting inland and coastal waters. These events have been exacerbated by man-made floodplain drainage, leading to large-scale fish kills and ecological degradation. This paper presents a new method to identify estuarine catchment areas that are most likely to generate hypoxic conditions. The method uses established blackwater risk factors, including vegetation type, inundation extent and duration, ground-truthed in eastern Australia. A catchment is at higher risk of blackwater generation if (i) it is located where floodwaters are high and/or drainage is impeded, (ii) the site topography includes an extensive, low-lying floodplain; and/or (iii) the land-use and environmental characteristics have a high deoxygenation potential. Blackwater impacts in an estuary are determined by the floodplain connectivity with the estuary, and the discharge characteristics of the catchment drainage system. Where multiple, proximate catchments have similar drainage conditions, compounding blackwater plumes can overwhelm the assimilation capacity of the estuary. Climate change may significantly increase the volume and frequency of blackwater events in estuarine environments as a result of reduced drainage due to sea level rise, higher temperatures, and more intense and sporadic rainfall events. It is recommended that management measures be introduced to mitigate the effects of climate change and avoid further widespread hypoxic blackwater events.

1 Introduction

Blackwater is the common name for dark coloured water characterised by low levels of dissolved oxygen (DO) (Howitt, Baldwin, Rees, & Williams, 2007; Moore, 2006). Blackwaters are typically associated with the presence of humic substances leached from decaying vegetation (Coble, Koenig, Potter, Parham, & McDowell, 2019) or floodplain sediments (Meyer, 1990; Rixen et al., 2008). This transfer of dissolved organic matter and nutrients from riparian zones and floodplains to adjacent waterways is a natural part of the nutrient cycle. However, excessive stimulation of microbial respiration, particularly via elevated levels of organic matter and higher temperatures, can lead to hypoxic conditions, whereby DO concentrations are reduced below 2mg/L (Rabalais, Turner, & Wiseman Jr., 2002; Vithana, Sullivan, & Shepherd, 2019). Indeed, hypoxic blackwater plumes have been linked to decreased aquatic ecosystem health, including mass fish kills, and detrimental impacts on sessile flora and fauna (Hladyz, Watkins, Whitworth, & Baldwin, 2011; Pahor & Newton, 2013; Vaquer-Sunyer & Duarte, 2008). Blackwater may also affect the broader estuarine environment through disrupted trophic levels, interrupted life cycles, reductions in suitable habitat, overcrowding, and forced migration (Rabalais et al., 2002; Vaquer-Sunyer & Duarte, 2008).

Globally, hypoxia is frequently associated with the decomposition of autochthonous algal blooms fuelled by the eutrophication of inland and coastal waterways, as exemplified by the infamous dead zones of the Gulf of Mexico (Diaz, 2001; Górniak, 2017), the Baltic (Conley et al., 2011) and Black Seas (Rabalais et al., 2002). However, hypoxic conditions can also develop following direct, precipitous carbon loading of lakes, rivers or estuaries as a result of extended catchment inundation, in what are commonly known as blackwater events (Moore, 2006). Globally, flood-induced blackwater events are widespread, having been reported on the Paraguay River, Brazil (Hamilton, Sippel, Calheiros, & Melack, 1997), the Atchafalaya River, USA (Bonvillain et al., 2011; Pasco et al., 2016) and in Lake FilsØ, Denmark (Kragh, Martinsen, Kristensen, & Sand-Jensen, 2020). In Australia, blackwater events have affected inland rivers in arid and temperate regions of the Murray-Darling Basin (King, Tonkin, & Lieshcke, 2012; Whitworth, Baldwin, & Kerr, 2012) and the Edward-Wakool River system (Hladyz et al., 2011); tropical waters in the Katherine (Townsend, Boland, & Wrigley, 1992) and Mary (Townsend & Edwards, 2003) Rivers of the Northern Territory; and coastal estuaries, including the Hunter (Carney et al., 2015; Hitchcock, Westhorpe, Glamore, & Mitrovic, 2021), Clarence (Johnston, Kroon, Slavich, Cibilic, & Bruce, 2003) and Richmond (Walsh, Copeland, & Westlake, 2004) Rivers in northern New South Wales (NSW).

While eutrophic and blackwater hypoxic events may occur naturally, anthropogenic activities appear to have escalated their frequency and magnitude (Carstensen, Andersen, Gustafsson, & Conley, 2014; Kerr, Baldwin, & Whitworth, 2013; Paerl, 2006; Rabalais et al., 2002; Wong et al., 2010). Dead zones have spread exponentially since the 1960s (Diaz & Rosenberg, 2008), with scientifically confirmed accounts of hypoxia affecting over 500 catchments globally (Breitburg et al., 2018; Díaz & Rosenberg, 2011). This increase has been attributed to anthropogenic impacts, including wastewater discharges (Breitburg et al., 2018), modifications to floodplain hydrology following river regulation and water extraction (Whitworth et al., 2013), and the construction of drainage and flood mitigation works

(Moore, 2006), with changes to vegetation and land-use contributing to increased nutrient loads (Arellano et al., 2019; Conley et al., 2007; Godinho et al., 2019).

Efforts to mitigate the impacts of hypoxia have included nutrient reduction schemes, primarily aimed at improving the quality of industrial and municipal wastewater discharges (Conley, 2012), reducing the impacts of agricultural land-use practices (Tallis et al., 2019), changes to river regulation procedures (Kerr et al., 2013; King et al., 2012; Watts et al., 2018), and dilution/aeration techniques (Whitworth et al., 2013). However, effective mitigation requires a thorough understanding of the mechanisms that contribute to the formation and persistence of blackwater. To this aim, conceptual models have been developed to improve blackwater management for the Atchafalaya River (Pasco et al., 2016), Gulf of Mexico (Scavia et al., 2017) and San Francisco Bay (Cloern, Schraga, Nejad, & Martin, 2020) in the United States, and the Murray-Darling River system in Australia (Whitworth and Baldwin (2016)). For example, the Blackwater Risk Assessment Tool (BRAT) developed by Howitt (2007) and Hladyz (2011) describes the carbon load generated over the Murray-Darling floodplain via litter accumulation and decomposition rates, carbon leaching, microbial degradation and respiration. The carbon load is then converted to a volumetric biochemical oxygen demand (BOD) by considering the area, depth and duration of inundation (Howitt et al., 2007; Whitworth & Baldwin, 2016). Other key variables are temperature, re-aeration and dilution potential (Howitt et al., 2007). The Dissolved Oxygen-Dissolved Organic Carbon (DODOC) model developed by Mosley, Wallace, Rahman, Roberts, and Gibbs (2021) has subsequently integrated hydrologic capability with the BRAT ecological assessment to better represent the complex interactions between catchment hydrology and floodplain inundation (Gibbs, Wallace, & Mosley, 2022; Mosley et al., 2021). Consequently, environmental flow releases in the regulated, lowland inland rivers of Australia are now managed to avoid periods of high carbon production on floodplains (Saintilan, Kelleway, Mazumder, Kobayashi, & Wen, 2021).

Many of the same risk factors that apply to the generation of blackwater over the floodplains of inland rivers also apply to coastal floodplains. However, tidal flows present a different hydrodynamic regime to that experienced in riverine environments, and within many estuarine environments the retention and release of floodplain waters has been heavily modified by extensive flood mitigation and drainage schemes. Over the course of the 20th century, meandering channels with low hydraulic gradients and limited outlets have been replaced by extensive networks of drainage channels that have breached the natural hydraulic separation between an estuary and the adjacent coastal floodplains (Tulau, 2011). Blackwaters that were once predominately retained within extensive tracts of freshwater and tidal wetlands, allowing the carbon cycle to complete and the water column to become re-aerated, are now discharged swiftly to the estuary (Johnston, Slavich, Sullivan, & Hirst, 2003).

These floodplain drainage schemes have been directly linked to blackwater events that resulted in major fish kills throughout the northern estuaries of NSW (Walsh et al., 2004). Such events closed the Macleay River to fishing for 3 months in 2001 (Walsh et al., 2004), and the Richmond River for 4.5 months in 2001 (Steffe, Macbeth, & Murphy, 2007) and 2 months in 2008 (Wong et al., 2010). Consequently, analyses of blackwater events in the Clarence (Johnston et al., 2003) and Richmond (Wong et al., 2010) Rivers of Australia have identified three characteristic stages of an estuarine blackwater event (Figure 1):

1. Initially low-lying floodplain areas are inundated as floodwaters rise. The concentration of dissolved organic carbon (DOC) in the water column starts to increase and microbial metabolization of DOC rapidly reduces the DO concentration (Stage 1).
2. Floodplain waters become anoxic and the deoxygenation potential (DOP) increases as the BOD continues to rise (Stage 2).
3. The assimilation capacity of the river decreases as the floodwaters recede and the high oxygen demand of the blackwaters discharged from the floodplain drainage systems has a substantial impact on the adjacent waterway (Stage 3). This stage may be exacerbated by the drainage of acidic groundwaters from behind the flood mitigation structures.

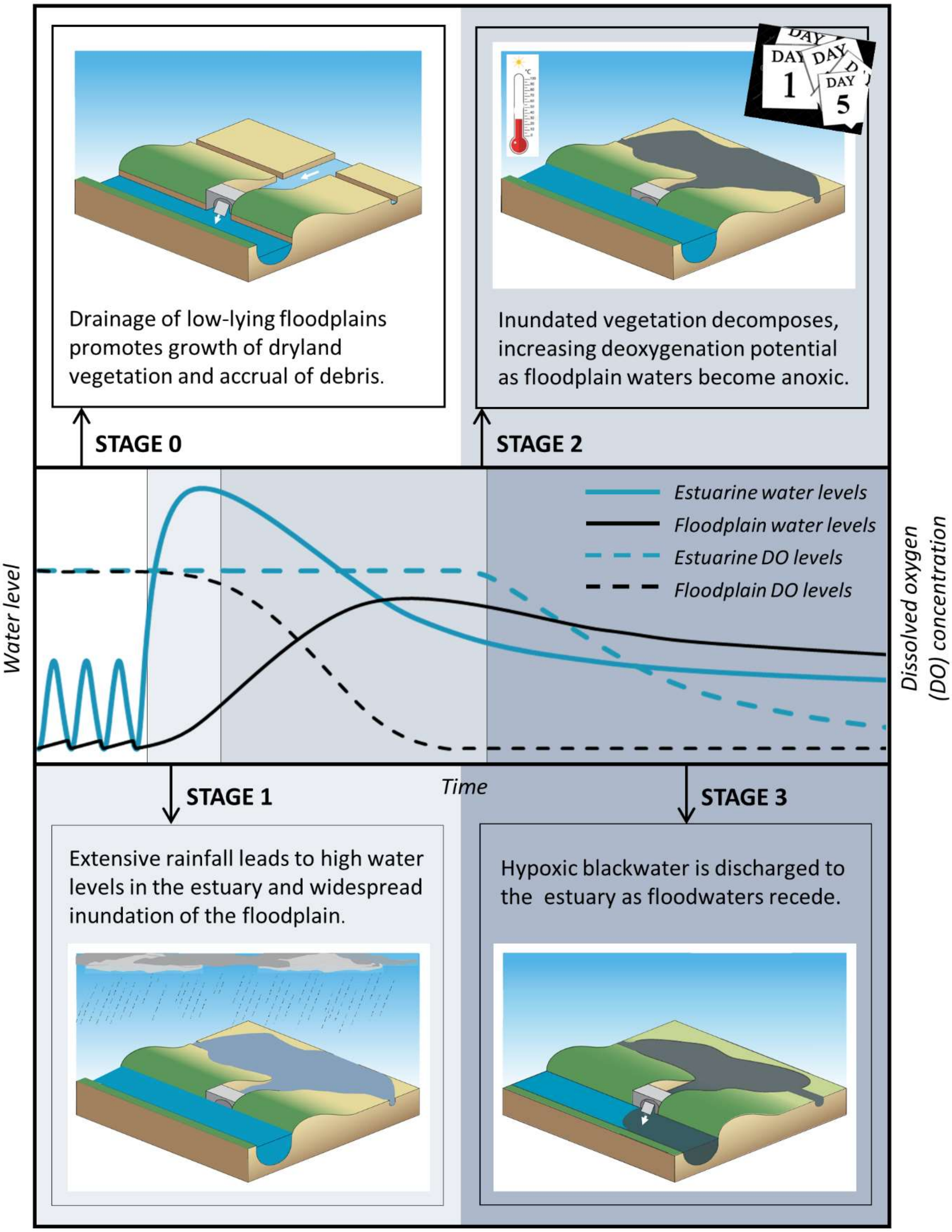

Figure 1. Conceptual stages of a blackwater event in an estuary (graph adapted from (Johnston et al., 2003))

The influence of constructed drainage systems and tidal floodgates on the magnitude and frequency of hypoxic blackwater events is evident in each of the three stages identified in Figure 1. Indeed, the construction of drainage schemes on estuarine floodplains has increased the potential for blackwater generation for a number of reasons. First, enhanced drainage promotes dry-land pastural grasses and agricultural crops in favour of water-tolerant vegetation species. These dry-land species are more susceptible to inundation and can provide a highly labile source of carbon for microbial metabolisation (Eyre, Kerr, & Sullivan, 2006; Johnston et al., 2003). Second, the reduced frequency of floodplain inundation increases the availability of carbon as organic debris accumulates between flood events (Ning, Petrie, Gawne, Nielsen, & Rees, 2015; Pahor & Newton, 2013). Finally, enhanced drainage intensifies the impact of blackwater by promoting the rapid discharge of anoxic floodwaters with high DOP directly to the estuary and by increasing the volume of blackwater that is transferred to the estuary (Wong et al., 2010).

Studies to date have focussed on the first two impacts of constructed drainage schemes; developing a detailed understanding of the local mechanisms by which blackwater is generated over estuarine floodplains. However, there have been limited investigations into the hydrodynamic interactions between the estuary and floodplain. Indeed, variability of rainfall and inundation across various drainage catchments within the floodplain has been identified as a primary difficulty in prioritising areas for blackwater management (Moore, 2006). Estuarine water levels are fundamental to the retention of water on the floodplains and the release of impounded water to the estuary. The former presents a limitation to the volume of blackwater that may be generated on the floodplain, while the latter is a determining factor regarding blackwater impacts upon the estuarine environment.

This paper presents a methodology to address this knowledge gap by incorporating the hydrodynamic regime and the topographic constraints underlying the generation of hypoxic blackwater in estuarine floodplains. The methodology quantifies the relative potential for blackwater contribution from each drainage catchment within an estuary. Water quality surveys from historic blackwater events in south-eastern Australia are used to explore the validity of the blackwater risk assessment. The results provide insights into the susceptibility of various catchments within an estuary to blackwater under current and future climate conditions. It is anticipated that this approach may be used to optimise strategic monitoring programmes and future management options.

2 Methodology

2.1 Blackwater risk factors

Differentiating the potential for blackwater generation between various catchments within an estuary requires the identification and quantification of risk factors that may contribute to a blackwater event. These include biological (carbon availability and microbial metabolization), chemical (for example, inorganic reactions, acidity and salinity) and physical (primarily temperature and pressure) mechanisms affecting the DOP of the floodwaters. Further, the extent and duration of inundation over the catchment is critical to the volume of blackwater that may be generated. An overview and the assessment of these risk factors is presented in the following sections.

2.1.2 BOD and carbon availability

BOD is a critical factor contributing to changes in DO levels within a water column, with the rate of oxidation assumed to be directly proportional to the BOD (Cox, 2003). BOD accounts for both the chemical oxidation of inorganic cations such as Fe^{2+}, Mn^{2+} and S^{2-} (Johnston, Slavich, & Hirst, 2005; Vithana et al., 2019; Wong et al., 2010), and the microbial decomposition of biodegradable organic matter (Hladyz et al., 2011).

In coastal estuaries of southeast Australia, the impacts of chemical oxidation are associated with acid sulfate soils (ASS) (Johnston et al., 2003). ASS are chemically stable when undisturbed, however constructed drainage systems have exposed large floodplain areas to oxygen, producing sulphuric acid and, via dissolution, metallic cations. Secondary oxidation of these ions can create a significant oxygen demand within the water column (Johnston et al., 2003; Lin, Wood, Haskins, Ryffel, & Lin, 2004) and the associated acidity has been independently attributed to fish kills (Walsh et al., 2004). Analysis of the geochemical signature of floodwaters in the main channel of the Clarence (Johnston et al., 2003) and Richmond Rivers (Wong et al., 2010) identified the anaerobic decomposition of floodplain vegetation as the primary process leading to generation of hypoxic blackwater conditions. Further, mesocosm experiments in the Richmond (Eyre et al., 2006) and Edward-

Wakool (Hladyz et al., 2011) Rivers determined the BOD of a variety of vegetation types and confirmed the potential for microbial decomposition of inundated floodplain vegetation to be sufficient to trigger a blackwater event.

The rate at which vegetation decays and deoxygenates water during periods of prolonged inundation differs depending on the vegetation type (Eyre et al., 2006; Johnston et al., 2005; Whitworth & Baldwin, 2016), with DOP being a factor of, *inter alia*, the labile carbon concentration (often measured as dissolved organic carbon) and temperature (Wong et al., 2011). Labile carbon is the organic component that is readily bio-available, with a higher lability associated with faster decomposition rates (Zhang et al., 2019). For example, when examining the impacts of flooding observed in the Clarence River, Johnston et al. (2003) attributed the relatively high oxygen demand from one catchment to the dominance of labile dryland pasture species compared to another that was vegetated predominately by recalcitrant *Melaleuca quinquenervia* forest. Thus, floodplains dominated by endemic wetland plant species would be less likely to generate blackwater than those that have been drained and revegetated with pasture grasses or crops that are less tolerant of inundation (Vithana et al., 2019; Wong et al., 2011). Research determining the oxygen demand of various vegetation, litter and soil types has subsequently been used to hypothesise the relative risk and potential contribution of different land-uses to blackwater events (Liu, Watts, Howitt, & McCasker, 2019).

2.1.2.1 Quantifying the DOP risk factor

It is difficult to establish strong links between land-use (for which spatial data is readily available) and BOD (Amiri & Nakane, 2008). However, a review of Australian literature identified five vegetation types typical of coastal floodplains for which experimental data regarding DOP has been established. Experimental methods differ between the various studies, making direct comparison difficult and there is limited data available regarding the spatial distribution of vegetation on coastal floodplains. Consequently, a risk-based approach linking vegetation types with comparative DOP was devised for this study, as detailed in Table 1. The vegetation types and corresponding risk factors were then assigned to each land-use identified in the 2017 (released in June 2020) Australian Land Use and Management (ALUM) classification (DPIE, 2020). Full details are presented in the Supplementary Material.

Table 1. Blackwater generation risk factors for typical vegetation types in coastal NSW

Vegetation Type	Water Tolerance		Comparative Deoxygenation Potential		Risk Factor**
	Rating	Score	Rating	Score	
Dryland grasses (e.g. pasture)	Low	3	High [a, c, e] Medium [b]	3	**3**
Forestry (other than tea tree) *	Low	3	High [b, c]	3	**3**
Tea tree leaves*	Low	3	Low [d] Low – Medium [a] Medium [e]	2	**2**
Sugar cane+	Medium	2	Low – Medium [a]	2	**2**
Freshwater wetland grasses (e.g. Grey rush)	High	1	Low [a] Medium [d]	1	**1**

[a] Eyre et al. (2006)
[b] Whitworth and Baldwin (2016)
[c] Liu et al. (2019)
[d] Johnston et al. (2005)
[e] Southern Cross GeoScience (2019)

* Low water tolerance is attributed to the presence of readily available leaf litter, rather than the likelihood of plants dying.

+ Sugar cane is relatively tolerant to water, but the presence of waste after harvest increases the DOP.

** The risk factor is the average of the scores for water tolerance and comparative DOP.

2.1.3 Floodplain inundation characteristics

Flood mitigation and drainage systems have been implemented to increase floodplain productivity by limiting floodplain inundation and increasing drainage efficiency. This reduces the risk of blackwater generation during smaller, localised rainfall events, as inundated catchments can drain freely when downstream waterways are not in flood. However, regardless of the efficiency and scale of drainage infrastructure, floodplain drainage is limited by the receiving (downstream) water level. Consequently, widespread blackwater generation is more commonly associated with extensive flooding when floodplain drainage is restricted by the rate of floodwater recession in the estuary.

2.1.3.1 Inundation duration

To determine the potential for blackwater generation in a floodplain, it is important to quantify the inundation duration required to generate and sustain a blackwater event. This will vary depending on catchment characteristics, seasonal and antecedent conditions, and the unique hydrologic and hydraulic profile of each flood event.

The microbial metabolisation of highly labile carbon sources can rapidly deoxygenate a water column. Organic compounds on the floodplains will start to decompose within hours of inundation (Vithana et al., 2019; Wallace, Ganf, & Brookes, 2008), with the most labile fractions leached of carbon within the first 24 hours. In-situ mesocosm experiments on the floodplain of the Richmond River by Eyre et al. (2006) indicated that microbial metabolisation of harvested sugar cane and dropped tea tree leaves can reduce the dissolved oxygen levels in a 300 mm deep water column to 3 – 4 mg/L within 10 hours, while slashed pasture grass can deoxygenate the same volume of river water almost completely (DO < 1 mg/L) under the same conditions. Similar experiments have shown that DO was reduced to near 0 mg/L over a period of two to three days for a variety of vegetation types (Johnston et al., 2005; Liu et al., 2019; Vithana et al., 2019).

After prolonged immersion, living plants may start to die and more recalcitrant plants decompose, contributing new carbon sources to the water column (Hladyz et al., 2011). Additionally, experiments by Vithana et al. (2019) and Liu et al. (2019) suggest that both DOC and BOD can continue to rise for more than two weeks after initial inundation. Similarly, Wong et al. (2011) showed that chemical oxygen demand (COD) peaked approximately 15 to 20 days after the flood peak in a backswamp on the Clarence River, NSW. This suggests that the DOP is likely to persist for floodplain inundation durations of at least two weeks.

During the 2001 floods in the Richmond, Clarence and Macleay Rivers, it was reported that river water started to deoxygenate as floodplains began to drain, becoming completely deoxygenated within 1 to 3 days, depending on site conditions (Walsh et al., 2004). Mass deoxygenation of coastal estuaries in NSW is typically observed 4 to 6 days after the peak of a flood event (Johnston et al., 2003; Southern Cross GeoScience, 2019; Wong et al., 2010). In part, this reflects the recession of the flood hydrograph and the limited drainage from the floodplain to the estuary during prolonged floods. However, similar observations were made by Bonvillain et al. (2011) following flooding of the Atchafalaya River Basin (USA) in September 2008, where hypoxic conditions were recorded within 3 days and extensive fish kills occurred within 5 days.

Both experimental evidence and recorded observations indicate that floodplain inundation of less than 24 hours can generate blackwater during flood events. However, the limited volume of blackwater generated during this short period is unlikely to have a significant impact on receiving waters. Conversely, the longer that floodwaters are retained on a floodplain, the greater the volume of water that can be deoxygenated (Hladyz et al., 2011), the higher the DOP of the floodwaters (Eyre et al., 2006), and the greater the risk of a blackwater event when those waters are discharged to the receiving estuary (Howitt et al., 2007).

2.1.3.2 Inundation depth and extent

While there are no known long-term records of floodplain inundation within estuaries of NSW, the Department of Planning and Environment maintains a network of water level gauges throughout the estuarine channels (MHL, 2023). These gauges provide continuous long-term, historic water level records which were adopted to represent the depth and duration of floodplain inundation as onsite drainage is controlled by the downstream water levels. The spatial extent of inundation across the floodplain was determined by extrapolating these historic estuarine water levels using ground-truthed digital elevation models (DEMs) with a 5 metre grid resolution (Geoscience Australia, 2018).

2.1.3.3 Inundation depth and duration matrices

Flood hydrographs are highly variable. The influence of the hydrograph shape on the potential for blackwater generation is illustrated in Figure 2. For example, flood events 1 and 2 generate approximately the same volume of flow within the estuary, whereas the higher peak water levels generated during event 2 have a shorter duration. Despite the higher peak flood levels, for floodplain areas below 1m AHD (Australian Height Datum, which equates approximately to mean sea level), the inundation conditions presented by flood event 1 (Figure 2) are likely to generate more hypoxic blackwater than those of event 2, as inundation would be maintained over a longer period of time. Floodplain areas above 2m AHD would only generate blackwater during flood event 3 as they would not be inundated during event 1 and there would be insufficient inundation duration during event 2.

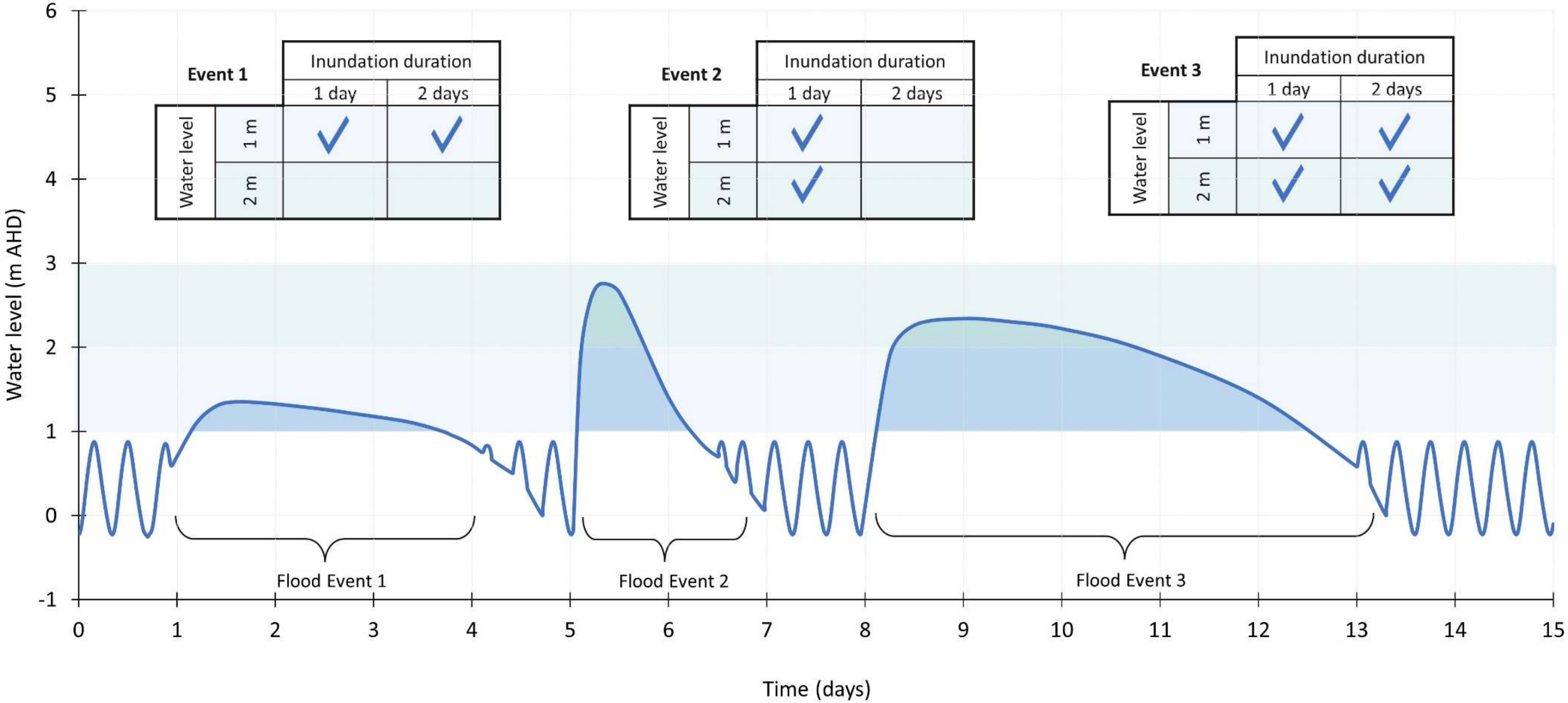

Figure 2. A conceptual hydrograph depicts three different flood events to highlight the blackwater potential risks for each event. At a floodplain elevation of 1m AHD, all floods contribute to the blackwater risk but for different inundation periods. At an elevation of 2m AHD, only flood events 2 and 3 would contribute blackwater. Flooding that persists over a broader area and a longer period (Flood Event 3) has a higher likelihood of producing larger volumes of blackwater.

Based on the conceptual model depicted in Figure 2, inundation risk matrices can be established at each water level gauge by identifying the historic frequency at which various combinations of inundation depth and duration have been exceeded. As such, the inundation duration was calculated at 0.1m increments in water level between 0.1m and 5.0m AHD. This covers the range of water levels and topographic elevations typical of estuarine floodplains. Additionally, as the tidal cycle will restrict discharges from the floodplain drainage systems during flood events, the long-term average mean high water (MHW) level (as documented by Fitzhenry, Alley, Hesse, and Couriel (2012)) was adopted as the minimum floodplain inundation level at each gauge location.

Within the estuaries of NSW, recorded flooding events rarely exceed five days. As the critical duration of inundation for the generation of blackwater may be achieved during floods with a duration of less than one day, event durations between one and five days were adopted for the inundation matrices. For each day a flood event exceeded any particular water level, it was assumed to contribute to the blackwater risk for that duration. This ensured that longer duration events contributed more blackwater risk than events of short duration, although the matrix could be extended to incorporate additional flood durations for estuaries regularly subject to longer floods.

To maximise the available data and account for any differences in the data record at each gauge, the full data record was analysed for each water level monitoring station. These results were then normalised by the length of the data record to calculate the average recurrence interval of each incremental inundation level at each gauge location.

2.2 Aggregated blackwater risk assessment

For each catchment, a blackwater contribution factor was calculated using spatial analysis tools within Geographic Information System (GIS) over a 5m square grid. This information was used to determine the area inundated and the land-use risk factor associated with that area for every 0.1m increment in water level (as illustrated in Figure 3). The blackwater contribution factor corresponding to the water level was then calculated for all combinations of inundation duration and frequency. A statistical mean of the factors calculated from the matrix of inundation levels affecting each catchment was adopted as the aggregated blackwater risk factor for that catchment. This factor was then used to rank the catchments according to their relative potential to generate blackwater.

2.3 Study area

The methodology described in Section 2 was applied to seven major estuaries within NSW, including (from north to south, as indicated in Figure 4):

- Tweed River;
- Richmond River;
- Clarence River;
- Macleay River;
- Hastings River;
- Manning River; and
- Shoalhaven River.

Each selected estuary has been previously identified as blackwater pollution sites resulting from the clearing and drainage of coastal wetlands (Fletcher and Fisk, 2017). In particular, the Richmond River has been the focus of detailed investigations into the causes of blackwater events that resulted in mass fish kills.

Details of government water level gauges used in this assessment are identified in the Supplementary Material, including gauge locations and historic flow distribution curves.

3 Results

The calculated aggregated blackwater risk factors provide an objective, data-driven evidence base to identify which catchments present the highest potential risk of generating blackwater. The ranking of catchments based on blackwater risk can be used to inform and prioritise floodplain management options. Ongoing and future monitoring programs may be optimised and used to further validate and refine the assessment methodology.

The risk factors and catchment ranking within each estuary are tabulated with a statistical analysis of the corresponding historic water levels in the Supplementary Material. Maps indicating the distribution of blackwater risk are also provided, with sample results for the Richmond River presented in Figure 5. These maps incorporate the median extent of

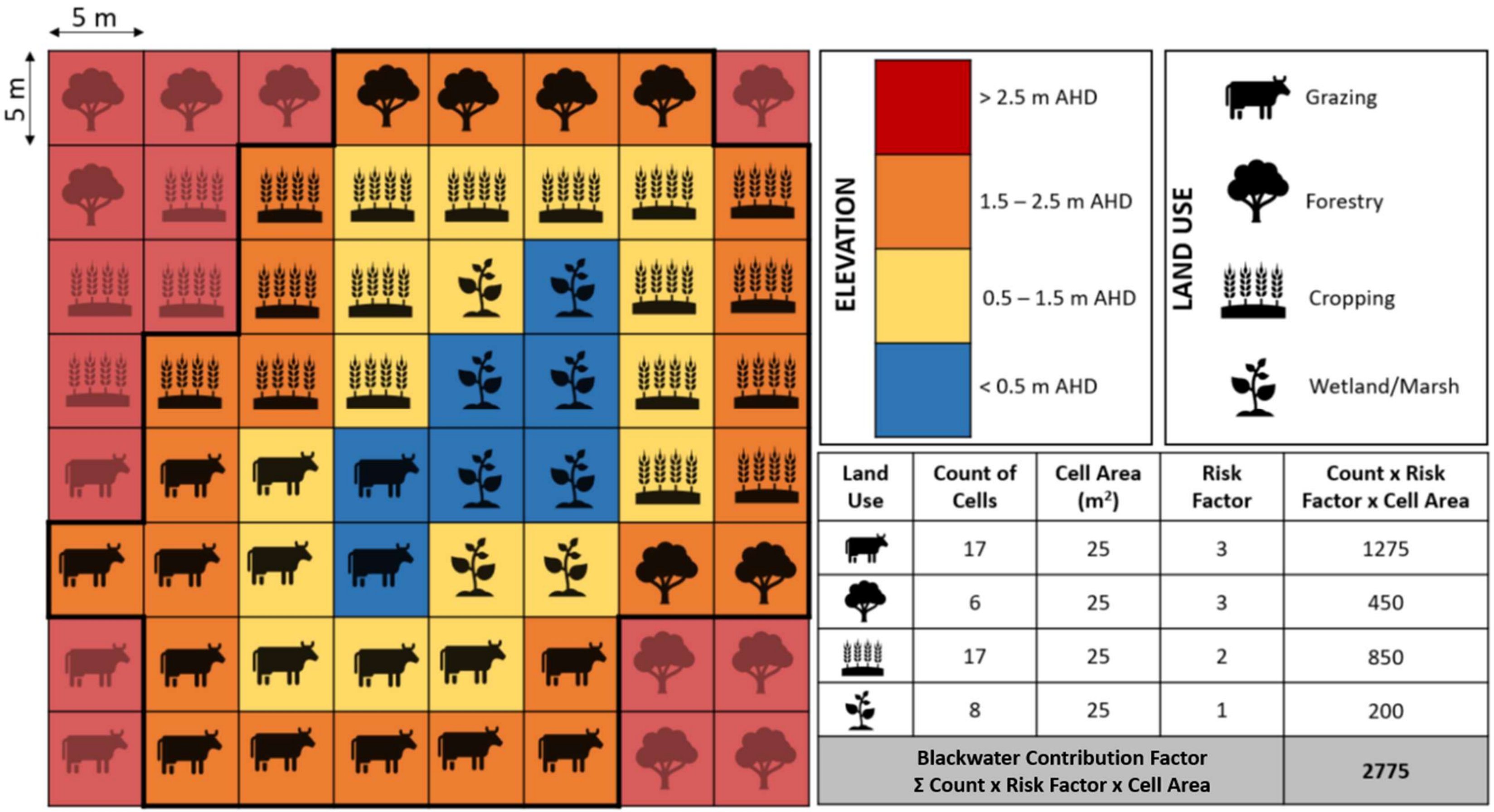

Land Use	Count of Cells	Cell Area (m^2)	Risk Factor	Count x Risk Factor x Cell Area
	17	25	3	1275
	6	25	3	450
	17	25	2	850
	8	25	1	200
Blackwater Contribution Factor Σ Count x Risk Factor x Cell Area				**2775**

Figure 3. An example calculation of a catchment blackwater contribution factor for an inundation level of 2.5 m AHD. The coloured matrix depicts the land-use type and elevation. The number of each land-use cells multiplied by the area and risk factor summed for the catchment is the blackwater contribution factor for that catchment. Within an estuary, multiple catchments were calculated to rank priority risk areas.

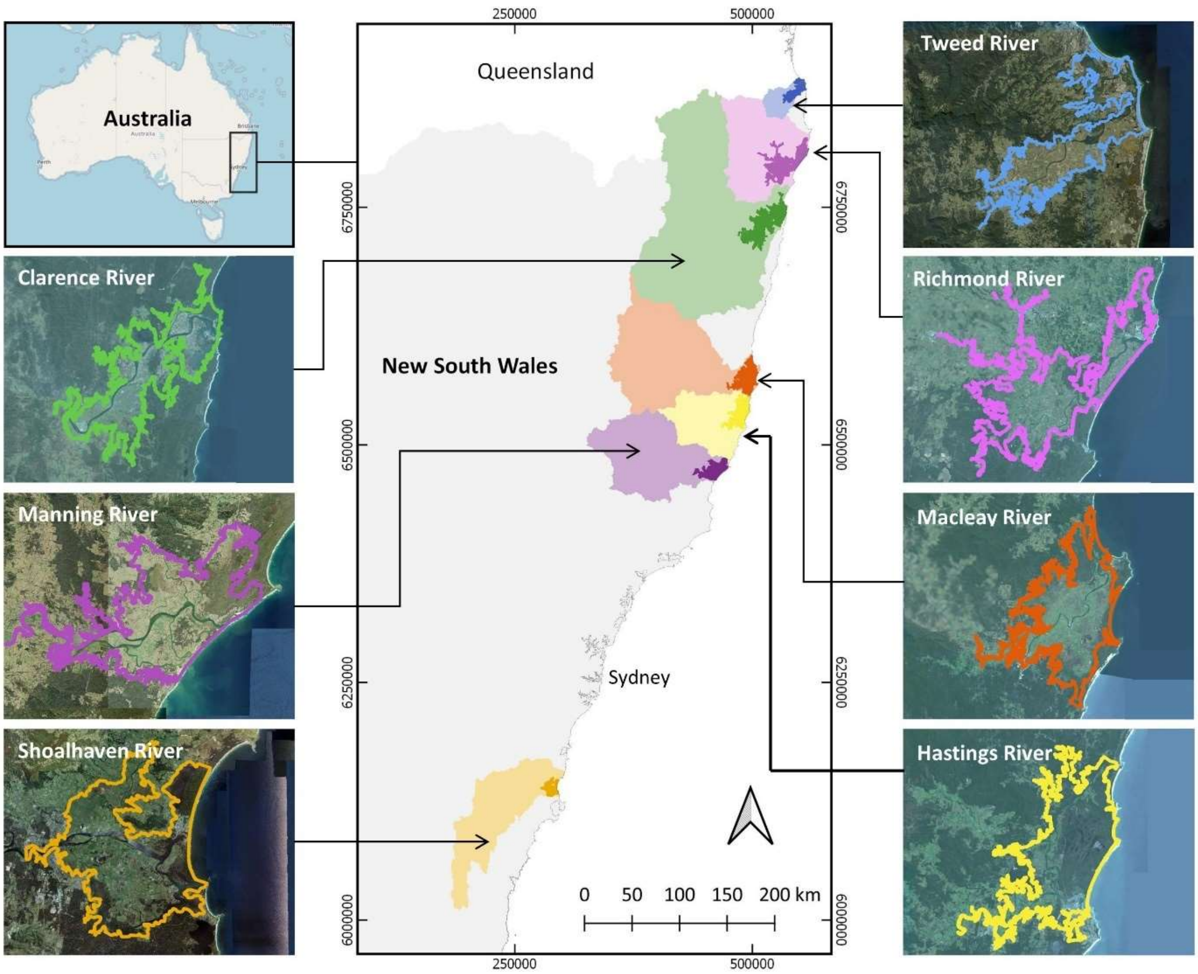

Figure 4. Selected estuaries (shaded) and estuarine floodplain areas below 5m AHD (outlined) defining the study area.

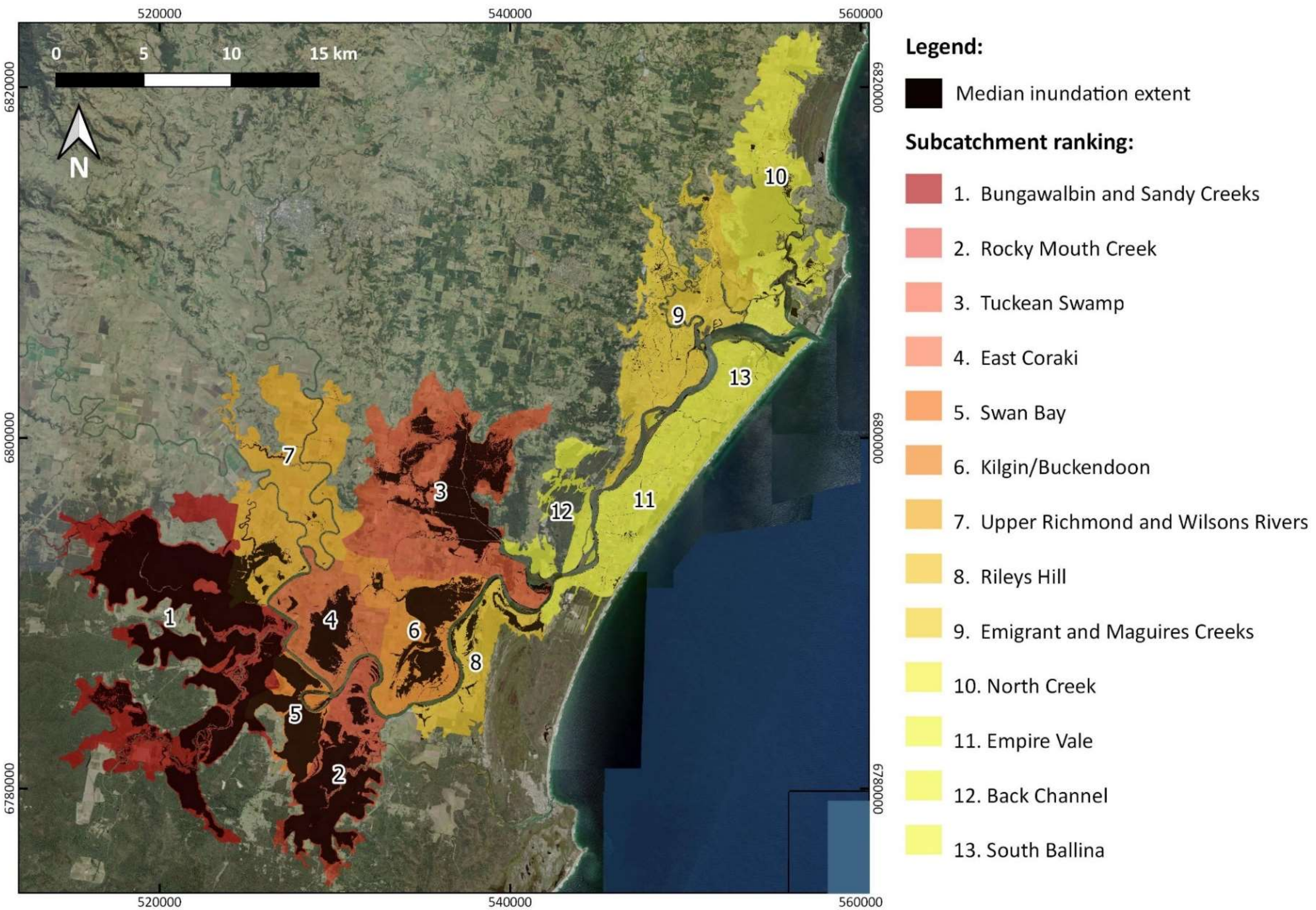

Figure 5. Ranking of catchments by aggregated blackwater risk factor and extent of inundation under median water levels for the Richmond River estuary (maps of results for all estuaries within the study area are included in the Supplementary Material).

inundation corresponding to the historic water levels in the estuary to provide an indication of the areal extent of potential blackwater generation within each catchment.

3.1 Validation of results

In the Richmond River the highest risk catchments were identified as Bungawalbyn and Sandy Creeks (ranked 1), Rocky Mouth Creek (ranked 2), and the Tuckean Swamp (ranked 3). These results correlate well with several previous scientific investigations and help to validate the assessment outcomes. Exceptionally low oxygen levels were previously recorded at Bungawalbyn and Rocky Mouth Creeks following the February 2001 flood (Eyre et al., 2006). Similarly, Wong et al. (2010) identified the Tuckean, Bungawalbyn, Sandy and Rocky Mouth Creek catchments as primary sources of DOP following the January 2008 flood. The same three catchments were attributed the highest risk of blackwater generation and impact by an expert panel under the Richmond Estuary Ecosystem Health Monitoring Strategy (Moore, 2006) and identified as the three top priority areas for blackwater management within the Richmond River floodplain by a collaborative Australian Research Council project (Southern Cross GeoScience, 2019). The latter study prioritised lower Bungawalbyn Creek as the largest blackwater generator on the floodplain.

The validity of the blackwater risk methodology is strengthened by a review of water quality, fish and crustacean mortality data undertaken by Walsh et al. (2004) following major flooding in February and March 2001. This investigation also identified blackwater risk areas within the Richmond River as Rocky Mouth Creek, Bungawalbyn Creek and Tuckean Swamp. Additionally, Walsh et al. (2004) prioritised the Coldstream River (ranked 1 under this study's methodology) and Everlasting Swamp (in the Sportsmans Creek catchment, ranked 2) in the Clarence River, and Belmore Swamp (ranked 2), the Swan Pool (Kinchela Creek, ranked 1) and Seven Oaks wetland (Collombatti-Clybucca, ranked 3) in the Macleay River, further supporting this study's methodology.

3.2 Limitations of methodology

3.2.1 Land use, ambient and antecedent conditions

Due to the relative homogeneity of land-use across the study area, the catchment rankings presented herein are highly influenced by the catchment size and inundation extent. The

Spearman's rank correlation between the aggregated blackwater risk factor and the area flooded at the median inundation level varied from 0.82 to 0.97 throughout each estuary, with the exception of the Shoalhaven River, where it was 0.55. Within the Shoalhaven River, the largest discrepancy was within the Comerong Island catchment, where over 12% of the land area is below the median inundation level but does not contribute to the blackwater risk factor as it is a tidal wetland. Further refinement of the weighting of blackwater risk factors may therefore be required in landscapes with more diverse land uses.

Where land-use is more critical in the assessment of blackwater risk, a weighting factor scaled to BOD may provide greater differentiation than the direct rank-order weighting adopted in this study. Scaled weightings may vary with time of inundation, as indicated by the results of the mesocosm and inundation experiments on which the rank-order weightings were based, (e.g. Liu et al. (2019) and Vithana et al. (2019)). The depth of inundation may also influence the rate of deoxygenation as shallow waters are likely to be warmer (increasing microbial metabolisation rates and reducing oxygen saturation levels) and subject to photochemical deoxygenation processes (Southern Cross GeoScience, 2019).

Indeed, decomposition rates are strongly affected by environmental factors such as temperature, solar radiation, salinity and acidity (Voß, Fernández, & Schäfer, 2015) and BOD has been shown to respond to plant density, shadowing, soil mineralogy and light transmission (Cox, 2003; Voß et al., 2015). Conversely, the bioavailability of organic matter has generally been found to respond more directly to land management practices, such as chemical and nutrient application, harvesting practices and stocking rates (Voß et al., 2015). Thus the potential for blackwater generation over various catchment areas may alternatively be differentiated by assessing variations in land management (both historic and current) and intensity of use (Barlow, Christy, & Weeks, 2009; Buck, Niyogi, & Townsend, 2004) rather than vegetation types or land-use categories, as the accumulation of surface litter is likely to drive the majority of oxygen demand in many environments (Mehring et al., 2014).

Similarly, seasonal changes and antecedent conditions will also impact the potential BOD. By reviewing antecedent weather conditions in the Richmond River, Wong, Walsh, and Morris (2018) found that fish kills were more common when the previous six months had been drier than usual prior to the blackwater flooding event. Conversely, wetter than average conditions are likely to reduce the amount of DOC that is available, thereby lowering the risk of blackwater generation (Hladyz et al., 2011). Antecedent conditions will influence the accumulation of organic matter and the bioavailability of carbon on the floodplain. Vegetation stress due to drought, for example, may increase litterfall (Whitworth et al., 2012), with the accumulation of organic debris increasing as the time between flood events is extended (Wong et al., 2018; Xiong, 1997). The amount of carbon leached from organic matter also reduces when the litter has been previously inundated.

Nevertheless, the spatial and temporal variability of environmental influences on BOD is unlikely to affect the intrinsic risk across a catchment or estuary within the study area presented in this assessment (refer to Supplementary Material). Indeed, current literature suggests that various vegetation and land cover types all have the ability to deoxygenate a waterbody (Kobayashi et al., 2009; Liu et al., 2019; O'Connell, Baldwin, Robertson, & Rees, 2000). Under equivalent environmental conditions, it would therefore be the extent and duration of inundation throughout a catchment which provides the greatest risk differential for blackwater generation.

3.2.2 Water level data

The accuracy of the assessment with respect to inundation characteristics relies on the suitability of the water level data available. In this regard, the results for the Shoalhaven River may also have been adversely affected by the limited distribution of water level data within major tributaries of the estuary. No gauges are located within the estuarine reaches of Broughton Creek, while water levels on the Crookhaven River are only recorded at the downstream limits of the estuary (refer to Supplementary Material). As the inundation extents were estimated by a direct extrapolation of the estuarine water levels, it is important to obtain a representative distribution of flood conditions throughout the estuary. If the adopted water levels are lower than those typically experienced at any catchment (as may occur when upstream water levels are poorly represented), the inundated area, and corresponding aggregated blackwater risk factor, will be underestimated.

4 Discussion

4.1 Floodplain inundation characteristics

Results from the catchment rankings provide insights into the influence of estuarine hydrodynamics on the blackwater risk profiles. For example, in the Tweed River the median extent of inundation over the Stotts Creek catchment (3.9km^2) exceeds that experienced in the Condong catchment (2.2km^2), yet Condong presents a higher overall blackwater risk than Stotts Creek (Figure 5). This reflects the differences in catchment size and topography as well as the water surface elevations.

As illustrated in Figure 6, Stotts Creek presents a relatively flat, low-lying floodplain below the local median inundation level of 0.7m AHD. However, the topography rises steeply, with limited additional catchment area contributing to potential blackwater generation at higher water levels. Conversely, the Condong catchment would produce limited volumes of blackwater until the surface water levels exceed 0.5m AHD. Once inundation levels reach 1.2m AHD, the area contributing to blackwater generation in the Condong catchment would exceed the Stotts Creek catchment and the risk factor would increase accordingly. At higher inundation levels (experienced during more significant, but less frequent rainfall events), the large potential volumetric contribution of blackwater from the Condong catchment outweighs that of the Stotts Creek catchment. In general, both greater topographic exposure and higher inundation levels increase the overall blackwater risk presented by any particular catchment to the receiving estuary.

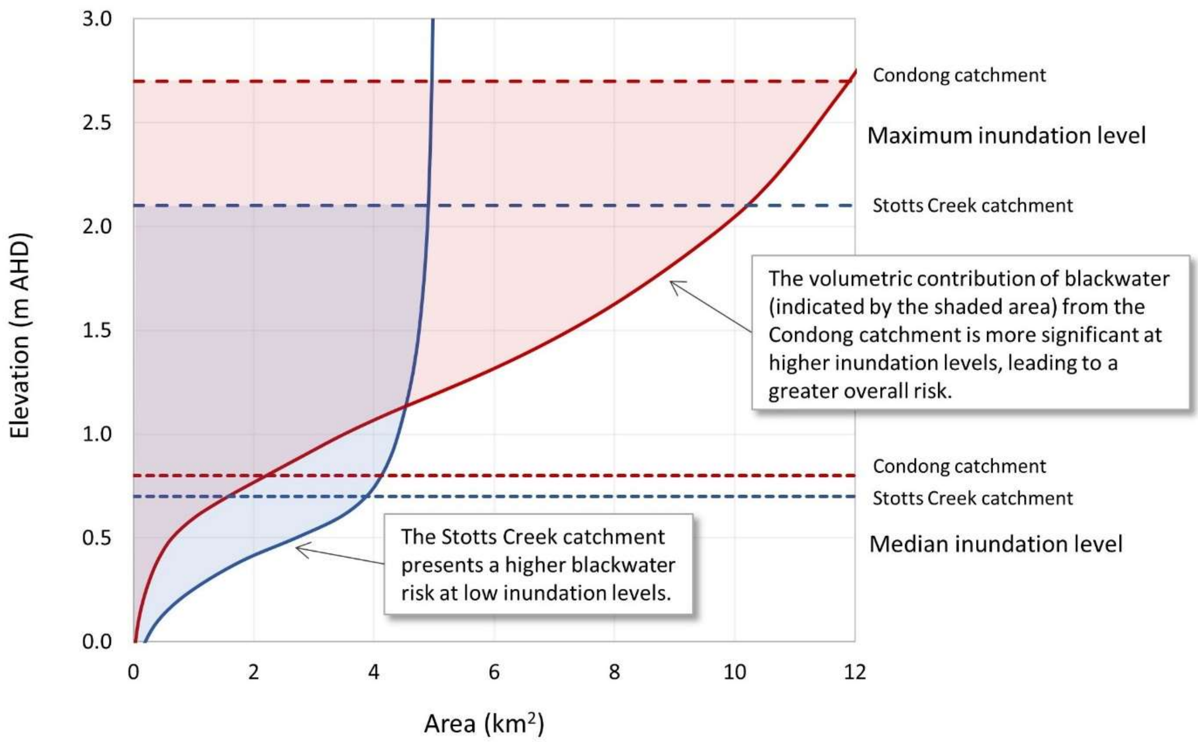

Figure 6. Hypsographic graph of the Stotts Creek (blue) and Condong (red) catchments in the Tweed River estuary, illustrating the changing risk profiles based on inundation levels.

Comparing the Stotts Creek and Condong catchments (Figure 6) also highlights the sensitivity of the method to the duration and frequency of flood events. This was further investigated by modifying the inundation matrix to assess the aggregated blackwater risk factor. Removing the 1 and 2 day inundation durations from the aggregated blackwater risk assessment matrix reduced the overall inundation levels, as lower water levels are experienced during the rising and falling limbs of a flood hydrograph. Conversely, limiting the analysis to flood events with a recurrence interval of 2 to 5 years or 3 to 5 years typically increased the median inundation levels as fewer minor events were included in the statistics. Importantly, the relative risk remained consistent throughout this sensitivity analysis, with Spearman's rank correlation remaining above 0.9 in all estuaries except the Shoalhaven River (detailed in the Supplementary Material). Notably, the ranking of catchments within the Shoalhaven River was more sensitive to the influence of shorter duration events, although the correlation between the top five ranked catchments remained above 0.9 in all analyses.

The robustness of the assessment to variations in the flood duration and recurrence interval reflects the consistency of the hydrodynamic response to flood events throughout each estuary. As illustrated in Figure 7, peak flood levels are typically highest in the upper estuary, where water levels rise rapidly and remain high due to restricted drainage from elevated tailwaters in the mid- and lower portions of the estuary. Flood profiles in the lower estuary are further moderated as the hydraulic energy and flow volumes are dispersed over the low-lying floodplains. Additionally, in the lower estuary water levels are less affected by flood flows as offshore waters can assimilate large flood volumes. These effects are exemplified in the comparison between the Condong (located in the upper estuary and subject to higher inundation levels) and Stotts Creek (mid-estuary) catchments (Figure 6).

Based on these spatial differences in drainage across an estuary, the free-draining lower reaches of an estuary typically have a lower risk of blackwater generation. The environmental impacts of blackwater discharged from these downstream catchments may also be mitigated by high tidal flushing and reduced residence times due to their proximity to the ocean (Johnston et al., 2003; Rabalais et al., 2002). To this aim, Eyre and Twigg (1997) indicated that dissolved oxygen levels were higher in parts of the estuary with higher salinity (or increased tidal flushing) for the first seven weeks after the flood event. In contrast, the upper estuary is likely to have a higher blackwater risk as residence times may be prolonged (i.e. any blackwater released would remain in the estuary for extended periods) and flood levels tend to remain elevated for longer periods (i.e. any blackwater generated may discharge into an estuary with less assimilation capacity).

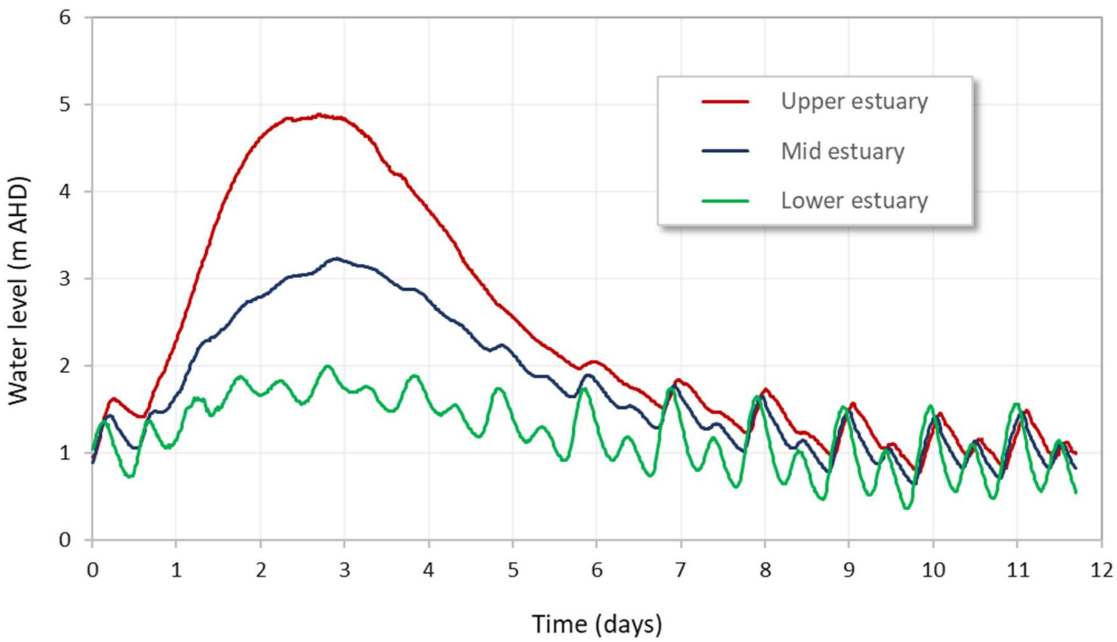

Figure 7. Spatial illustration of typical water level response to a flood in the lower, mid and upper reaches of an estuary from an event recorded in the Richmond River in June 2005. The upper estuary was measured at Coraki (refer to Supplementary Material for gauge locations) and represents conditions for the Upper Richmond and Wilsons River catchments (Figure 5). The mid estuary was measured at Woodburn (Rocky Mouth Creek catchment) and the lower estuary at Wardell (Empire Vale and Back Channel catchments.

As inundation levels and inundation durations are often spatially correlated within an estuary, the risk factors for blackwater generation and impact may be simplified to the estuarine water levels, floodplain geomorphology, and the potential for BOD generation. These primary factors are conceptualised in Figure 8 for an idealised system. Based on these factors, a catchment may present a higher risk of blackwater generation and impact if:

- it is located in a portion of the estuary where floodwaters are maintained at higher levels and/or for longer durations (Figure 8(a));
- the topography contains an extensive, low-lying floodplain that can accommodate large volumes of floodwater (Figure 8(b)); and/or
- the land use and environmental characteristics have a higher potential to generate BOD (Figure 8(c)).

The environmental impact of blackwater in an estuary is then determined by the floodplain connectivity with the estuary and the discharge characteristics of the catchment drainage system (Figure 8(d)). Modern drainage systems facilitate the rapid transfer of DOP to the estuary, with substantial volumes of blackwater discharged as the flood recedes (Figure 8(a)). These discharges can be particularly harmful when there is limited assimilative capacity in the estuary. The impact from any individual catchment discharge is also affected by discharges from nearby catchments as individual blackwater plumes can intermix. The dilution capacity and potential environmental impacts from these blackwater plumes are highlighted in Figure 9.

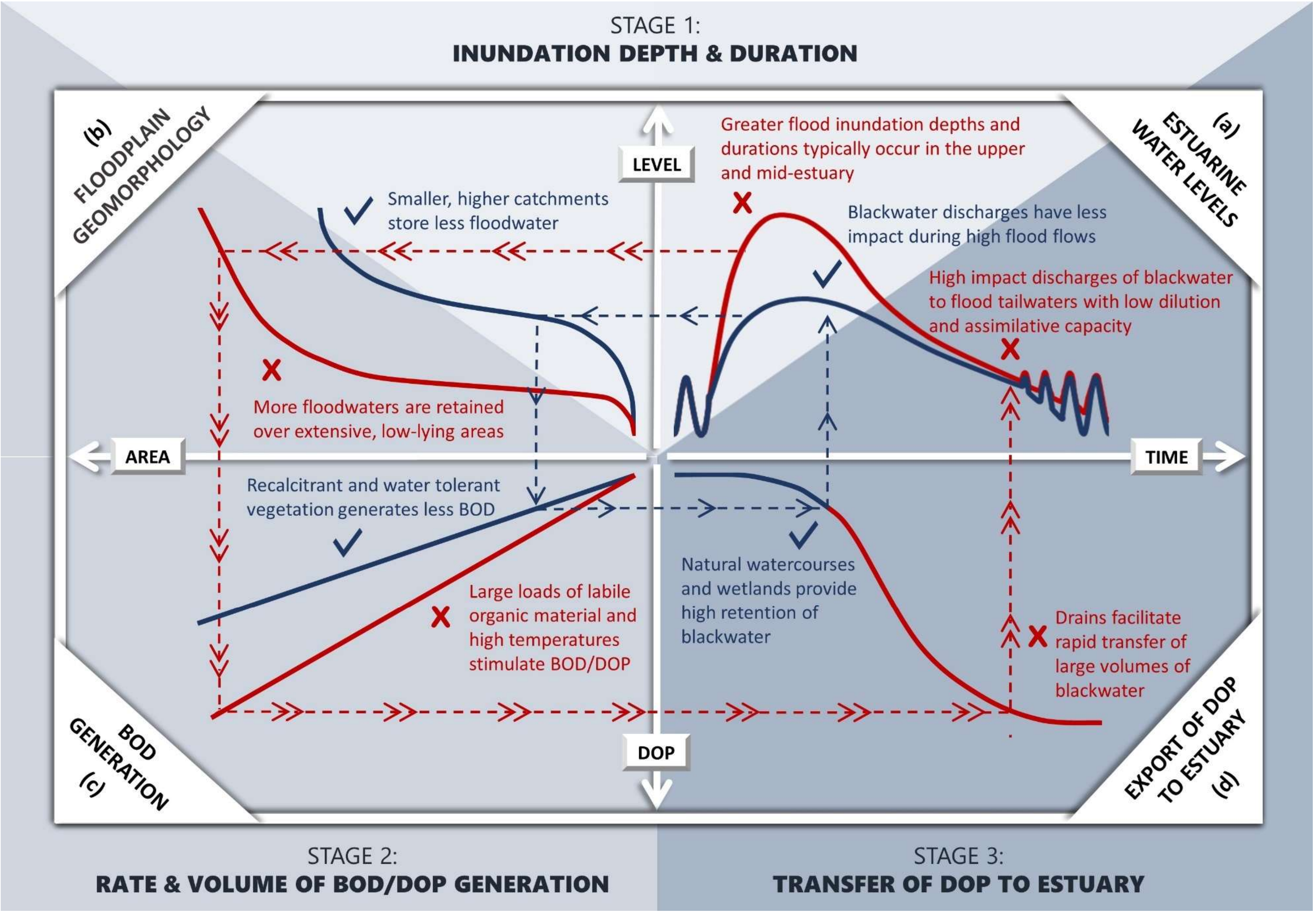
STAGE 1:
INUNDATION DEPTH & DURATION
(a) ESTUARINE WATER LEVELS
(b) FLOODPLAIN GEOMORPHOLOGY
(c) BOD GENERATION
(d) EXPORT OF DOP TO ESTUARY
LEVEL
AREA
TIME
DOP
Greater flood inundation depths and durations typically occur in the upper and mid-estuary
Blackwater discharges have less impact during high flood flows
High impact discharges of blackwater to flood tailwaters with low dilution and assimilative capacity
Smaller, higher catchments store less floodwater
More floodwaters are retained over extensive, low-lying areas
Recalcitrant and water tolerant vegetation generates less BOD
Large loads of labile organic material and high temperatures stimulate BOD/DOP
Natural watercourses and wetlands provide high retention of blackwater
Drains facilitate rapid transfer of large volumes of blackwater
STAGE 2:
RATE & VOLUME OF BOD/DOP GENERATION
STAGE 3:
TRANSFER OF DOP TO ESTUARY

Figure 8. Conceptual diagram of the key risk factors for blackwater generation on an estuarine floodplain. The diagram should be read counter clockwise from the top right corner. A high-risk scenario is realised by following the progression of a blackwater event via the red arrows from Stages 1 to 3. Commencing in quadrant (**a**), high flood levels in the estuary lead to extensive inundation (**b**) during Stage 1. Increased biochemical oxygen demand (BOD) generated at Stage 2 (**c**) will result in a high deoxygenation potential (DOP). The greatest impacts occur when the blackwater discharges at Stage 3 (**d**) overwhelm the assimilative capacity of the receiving waters (a). An alternative low risk scenario is proposed via the blue arrows.

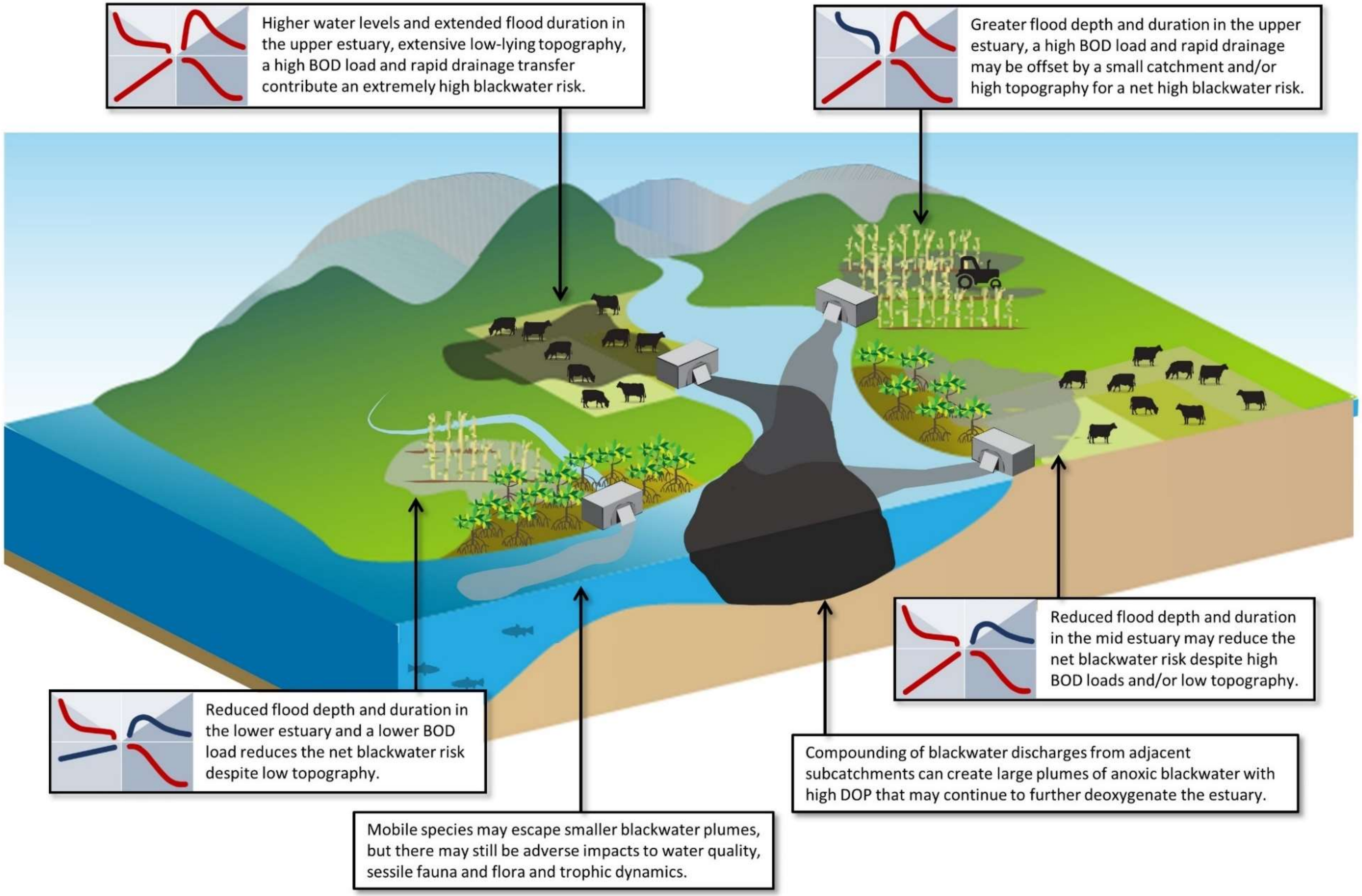
Higher water levels and extended flood duration in the upper estuary, extensive low-lying topography, a high BOD load and rapid drainage transfer contribute an extremely high blackwater risk.
Greater flood depth and duration in the upper estuary, a high BOD load and rapid drainage may be offset by a small catchment and/or high topography for a net high blackwater risk.
Reduced flood depth and duration in the mid estuary may reduce the net blackwater risk despite high BOD loads and/or low topography.
Reduced flood depth and duration in the lower estuary and a lower BOD load reduces the net blackwater risk despite low topography.
Compounding of blackwater discharges from adjacent subcatchments can create large plumes of anoxic blackwater with high DOP that may continue to further deoxygenate the estuary.
Mobile species may escape smaller blackwater plumes, but there may still be adverse impacts to water quality, sessile fauna and flora and trophic dynamics.

558

Figure 9. Conceptual diagram of common blackwater risk factors and compounding discharges within an estuary. The risk from each drainage catchment is described with reference to the four risk factors illustrated in Figure 8.

4.2 Spatial distribution of floodplain drainage

Impacts of compounding blackwater plumes are typified by the blackwater risk profiles of the Clarence and Richmond Rivers. The inundation extent at the median inundation level for the Clarence River (285 km^2) is more than twice the Richmond River (137 km^2). However, the impact of blackwater events in the Richmond River has been more severe, with extensive fish kills regularly reported after comparable flood events (Walsh et al., 2004). This has previously been attributed to the substantially larger river discharges and assimilation capacity of the Clarence River, which also provides opportunities for fish to seek refuge in the less affected parts of the estuary (Walsh et al., 2004).

Results from the aggregated blackwater risk analysis indicate that the highest ranked sub-catchments in the Clarence River discharge to different parts of the estuary. As such, blackwater discharges are likely to impact the estuary at different stages of a flood event. In comparison, the Richmond River has four of the five highest ranking sub-catchments discharging into the estuary within a 20km reach. With such close proximity, these individual plumes are likely to intermix, resulting in compounding impacts that are more likely to overwhelm the assimilation capacity of the estuary. These potential compounding impacts are illustrated in Figure 9.

4.3 Climate change impacts

Investigating the sensitivity of spatial and temporal factors on blackwater generation also provides insights into how climate change may influence future blackwater conditions. Climate change has been predicted to increase temperatures (Masson-Delmotte et al., 2021), and create more intense and sporadic rainfall conditions (Dey, Lewis, Arblaster, & Abram, 2019). These impacts are expected to exacerbate hypoxic blackwater events (Carstensen et al., 2014; Godinho et al., 2019; Koehn, 2022; Vaquer-Sunyer & Duarte, 2008), with larger floods increasing the spatial and temporal inundation patterns, while warmer conditions may increase the microbial reaction rates (Wong et al., 2010). Changes in flood frequency and meteorological conditions may also encourage the accumulation of organic matter between floods providing high BOD potential.

In estuarine environments these effects will be further compounded by sea level rise, which is expected to increase standing water levels and reduce drainage (Waddington et al., 2022).

Higher downstream water levels may lead to increased spatial inundation, while reduced drainage will extend the temporal inundation. Overall, both factors will likely increase blackwater generation risk.

The potential for blackwater generation from sea level rise was investigated by examining the projected increase in area inundated for incremental increases in water levels across the floodplain sub-catchments. Unsurprisingly, the larger Clarence, Richmond and Macleay River systems, which already suffer the highest rate of fish mortality from blackwater events, would experience the greatest increases under rising sea levels. Normalising the increase in area inundated by the total catchment area (Figure 10(a)) indicates that the future risk of blackwater creation in the Tweed River is likely to be substantially higher than in other estuaries. This is primarily attributable to the topography of the Tweed River floodplain, where there is a greater increase in the area inundated by higher water levels.

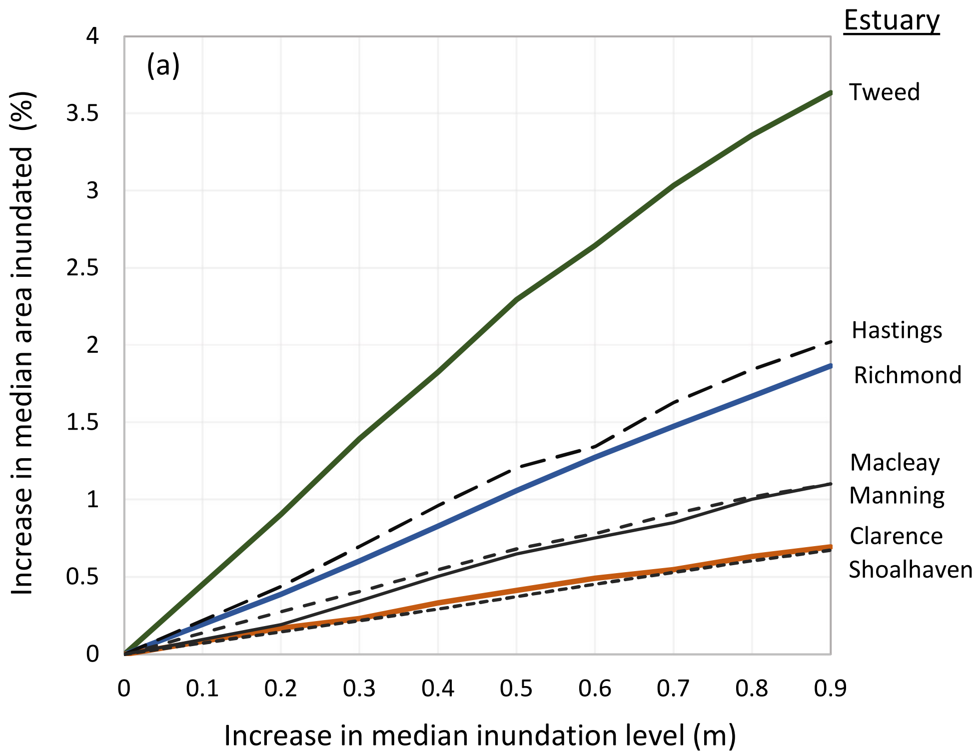

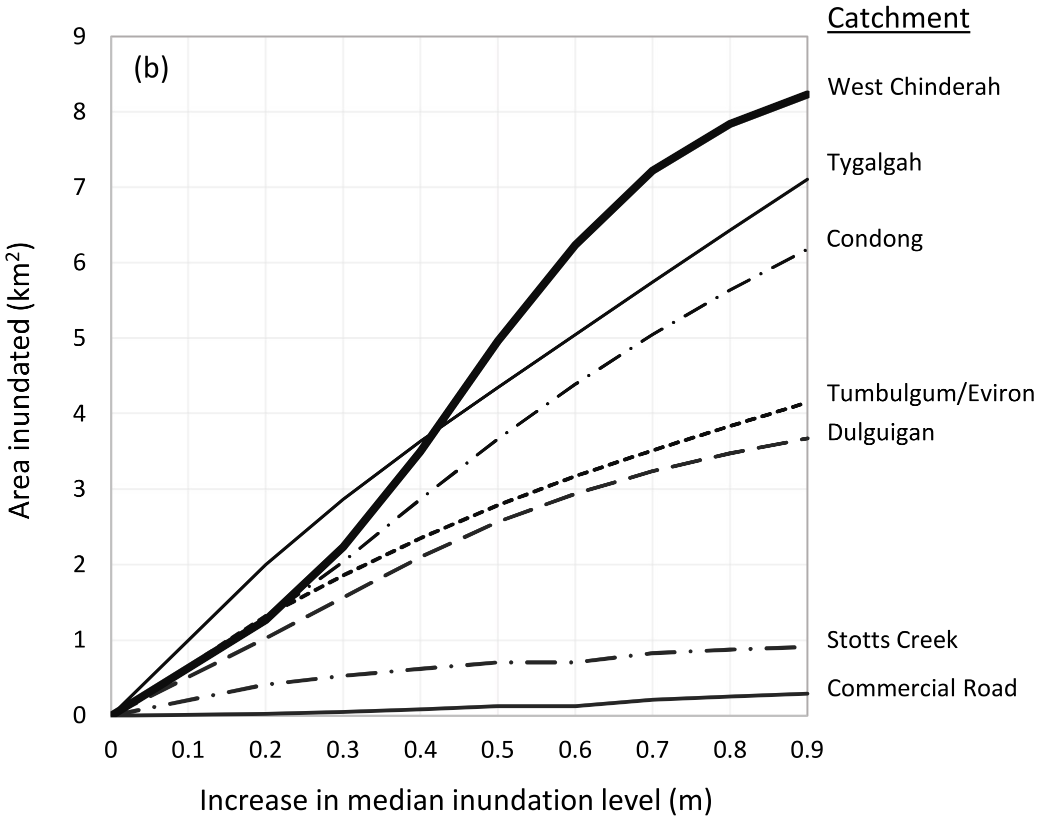

Figure 10. The (**a**) increase in median area inundated after an incremental rise in water level expressed as a percentage of the total catchment area. Within any given estuary (the Tweed River is used as an example here) the sub-catchments most extensively inundated and the locations discharging the most blackwater may change (**b**).

This analysis can be further extended to identify which catchments within a particular estuary present an increased risk of blackwater generation under existing or future conditions. For example, while the West Chinderah catchment of the Tweed River estuary currently presents a relatively moderate risk, the potential for blackwater generation may increase exponentially once the median inundation level rises by approximately 0.3m (Figure 10(c)).

4.4 Management and mitigation of blackwater risk

The improved understanding of estuarine blackwater events, as provided by this assessment, enables a nuanced assessment of potential mitigation measures. In areas identified as low risk for blackwater generation, minor changes to land management may mitigate blackwater generation by reducing the bioavailability of carbon. For example, the removal of cuttings from slashed pastures has been suggested as an effective means of reducing the DOP of grazing lands (Eyre et al., 2006). Alternatively, mechanical oxygenation has been employed to mitigate blackwater impacts in the Swan and Canning Rivers of Western Australia (Greenop, Lovatt, & Robb, 2001), although this is generally regarded as an emergency response measure as it is substantially limited by the area that can be serviced and operational costs (Baldwin, Boys, Rohlfs, Ellis, & Pera, 2022).

As the potential for blackwater generation increases, the impact of effective mitigation measures on current land uses is also likely to increase. Where the median inundation level is relatively shallow, the depth and density of floodplain drains may be reduced to encourage the growth of water-tolerant vegetation and facilitate reaeration of the water column (Hamilton et al., 1997; Rixen et al., 2008). However, in areas subject to prolonged, deep inundation, reaeration will be hampered by the lower ratio of the air-water interface to flood volume and there is likely to be greater plant morbidity and contribution to BOD. Such conditions are typified in the low energy backswamp environments, which may be best suited to reinstatement into natural wetland systems. Indeed, tidal restoration and the reinstatement of coastal and floodplain wetlands has been identified as the preferred management measure for the mitigation of blackwater events in the coastal estuaries of NSW (Moore, 2006).

Social and economic ramifications accompanying land-use change may be significant due to the level of development throughout the floodplains (Moore, 2006; Southern Cross GeoScience, 2019). Identification of areas at highest risk of backwater generation (as discussed in this paper) is recommended to support trials and further investigations into these options. This will ensure that decisions to reinstate wetland systems are evidence-based and transparent, optimising water quality benefits and ongoing floodplain productivity.

5 Conclusion

Hypoxic blackwater events occur worldwide and affect both inland and coastal waters. The mechanisms underpinning these events are associated with the microbial metabolisation of carbon and the accumulation/discharge of deoxygenated water during and post flood events. This paper presents a methodology developed to prioritise catchments within an estuarine floodplain based on their potential to generate hypoxic blackwater and to identify those catchments from which blackwater discharges are likely to have the most significant impact on the estuary. Local topography and changes to the flood hydrograph as it progresses along an estuary are shown to influence the extent and duration of inundation over the floodplain. In turn, inundation characteristics are identified as critical factors in determining the volume of blackwater generated and the DOP discharged to the receiving waters. Concerns related to increased blackwater generation from climate change, and sea level rise in particular, are highlighted.

It is anticipated that this research will be used to inform evidence-based decision making to manage catchment risks to water quality. This may enable a strategic approach to future investments in floodplain and estuarine research and management measures to optimise economic, social and environmental outcomes.

Acknowledgements

The blackwater risk assessment methodology presented herein was developed with funding from the New South Wales Marine Estate Management Strategy (MEMS). Katrina Waddington was supported by a scholarship jointly funded by UNSW Sydney and MEMS. The authors would like to thank Anna Blacka from UNSW Sydney for her assistance with the preparation of figures. We also thank Danial Khojasteh for his constructive comments which helped us to greatly improve this manuscript.

Declaration

The authors declare that they have no known competeing financial interests or personal relationships that could have appeared to influence the work reported in this paper.

Data availability statement

Water level data was sourced from the NSW Water Level Data Collection Program (MHL, 2023) available at https://mhl.nsw.gov.au/Data-Level. Land-use mapping was based on the Australian Land Use and Management (ALUM) classification (DPIE, 2020). Climate (monthly temperature) data presented in the Supplementary Material was downloaded from the Climate Data Online service of the Australia Bureau of Meteorology website Climate Data Online - Map search (bom.gov.au). Mapping was undertaken using the QGIS software, which can be freely downloaded from Discover QGIS. Digital elevation data (Geoscience Australia,

2018) was obtained from the National Elevation Data Framework spatial dataset Elvis (fsdf.org.au) managed by Geoscience Australia Digital Elevation Data | Geoscience Australia (ga.gov.au).

References

Amiri, B. J., & Nakane, K. (2008). Entire catchment and buffer zone approaches to modeling linkage between river water quality and land cover—A case study of Yamaguchi Prefecture, Japan. *Chinese Geographical Science, 18*(1), 85-92. doi:10.1007/s11769-008-0085-6

Arellano, A., Bianchi, T. S., Osburn, C., D'Sa, E., Ward, N. D., Oviedo-Vargas, D., . . . Kurian, G. (2019). Mechanisms of Organic Matter Export in Estuaries with Contrasting Carbon Sources. *Journal of Geophysical Research: Biogeosciences, 124*(10), 3168-3188.

Baldwin, D. S., Boys, C. A., Rohlfs, A.-M., Ellis, I., & Pera, J. (2022). Field trials to determine the efficacy of aerators to mitigate hypoxia in inland waterways. *Marine and Freshwater Research, 73*(2), 211-222. doi:https://doi.org/10.1071/MF20365

Barlow, K., Christy, B., & Weeks, A. (2009). *Nutrient generation and transport at the catchment scale.* Paper presented at the 18th World IMACS Congress and MODSIM09 International Congress on Modelling and Simulation.

Bonvillain, C. P., Halloran, B. T., Boswell, K. M., Kelso, W. E., Harlan, A. R., & Rutherford, D. A. (2011). Acute Physicochemical Effects in a Large River-Floodplain System Associated with the Passage of Hurricane Gustav. *Wetlands, 31*(5), 979. doi:10.1007/s13157-011-0213-4

Breitburg, D., Levin, L. A., Oschlies, A., Grégoire, M., Chavez, F. P., Conley, D. J., . . . Zhang, J. (2018). Declining oxygen in the global ocean and coastal waters. *Science, 359*(6371), eaam7240. doi:doi:10.1126/science.aam7240

Buck, O., Niyogi, D. K., & Townsend, C. R. (2004). Scale-dependence of land use effects on water quality of streams in agricultural catchments. *Environmental Pollution, 130*(2), 287-299. doi:https://doi.org/10.1016/j.envpol.2003.10.018

Carney, R. L., Mitrovic, S. M., Jeffries, T., Westhorpe, D., Curlevski, N., & Seymour, J. R. (2015). River bacterioplankton community responses to a high inflow event. *Aquatic Microbial Ecology, 75*(3), 187-205.

Carstensen, J., Andersen, J. H., Gustafsson, B. G., & Conley, D. J. (2014). Deoxygenation of the Baltic Sea during the last century. *Proceedings of the National Academy of Sciences, 111*(15), 5628-5633. doi:doi:10.1073/pnas.1323156111

Cloern, J. E., Schraga, T. S., Nejad, E., & Martin, C. (2020). Nutrient Status of San Francisco Bay and Its Management Implications. *Estuaries and Coasts, 43*(6), 1299-1317. doi:10.1007/s12237-020-00737-w

Coble, A. A., Koenig, L. E., Potter, J. D., Parham, L. M., & McDowell, W. H. (2019). Homogenization of dissolved organic matter within a river network occurs in the smallest headwaters. *Biogeochemistry, 143*(1), 85-104.

Conley, D. J. (2012). Save the Baltic Sea. *Nature, 486*(7404), 463-464. doi:10.1038/486463a

Conley, D. J., Carstensen, J., Ærtebjerg, G., Christensen, P. B., Dalsgaard, T., Hansen, J. L. S., & Josefson, A. B. (2007). LONG-TERM CHANGES AND IMPACTS OF HYPOXIA IN DANISH COASTAL WATERS. *Ecological Applications, 17*(sp5), S165-S184. doi:10.1890/05-0766.1

Conley, D. J., Carstensen, J., Aigars, J., Axe, P., Bonsdorff, E., Eremina, T., . . . Zillén, L. (2011). Hypoxia Is Increasing in the Coastal Zone of the Baltic Sea. *Environmental Science & Technology, 45*(16), 6777-6783. doi:10.1021/es201212r

Cox, B. A. (2003). A review of currently available in-stream water-quality models and their applicability for simulating dissolved oxygen in lowland rivers. *Science of The Total Environment, 314-316*, 335-377. doi:https://doi.org/10.1016/S0048-9697(03)00063-9

Dey, R., Lewis, S. C., Arblaster, J. M., & Abram, N. J. (2019). A review of past and projected changes in Australia's rainfall. *WIREs Climate Change, 10*(3), e577. doi:https://doi.org/10.1002/wcc.577

Diaz, R. J. (2001). Overview of Hypoxia around the World. *Journal of environmental quality, 30*(2), 275-281. doi:10.2134/jeq2001.302275x

Diaz, R. J., & Rosenberg, R. (2008). Spreading Dead Zones and Consequences for Marine Ecosystems. *Science, 321*(5891), 926-929. doi:doi:10.1126/science.1156401

Díaz, R. J., & Rosenberg, R. (2011). Introduction to Environmental and Economic Consequences of Hypoxia. *International Journal of Water Resources Development, 27*(1), 71-82. doi:10.1080/07900627.2010.531379

DPIE. (2020). NSW Landuse 2017 Version 1.2. Retrieved from https://datasets.seed.nsw.gov.au/dataset/nsw-landuse-2017-v1p2-f0ed

Eyre, B., & Twigg, C. (1997). Nutrient behaviour during post-flood recovery of the Richmond River Estuary, Northern NSW, Australia. *Estuarine, Coastal and Shelf Science, 44*(3), 311-326.

Eyre, B. D., Kerr, G., & Sullivan, L. A. (2006). Deoxygenation potential of the Richmond River Estuary floodplain, northern NSW, Australia. *River Research and Applications, 22*(9), 981-992. doi:10.1002/rra.950

Fitzhenry, M., Alley, K., Hesse, S., & Couriel, E. (2012). *OEH NSW Tidal Planes Analysis: 1990 - 2010 Harmonic Analysis*. Retrieved from

Geoscience Australia. (2018). Retrieved from https://elevation.fsdf.org.au/

Gibbs, M. S., Wallace, T., & Mosley, L. M. (2022). Constraining organic matter composition and dynamics as a dominant driver of hypoxic blackwater risk during river Murray floodplain inundation. *Hydrological processes, 36*(3), e14529. doi:https://doi.org/10.1002/hyp.14529

Godinho, F. N., Segurado, P., Franco, A., Pinheiro, P., Pádua, J., Rivaes, R., & Ramos, P. (2019). Factors related to fish kill events in Mediterranean reservoirs. *Water Research, 158*, 280-290. doi:https://doi.org/10.1016/j.watres.2019.04.027

Górniak, A. (2017). A new version of the Hydrochemical Dystrophy Index to evaluate dystrophy in lakes. *Ecological Indicators, 78*, 566-573. doi:https://doi.org/10.1016/j.ecolind.2017.03.030

Greenop, B., Lovatt, K., & Robb, M. (2001). The use of artificial oxygenation to reduce nutrient availability in the Canning River, Western Australia. *Water Sci Technol, 43*(9), 133-144.

Hamilton, S. K., Sippel, S. J., Calheiros, D. F., & Melack, J. M. (1997). An anoxic event and other biogeochemical effects of the Pantanal wetland on the Paraguay River. *Limnology and Oceanography, 42*(2), 257-272.

Hitchcock, J. N., Westhorpe, D., Glamore, W., & Mitrovic, S. (2021). Estuarine zooplankton responses to flood pulses and a hypoxic blackwater event.

Hladyz, S., Watkins, S. C., Whitworth, K. L., & Baldwin, D. S. (2011). Flows and hypoxic blackwater events in managed ephemeral river channels. *Journal of Hydrology, 401*(1), 117-125. doi:https://doi.org/10.1016/j.jhydrol.2011.02.014

Howitt, J. A., Baldwin, D. S., Rees, G. N., & Williams, J. L. (2007). Modelling blackwater: Predicting water quality during flooding of lowland river forests. *Ecological Modelling, 203*(3), 229-242. doi:https://doi.org/10.1016/j.ecolmodel.2006.11.017

Johnston, S., Kroon, F., Slavich, P., Cibilic, A., & Bruce, A. (2003). Restoring the balance-guidelines for managing floodgates and drainage systems on coastal floodplains.

Johnston, S. G., Slavich, P. G., & Hirst, P. (2005). Changes in surface water quality after inundation of acid sulfate soils of different vegetation cover. *Soil Research, 43*(1), 1-12. doi:https://doi.org/10.1071/SR04073

Johnston, S. G., Slavich, P. G., Sullivan, L. A., & Hirst, P. (2003). Artificial drainage of floodwaters from sulfidic backswamps: effects on deoxygenation in an Australian estuary. *Marine and Freshwater Research, 54*(6), 781-795. doi:https://doi.org/10.1071/MF02016

Kerr, J. L., Baldwin, D. S., & Whitworth, K. L. (2013). Options for managing hypoxic blackwater events in river systems: A review. *Journal of Environmental Management, 114*, 139-147. doi:https://doi.org/10.1016/j.jenvman.2012.10.013

King, A. J., Tonkin, Z., & Lieshcke, J. (2012). Short-term effects of a prolonged blackwater event on aquatic fauna in the Murray River, Australia: considerations for future events. *Marine and Freshwater Research, 63*(7), 576-586. doi:https://doi.org/10.1071/MF11275

Kobayashi, T., Ryder, D. S., Gordon, G., Shannon, I., Ingleton, T., Carpenter, M., & Jacobs, S. J. (2009). Short-term response of nutrients, carbon and planktonic microbial communities to floodplain wetland inundation. *Aquatic Ecology, 43*(4), 843-858. doi:10.1007/s10452-008-9219-2

Koehn, J. D. (2022). Key steps to improve the assessment, evaluation and management of fish kills: lessons from the Murray–Darling River system, Australia. *Marine and Freshwater Research, 73*(2), 269-281. doi:https://doi.org/10.1071/MF20375

Kragh, T., Martinsen, K. T., Kristensen, E., & Sand-Jensen, K. (2020). From drought to flood: Sudden carbon inflow causes whole-lake anoxia and massive fish kill in a large shallow lake. *Science of The Total Environment, 739*, 140072. doi:https://doi.org/10.1016/j.scitotenv.2020.140072

Lin, C., Wood, M., Haskins, P., Ryffel, T., & Lin, J. (2004). Controls on water acidification and de-oxygenation in an estuarine waterway, eastern Australia. *Estuarine, Coastal and Shelf Science, 61*(1), 55-63.

Liu, X., Watts, R. J., Howitt, J. A., & McCasker, N. (2019). Carbon and nutrient release from experimental inundation of agricultural and forested floodplain soil and vegetation: influence of floodplain land use on the development of hypoxic blackwater during floods. *Marine and Freshwater Research*. doi:10.1071/mf18452

Masson-Delmotte, V., Zhai, P., Priani, A., Connors, S. L., Pean, C., Berger, S., . . . Zhou, B. (2021). *IPCC: Climate Change 2021: The Physical Science Basis. Contribution of Working Group I to the Sixth Assessment Report of the Intergovernmental Panel on Climate Change.* Retrieved from

Mehring, A. S., Kuehn, K. A., Tant, C. J., Pringle, C. M., Lowrance, R. R., & Vellidis, G. (2014). Contribution of surface leaf-litter breakdown and forest composition to benthic oxygen demand and ecosystem respiration in a South Georgia blackwater river. *Freshwater Science, 33*(2), 377-389. doi:10.1086/675507

Meyer, J. L. (1990). A blackwater perspective on riverine ecosystems. *BioScience, 40*(9), 643-651.

MHL. (2023). New South Wales water level data collection program. Retrieved from https://mhl.nsw.gov.au/Data-Level

Moore, A. (2006). Blackwater and fish kills in the Richmond River estuary. Defining the issues - Assessing the risks - Providing management options. *Southern Cross University: Lismore, NSW, Australia*.

Mosley, L. M., Wallace, T., Rahman, J., Roberts, T., & Gibbs, M. (2021). An integrated model to predict and prevent hypoxia in floodplain-river systems. *Journal of Environmental Management, 286*, 112213. doi:https://doi.org/10.1016/j.jenvman.2021.112213

Ning, N. S. P., Petrie, R., Gawne, B., Nielsen, D. L., & Rees, G. N. (2015). Hypoxic blackwater events suppress the emergence of zooplankton from wetland sediments. *Aquatic Sciences, 77*(2), 221-230. doi:10.1007/s00027-014-0382-3

O'Connell, M., Baldwin, D. S., Robertson, A. I., & Rees, G. (2000). Release and bioavailability of dissolved organic matter from floodplain litter: influence of origin and oxygen levels. *Freshwater Biology, 45*(3), 333-342. doi:10.1111/j.1365-2427.2000.00627.x

Paerl, H. W. (2006). Assessing and managing nutrient-enhanced eutrophication in estuarine and coastal waters: Interactive effects of human and climatic perturbations. *Ecological Engineering, 26*(1), 40-54. doi:https://doi.org/10.1016/j.ecoleng.2005.09.006

Pahor, S., & Newton, G. (2013). *Understanding blackwater events in rivers* (Vol. 22): Australian Network for Plant Conservation Inc.

Pasco, T. E., Kaller, M. D., Harlan, R., Kelso, W. E., Rutherford, D. A., & Roberts, S. (2016). Predicting Floodplain Hypoxia in the Atchafalaya River, Louisiana, USA, a Large, Regulated Southern Floodplain River System. *River Research and Applications, 32*(5), 845-855. doi:https://doi.org/10.1002/rra.2903

Rabalais, N. N., Turner, R. E., & Wiseman Jr., W. J. (2002). Gulf of Mexico Hypoxia, A.K.A. “The Dead Zone”. *Annual Review of Ecology and Systematics, 33*(1), 235-263. doi:10.1146/annurev.ecolsys.33.010802.150513

Rixen, T., Baum, A., Pohlmann, T., Balzer, W., Samiaji, J., & Jose, C. (2008). The Siak, a tropical black water river in central Sumatra on the verge of anoxia. *Biogeochemistry, 90*(2), 129-140. doi:10.1007/s10533-008-9239-y

Saintilan, N., Kelleway, J. J., Mazumder, D., Kobayashi, T., & Wen, L. (2021). Incorporation of local dissolved organic carbon into floodplain aquatic ecosystems. *Aquatic Ecology, 55*(3), 779-790. doi:10.1007/s10452-021-09860-7

Scavia, D., Bertani, I., Obenour, D. R., Turner, R. E., Forrest, D. R., & Katin, A. (2017). Ensemble modeling informs hypoxia management in the northern Gulf of Mexico. *Proceedings of the National Academy of Sciences, 114*(33), 8823-8828. doi:doi:10.1073/pnas.1705293114

Southern Cross GeoScience. (2019). *Episodic estuarine hypoxia: resolving the geochemistry of coastal floodplain blackwaters – Summary of project findings* (Southern Cross GeoScience Technical Report No. 119). Retrieved from Southern Cross University, Lismore NSW 2480:

Steffe, A. S., Macbeth, W. G., & Murphy, J. J. (2007). Status of the recreational fisheries in two Australian coastal estuaries following large fish-kill events. *Fisheries Research, 85*(3), 258-269. doi:https://doi.org/10.1016/j.fishres.2007.02.003

Tallis, H., Polasky, S., Hellmann, J., Springer, N. P., Biske, R., DeGeus, D., . . . Weaver, S. K. (2019). Five financial incentives to revive the Gulf of Mexico dead zone and Mississippi basin soils. *Journal of Environmental Management, 233*, 30-38. doi:https://doi.org/10.1016/j.jenvman.2018.11.140

Townsend, S. A., Boland, K. T., & Wrigley, T. J. (1992). Factors contributing to a fish kill in the Australian wet/dry tropics. *Water Research, 26*(8), 1039-1044. doi:https://doi.org/10.1016/0043-1354(92)90139-U

Townsend, S. A., & Edwards, C. A. (2003). A fish kill event, hypoxia and other limnological impacts associated with early wet season flow into a lake on the Mary River floodplain, tropical northern Australia. *Lakes & Reservoirs: Research & Management, 8*(3-4), 169-176.

Tulau, M. J. (2011). Lands of the richest character: Agricultural drainage of backswamp wetlands on the north coast of New South Wales, Australia: Development, conservation and policy change: An environmental history.

Vaquer-Sunyer, R., & Duarte, C. M. (2008). Thresholds of hypoxia for marine biodiversity. *Proceedings of the National Academy of Sciences, 105*(40), 15452-15457. doi:doi:10.1073/pnas.0803833105

Vithana, C. L., Sullivan, L. A., & Shepherd, T. (2019). Role of temperature on the development of hypoxia in blackwater from grass. *Science of The Total Environment, 667*, 152-159. doi:https://doi.org/10.1016/j.scitotenv.2019.02.386

Voß, K., Fernández, D., & Schäfer, R. B. (2015). Organic matter breakdown in streams in a region of contrasting anthropogenic land use. *Science of The Total Environment, 527-528*, 179-184. doi:10.1016/j.scitotenv.2015.04.071

Wallace, T. A., Ganf, G. G., & Brookes, J. D. (2008). A comparison of phosphorus and DOC leachates from different types of leaf litter in an urban environment. *Freshwater Biology, 53*(9), 1902-1913. doi:10.1111/j.1365-2427.2008.02006.x

Walsh, S., Copeland, C., & Westlake, M. (2004). Major fish kills in the northern rivers of NSW in 2001: causes, impacts and responses. *NSW Department of Primary Industries. Fisheries final report series*(68), 55.

Watts, R. J., Kopf, R. K., McCasker, N., Howitt, J. A., Conallin, J., Wooden, I., & Baumgartner, L. (2018). Adaptive Management of Environmental Flows: Using Irrigation Infrastructure to Deliver Environmental Benefits During a Large Hypoxic Blackwater Event in the Southern Murray–Darling Basin, Australia. *Environmental Management, 61*(3), 469-480. doi:10.1007/s00267-017-0941-1

Whitworth, K. L., & Baldwin, D. S. (2016). Improving our capacity to manage hypoxic blackwater events in lowland rivers: the Blackwater risk assessment tool. *Ecological Modelling, 320*, 292-298.

Whitworth, K. L., Baldwin, D. S., & Kerr, J. L. (2012). Drought, floods and water quality: Drivers of a severe hypoxic blackwater event in a major river system (the southern Murray–Darling Basin, Australia). *Journal of Hydrology, 450-451*, 190-198. doi:https://doi.org/10.1016/j.jhydrol.2012.04.057

Whitworth, K. L., Kerr, J. L., Mosley, L. M., Conallin, J., Hardwick, L., & Baldwin, D. S. (2013). Options for managing hypoxic blackwater in river systems: case studies and framework. *Environmental Management, 52*(4), 837-850.

Wong, V., Walsh, S., & Morris, S. (2018). Climate affects fish-kill events in subtropical estuaries of eastern Australia. *Marine and Freshwater Research, 69*(11), 1641-1648.

Wong, V. N. L., Johnston, S. G., Burton, E. D., Bush, R. T., Sullivan, L. A., & Slavich, P. G. (2011). Anthropogenic forcing of estuarine hypoxic events in sub-tropical catchments: Landscape drivers and biogeochemical processes. *Science of The Total Environment, 409*(24), 5368-5375.

Wong, V. N. L., Johnston, S. G., Bush, R. T., Sullivan, L. A., Clay, C., Burton, E. D., & Slavich, P. G. (2010). Spatial and temporal changes in estuarine water quality during a post-flood hypoxic event. *Estuarine, Coastal and Shelf Science, 87*(1), 73-82. doi:https://doi.org/10.1016/j.ecss.2009.12.015

Xiong, S., Nilsson, C. (1997). Dynamics of leaf litter accumulation and its effects on riparian vegetation: A review. . *The Botanical Review, 69*. doi:10.1071/mf17307

Zhang, M., Cheng, X., Geng, Q., Shi, Z., Luo, Y., & Xu, X. (2019). Leaf litter traits predominantly control litter decomposition in streams worldwide. *Global Ecology and Biogeography, 28*(10), 1469-1486.

Supporting Information for

Hypoxic Blackwater Events – Identifying High Risk Catchments in Estuaries Now and Under Future Climate Scenarios

K. Waddington[1], A. Harrison[1], D. Rayner[1], T. Tucker[1] and W. Glamore[1]

[1]Water Research Laboratory, School of Civil and Environmental Engineering, UNSW Sydney, NSW 2093 Australia.

Contents of this file

Tables S1 to S30
Figures S1 to S114

Introduction

This supporting information includes:

- Representative vegetation types and associated risk factors assigned to the various land uses within the study area (Table S1).
- Water level data for each estuary (Figures S1 to S93 and Tables S2 to S15); including maps identifying the locations of water level gauges and floodplain catchments, details of each gauge record and flow distribution curves. Water levels representing the range of inundation durations (1 to 5 days) and recurrence intervals (1 to 5 years) assessed are presented for each water level gauge and the distribution of these levels to each catchment is tabulated. Note that where water gauges are not located within a suitable distance of the catchment drainage connection to the estuary, inundation elevations have been interpolated as tabulated herein. Water level data used and presented for the analysis was obtained from the WaterNSW Water Information Hub Real-time water data (waternsw.com.au).
- The results of the analysis, including median inundation level, blackwater contribution factor and ranking of each catchment within each estuary (Tables S16 to S22). The catchment ranking and extents of inundation under median blackwater levels are also mapped in Figures S94 to S107).
- A summary of the results of an analysis of the sensitivity of inundation level and ranking of aggregated blackwater risk factor to changes in inundation duration and flood frequency matrices (Table S23). The rank correlation refers to the correlation between ranking of catchments according to average aggregated blackwater risk factor was determined by comparing the base case with the modified case.
- Average annual temperature ranges within each catchment of the study area (Tables S24 to S30), obtained from the Climate Data Online service of the Australian Bureau of Meteorology Climate Data Online - Map search (bom.gov.au). The monthly average maximum temperatures presented in these tables refer to the average of all daily maxima for the month, as recorded in the 24 hours prior to 9am local time. The locations of each climate monitoring station are included in Figures S108 to S114, which show the

geographical distribution of average maximum daily temperatures across the various catchments for the warmest months of October to April. Typically, the average maximum daily temperatures do not vary by more than 5°C throughout each of the catchment areas, suggesting that, while higher temperatures are a contributing factor to blackwater events, differences in temperature are unlikely to affect the distribution of blackwater risk within each river system.

Both the water level and temperature data support the use of the methodology within coastal NSW with respect to the limitations discussed in Section 3.2 of the manuscript. This data indicates that there is insufficient variation in altitude or temperature to provide added differentiation in blackwater risk between the catchments studied. Throughout the selected study sites, the High High Water Solstice Spring (HHWSS) tide does not exceed 2.5m AHD (Australian Height Datum) (Couriel et al., 2012). Further, estuarine flood levels (and hence inundation levels across the floodplains) are typically limited to <5m AHD.

With regard to temperature, more frequent and severe blackwater events have been recorded during summer months (Wong et al., 2018). Nevertheless, Vithana et al. (2019) found that grasses inundated for one week produced a similar biochemical oxygen demand at temperatures of 20C, 27.5C and 35C. As demonstrated in this Supplementary Material, these temperatures are representative of the annual range experienced throughout coastal New South Wales (Australia), indicating that, under suitable inundation conditions, blackwater may be generated throughout the year within any of the catchments in the selected study area. Flooding may also occur at any time of the year throughout these catchments, justifying the inclusion of the full annual record of water levels in the analysis. It is noted that in alternative locations, the methodology may need to be modified to incorporate seasonal flooding and regional temperature variations.

Table S1. Blackwater risk factors for land uses associated with various vegetation types

Secondary Land Use Type[1]		Assigned Vegetation	Risk Factor
1.1.0	Nature conservation	Forestry	3
1.2.0	Managed Resource Protection	Forestry	3
1.3.0	Other minimal use	Forestry	3
2.1.0	Grazing native vegetation	Dryland Grasses	3
2.2.0	Production forestry	Forestry	3
3.1.0	Plantation forestry	Forestry	3
3.2.0	Grazing modified pastures	Grass	3
3.3.0	Cropping	Sugar Cane	2
3.4.0	Perennial horticulture	Forestry	3
3.5.0	Seasonal horticulture	Forestry	3
3.6.0	Land in transition	Forestry	3
4.1.0	Irrigated plantation forestry	Forestry	3
4.2.0	Grazing irrigated modified pastures	Dryland Grasses	3
4.3.0	Irrigated cropping	Sugar Cane	2
4.4.0	Irrigated perennial horticulture	Forestry	3
4.5.0	Irrigated seasonal horticulture	Forestry	3
4.6.0	Irrigated land in transition	Forestry	3
5.1.0	Intensive horticulture	Forestry	3
5.2.0	Intensive animal husbandry	Industry/Urban[2]	1
5.3.0	Manufacturing and industrial	Industry/Urban[2]	1
5.4.0	Residential and farm infrastructure	Industry/Urban[2]	1
5.5.0	Services	Industry/Urban[2]	1
5.6.0	Utilities	Industry/Urban[2]	1
5.7.0	Transport and communication	Industry/Urban[2]	1
5.8.0	Mining	Industry/Urban[2]	1
5.9.0	Waste treatment and disposal	Industry/Urban[2]	1
6.1.0	Lake	Water[3]	0
6.2.0	Reservoir/dam	Water[3]	0
6.3.0	River	Water[3]	0
6.4.0	Channel/aqueduct	Water[3]	0
6.5.0	Marsh/wetland	Freshwater Wetland	1
6.6.0	Estuary/coastal waters	Water[3]	0

[1] 2017 Australian Land Use and Management (ALUM) classification for NSW (DPIE, 2020)

[2] The runoff from urban and industrial areas is often associated with high BOD (USEPA, 2001), however the impact on water quality is more likely to be associated with the first flush of runoff due to the high proportion of impervious surfaces and with eutrophication due to high nutrient levels in the water column. Further, low levels of vegetation coverage are unlikely to produce as substantial an increase in deoxygenation potential as agricultural or nature conservation areas. Any land uses identified as industry/urban were therefore assigned a blackwater risk factor of one, noting that these areas account for a relatively small portion of the floodplain subcatchments, making the results reasonably insensitive to this assumption. This contrasts strongly to intensely developed catchments, such as those along the south-eastern coast of the USA, where point source loading of human sewage and animal waste have been identified as the principal anthropogenic sources of BOD (Mallin et al., 2002).

[3] Permanent waterbodies were assigned a zero risk factor, as were floodplain areas mapped as mangroves or saltmarsh (identified by macrophyte mapping supplied by NSW Department of Primary Industries – Fisheries). It was considered that these areas would not significantly contribute to blackwater generation as they are frequently inundated by tidal waters.

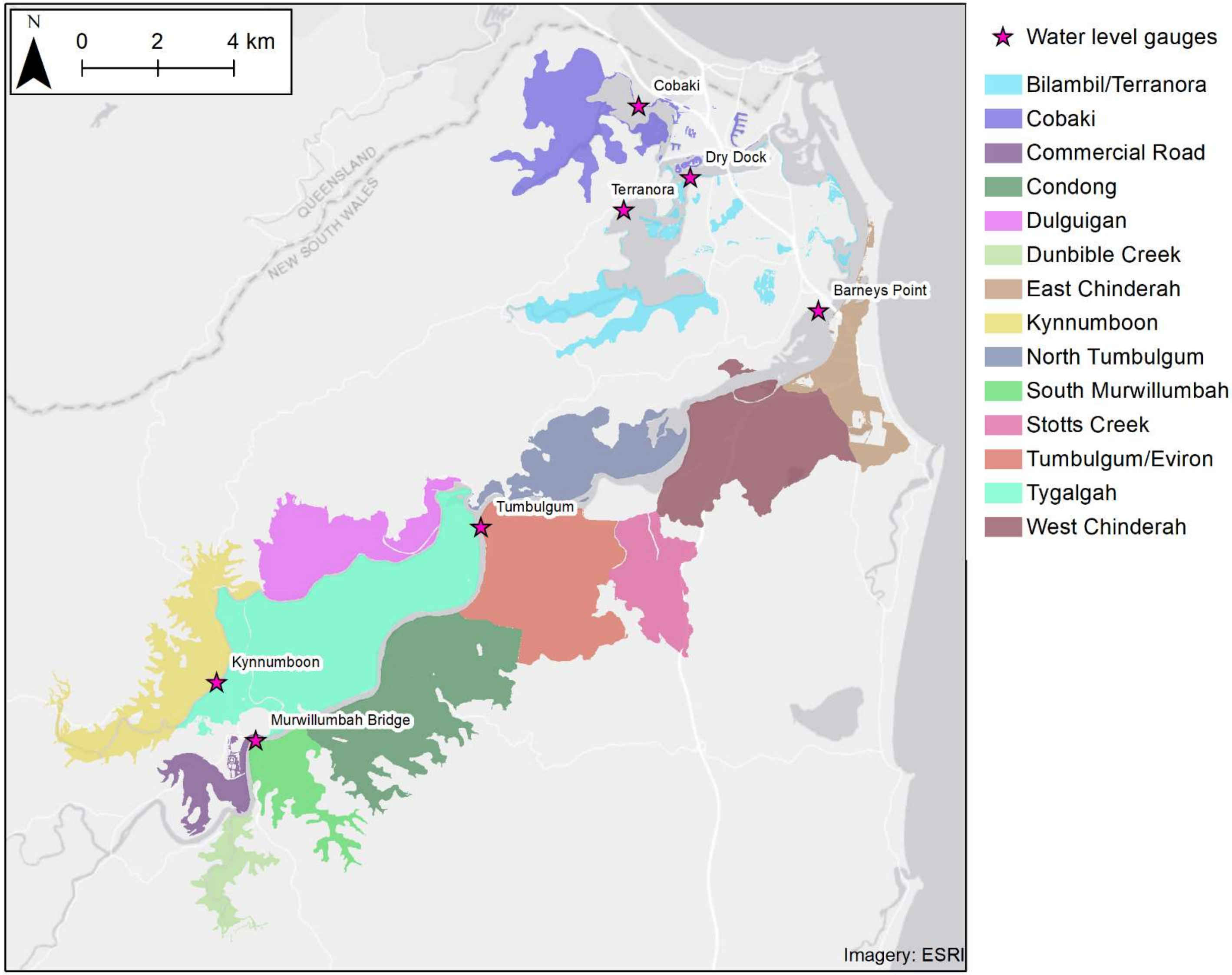

Figure S1. Water level gauge locations and catchment areas, Tweed River

Table S2. Details of water level gauges, Tweed River

Station	Length of record** (years)	Mean High Water level (m AHD)	Blackwater inundation level (m AHD)	
			Median	Maximum
Barneys Point (201426)	30.4	0.4	0.4*	1.3
Cobaki (201448)	31.2	0.4	0.4*	0.7
Terranora (201447)	30.8	0.4	0.4*	0.7
Tumbulgum (201432)	32.2	0.4	0.9	2.6
North Murwillumbah (201420)	27.8	0.4	0.7	2.8
Kynnumboon (201422)	26.8	0.5	1.4	3.8

* Mean High Water adopted as minimum blackwater inundation level
** Excluding data gaps in excess of 6 hours

Table S3. Distribution of water level gauges to catchments, Tweed River

Catchment	Water level station(s) adopted
Bilambil-Terranora	Terranora
Cobaki	Cobaki
East Chinderah	0.91 x Barneys Point + 0.09 x Tumbulgum
West Chinderah	0.76 x Barneys Point + 0.24 x Tumbulgum
Stotts Creek	0.41 x Barneys Point + 0.59 x Tumbulgum
North Tumbulgum	0.32 x Barneys Point + 0.68 x Tumbulgum
Tumbulgum-Eviron	0.22 x Barneys Point + 0.78 x Tumbulgum
Condong	0.69 x Tumbulgum + 0.31 x Nth Murwillumbah
Dulguigan	0.78 x Tumbulgum + 0.22 x Kynnumboon
Tygalgah	0.73 x Tumbulgum + 0.27 x Kynnumboon
Kynnumboon	Kynnumboon
South Murwillumbah	North Murwillumbah
Dunbible Creek	North Murwillumbah
Commercial Road	North Murwillumbah

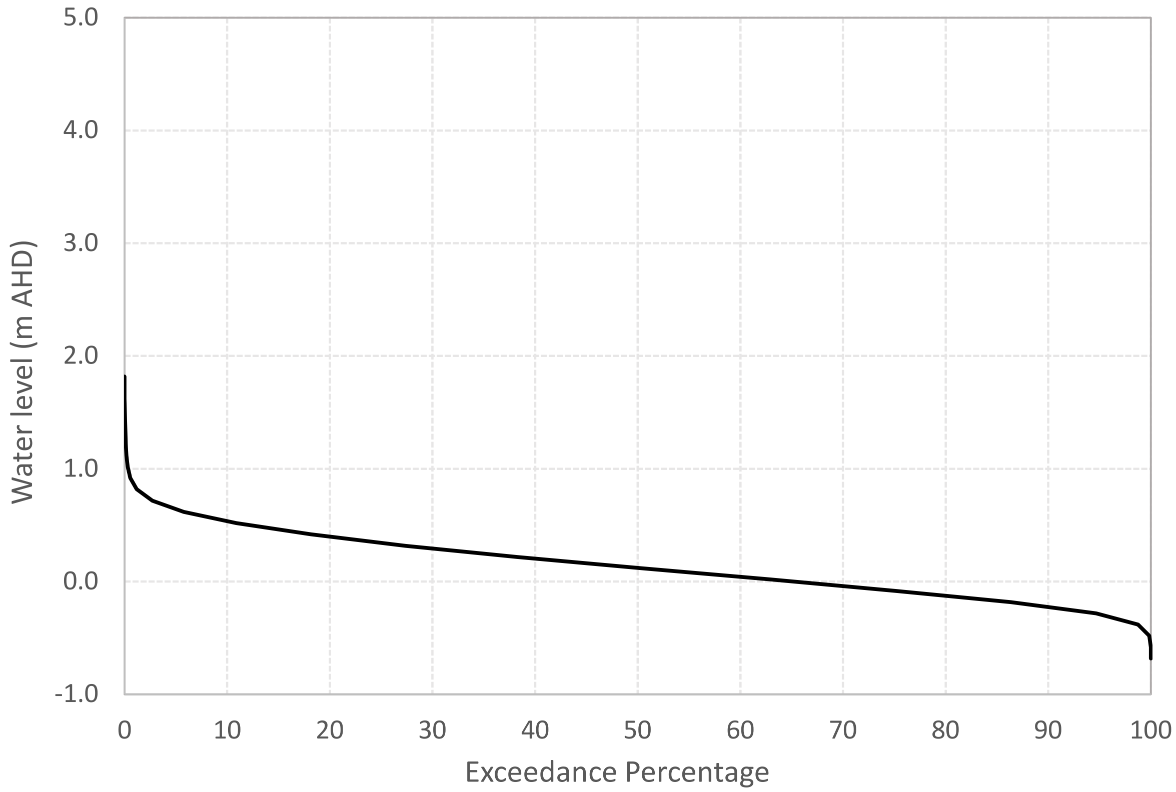

Figure S2. Frequency distribution of water levels at Barneys Point (Station 201426)

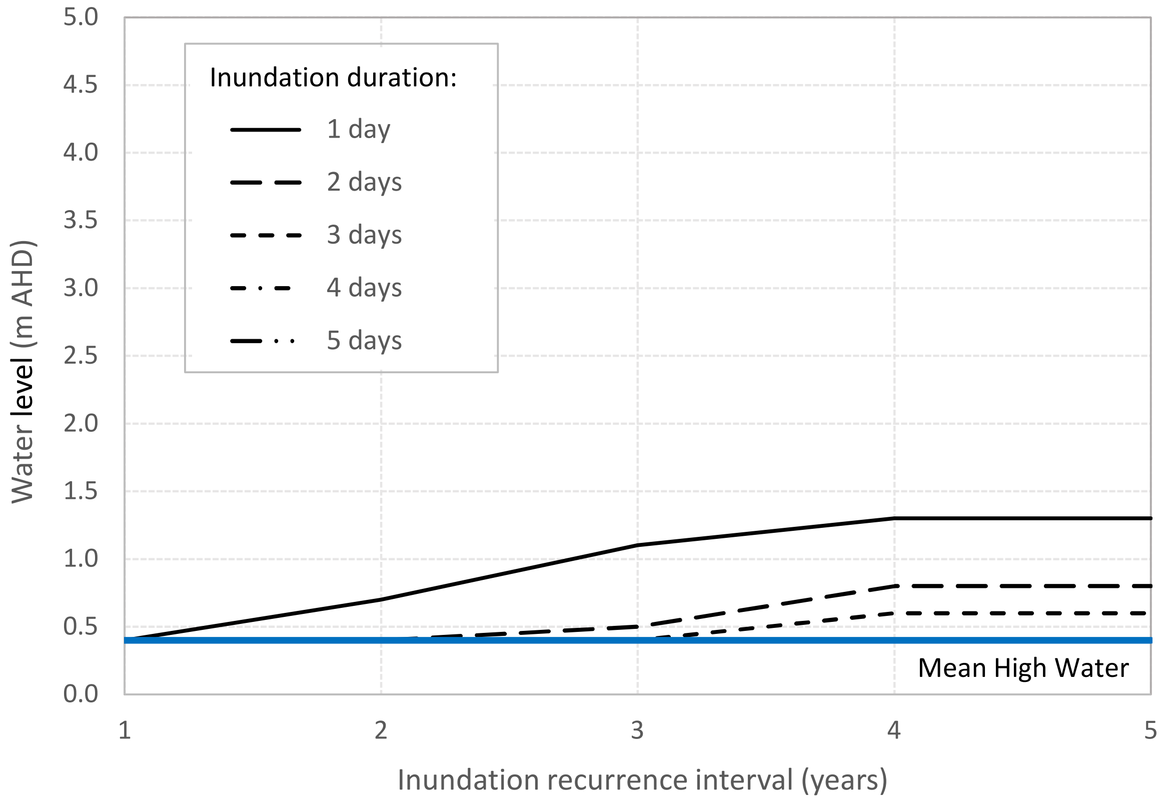

Figure S3. Water levels corresponding to inundation durations of 1 to 5 days with recurrence intervals of 1 to 5 years for Barneys Point (Station 201426)

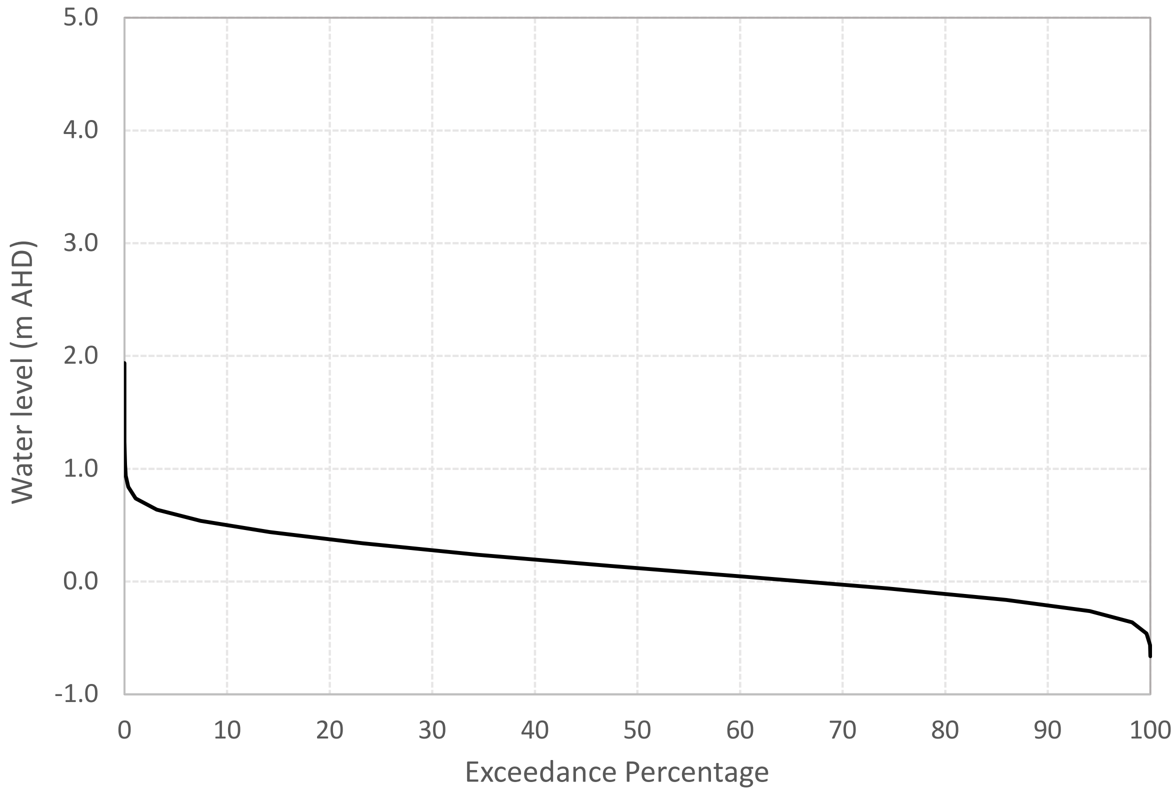

Figure S4. Frequency distribution of water levels at Cobaki (Station 201448)

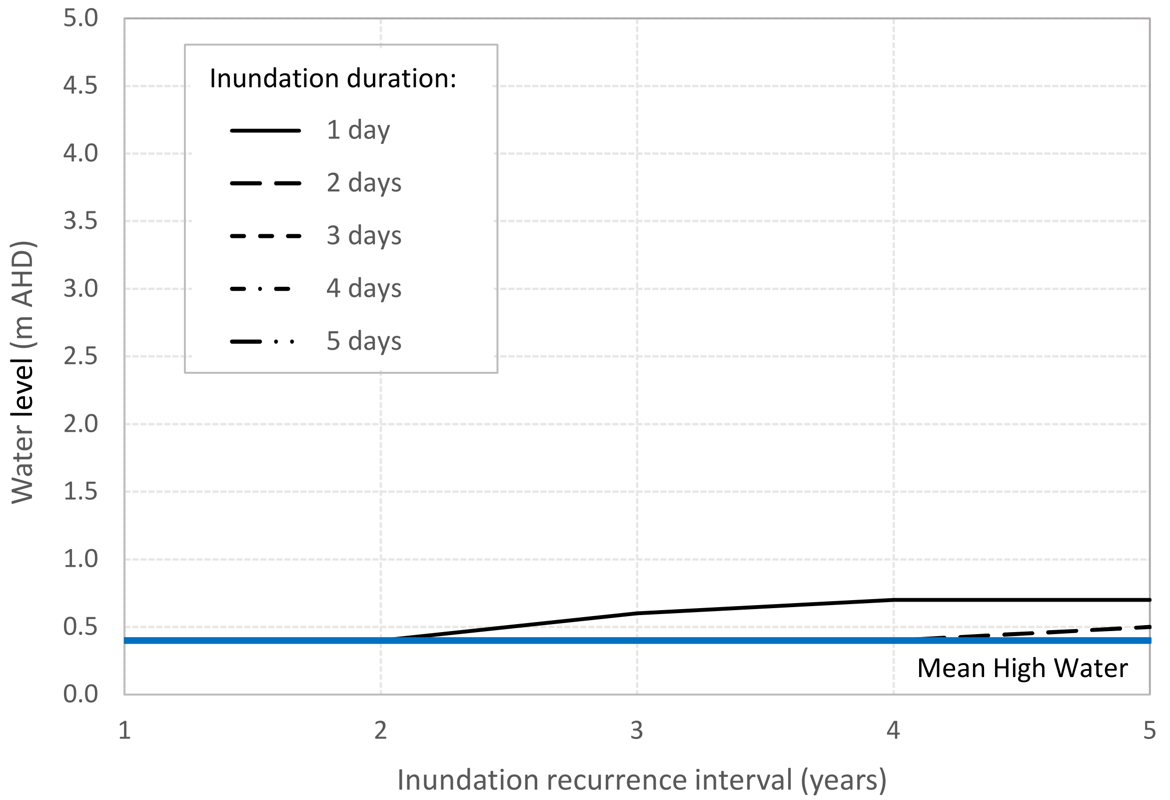

Figure S5. Water levels corresponding to inundation durations of 1 to 5 days with recurrence intervals of 1 to 5 years for Cobaki (Station 201448)

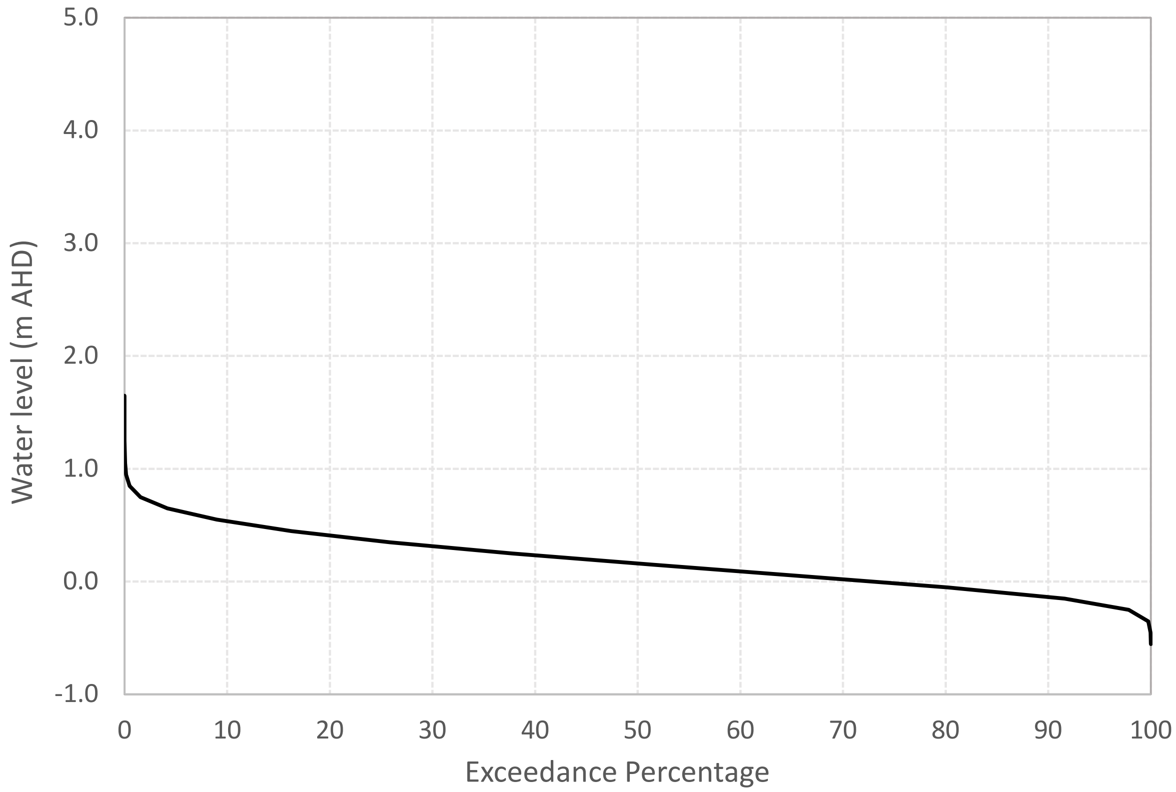

Figure S6. Frequency distribution of water levels at Terranora (Station 201447)

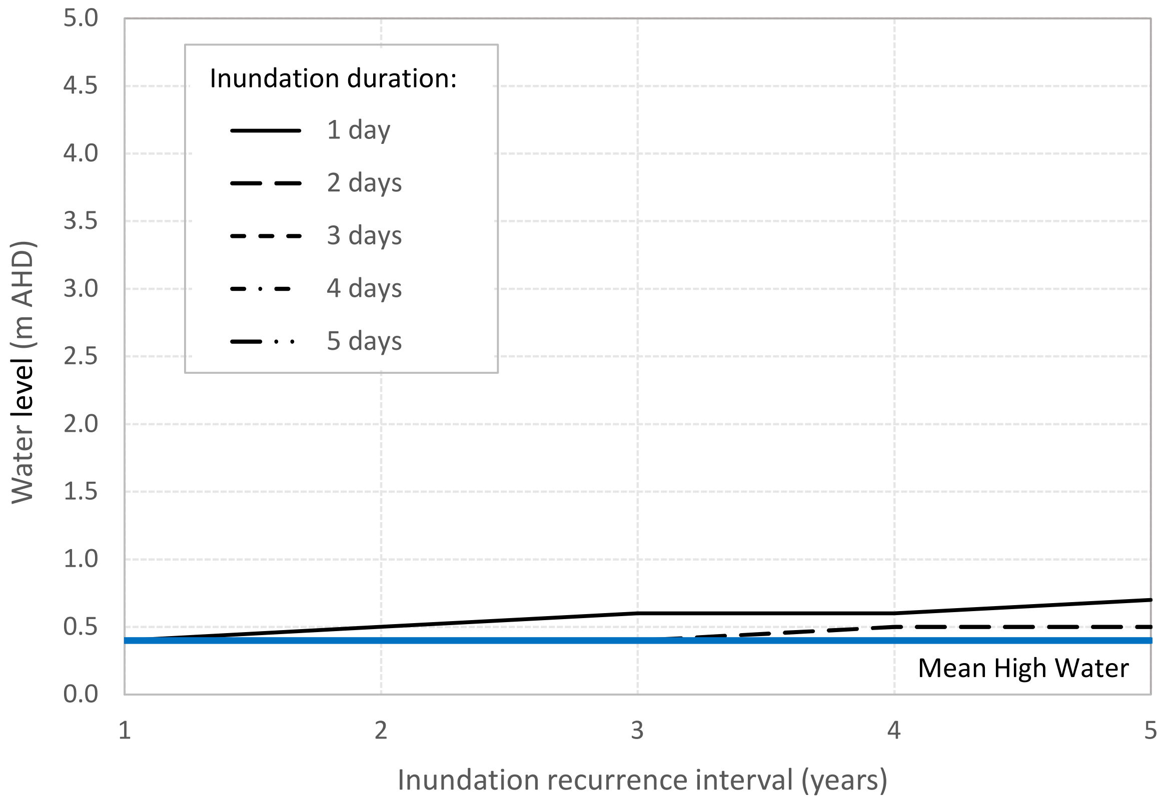

Figure S7. Water levels corresponding to inundation durations of 1 to 5 days with recurrence intervals of 1 to 5 years for Terranora (Station 201447)

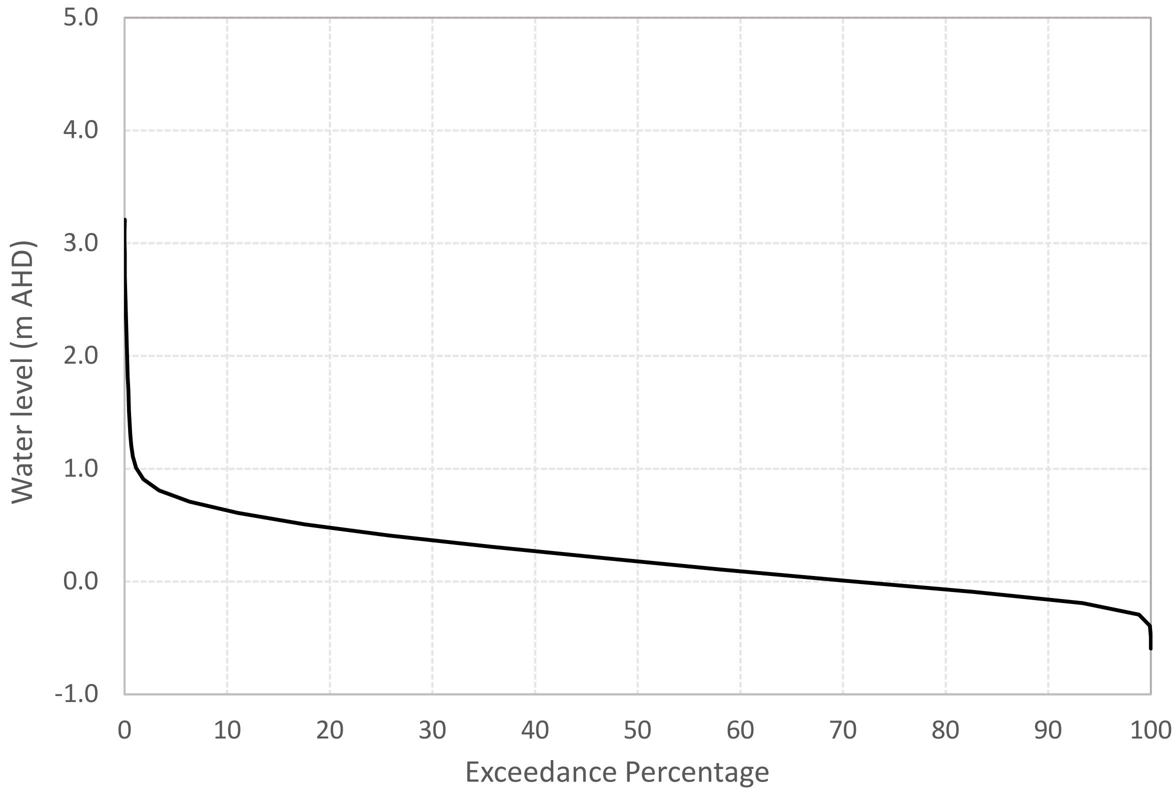

Figure S8. Frequency distribution of water levels at Tumbulgum (Station 201432)

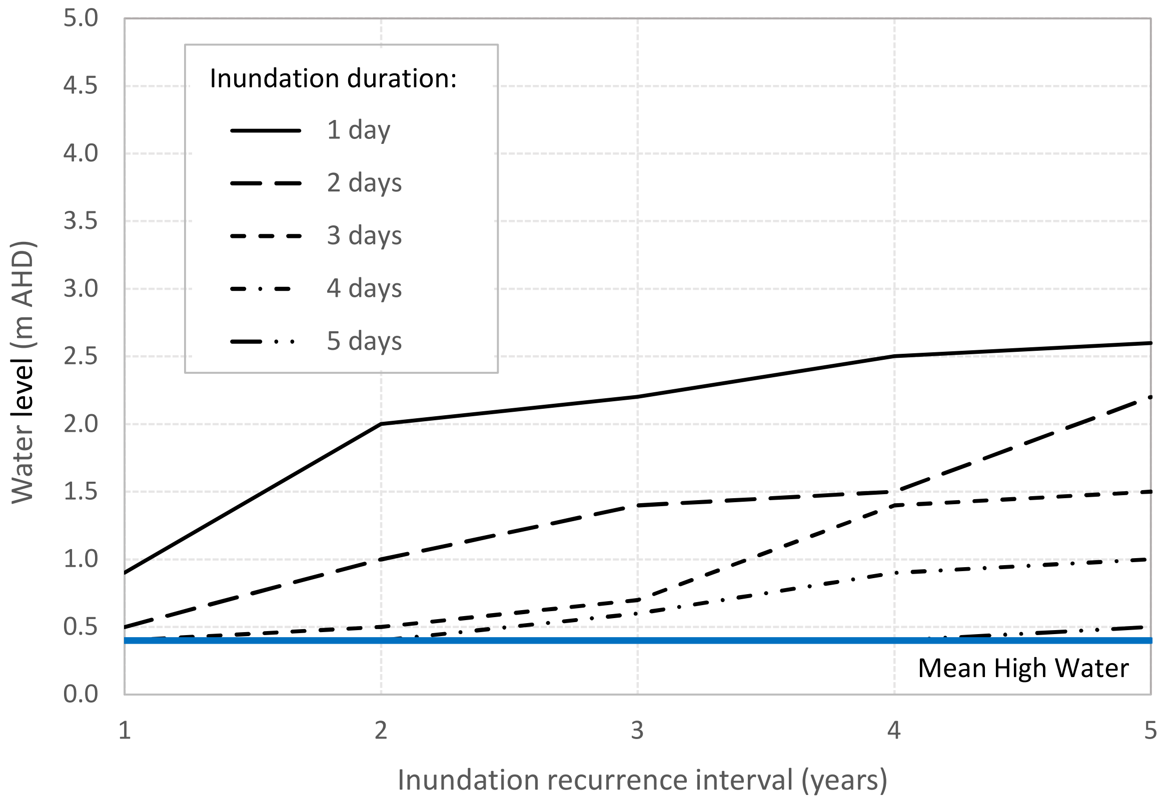

Figure S9. Water levels corresponding to inundation durations of 1 to 5 days with recurrence intervals of 1 to 5 years for Tumbulgum (Station 201432)

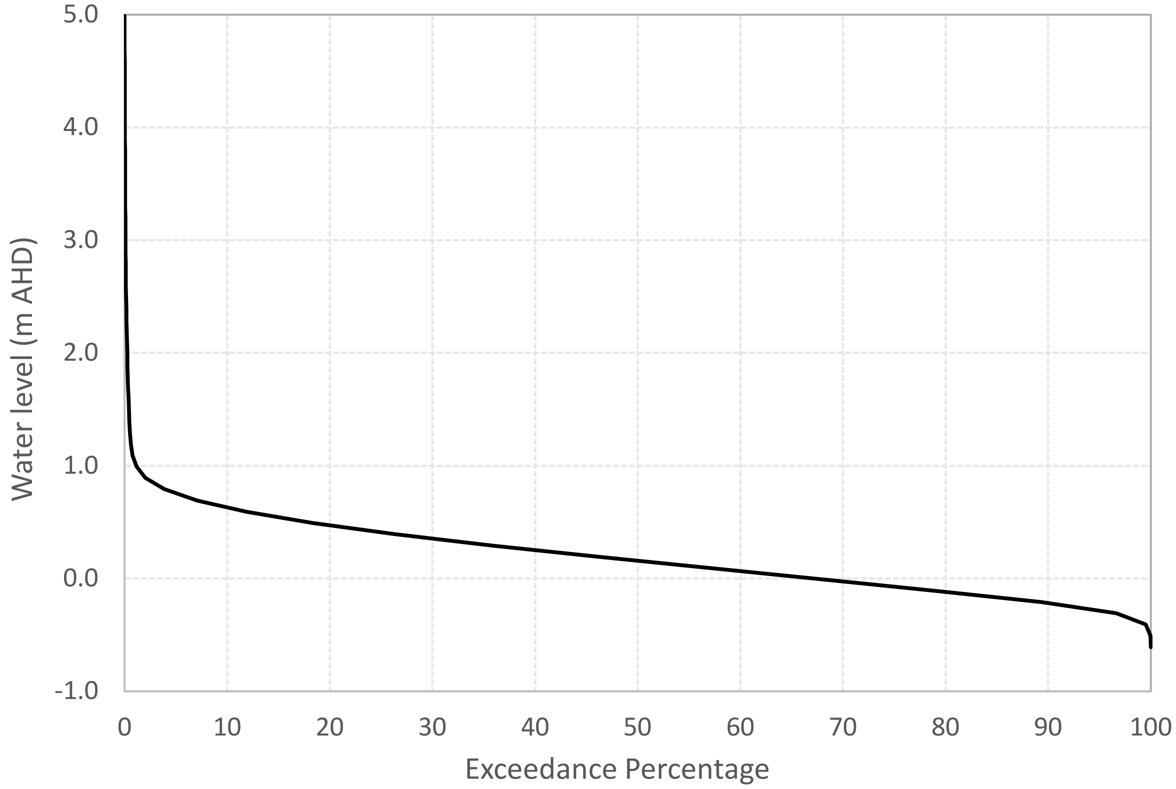

Figure S10. Frequency distribution of water levels at North Murwillumbah (Station 201420)

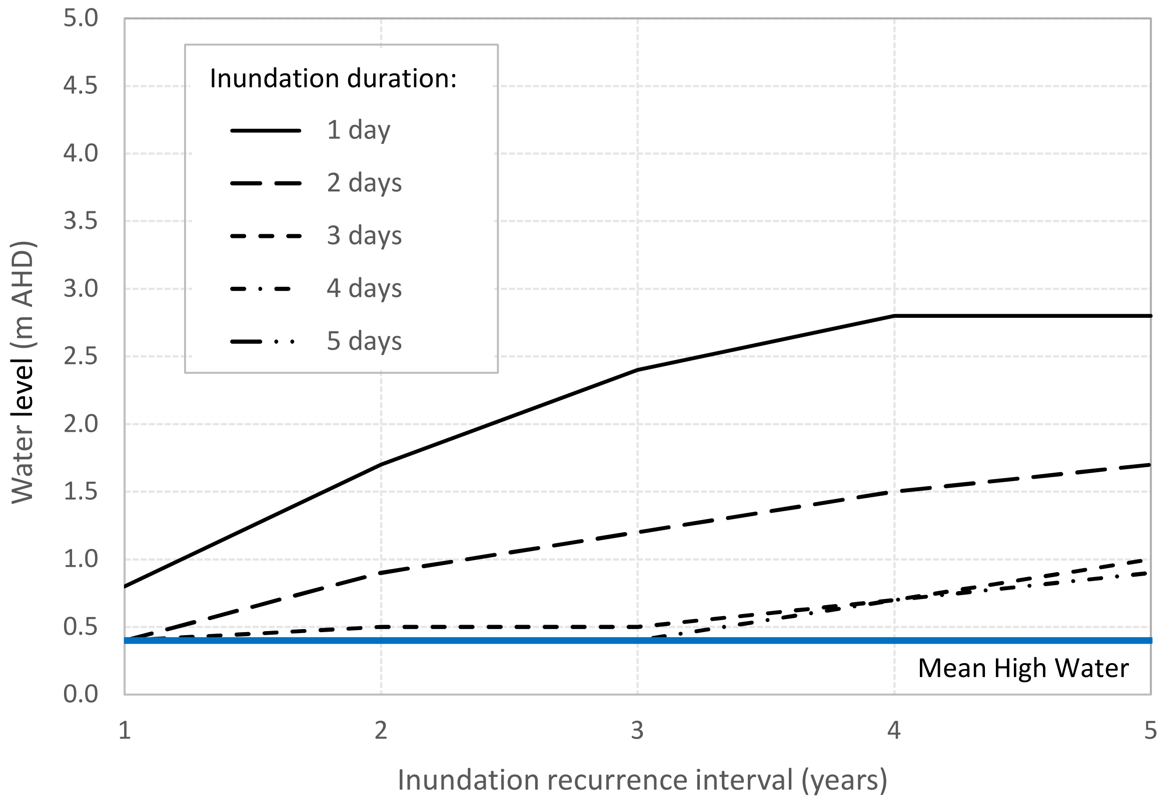

Figure S11. Water levels corresponding to inundation durations of 1 to 5 days with recurrence intervals of 1 to 5 years for North Murwillumbah (Station 201420)

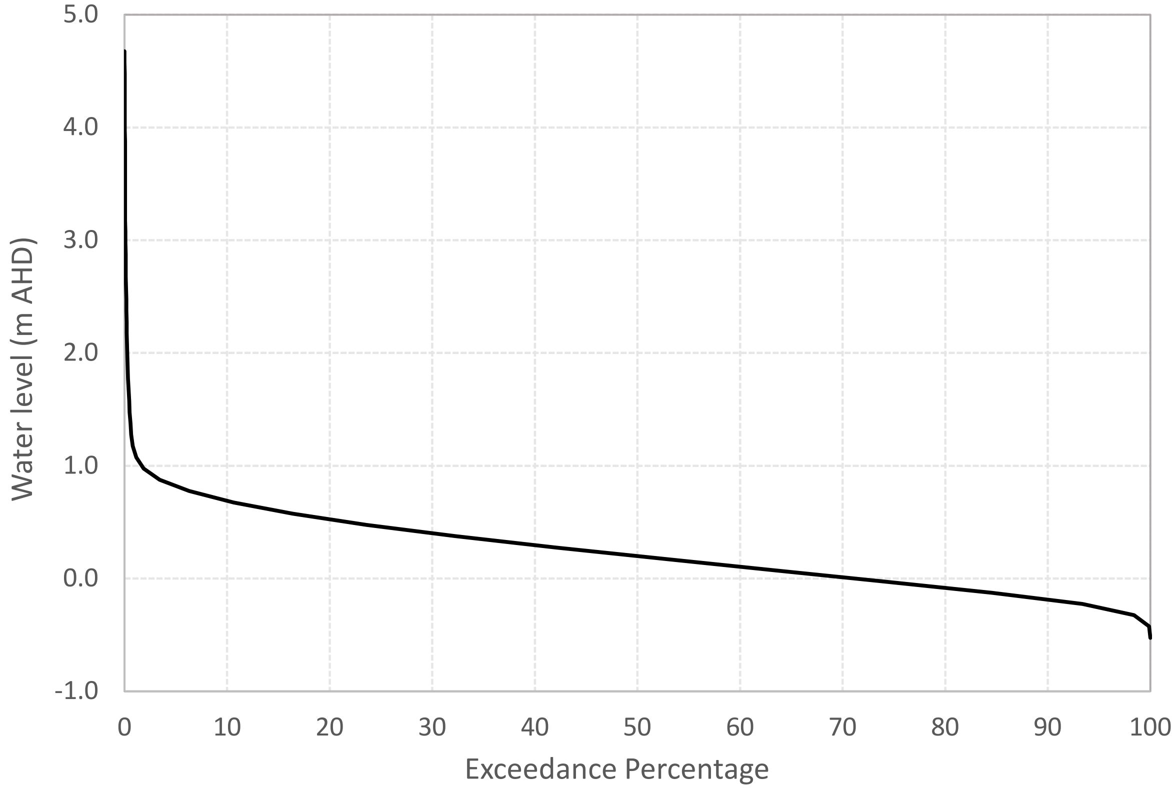

Figure S12. Frequency distribution of water levels at Kynnumboon (Station 201442)

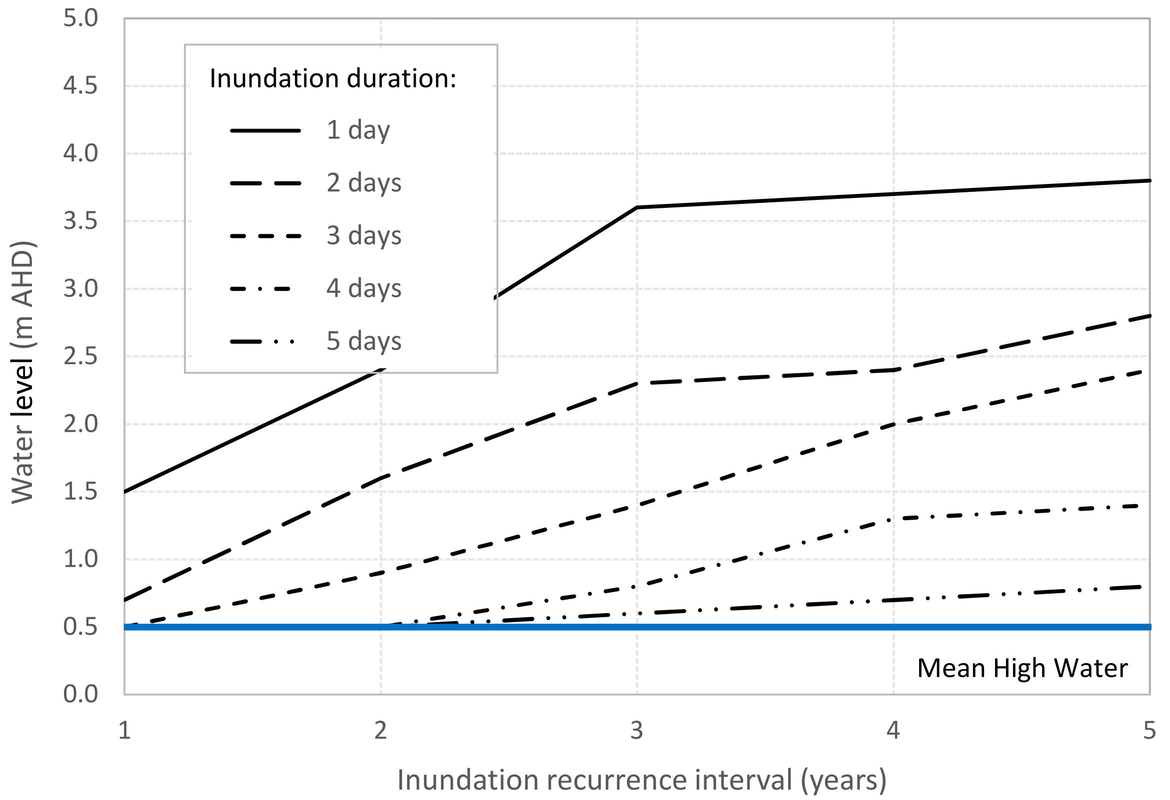

Figure S13. Water levels corresponding to inundation durations of 1 to 5 days with recurrence intervals of 1 to 5 years for Kynnumboon (Station 201442)

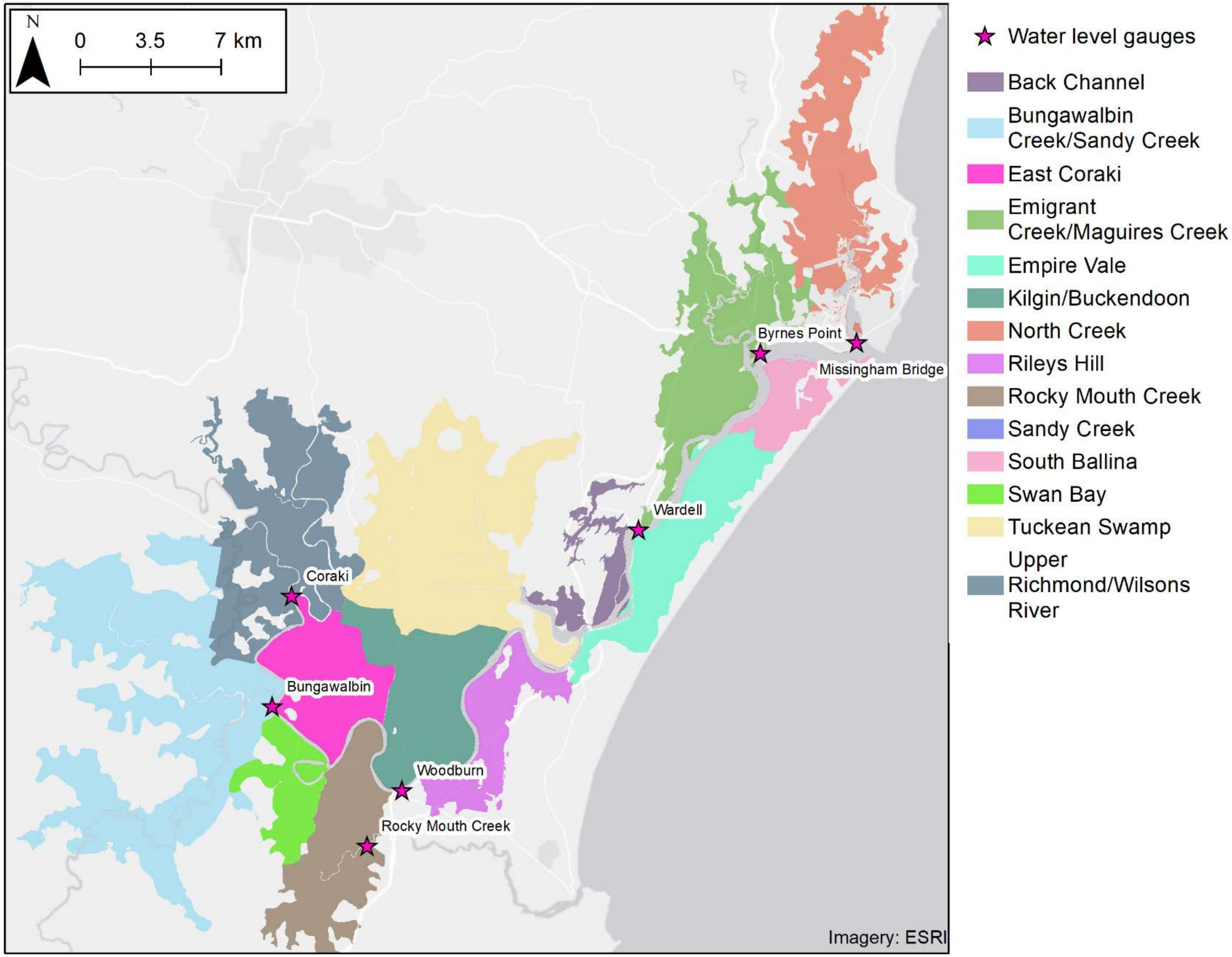

Figure S14. Water level gauge locations and catchment areas, Richmond River

Table S4. Details of water level gauges, Richmond River

Station	Length of record** (years)	Mean High Water level (m AHD)	Blackwater inundation level (m AHD)	
			Median	Maximum
Missingham Bridge (203465)	16.3	0.5	0.5*	0.5
Byrnes Point (203461)	29.3	0.4	0.4*	0.4
Wardell (203468)	17.3	0.5	0.5*	1.1
Woodburn (203412)	33.75	0.4	2.1	3.0
Bungawalbin (203450)	17.5	0.4	2.9	4.1
Coraki (203403)	32.25	0.4	2.1	1.4
Rocky Mouth Creek (203432)	25.5	0.4	1.5	2.0

* Mean High Water adopted as minimum blackwater inundation level

** Excluding data gaps in excess of 6 hours

Table S5. Distribution of water level gauges to catchments, Richmond River

Catchment	Water level station(s) adopted
North Creek	Missingham Bridge
South Ballina	Missingham Bridge
Emigrant Creek/Maguires Creek	Brynes Point
Empire Vale	0.18 x Brynes Point + 0.82 x Wardell
Back Channel	Wardell
Tuckean Swamp	0.82 x Wardell + 0.28 x Woodburn
Rocky Mouth Creek	Rocky Mouth Creek
Rileys Hill	0.41 x Wardell + 0.59 x Woodburn
Kilgin/Buckendoon	0.32 x Wardell + 0.68 x Woodburn
East Coraki	0.38 x Bungawalbin + 0.62 x Woodburn
Swan Bay	Bungawalbin
Bungawalbin Creek/Sandy Creek	Bungawalbin
Upper Richmond/Wilsons River	Coraki

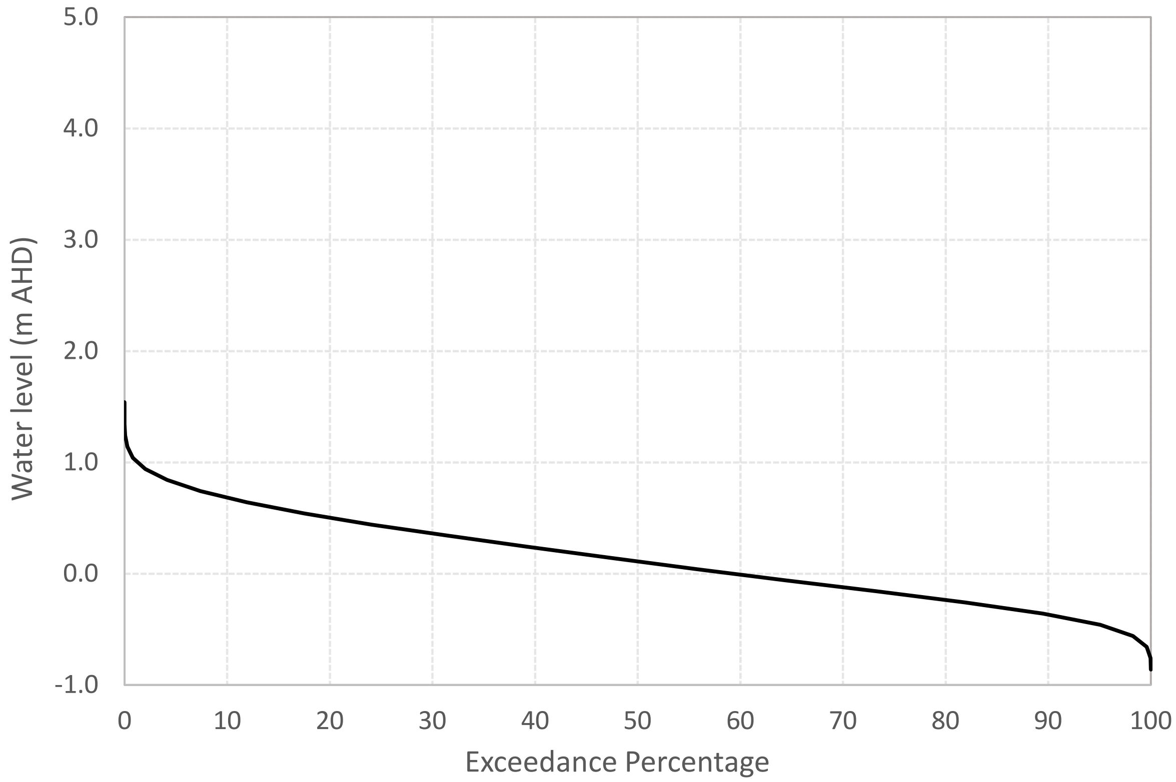

Figure S15. Frequency distribution of water levels at Missingham Bridge (Station 203465)

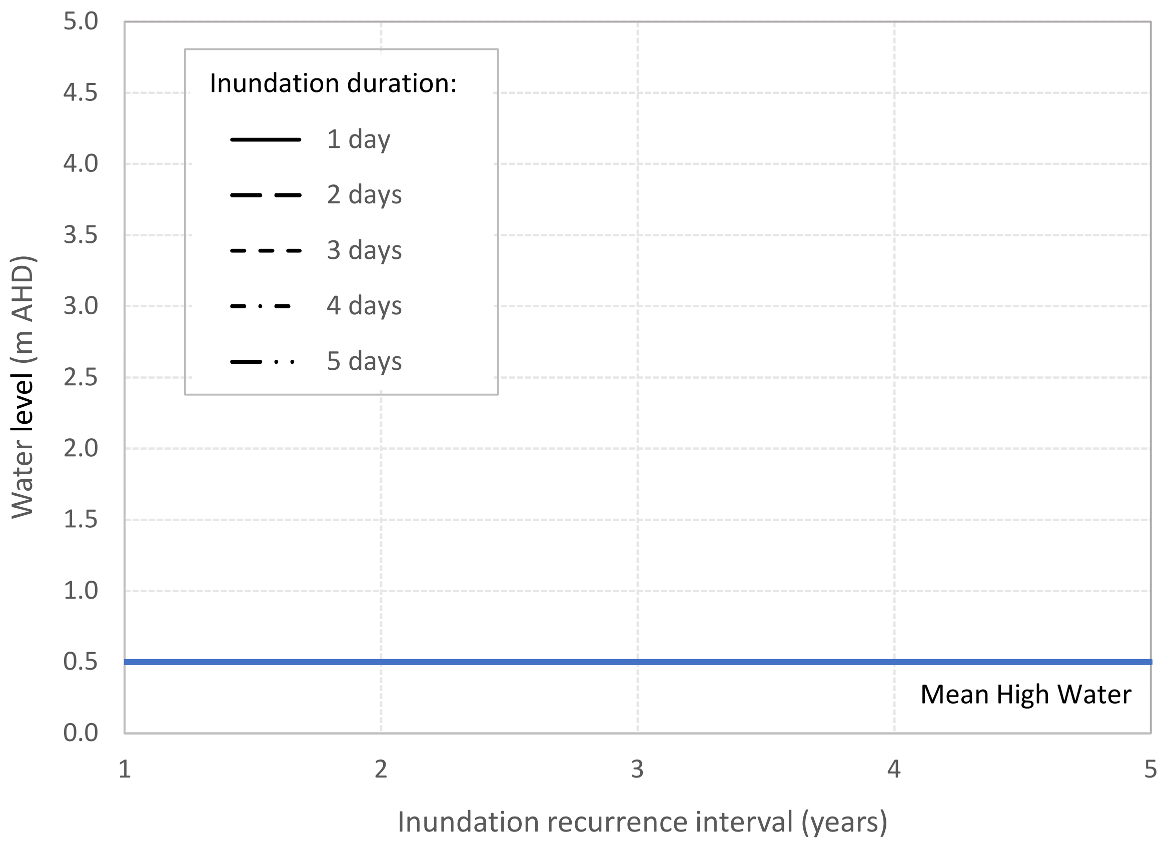

Figure S16. Water levels corresponding to inundation durations of 1 to 5 days with recurrence intervals of 1 to 5 years for Missingham Bridge (Station 203465)

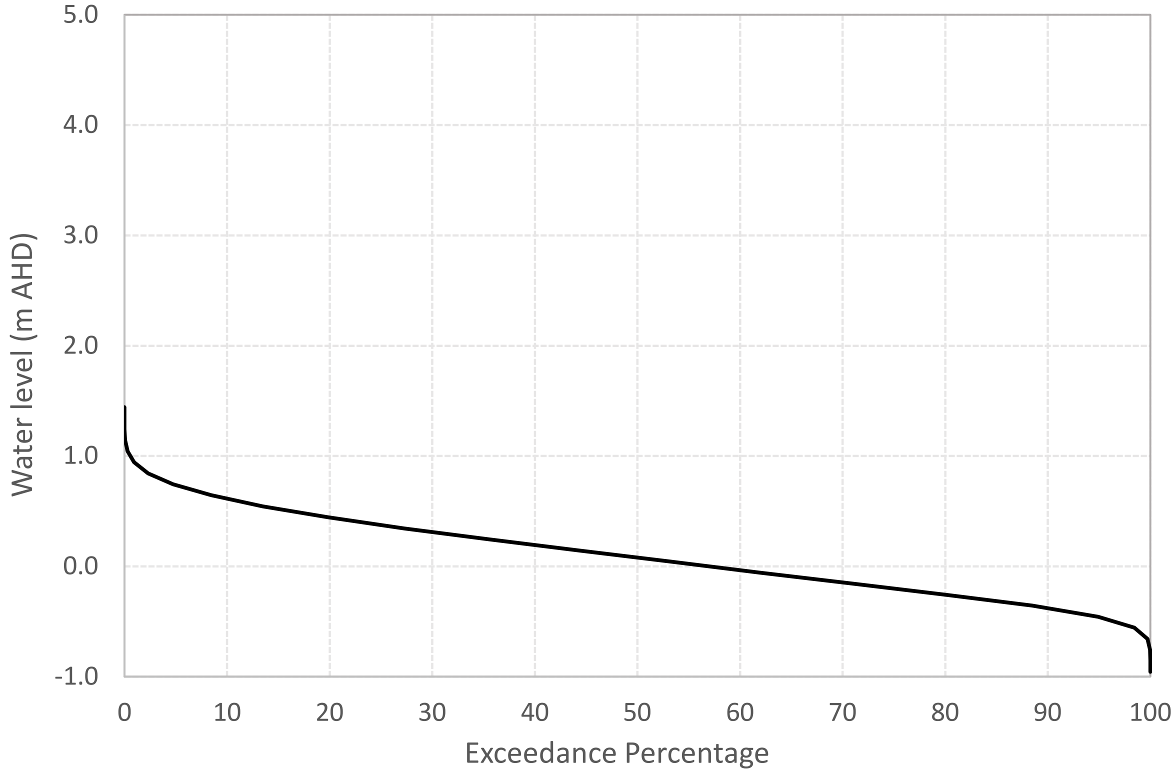

Figure S17. Frequency distribution of water levels at Byrnes Point (Station 203461)

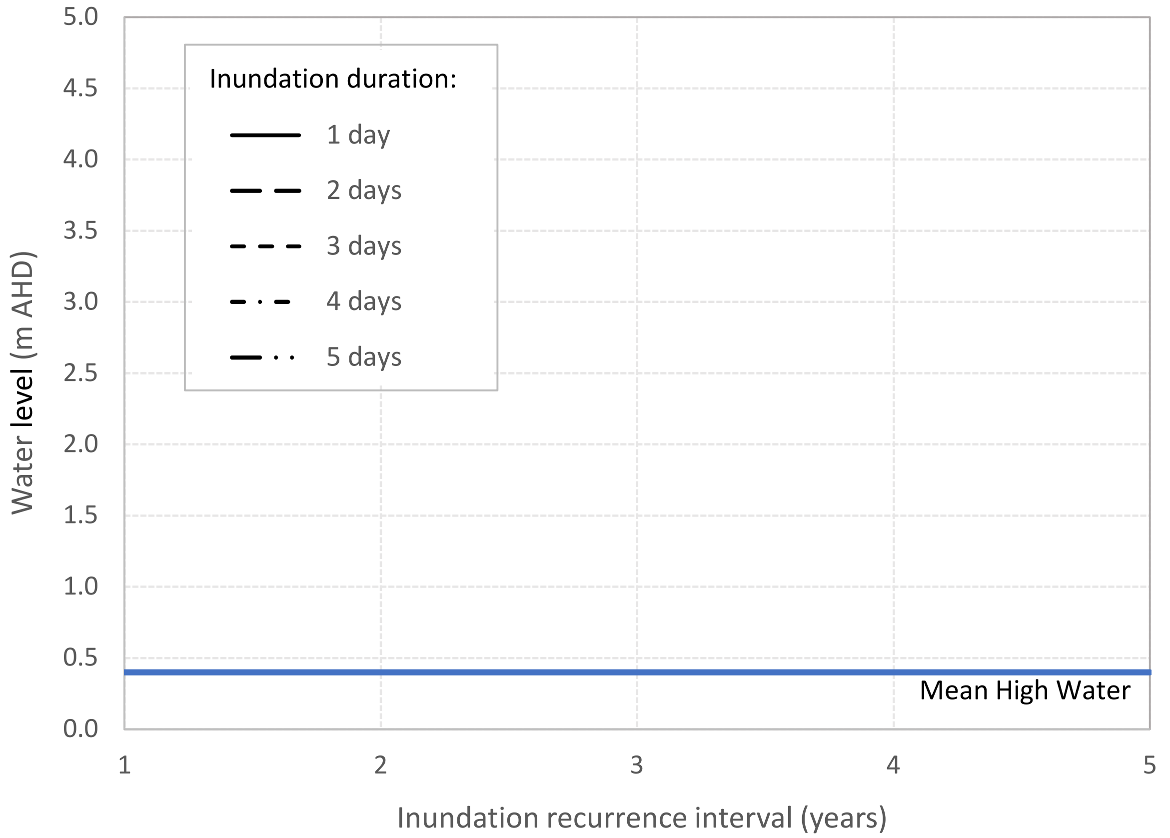

Figure S18. Water levels corresponding to inundation durations of 1 to 5 days with recurrence intervals of 1 to 5 years for Byrnes Point (Station 203461)

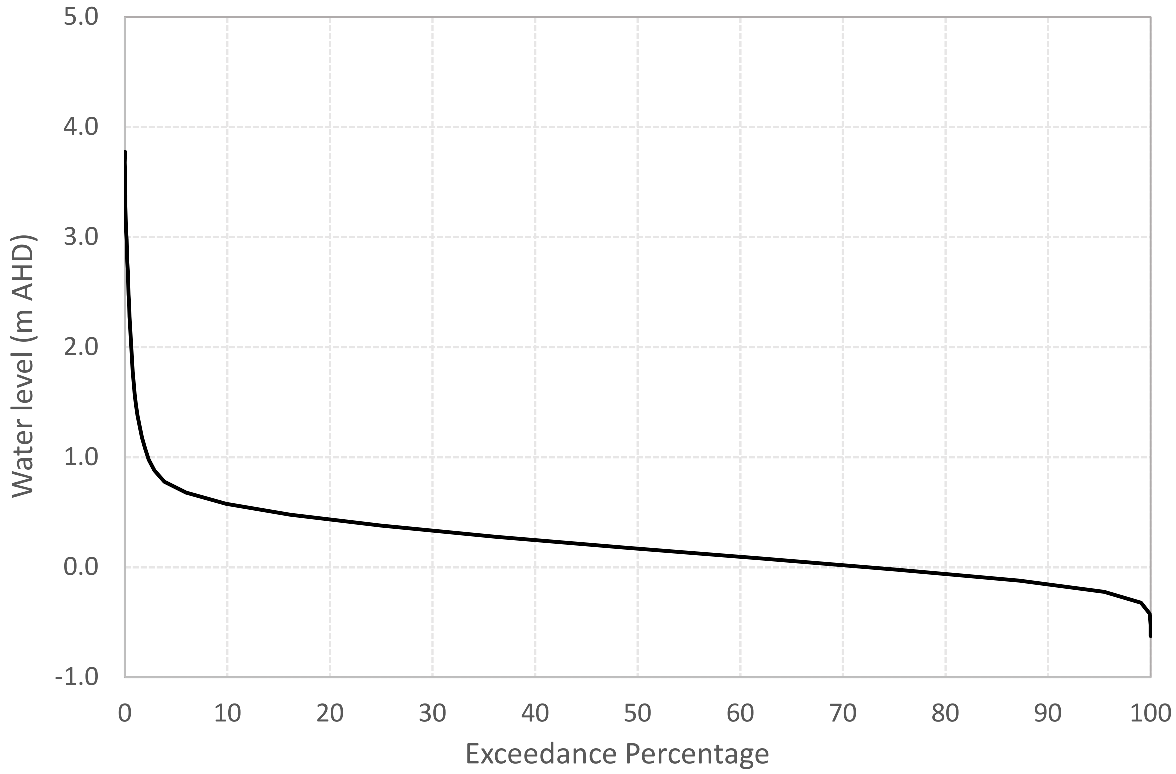

Figure S19. Frequency distribution of water levels at Wardell (Station 20)

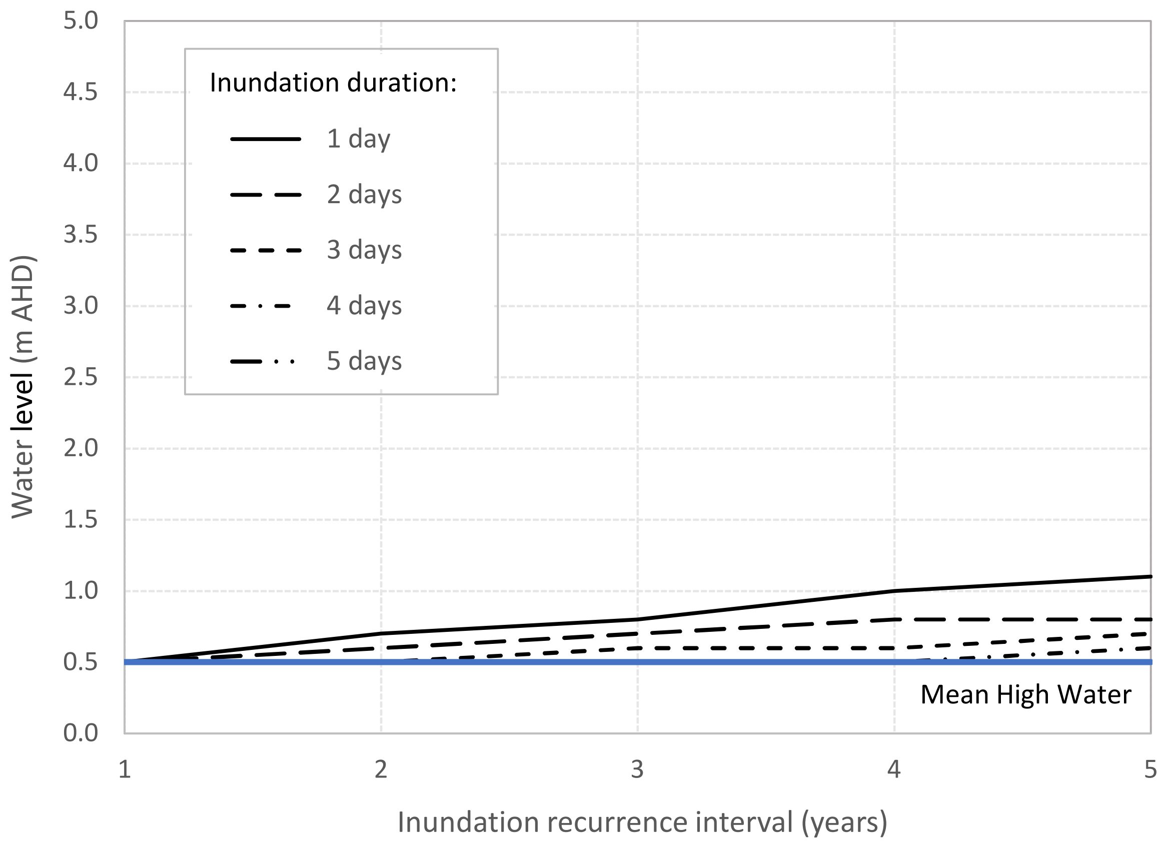

Figure S20. Water levels corresponding to inundation durations of 1 to 5 days with recurrence intervals of 1 to 5 years for Wardell (Station 20)

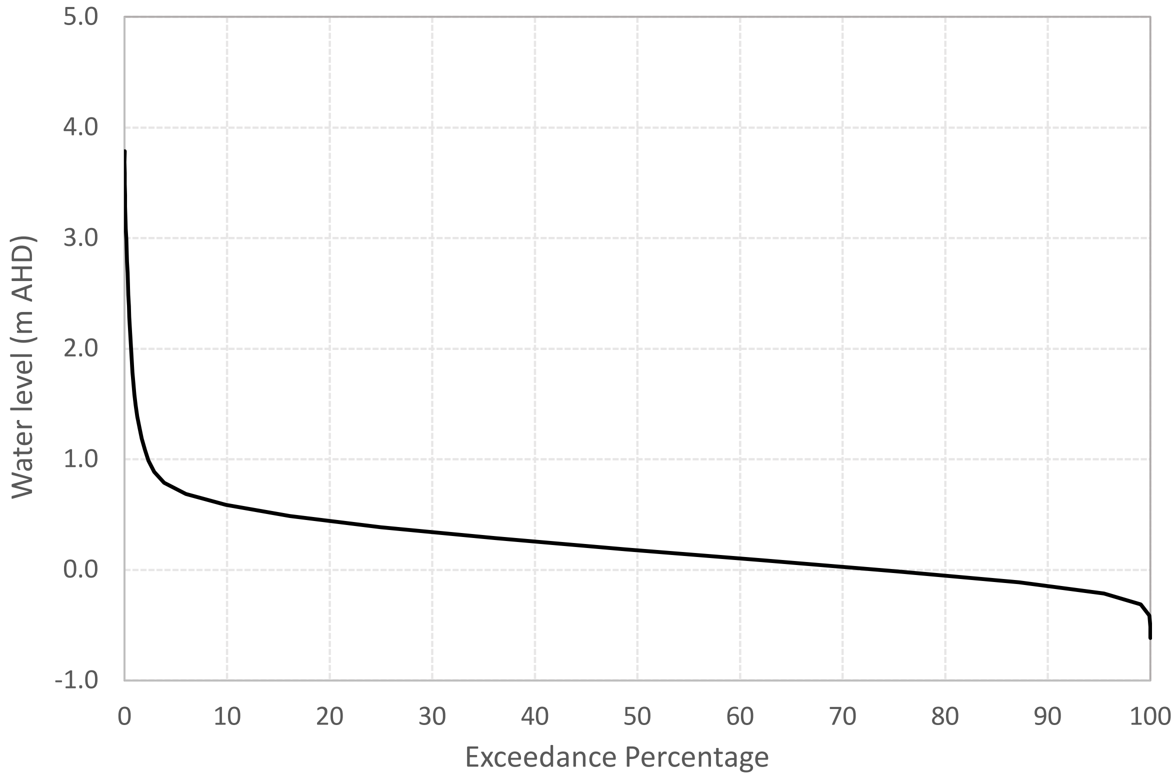

Figure S21. Frequency distribution of water levels at Woodburn (Station 203412)

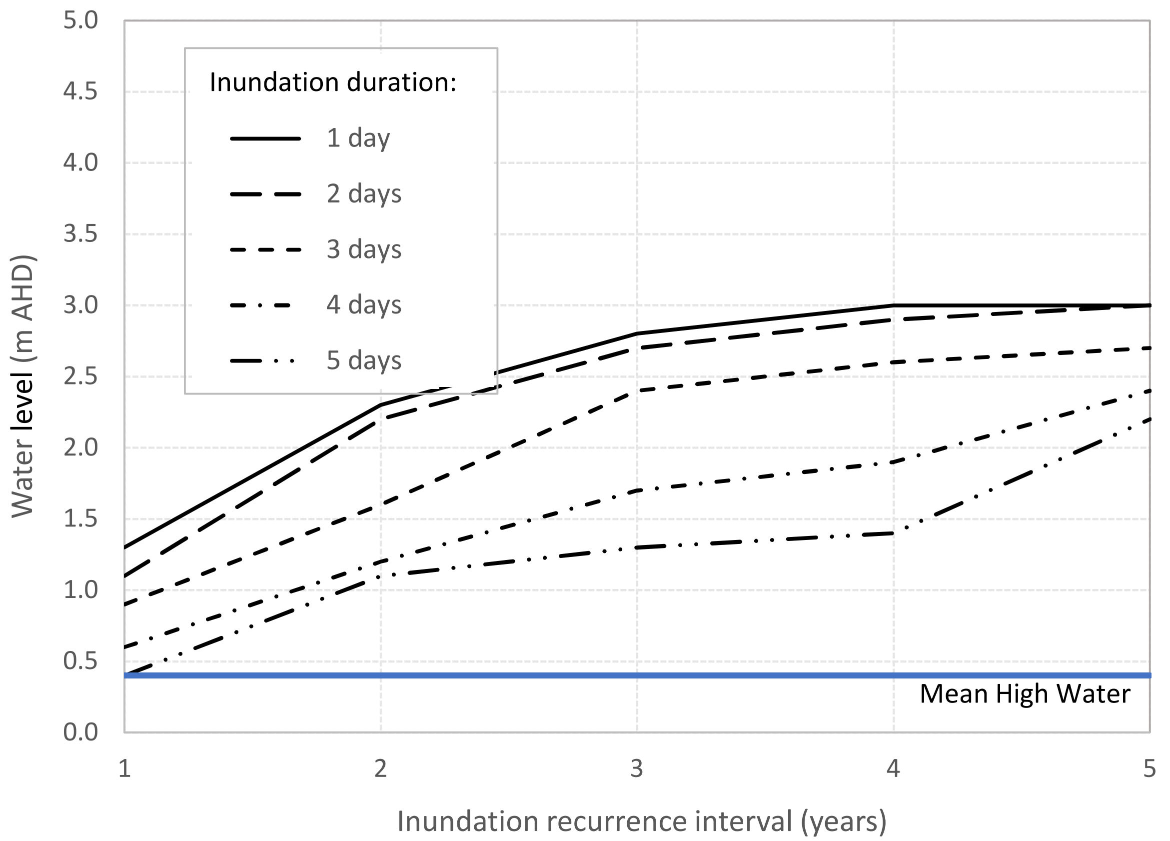

Figure S22. Water levels corresponding to inundation durations of 1 to 5 days with recurrence intervals of 1 to 5 years for Woodburn (Station 203412)

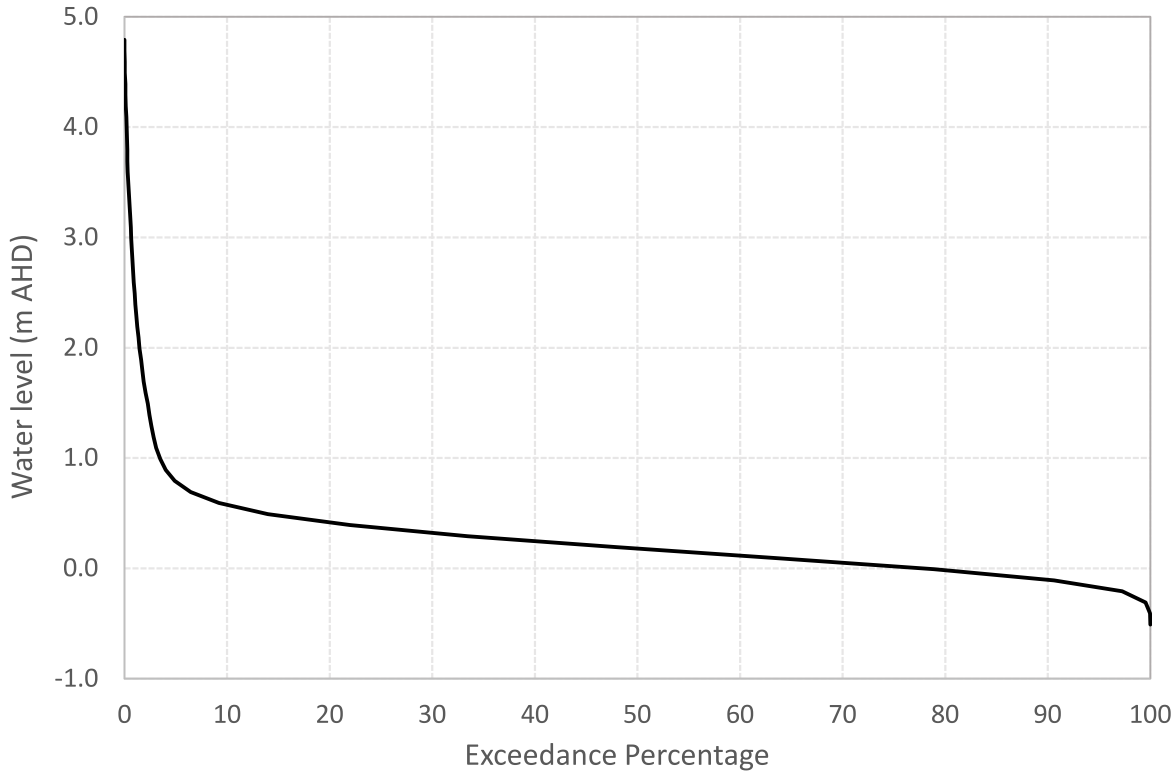

Figure S23. Frequency distribution of water levels at Bungawalbin (Station 203450)

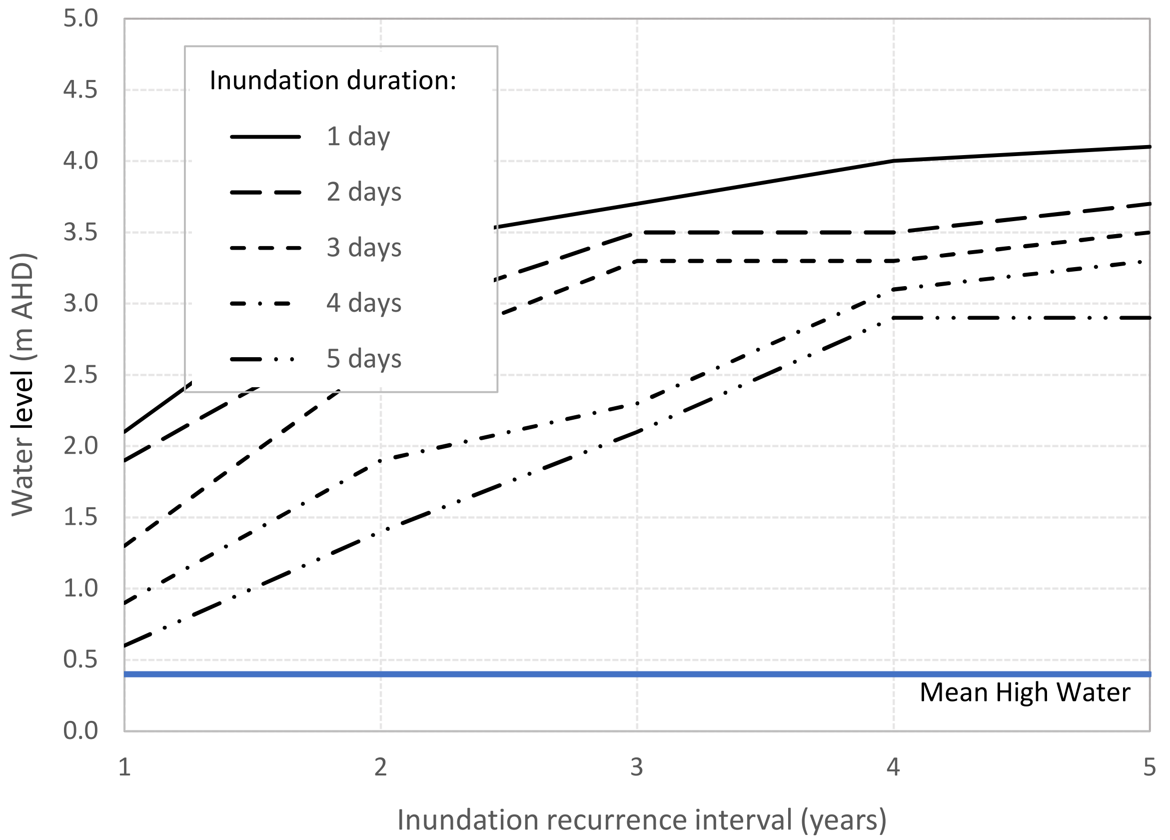

Figure S24. Water levels corresponding to inundation durations of 1 to 5 days with recurrence intervals of 1 to 5 years for Bungawalbin (Station 203450)

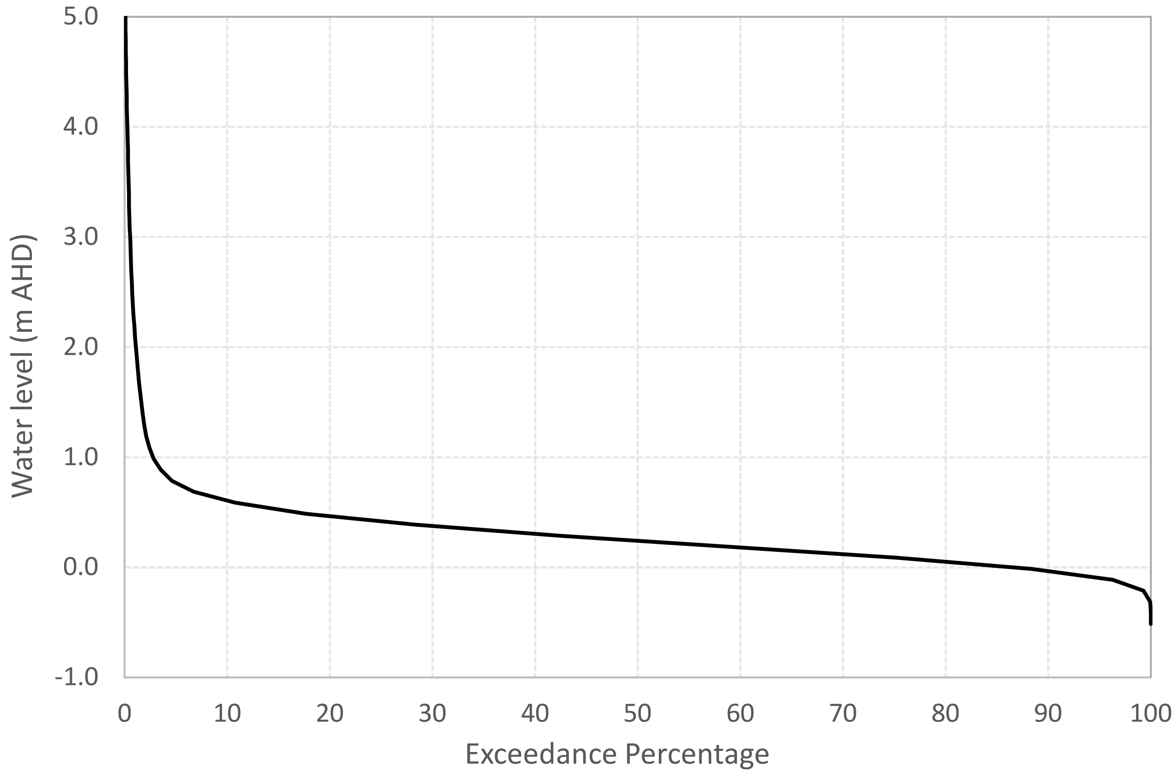

Figure S25. Frequency distribution of water levels at Coraki (Station 203403)

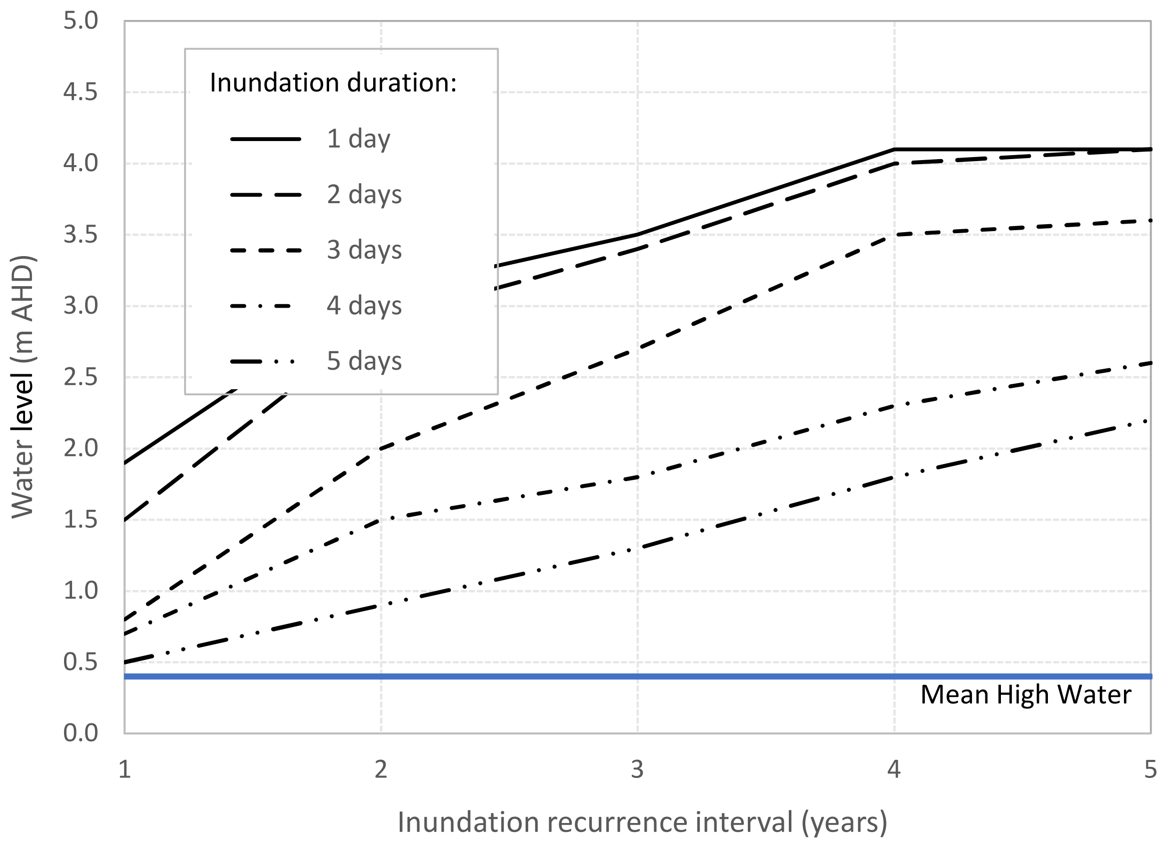

Figure S26. Water levels corresponding to inundation durations of 1 to 5 days with recurrence intervals of 1 to 5 years for Coraki (Station 203403)

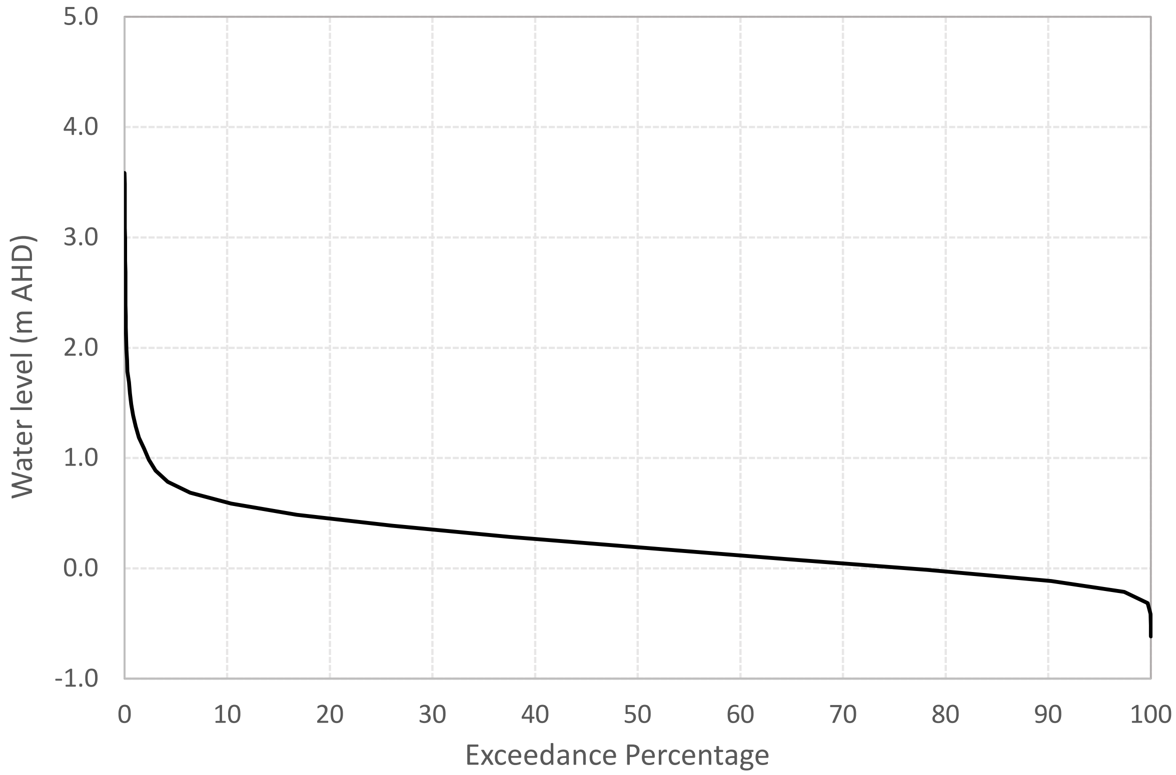

Figure S27. Frequency distribution of water levels at Rocky Mouth Creek (Station 203432)

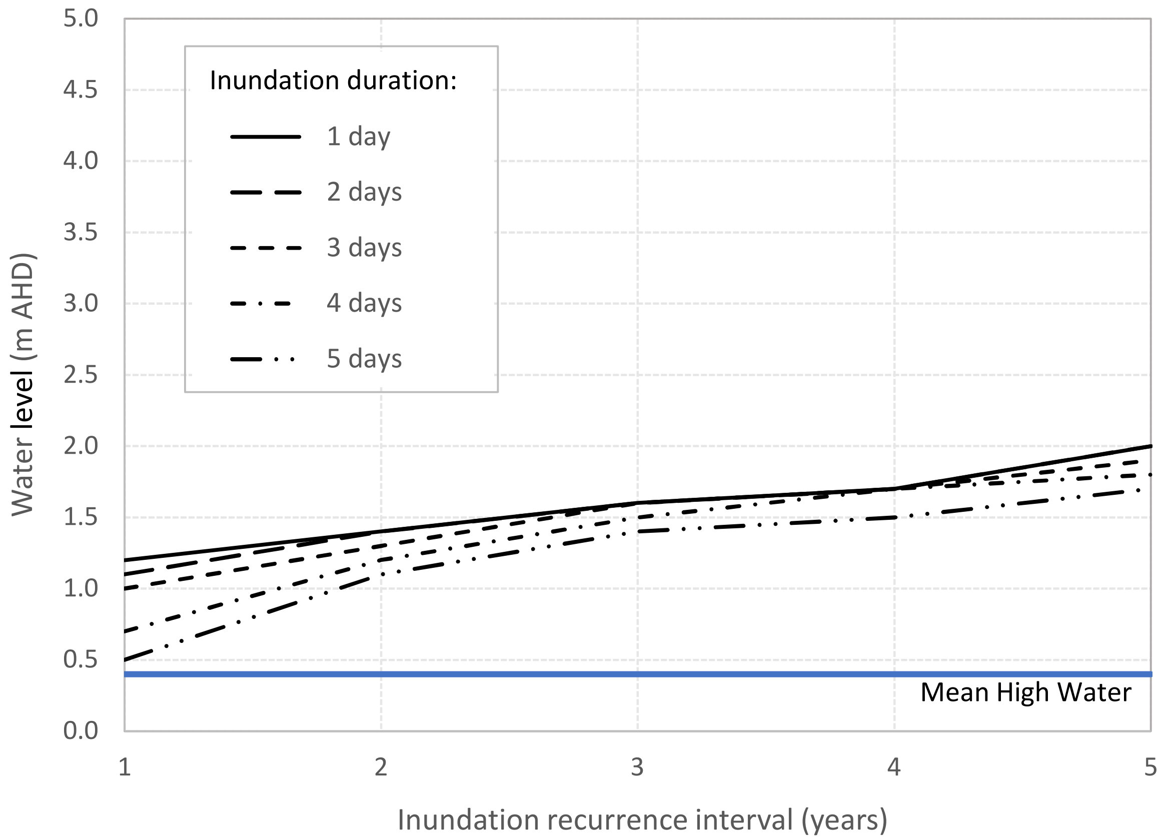

Figure S28. Water levels corresponding to inundation durations of 1 to 5 days with recurrence intervals of 1 to 5 years for Rocky Mouth Creek (Station 203432)

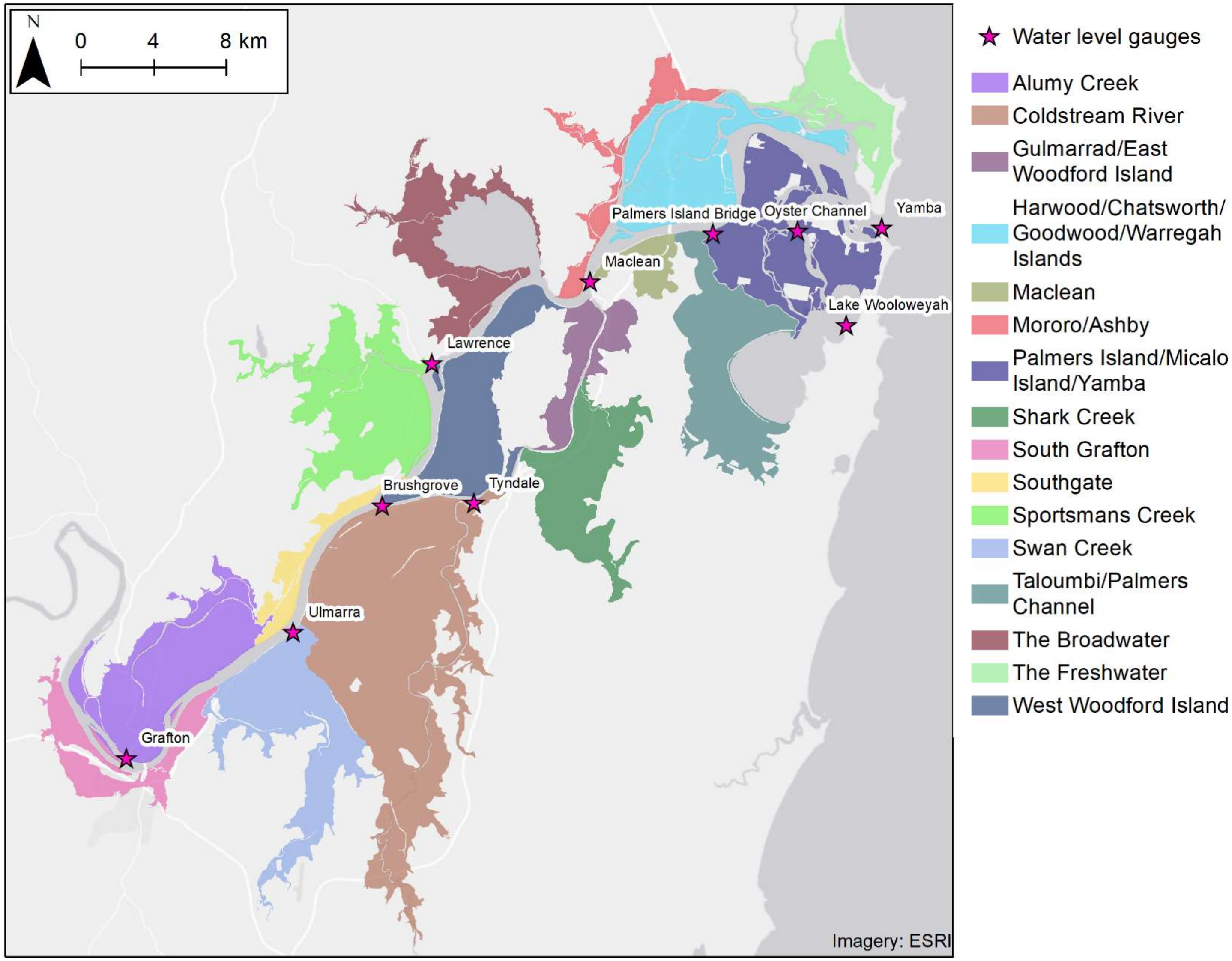

Figure S29. Water level gauge locations, Clarence River

Table S6. Details of water level gauges, Clarence River

Station	Length of record** (years)	Mean High Water level (m AHD)	Blackwater inundation level (m AHD)	
			Median	Maximum
Yamba (204454)	32.5	0.5	0.9	1.9
Oyster Channel (204451)	15.9	0.3	0.5	0.8
Palmers Island Bridge (204426)	17.8	0.3	0.9	1.8
Maclean (204410)	29.3	0.3	0.8	2.5
Tyndale (204465)	16.3	0.3	1.9	3.8
Brushgrove (204406)	27.7	0.3	1.4	4.1
Lawrence (204453)	10.8	0.3	1.9	3.4
Ulmarra (204480)	15.6	0.4	2.2	5.0
Grafton (204400)	28.9	0.4	1.5	6.2

* Mean High Water adopted as minimum blackwater inundation level
** Excluding data gaps in excess of 6 hours

Table S7. Distribution of water level gauges to catchments, Clarence River

Catchment	Water level station(s) adopted
Palmers Island/Micalo Island/Yamba	Oyster Channel
Taloumbi/Palmers Channel	Palmers Island Bridge
The Freshwater	0.76 x Yamba + 0.24 x Palmers Island Bridge
Mororo/Ashby	Palmers Island Bridge + 0.46 x Maclean
Harwood/Chatsworth/Goodwood/ Warregah Islands	0.31 x Yamba + 0.69 x Palmers Island Bridge
Maclean	0.69 x Palmers Island Bridge + 0.31 x Maclean
The Broadwater	0.64 x Maclean + 0.36 x Lawrence
West Woodford Island	0.23 x Maclean + 0.77 x Lawrence
Gulmarrad/East Woodford Island	0.89 x Maclean + 0.11 x Tyndale
Shark Creek	0.65 x Maclean + 0.35 x Tyndale
Coldstream River	Tyndale
Sportsmans Creek	Lawrence
Southgate	0.46 x Brushgrove + 0.54 x Ulmarra
Alumy Creek	0.83 x Ulmarra + 0.17 x Grafton
Swan Creek	0.60 x Ulmarra + 0.40 x Grafton
South Grafton	Grafton

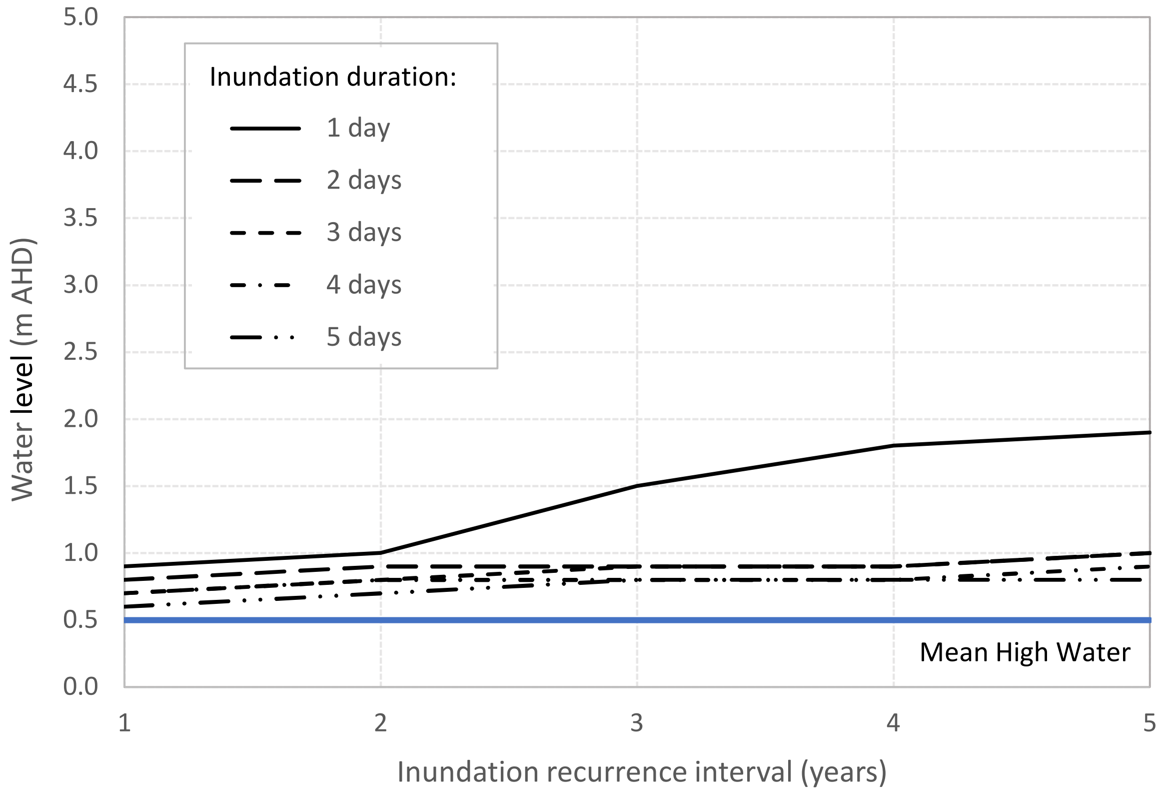

Figure S30. Frequency distribution of water levels at Yamba (Station 204454)

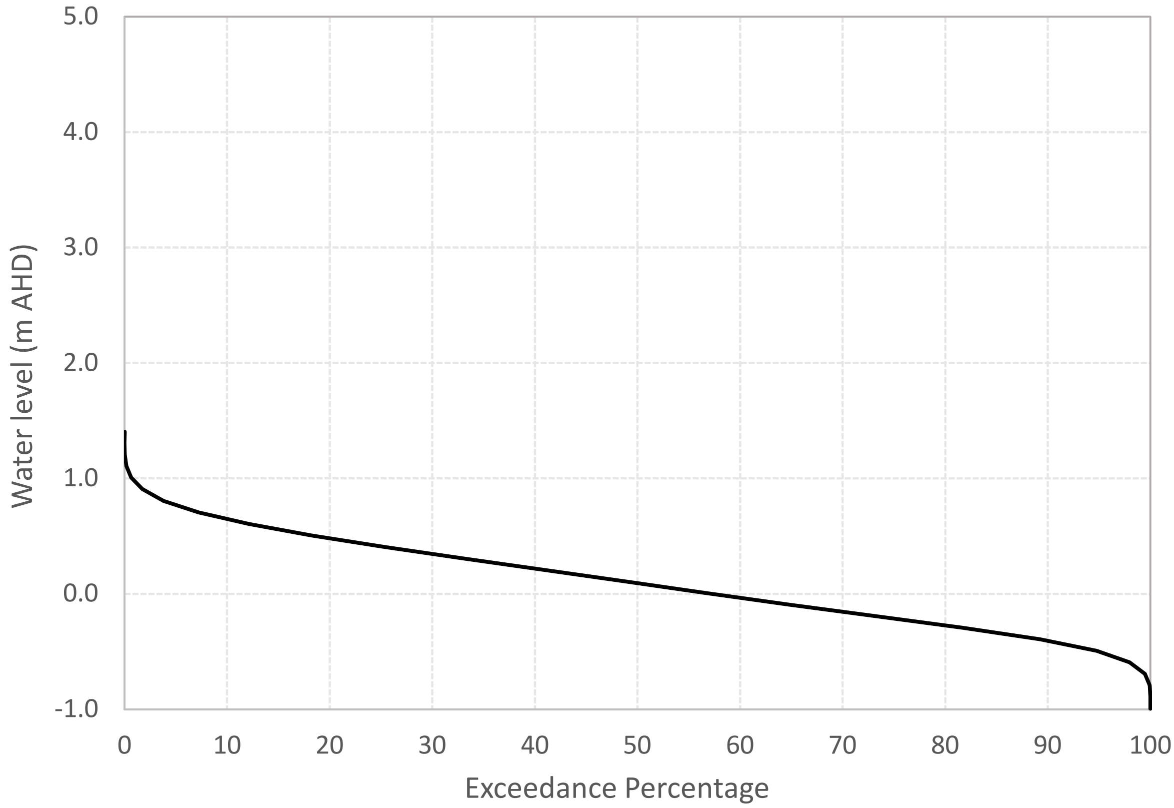

Figure S31. Water levels corresponding to inundation durations of 1 to 5 days with recurrence intervals of 1 to 5 years for Yamba (Station 204454)

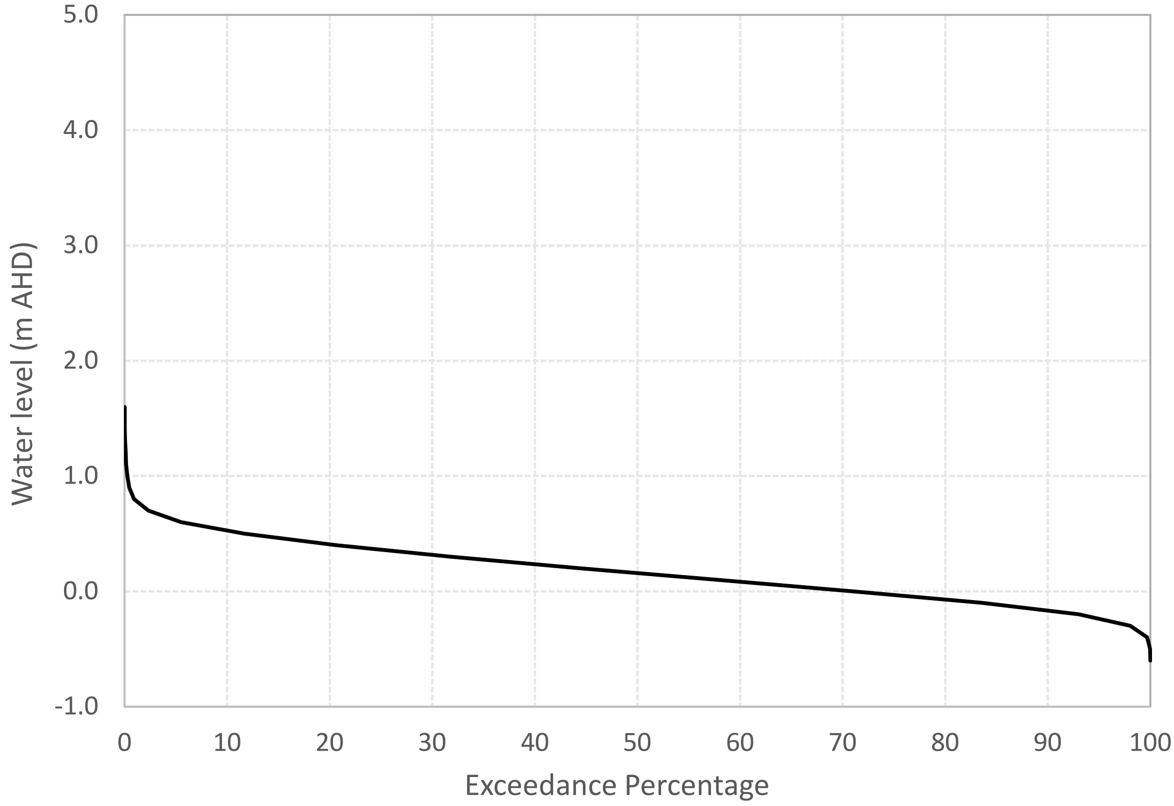

Figure S32. Frequency distribution of water levels at Oyster Channel (Station 204451)

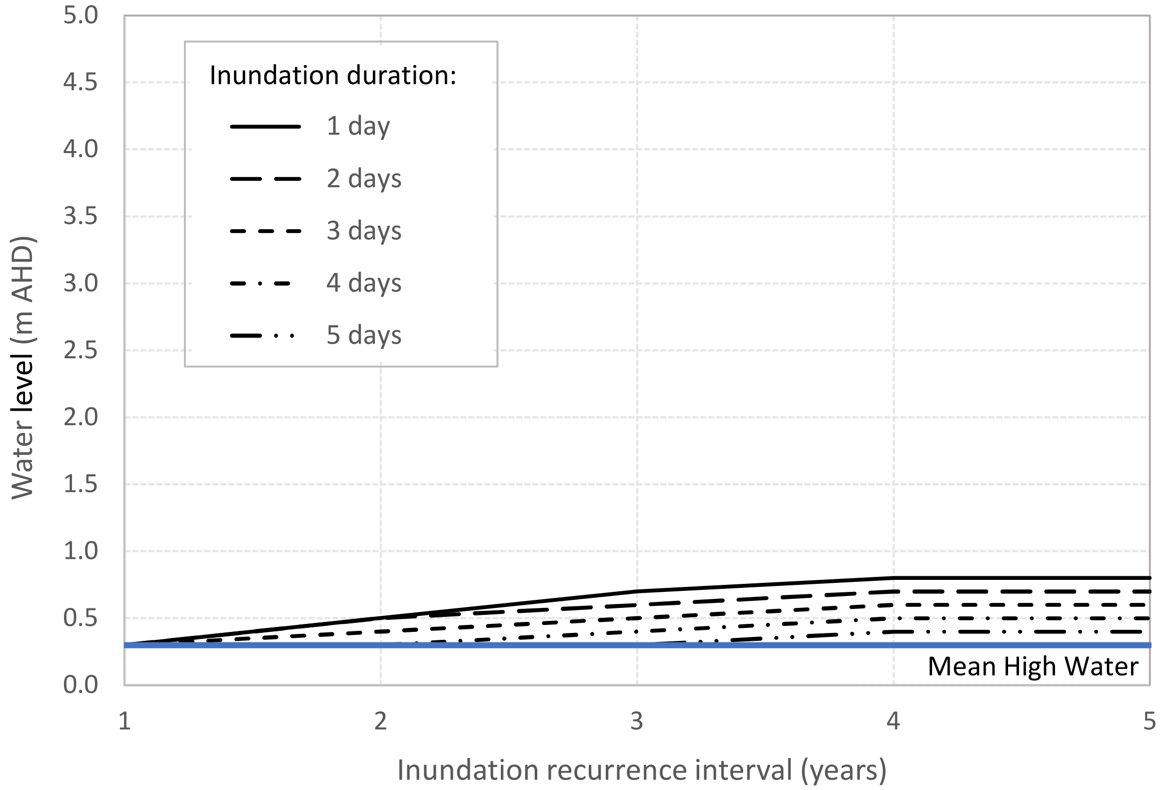

Figure S33. Water levels corresponding to inundation durations of 1 to 5 days with recurrence intervals of 1 to 5 years for Oyster Channel (Station 204451)

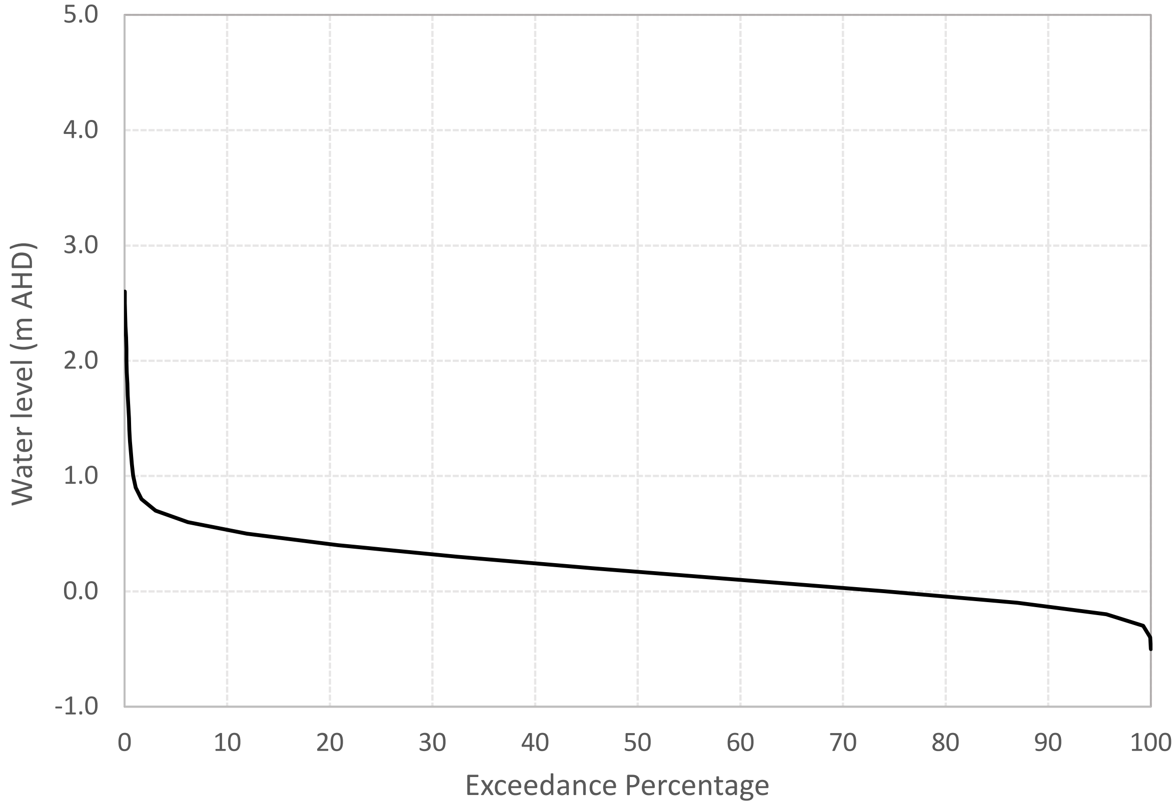

Figure S34. Frequency distribution of water levels at Palmers Island Bridge (Station 204426)

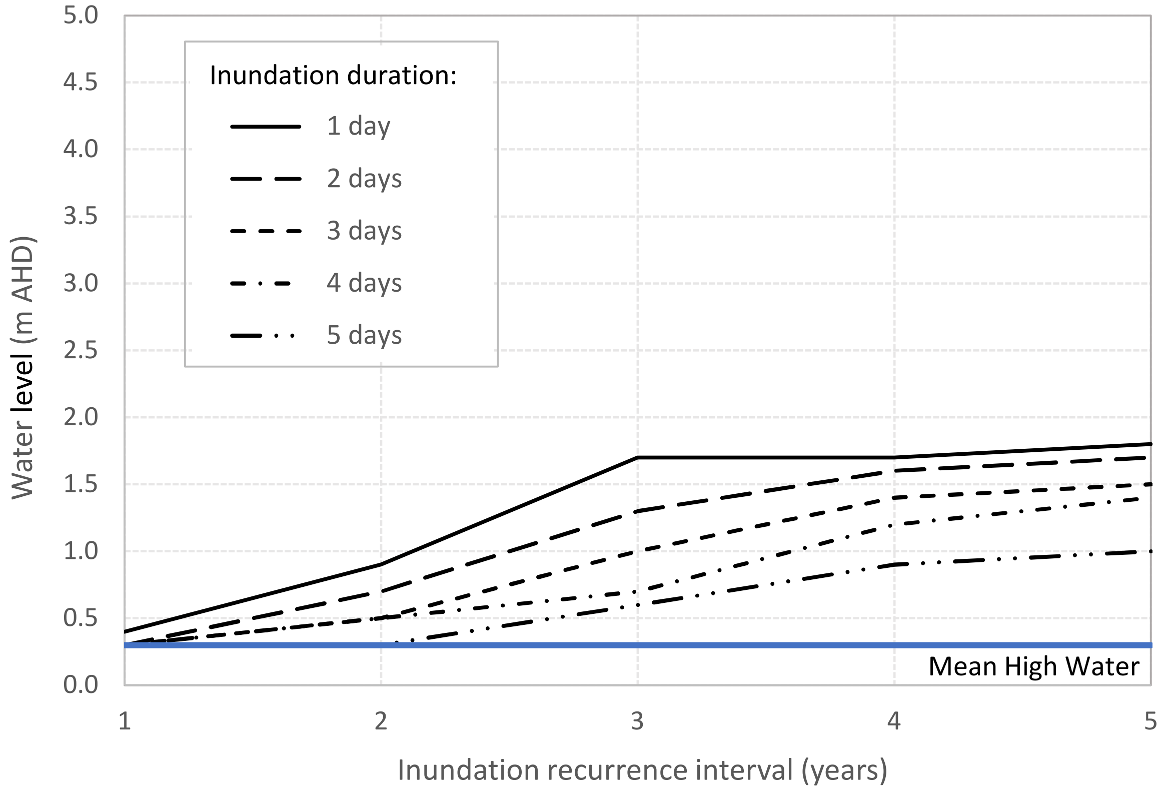

Figure S35. Water levels corresponding to inundation durations of 1 to 5 days with recurrence intervals of 1 to 5 years for Palmers Island Bridge (Station 204426)

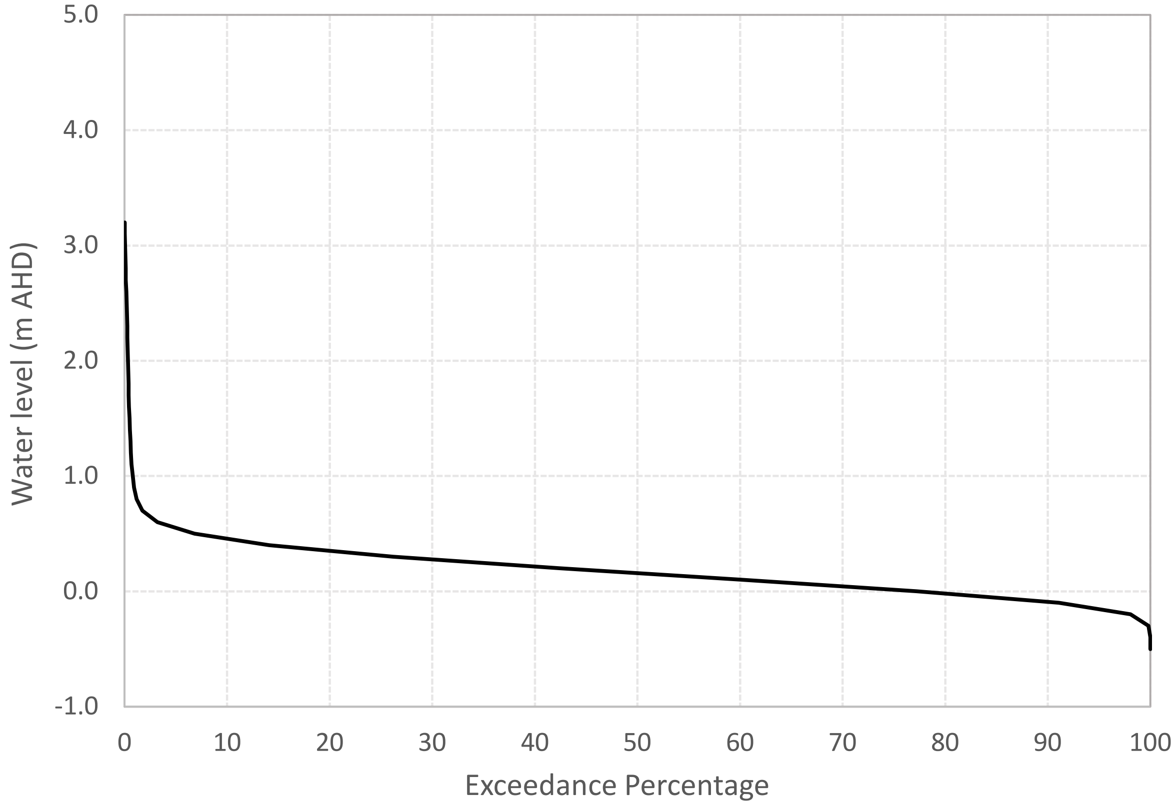

Figure S36. Frequency distribution of water levels at Maclean (Station 204410)

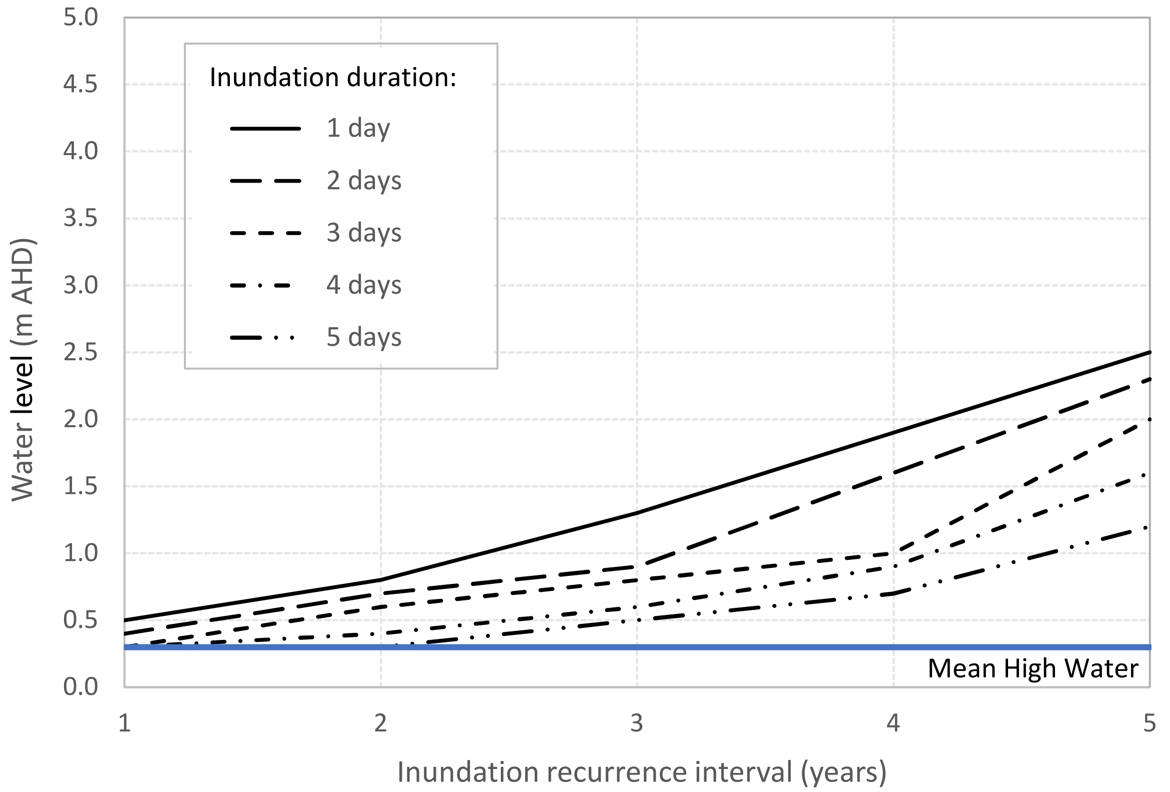

Figure S37. Water levels corresponding to inundation durations of 1 to 5 days with recurrence intervals of 1 to 5 years for Maclean (Station 204410)

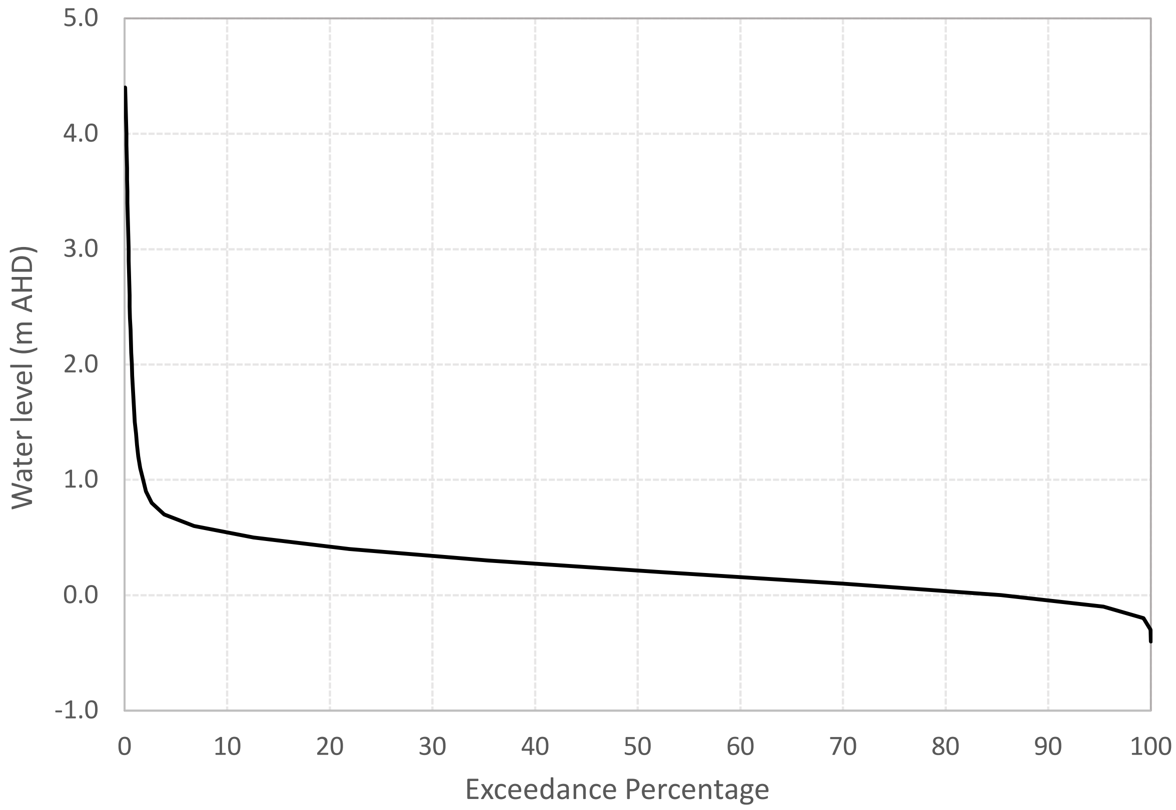

Figure S38. Frequency distribution of water levels at Tyndale (Station 204465)

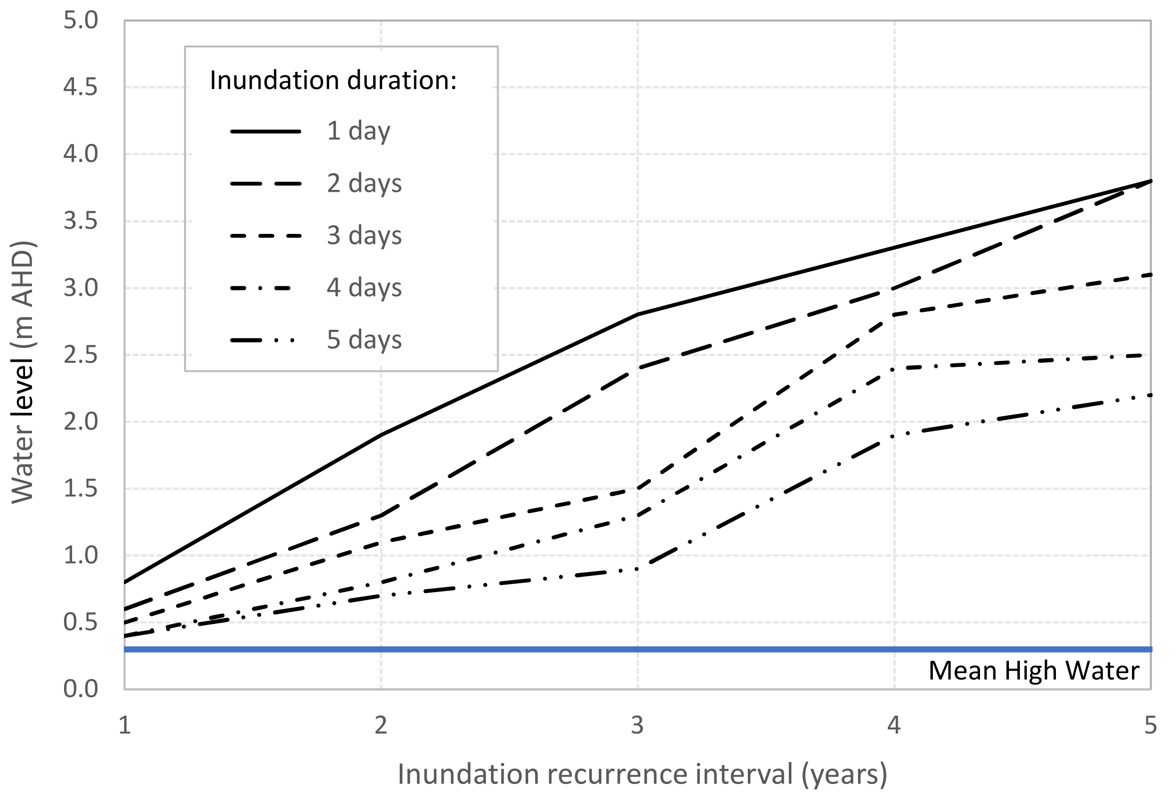

Figure S39. Water levels corresponding to inundation durations of 1 to 5 days with recurrence intervals of 1 to 5 years for Tyndale (Station 204465)

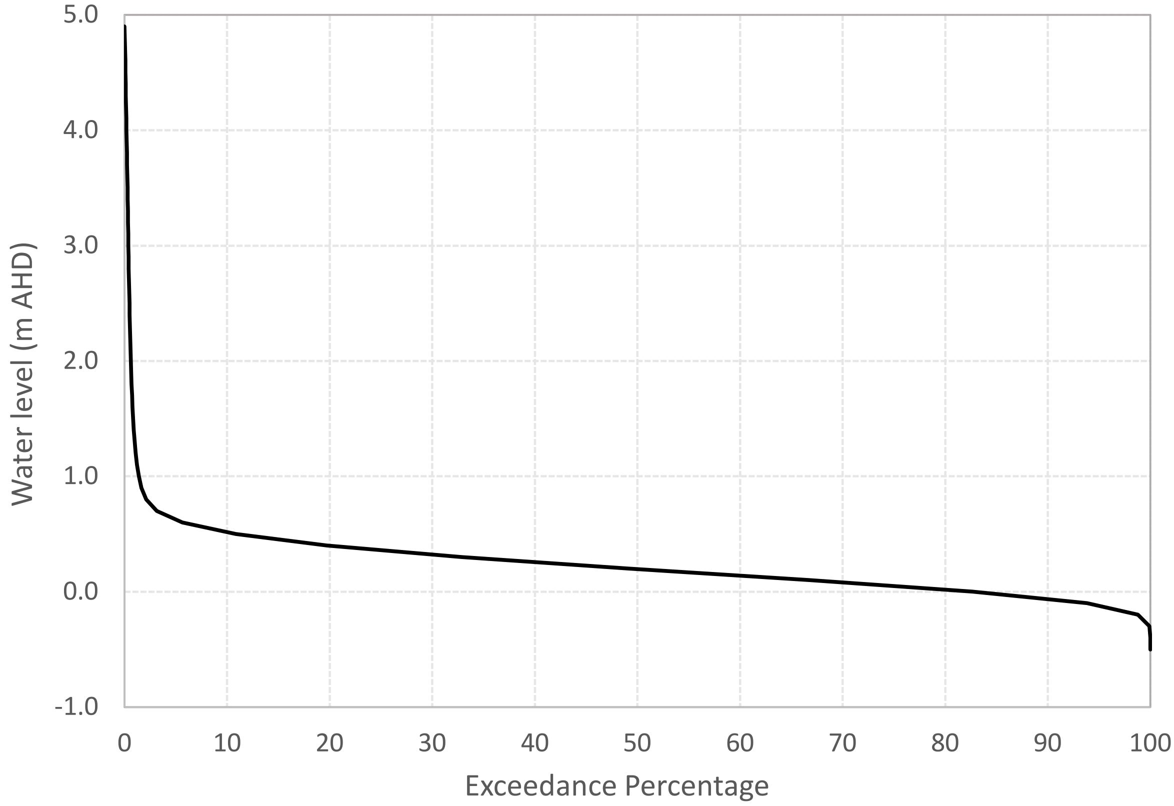

Figure S40. Frequency distribution of water levels at Brushgrove (Station 204406)

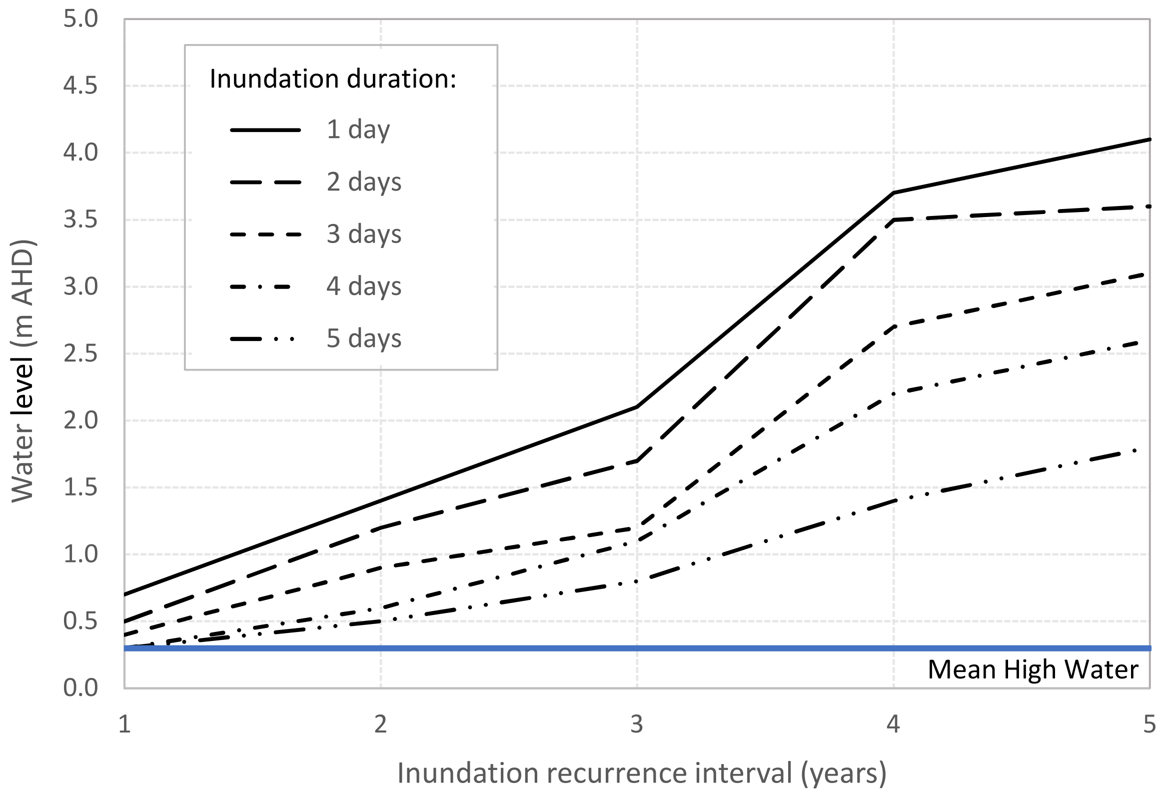

Figure S41. Water levels corresponding to inundation durations of 1 to 5 days with recurrence intervals of 1 to 5 years for Brushgrove (Station 204406)

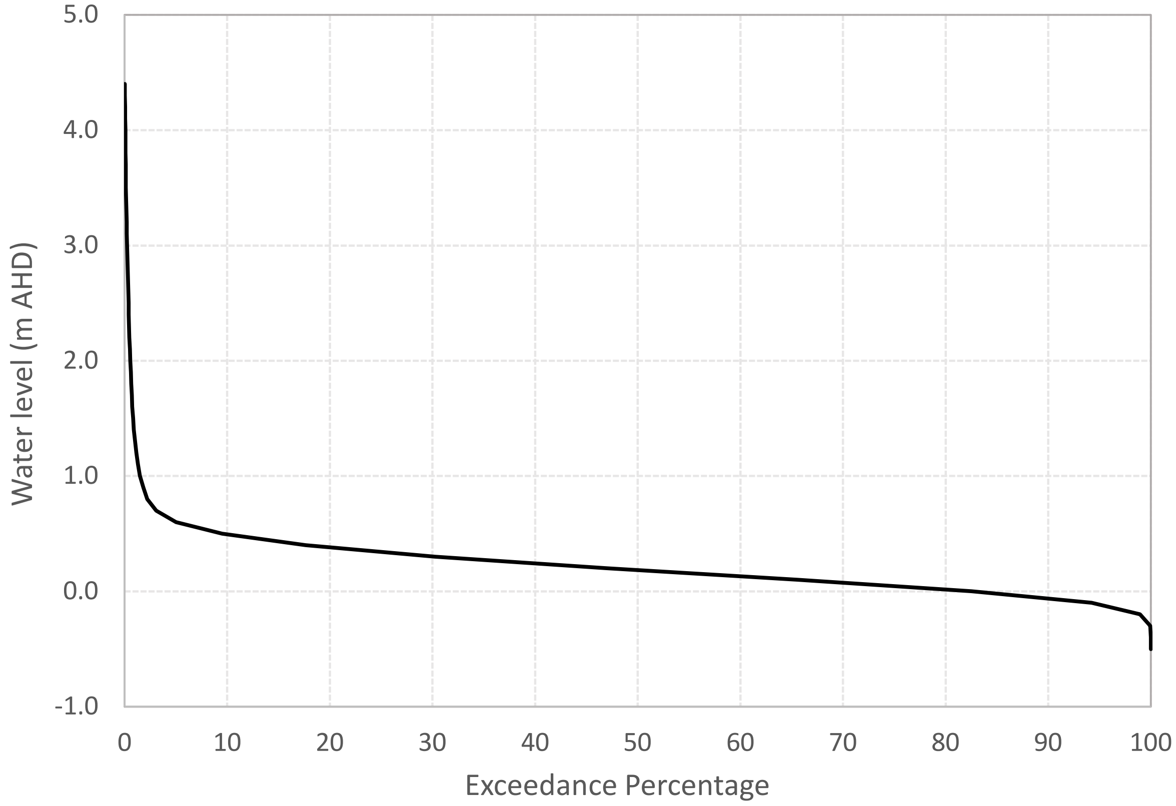

Figure S42. Frequency distribution of water levels at Lawrence (Station 204453)

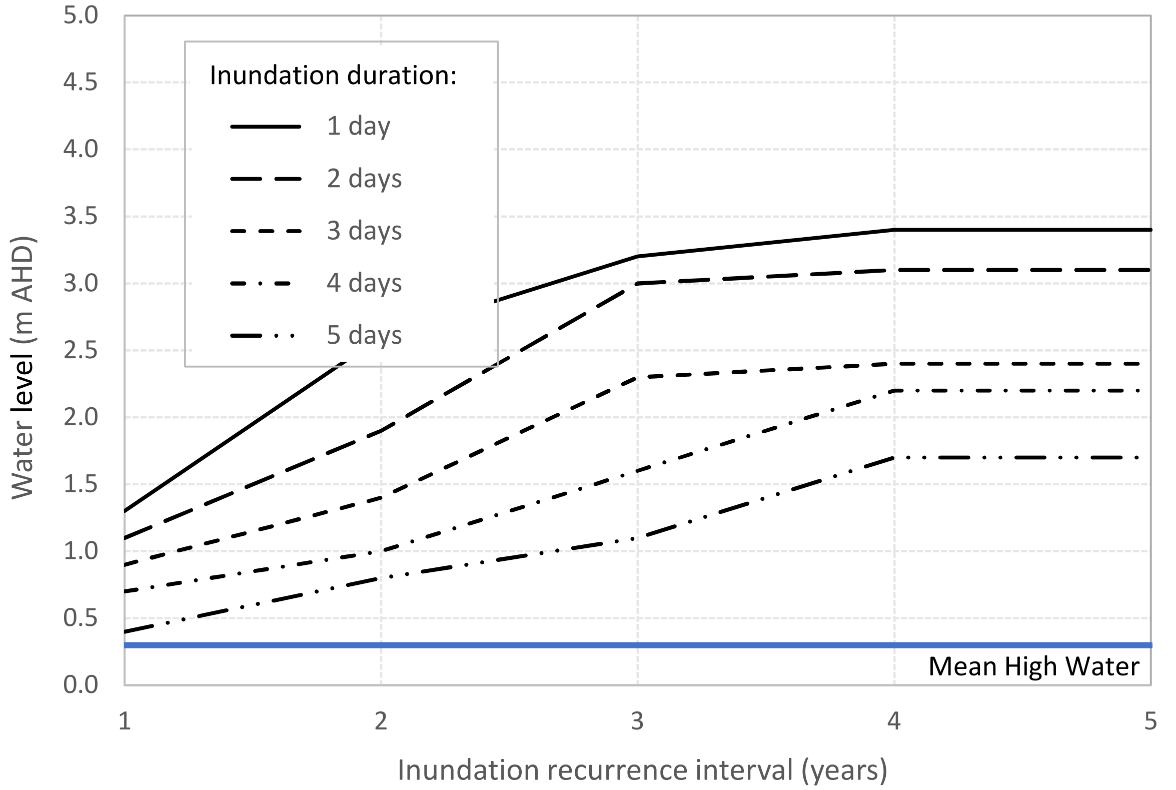

Figure S43. Water levels corresponding to inundation durations of 1 to 5 days with recurrence intervals of 1 to 5 years for Lawrence (Station 204453)

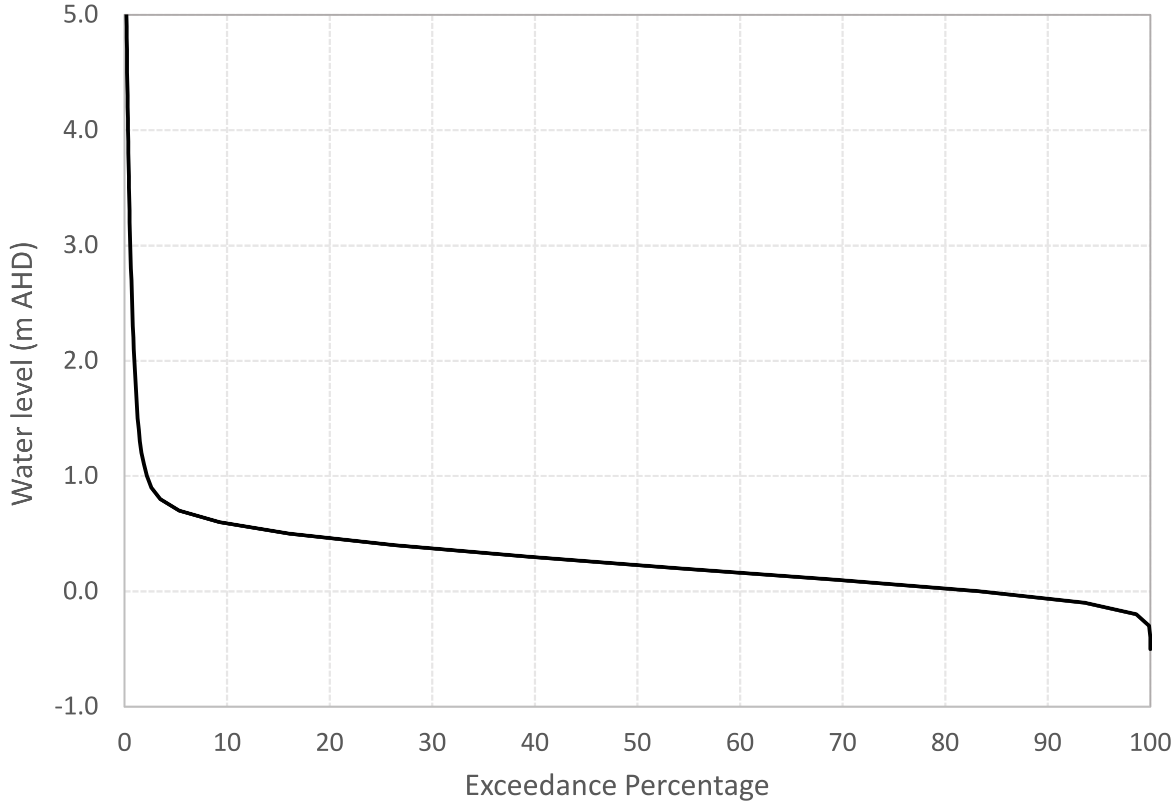

Figure S44. Frequency distribution of water levels at Ulmarra (Station 204480)

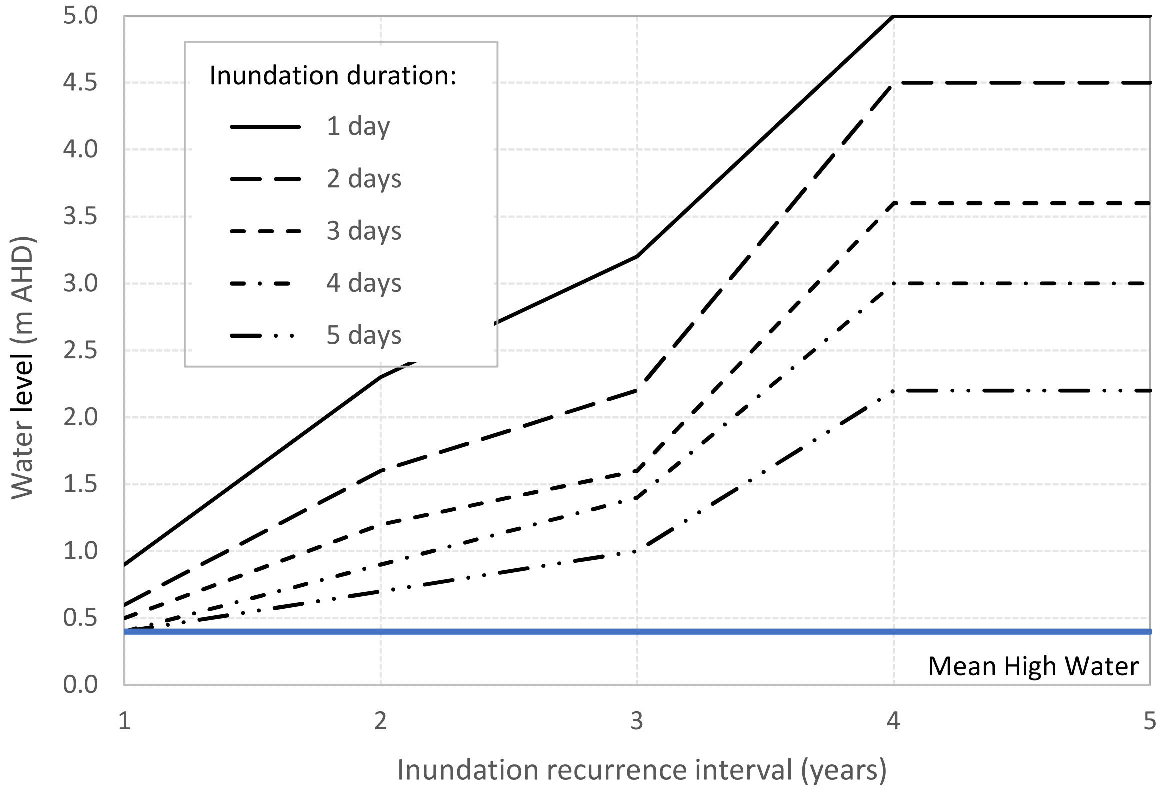

Figure S45. Water levels corresponding to inundation durations of 1 to 5 days with recurrence intervals of 1 to 5 years for Ulmarra (Station 204480)

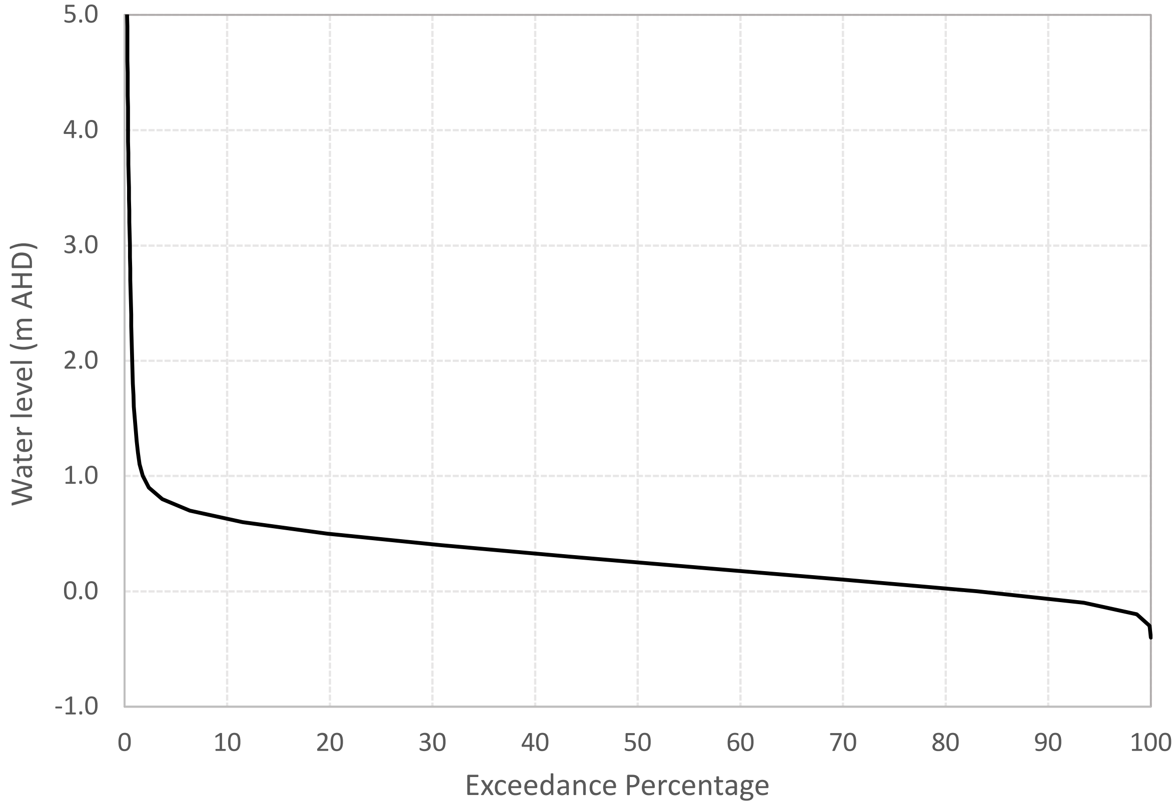

Figure S46. Frequency distribution of water levels at Grafton (Station 204400)

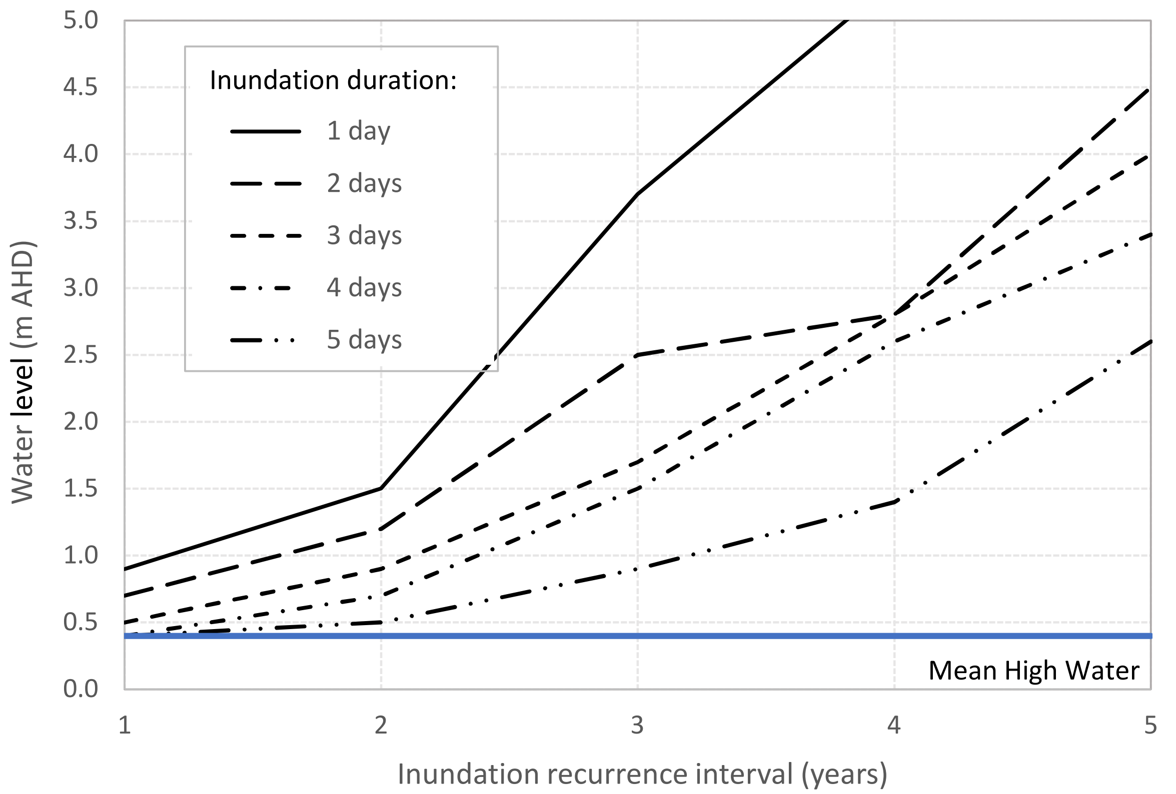

Figure S47. Water levels corresponding to inundation durations of 1 to 5 days with recurrence intervals of 1 to 5 years for Grafton (Station 204400)

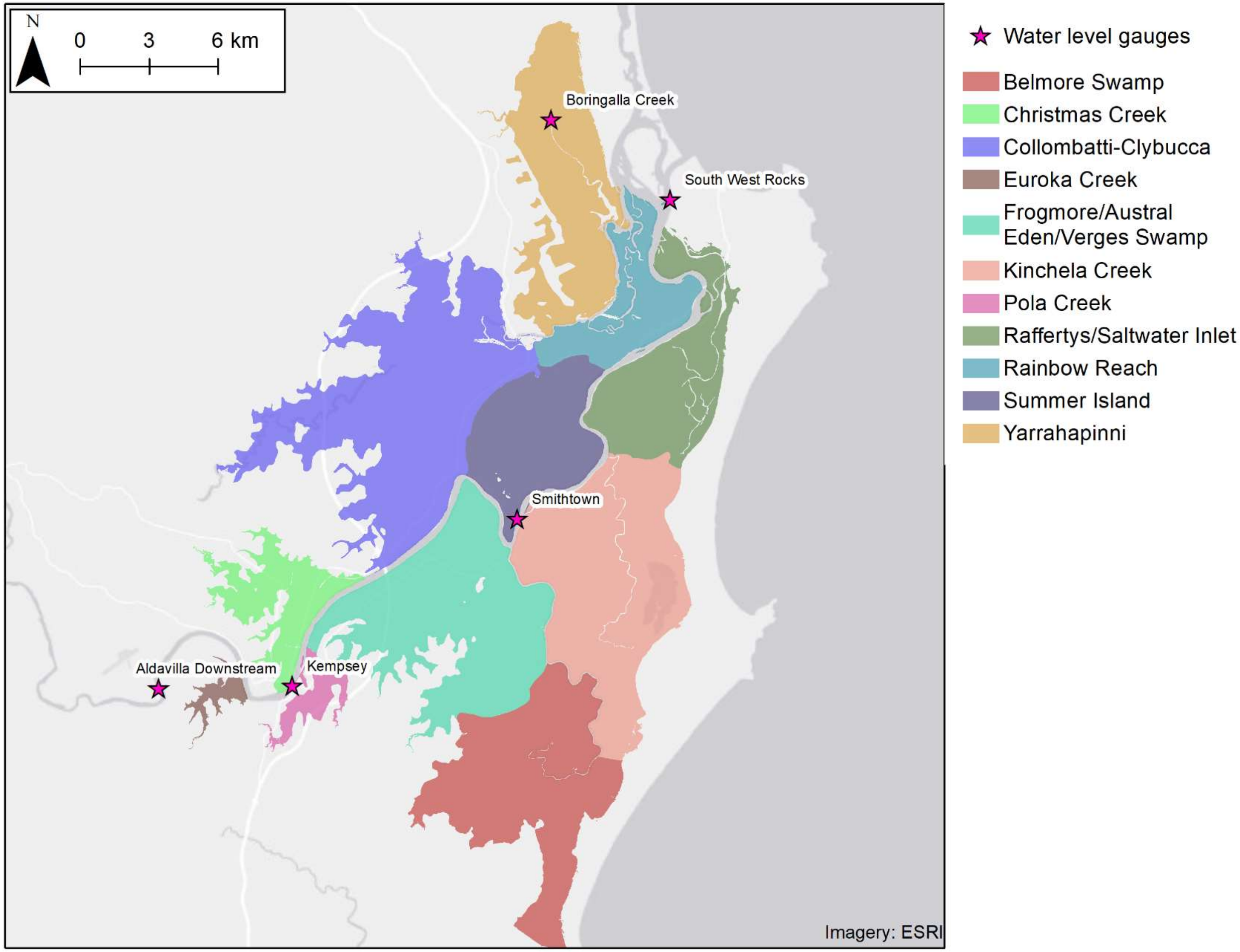

Figure S48. Water level gauge locations, Macleay River

Table S8. Details of water level gauges, Macleay River

Station	Length of record** (years)	Mean High Water level (m AHD)	Blackwater inundation level (m AHD)	
			Median	Maximum
South West Rocks (206456)	31.4	0.5	0.5*	0.5
Borigala Creek (206450)	11.9	N/A***	1.1	1.1
Smithtown (206406)	33.2	0.4	1.1	3.7
Kempsey (206402)	35.3	0.5	2.2	5.6
Aldavilla Downstream (206459)	11.9	0.5	1.4	6.7

* Mean High Water adopted as minimum blackwater inundation level

** Excluding data gaps in excess of 6 hours

*** Minimum level of 0.5 assumed from South West Rocks.

Table S9. Distribution of water level gauges to catchments, Macleay River

Catchment	Water level station(s) adopted
Belmore Swamp*	Assumed to be the same as Frogmore-Austral Eden-Verges Swamp
Christmas Creek	0.33 x Smithtown + 0.67 x Kempsey
Collombatti-Clybucca*	Assumed to be the same as Yarrahapinni
Euroka Creek	0.77 x Kempsey + 0.23 x Aldavilla Downstream
Frogmore-Austral/Eden-Verges Swamp	0.92 x Smithtown + 0.08 x Kempsey
Kinchela Creek	0.23 x South West Rocks + 0.77 x Smithtown
Pola Creek	0.09 x Smithtown + 0.91 x Kempsey
Raffertys-Saltwater Inlet	0.50 x South West Rocks + 0.50 x Smithtown
Rainbow Reach	0.82 x South West Rocks + 0.18 x Smithtown
Summer Island	0.35 x South West Rocks + 0.65 x Smithtown
Yarrahapinni	Borirgala Creek

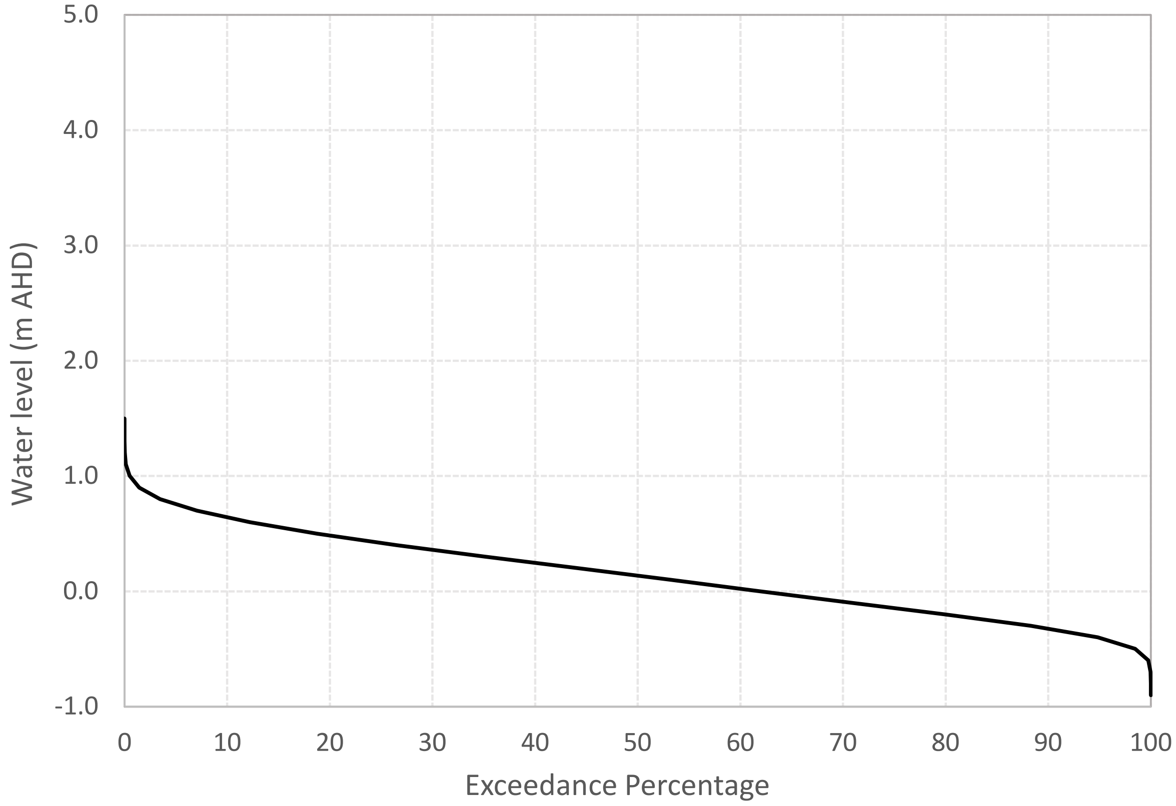

Figure S49. Frequency distribution of water levels at South West Rocks (Station 20646)

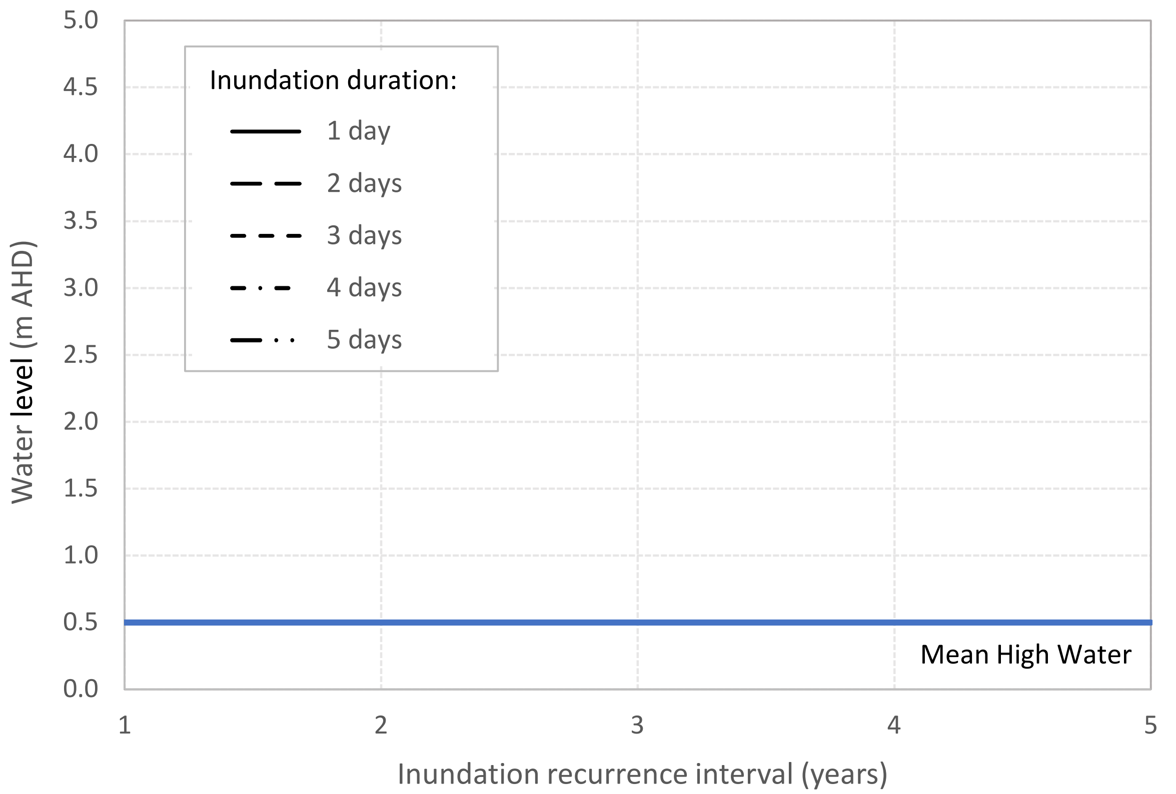

Figure S50. Water levels corresponding to inundation durations of 1 to 5 days with recurrence intervals of 1 to 5 years for South West Rocks (Station 20646)

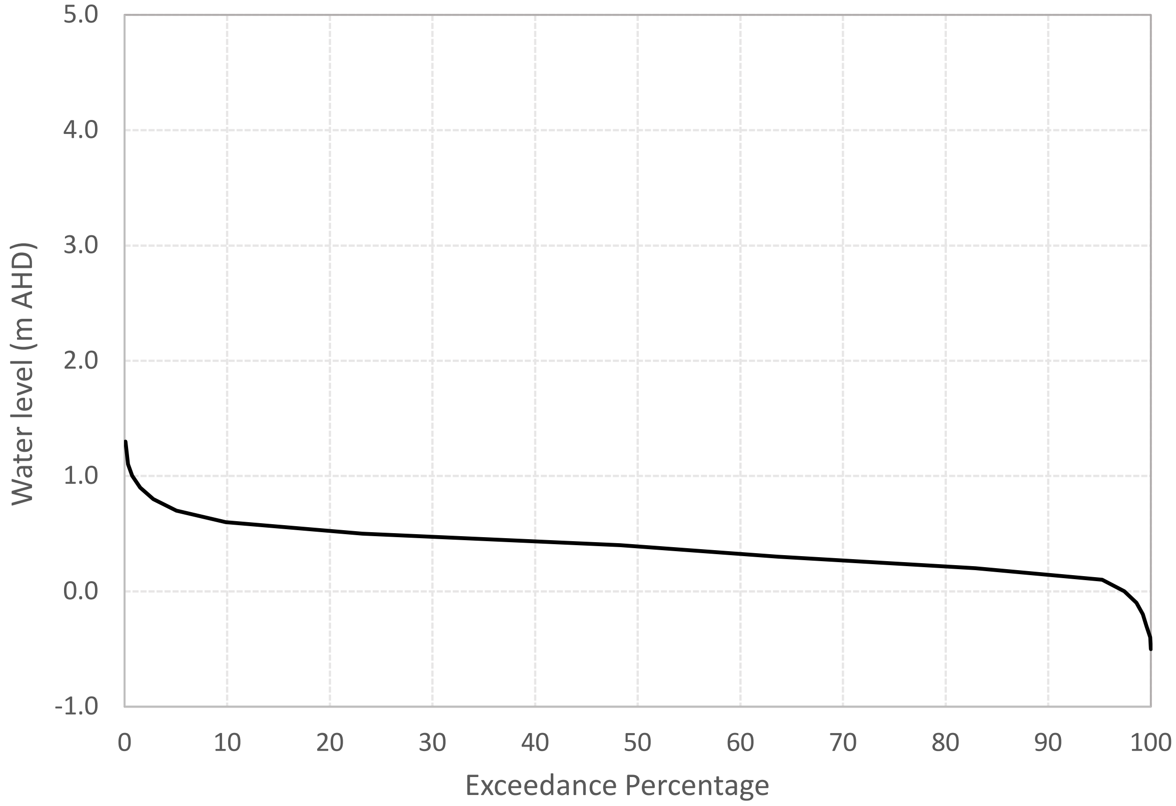

Figure S51. Frequency distribution of water levels at Borigala Creek (Station 206450)

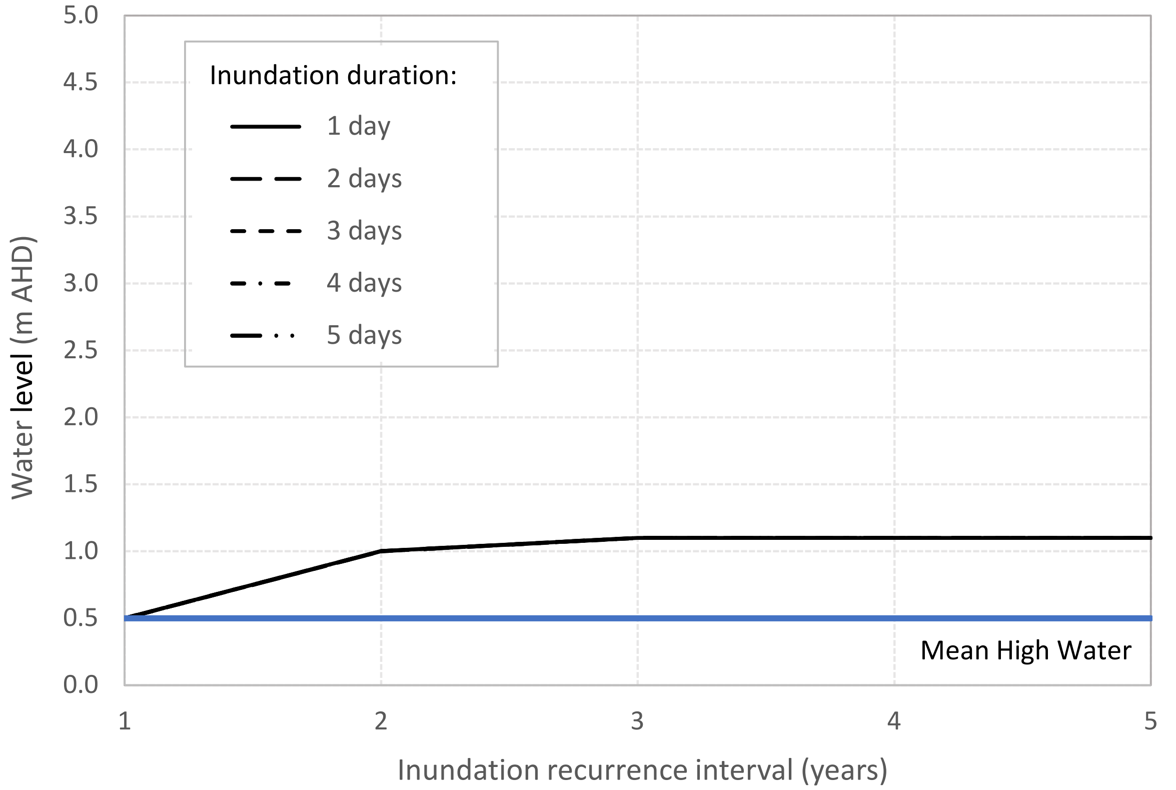

Figure S52. Water levels corresponding to inundation durations of 1 to 5 days with recurrence intervals of 1 to 5 years for Borigala Creek (Station 206450)

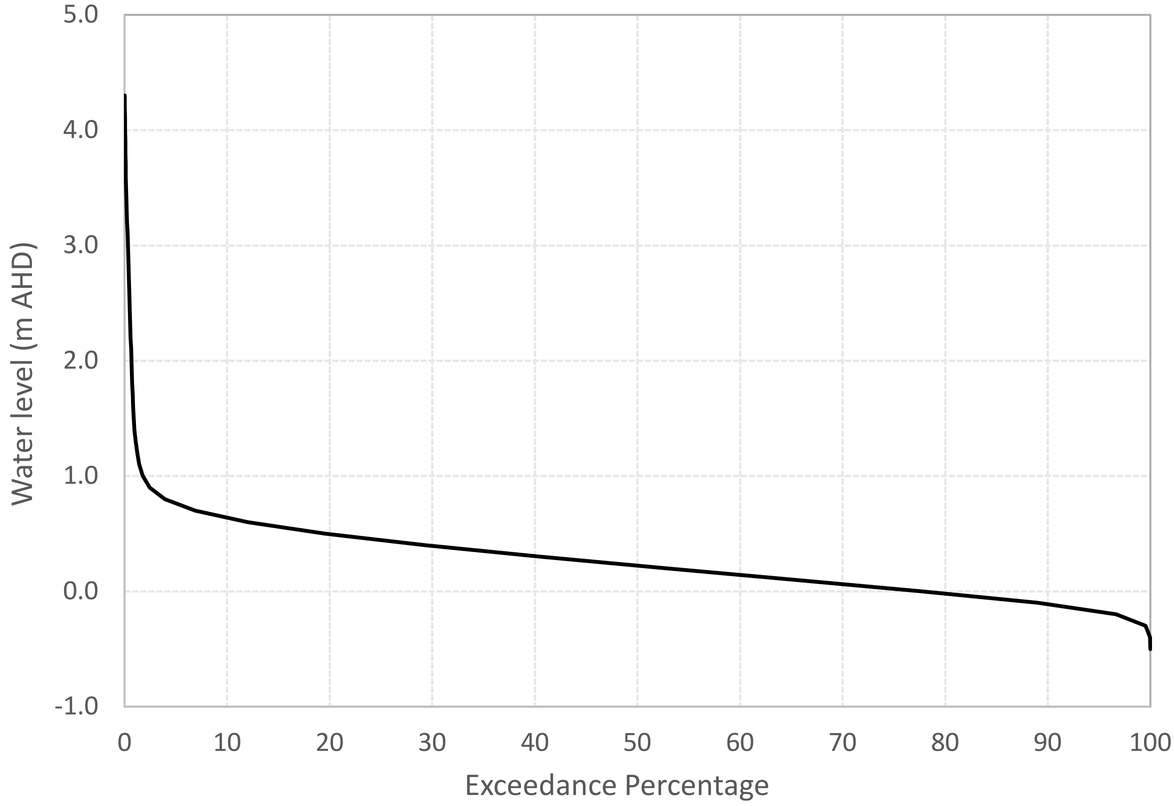

Figure S53. Frequency distribution of water levels at Smithtown (Station 206406)

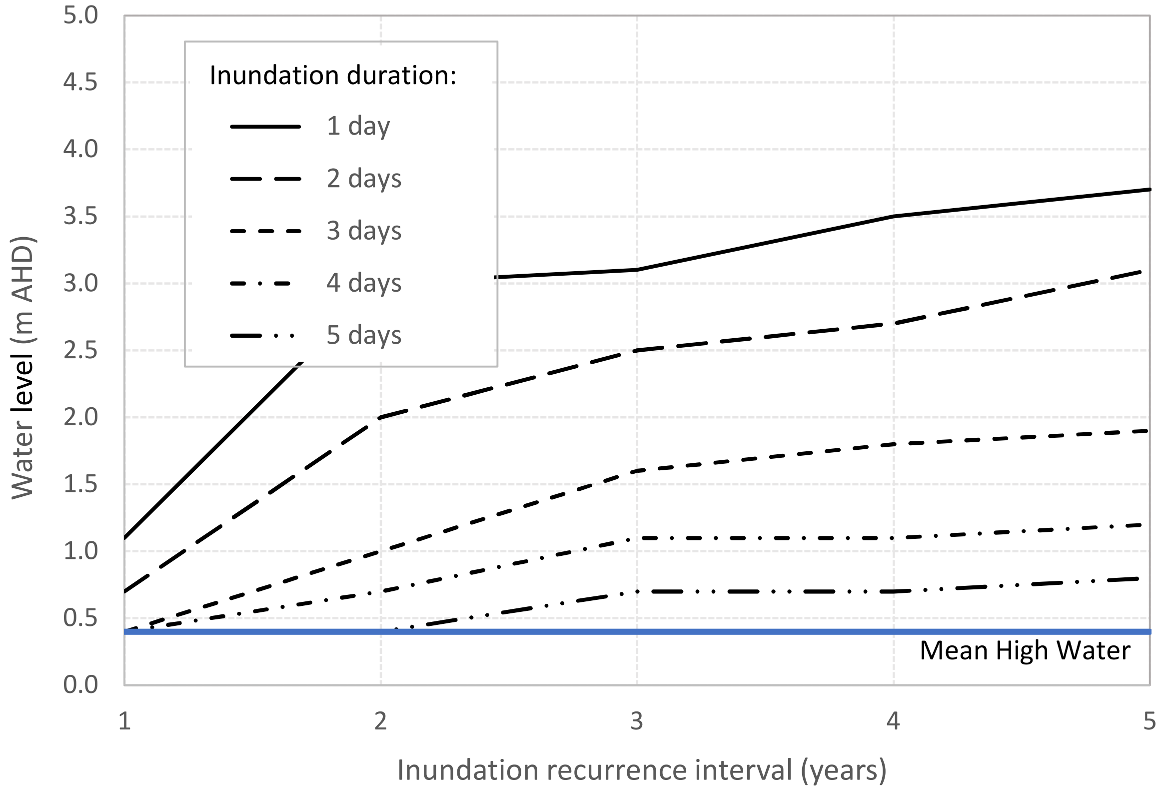

Figure S54. Water levels corresponding to inundation durations of 1 to 5 days with recurrence intervals of 1 to 5 years for Smithtown (Station 206406)

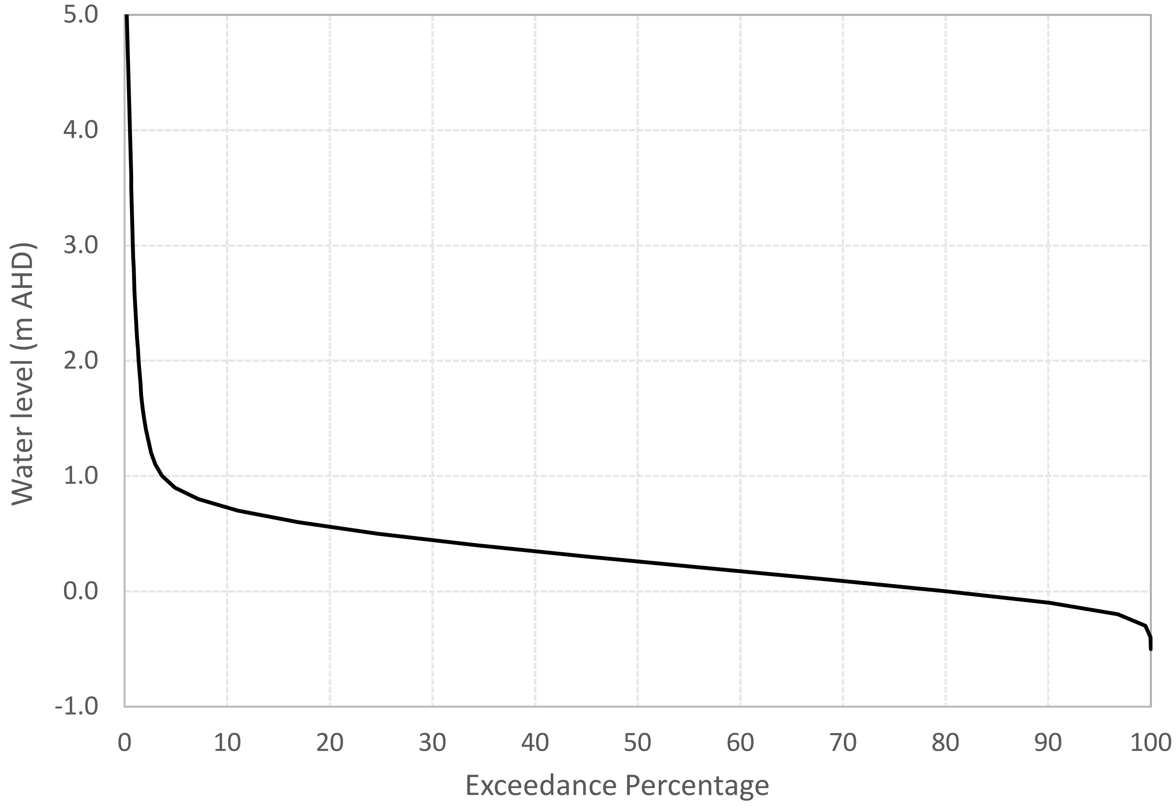

Figure S55. Frequency distribution of water levels at Kempsey (Station 206402)

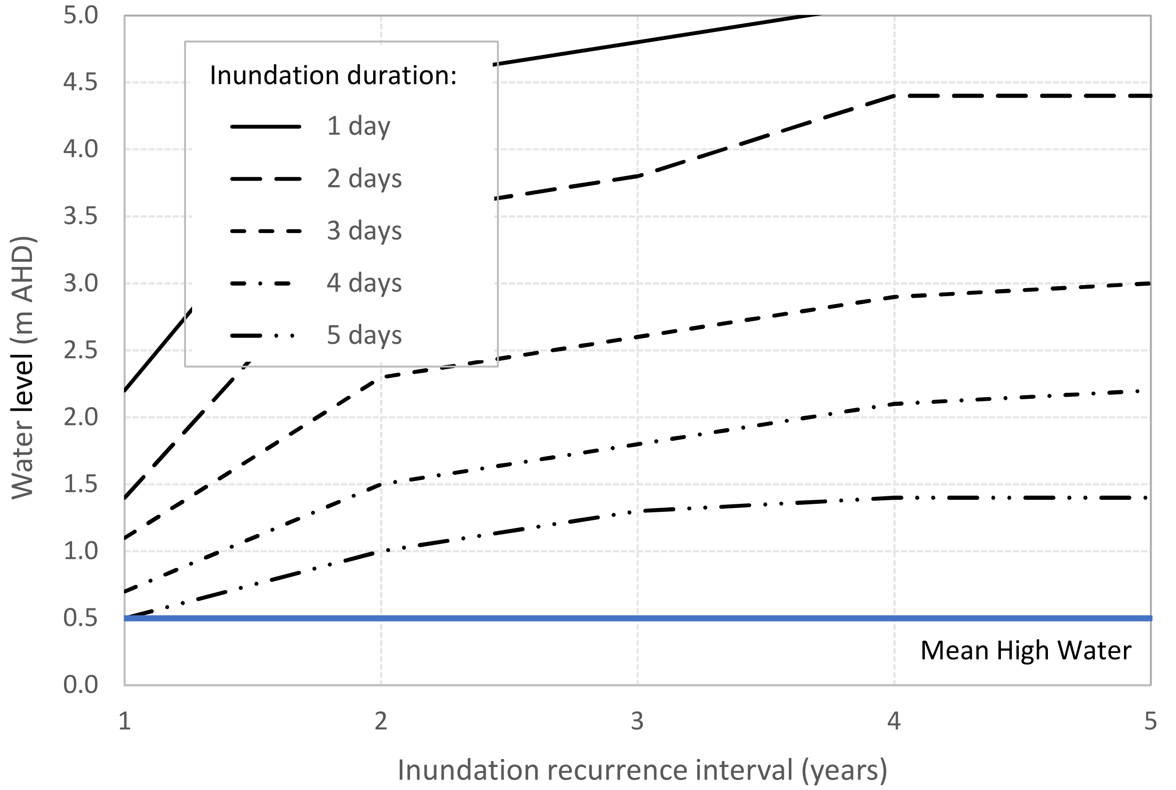

Figure S56. Water levels corresponding to inundation durations of 1 to 5 days with recurrence intervals of 1 to 5 years for Kempsey (Station 206402)

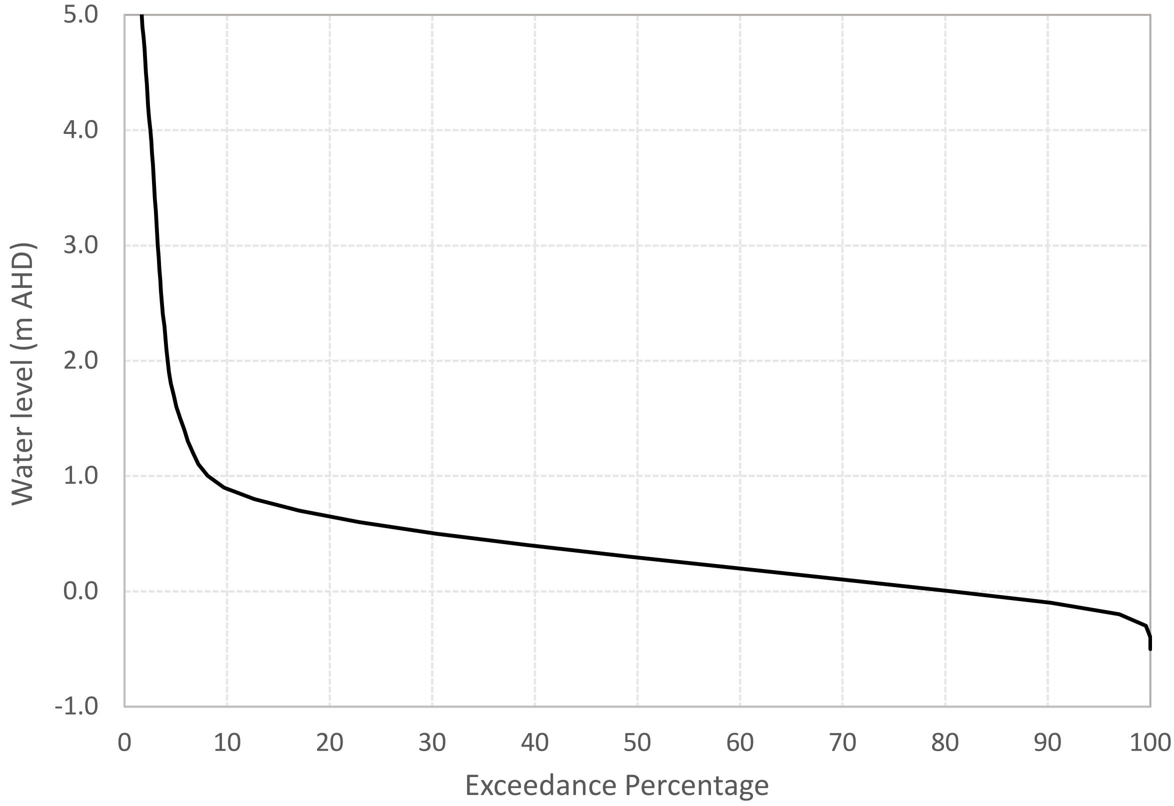

Figure S57. Frequency distribution of water levels at Aldavilla Downstream (Station 206459)

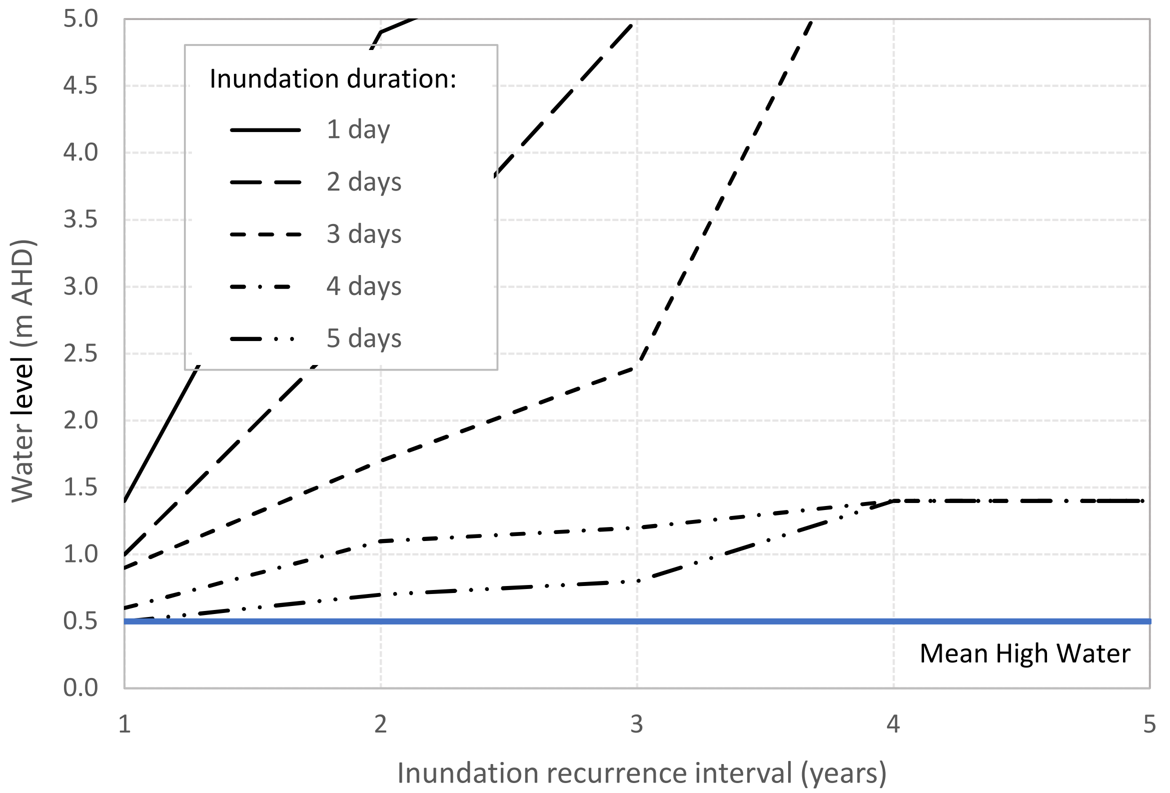

Figure S58. Water levels corresponding to inundation durations of 1 to 5 days with recurrence intervals of 1 to 5 years for Aldavilla Downstream (Station 206459)

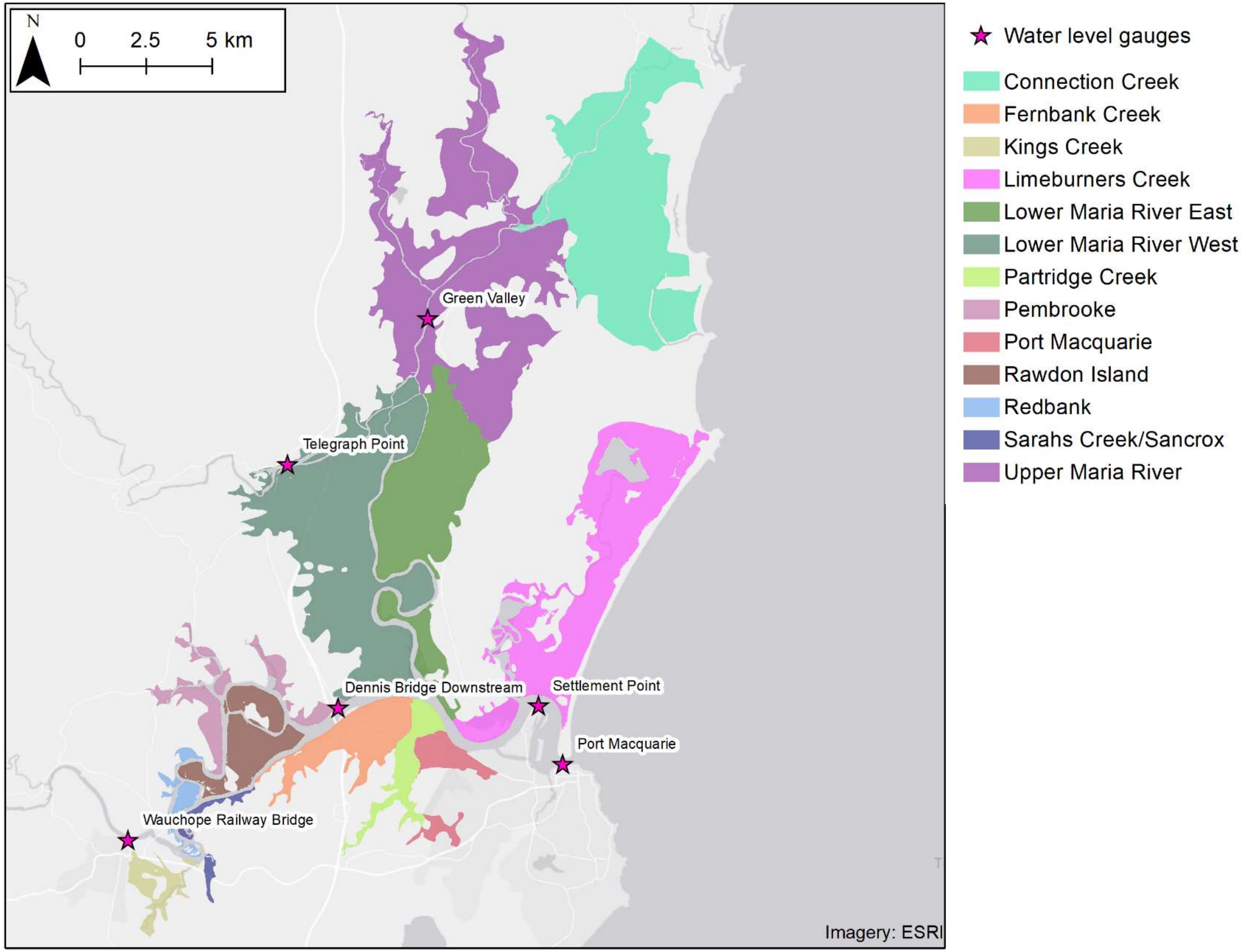

Figure S59. Water level gauge locations, Hastings River

Table S10. Details of water level gauges, Hastings River

Station	Length of record** (years)	Mean High Water level (m AHD)	Blackwater inundation level (m AHD)	
			Median	Maximum
Settlement Point (207418)	33.6	0.4	0.4*	0.8
Dennis Bridge D/S (207444)	24.8	0.5	0.5*	1.5
Wauchope Railway Bridge (207401)	32.9	0.5	0.8	4.2
Telegraph Point (207415)	30.3	0.4	0.7	2.1
Green Valley (207406)	26.2	0.4	1	1.9

* Mean High Water adopted as minimum blackwater inundation level

** Excluding data gaps in excess of 6 hours

Table S11. Distribution of water level gauges to catchments, Hastings River

Catchment	Water level station(s) adopted
Limeburners Creek	Settlement Point
Port Macquarie Airport	0.61 x Settlement Point + 0.39 x Dennis Bridge D/S
Partridge Creek	0.49 x Settlement Point + 0.51 x Dennis Bridge D/S
Fernbank Creek	Dennis Bridge D/S
Pembrooke	0.75 x Dennis Bridge D/S + 0.25 x Wauchope Railway Bridge
Rawdon Island	0.75 x Dennis Bridge D/S + 0.25 x Wauchope Railway Bridge
Redbank	0.49 x Dennis Bridge D/S + 0.51 x Wauchope Railway Bridge
Sarahs Creek-Sancrox	0.25 x Dennis Bridge D/S + 0.75 x Wauchope Railway Bridge
Kings Creek	0.23 x Dennis Bridge D/S + 0.77 x Wauchope Railway Bridge
Lower Maria River West	0.19 x Dennis Bridge D/S + 0.81 x Telegraph Point
Lower Maria River East	0.07 x Dennis Bridge D/S + 0.93 x Telegraph Point
Upper Maria River	Green Valley
Connection Creek	Green Valley
Limeburners Creek	Settlement Point

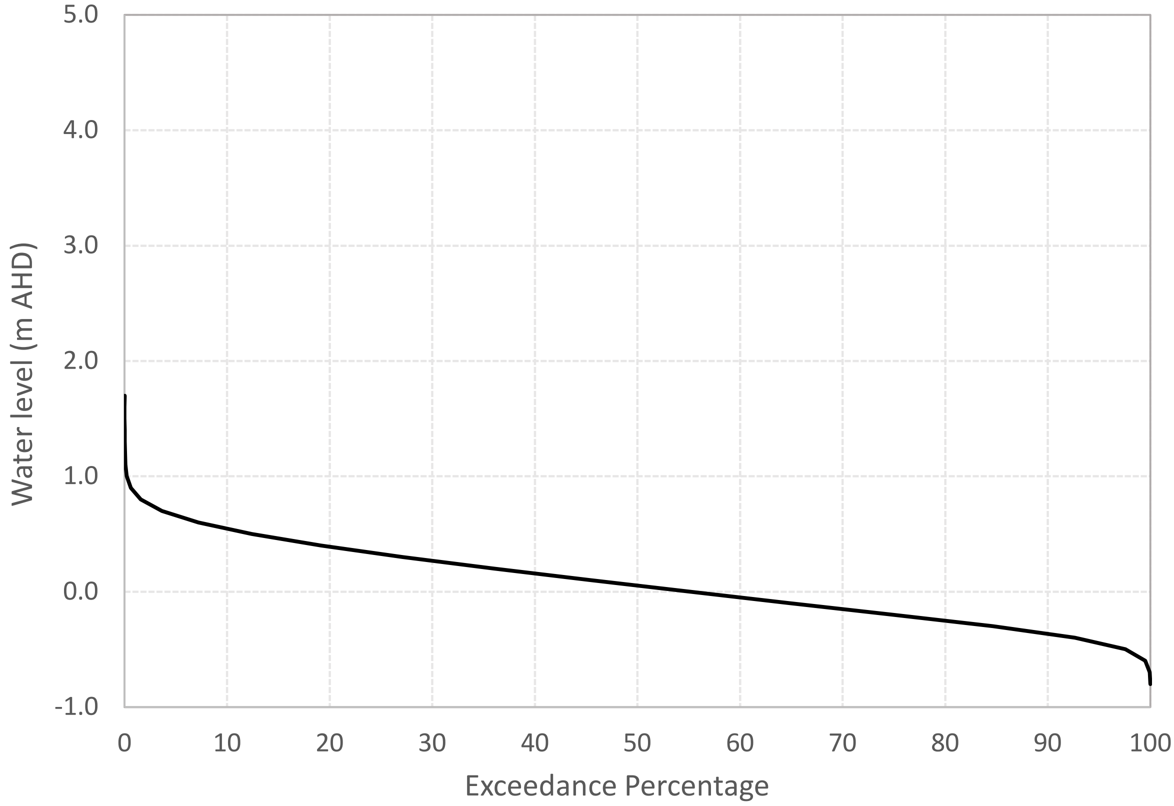

Figure S60. Frequency distribution of water levels at Settlement Point (Station 207418)

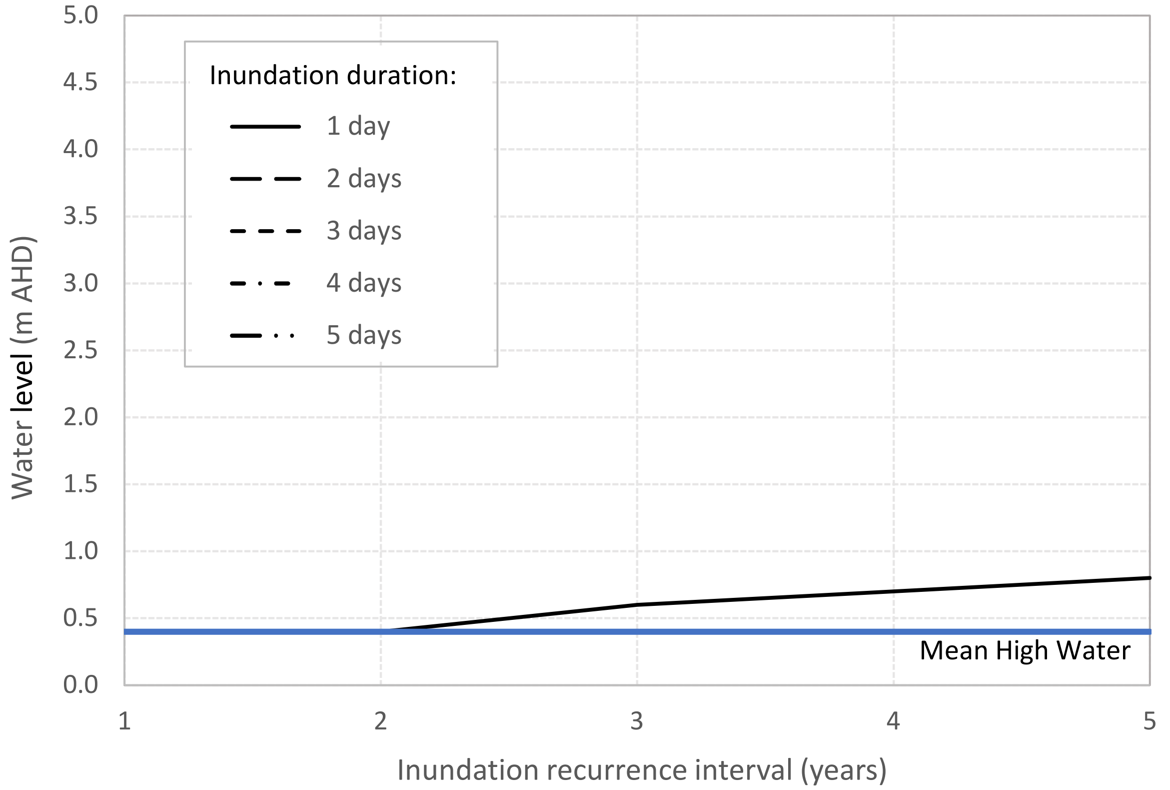

Figure S61. Water levels corresponding to inundation durations of 1 to 5 days with recurrence intervals of 1 to 5 years for Settlement Point (Station 207418)

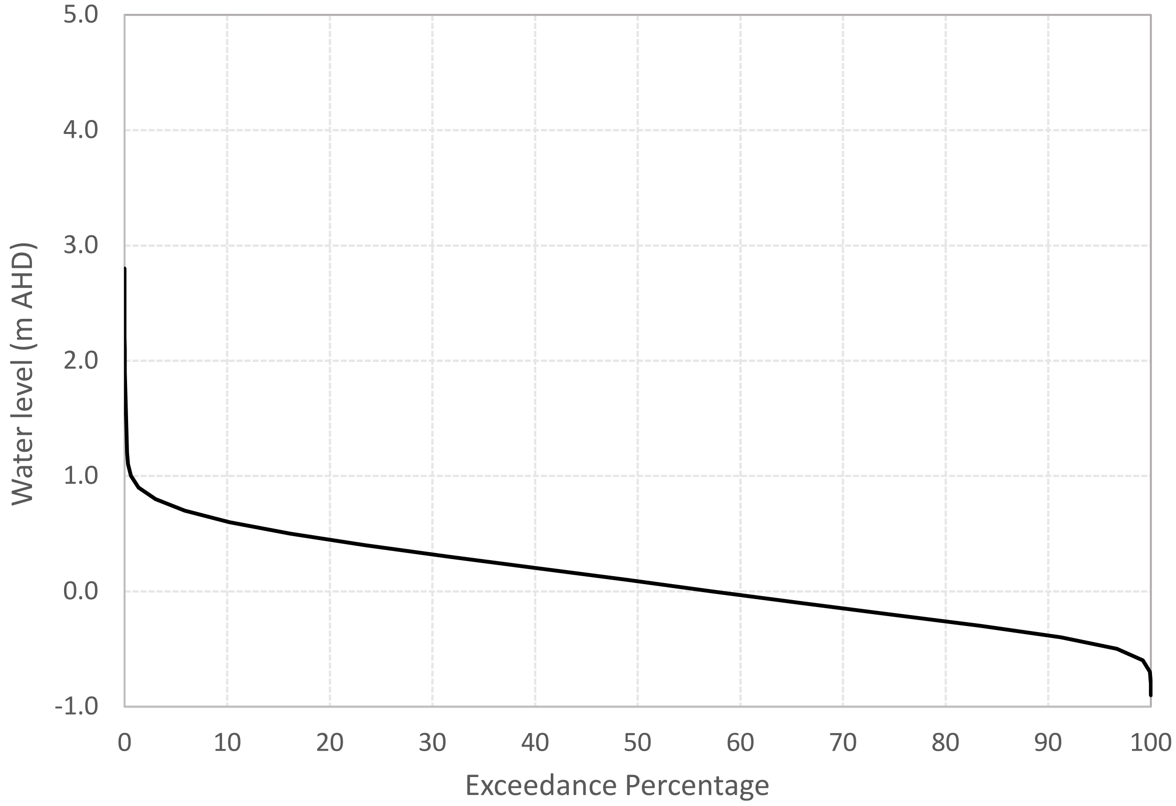

Figure S62. Frequency distribution of water levels at Dennis Bridge D/S (Station 207444)

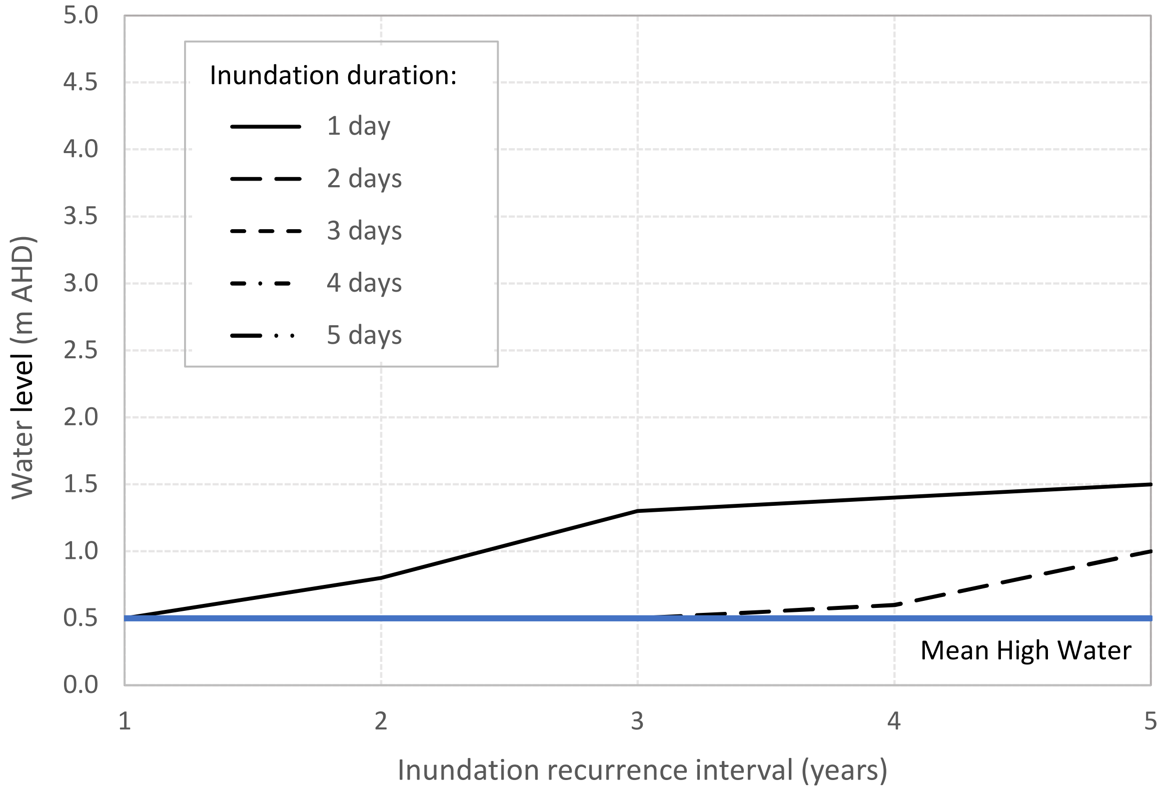

Figure S63. Water levels corresponding to inundation durations of 1 to 5 days with recurrence intervals of 1 to 5 years for Dennis Bridge Downstream (Station 207444)

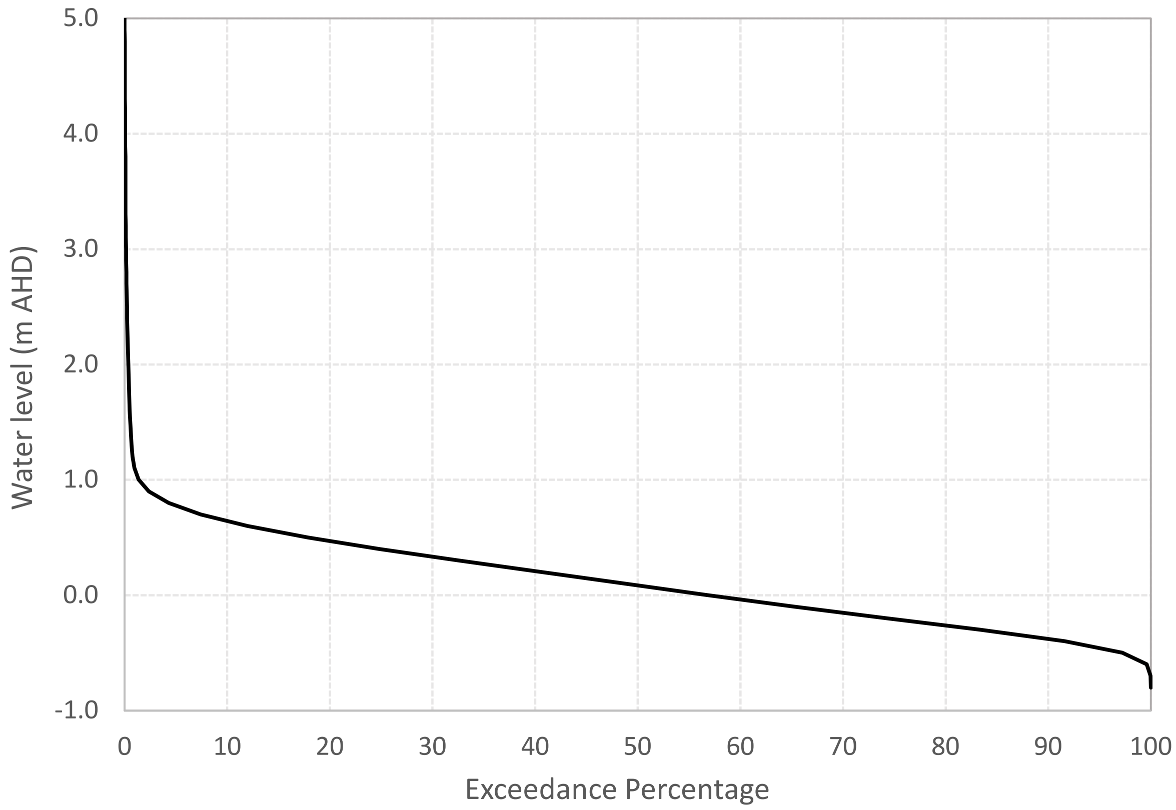

Figure S64. Frequency distribution of water levels at Wauchope Railway Bridge (St'n 207401)

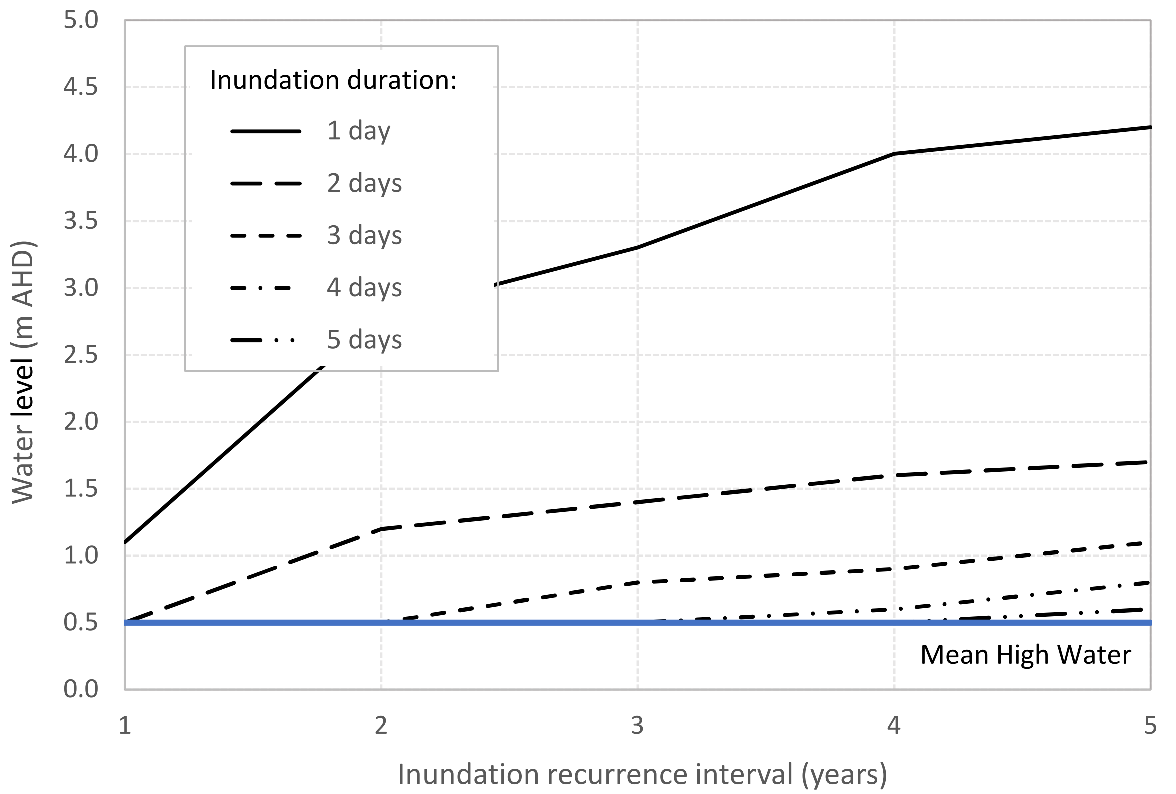

Figure S65. Water levels corresponding to inundation durations of 1 to 5 days with recurrence intervals of 1 to 5 years for Wauchope Railway Bridge (Station 207401)

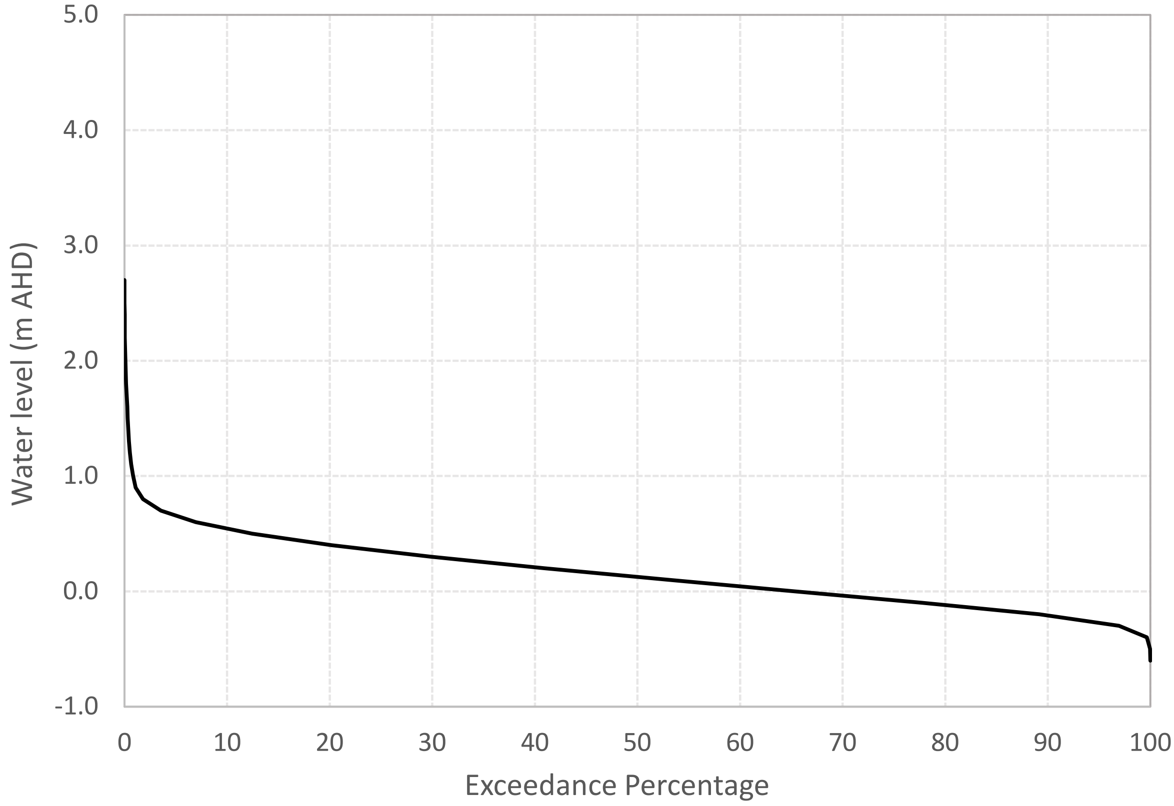

Figure S66. Frequency distribution of water levels at Telegraph Point (Station 207415)

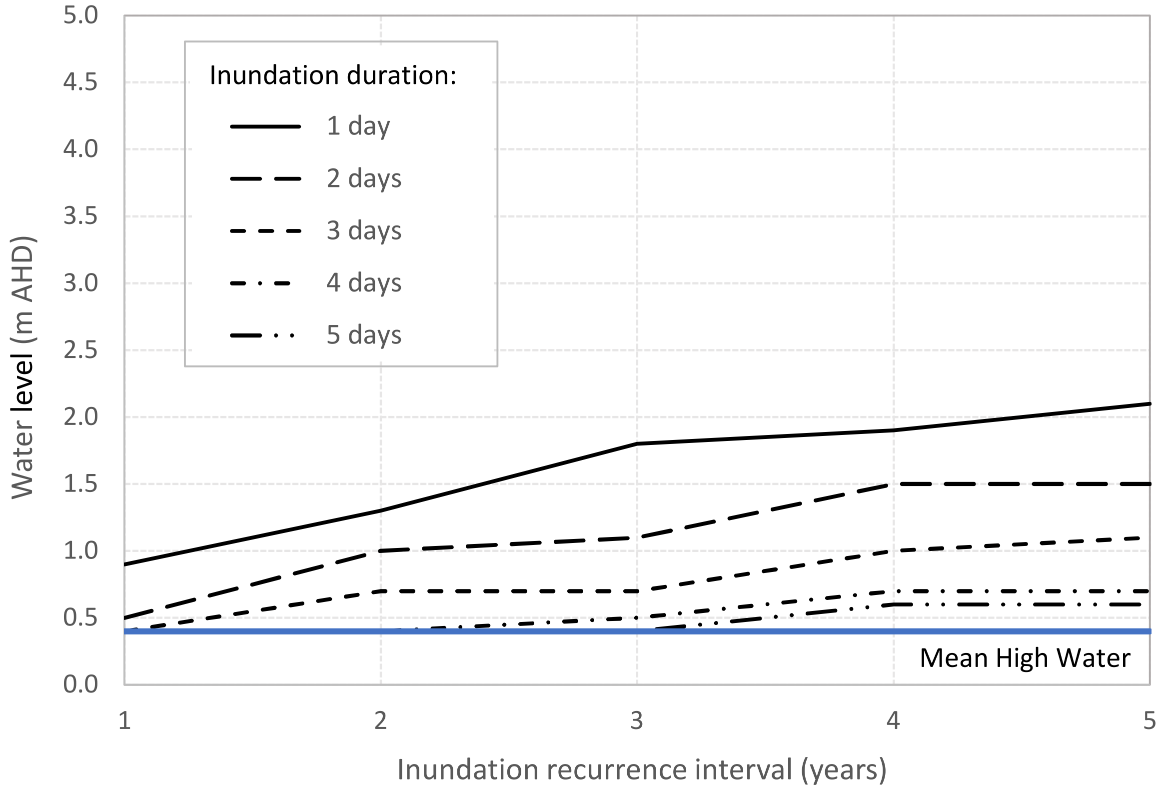

Figure S67. Water levels corresponding to inundation durations of 1 to 5 days with recurrence intervals of 1 to 5 years for Telegraph Point (Station 207415)

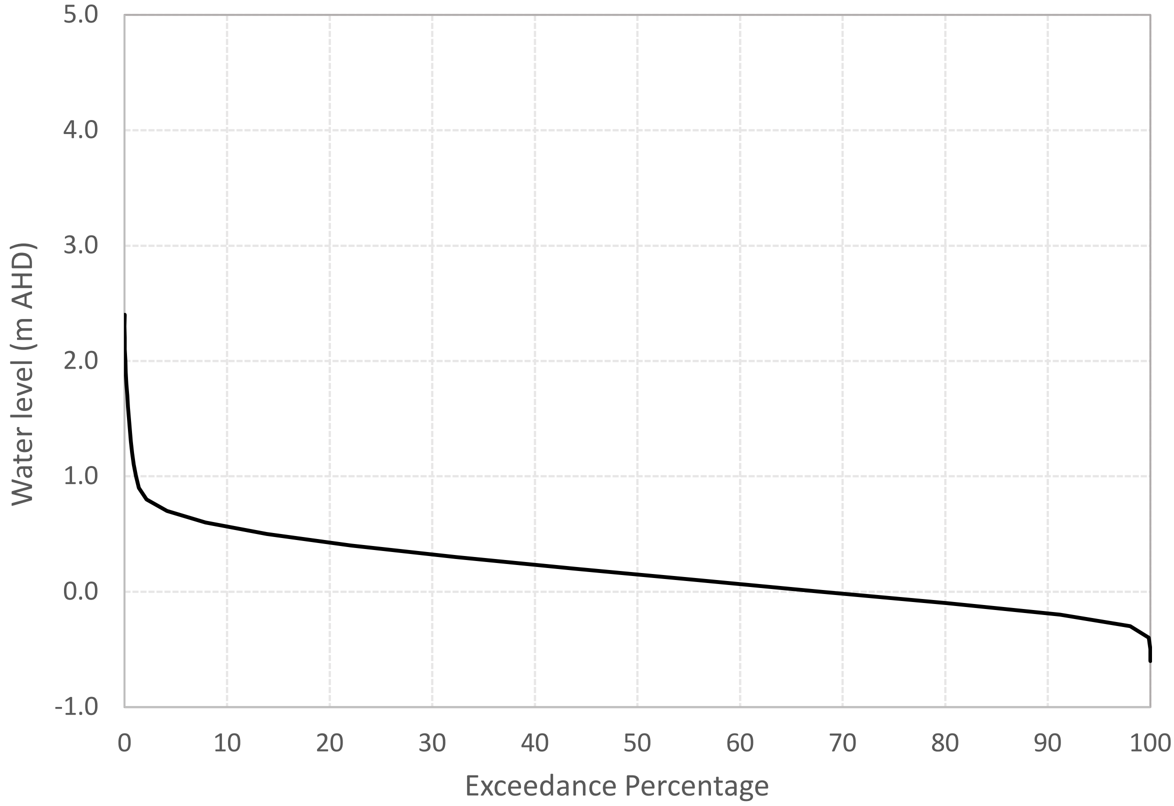

Figure S68. Frequency distribution of water levels at Green Valley (Station 207406)

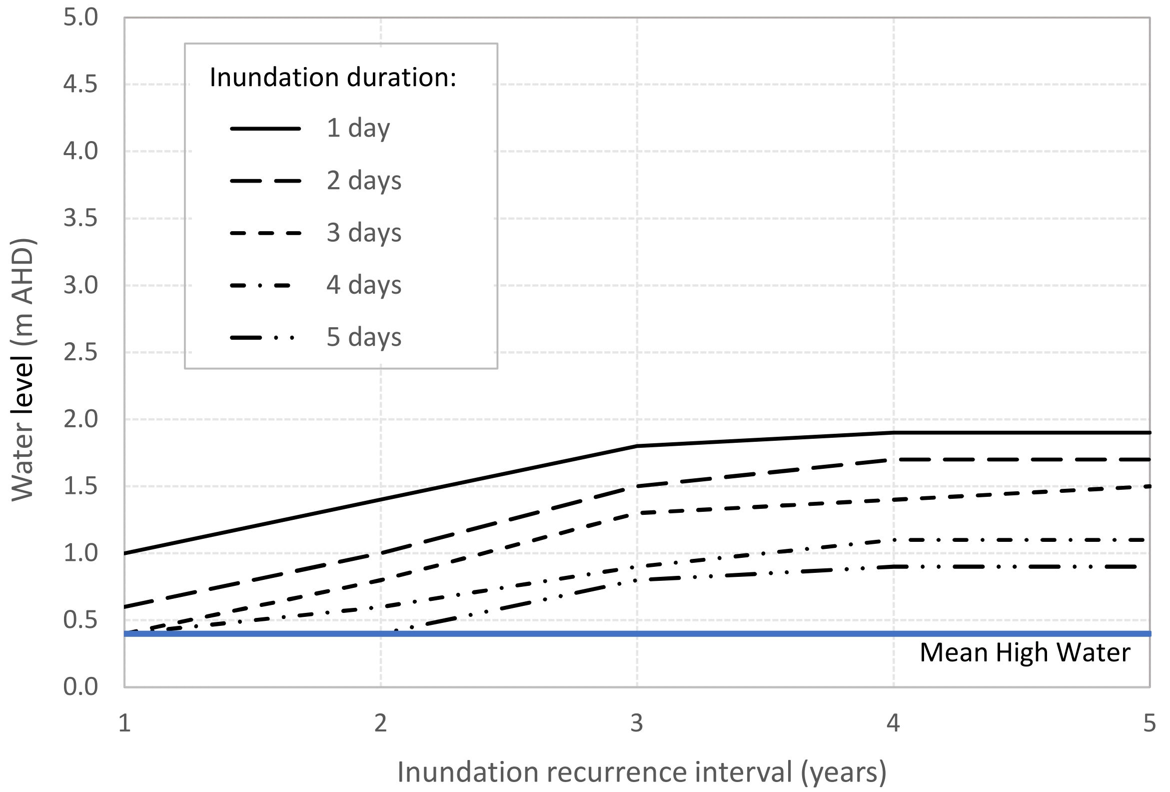

Figure S69. Water levels corresponding to inundation durations of 1 to 5 days with recurrence intervals of 1 to 5 years for Green Valley (Station 207406)

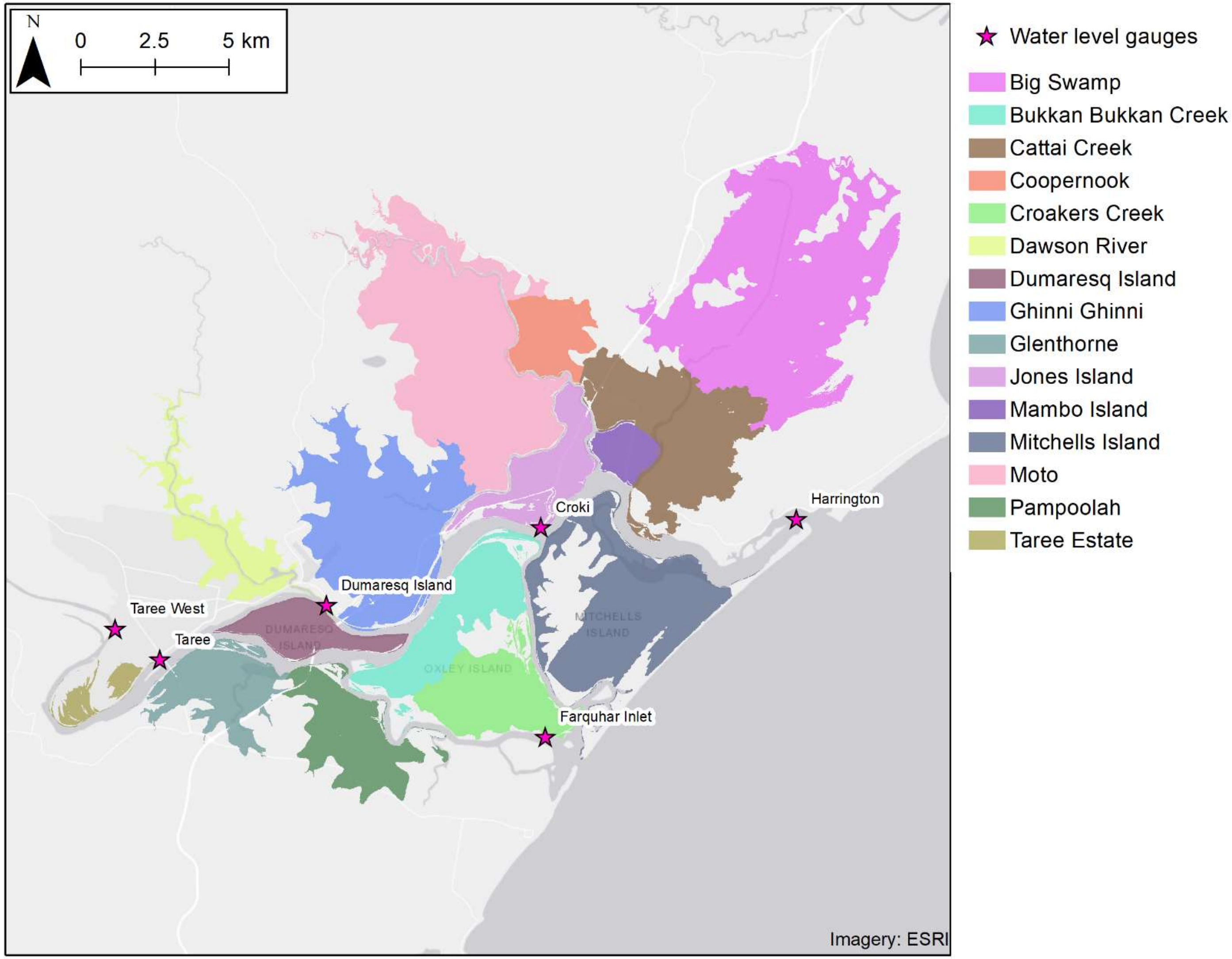

Figure S70. Water level gauge locations, Manning River

Table S12. Details of water level gauges, Manning River

Station	Length of record** (years)	Mean High Water level (m AHD)	Blackwater inundation level (m AHD)	
			Median	Maximum
Harrington (208425)	28.5	0.4	0.4*	0.5
Croki (208404)	27.7	0.4	0.6	1.6
Dumaresq Island (208430)	17.7	0.4	0.7	2
Taree (208410)	33.3	0.5	0.6	2.2
Taree West (208420)	10.0	0.5	1	4.6
Farquhar Inlet (208415)	32.0	0.4	0.5	1.3

* Mean High Water adopted as minimum blackwater inundation level

** Excluding data gaps in excess of 6 hours

Table S13. Distribution of water level gauges to catchments, Manning River

Catchment	Water level station(s) adopted
Harrington	Harrington
Mitchells Island	0.71 x Harrington + 0.29 x Croki
Cattai Creek	0.30 x Harrington + 0.70 x Croki
Big Swamp	Assumed the same levels as Cattai Creek
Mambo Island	0.28 x Harrington + 0.72 x Croki
Moto	0.22 x Harrington + 0.78 x Croki
Coopernook	Assumed to be the same as Moto
Ghinni Ghinni	0.65 x Croki + 0.65 x Dumaresq Island
Jones Island	Croki
Dumaresq Island	Dumaresq Island
Dawson River	Dumaresq Island
Glenthorne	Dumaresq Island
Taree Estate	0.67 x Taree + 0.33 x Taree West
Old Bar	Farquhar Inlet
Croakers Creek	Farquhar Inlet
Bukkan Bukkan Creek	0.34 x Farquhar Inlet + 0.66 x Croki
Pampoolah	0.34 x Farquhar Inlet + 0.66 x Dumaresq Island

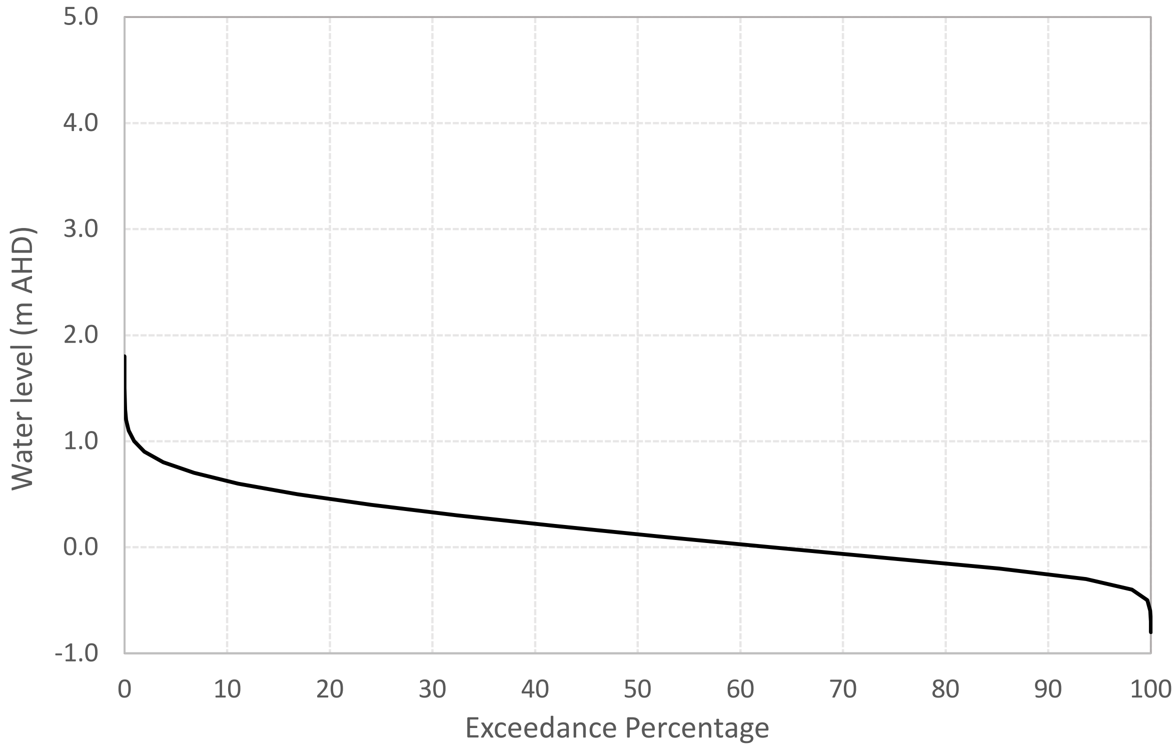

Figure S71. Frequency distribution of water levels at Harrington (Station 208425)

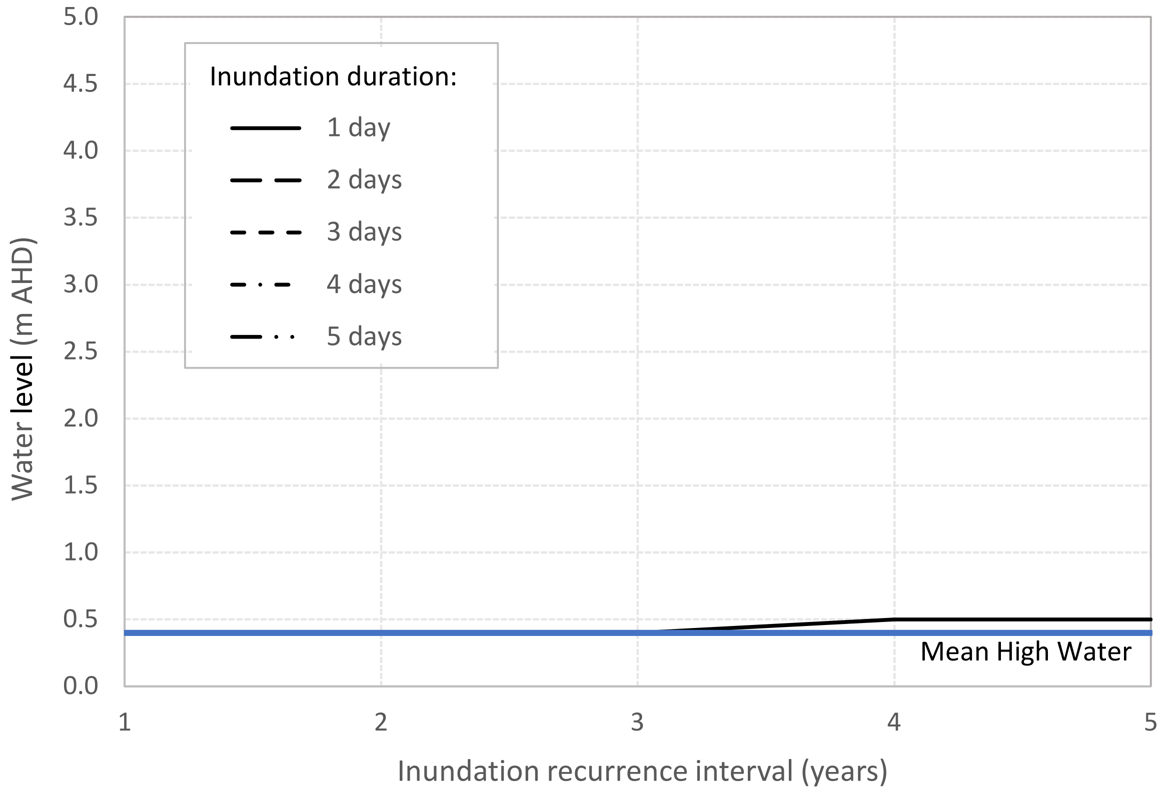

Figure S72. Water levels corresponding to inundation durations of 1 to 5 days with recurrence intervals of 1 to 5 years for Harrington (Station 208425)

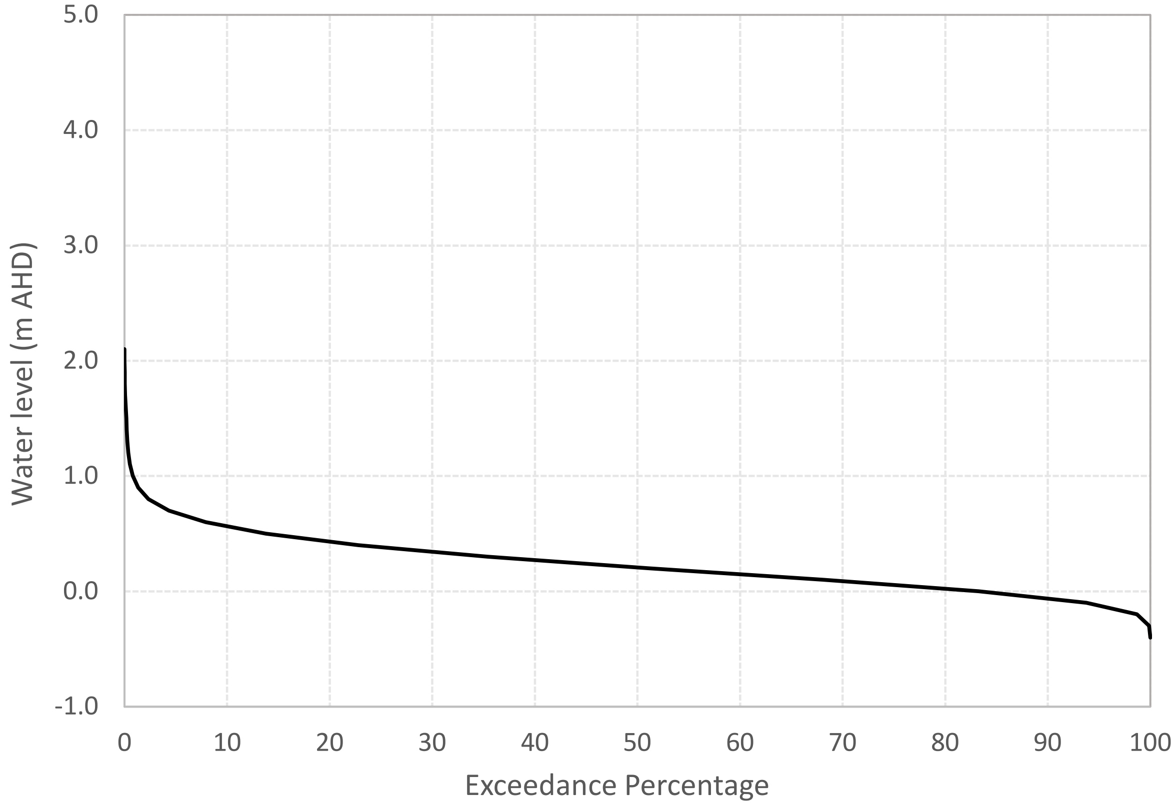

Figure S73. Frequency distribution of water levels at Croki (Station 208404)

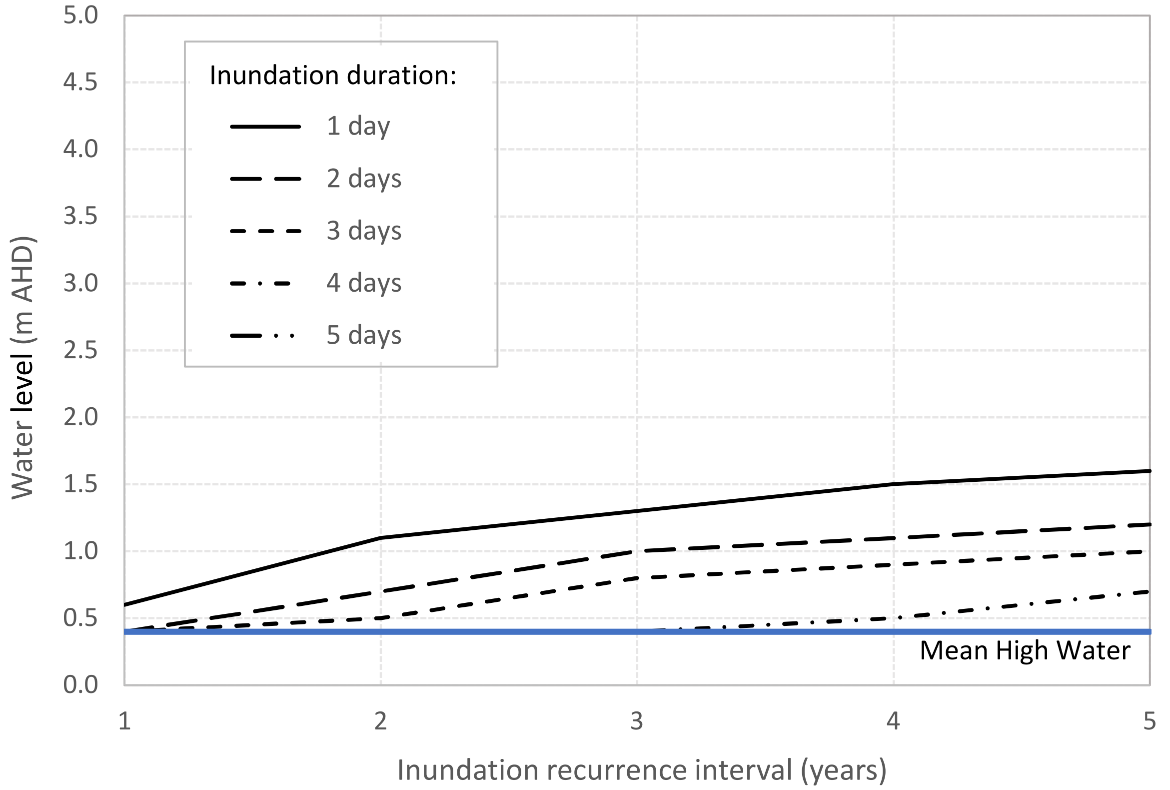

Figure S74. Water levels corresponding to inundation durations of 1 to 5 days with recurrence intervals of 1 to 5 years for Croki (Station 208404)

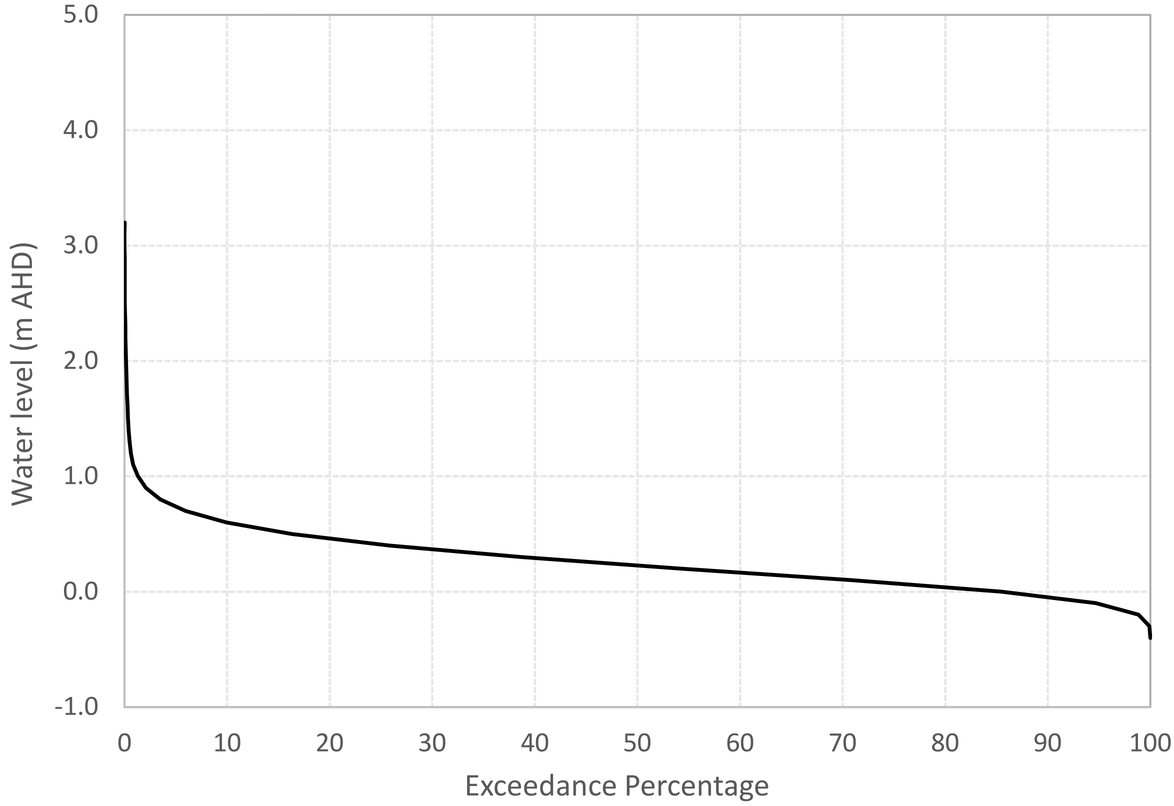

Figure S75. Frequency distribution of water levels at Dumaresq Island (Station 208430)

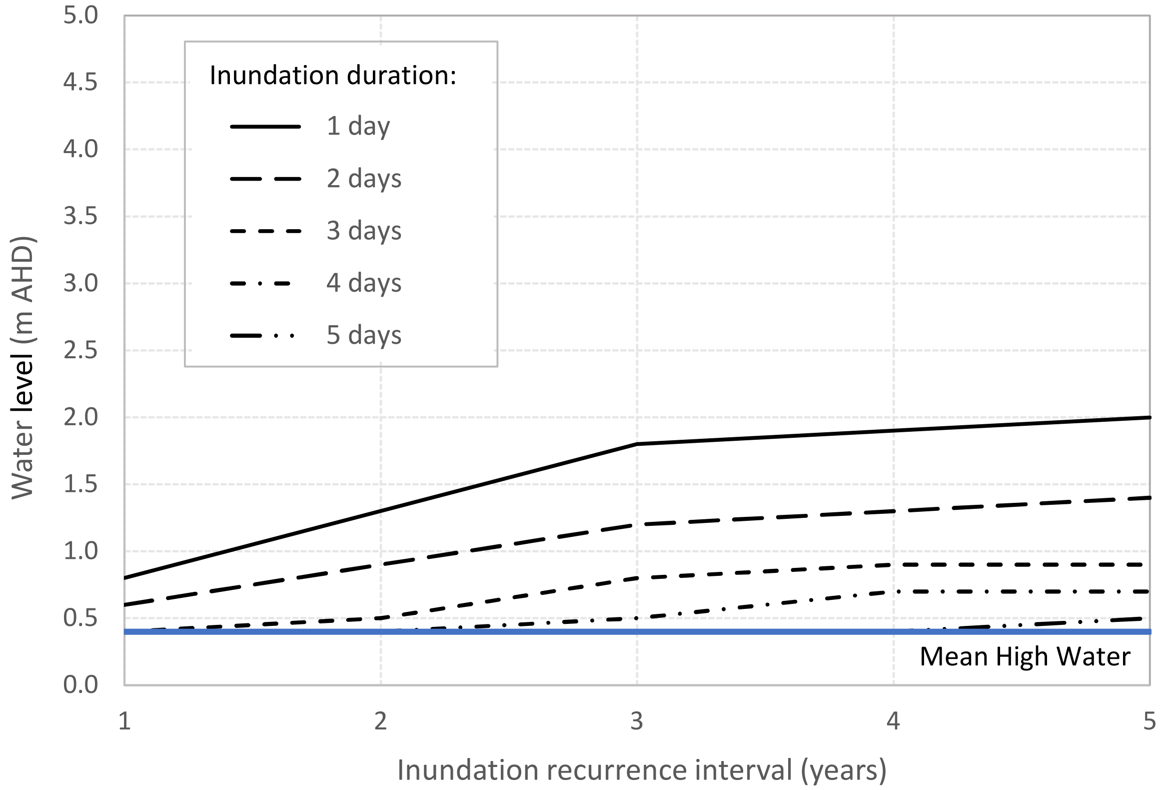

Figure S76. Water levels corresponding to inundation durations of 1 to 5 days with recurrence intervals of 1 to 5 years for Dumaresq Island (Station 208430)

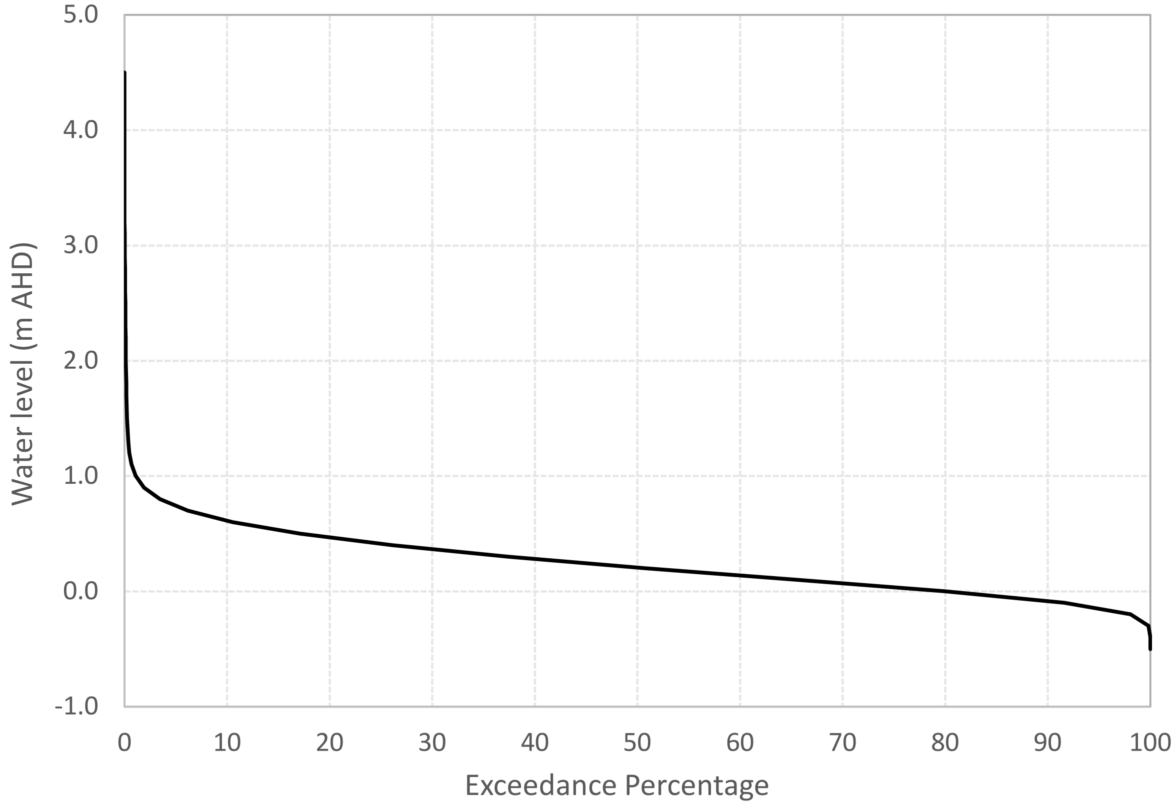

Figure S77. Frequency distribution of water levels at Taree (Station 208410)

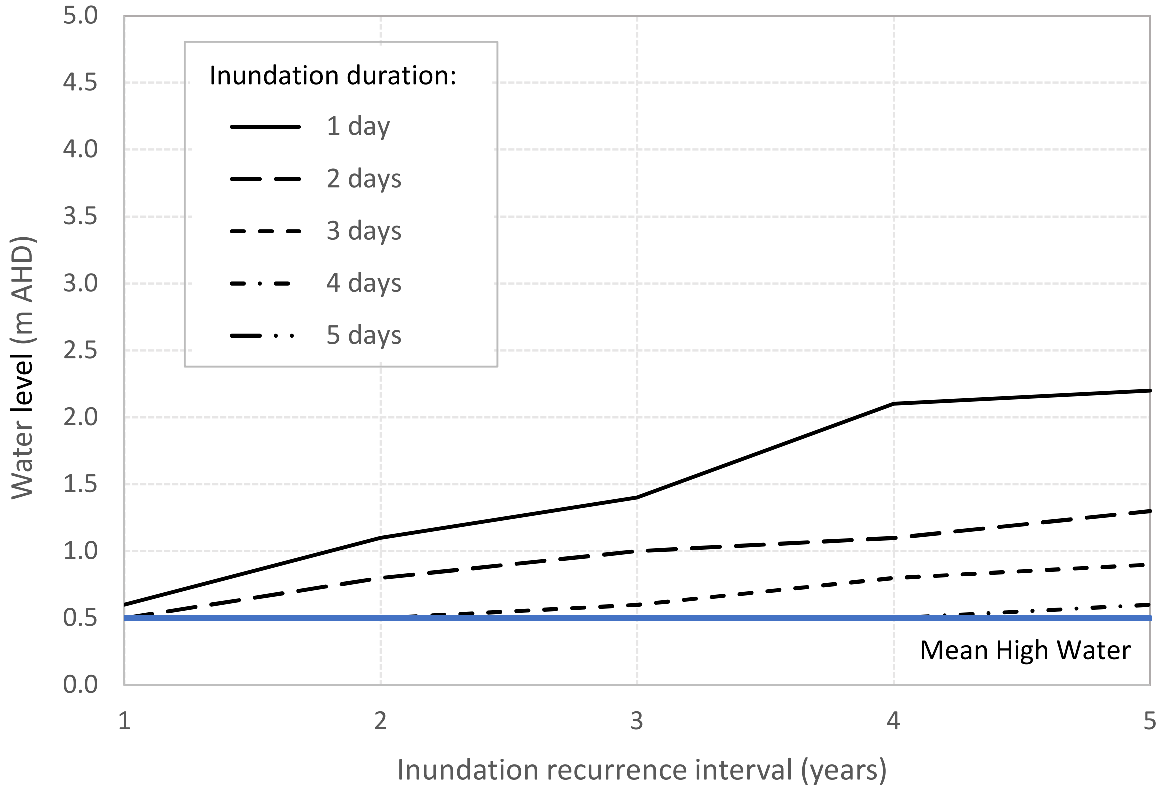

Figure S78. Water levels corresponding to inundation durations of 1 to 5 days with recurrence intervals of 1 to 5 years for Taree (Station 208410)

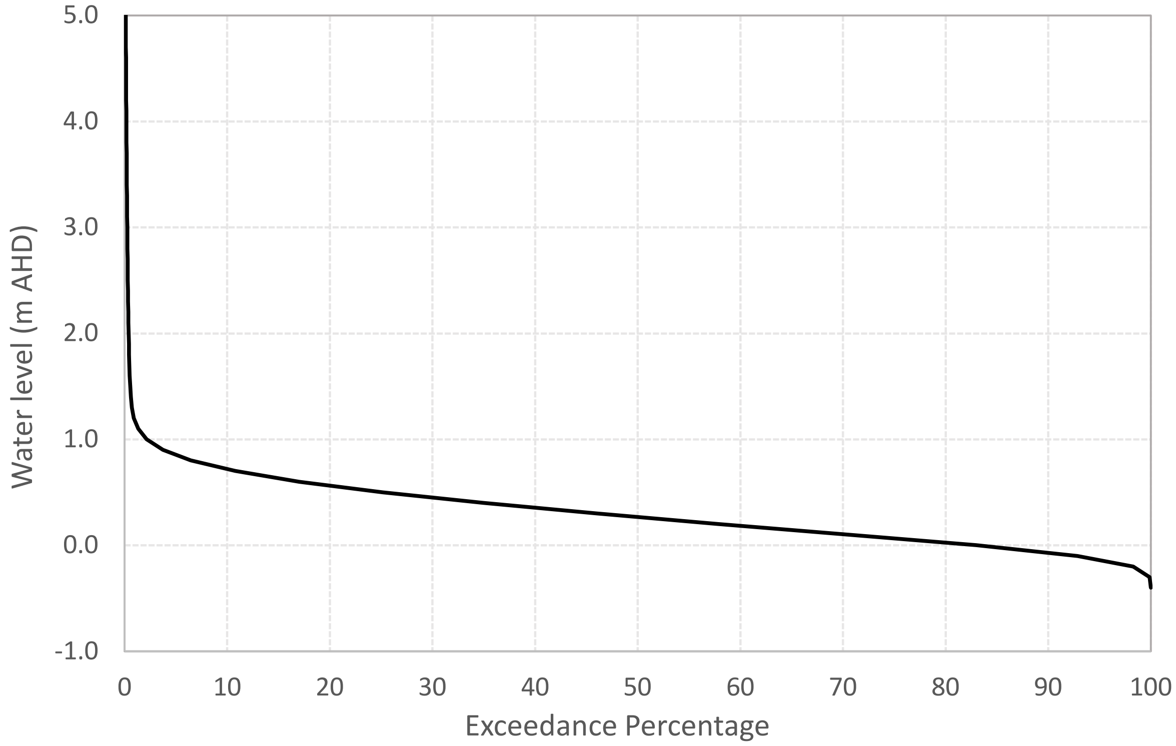

Figure S79. Frequency distribution of water levels at Taree West (Station 208420)

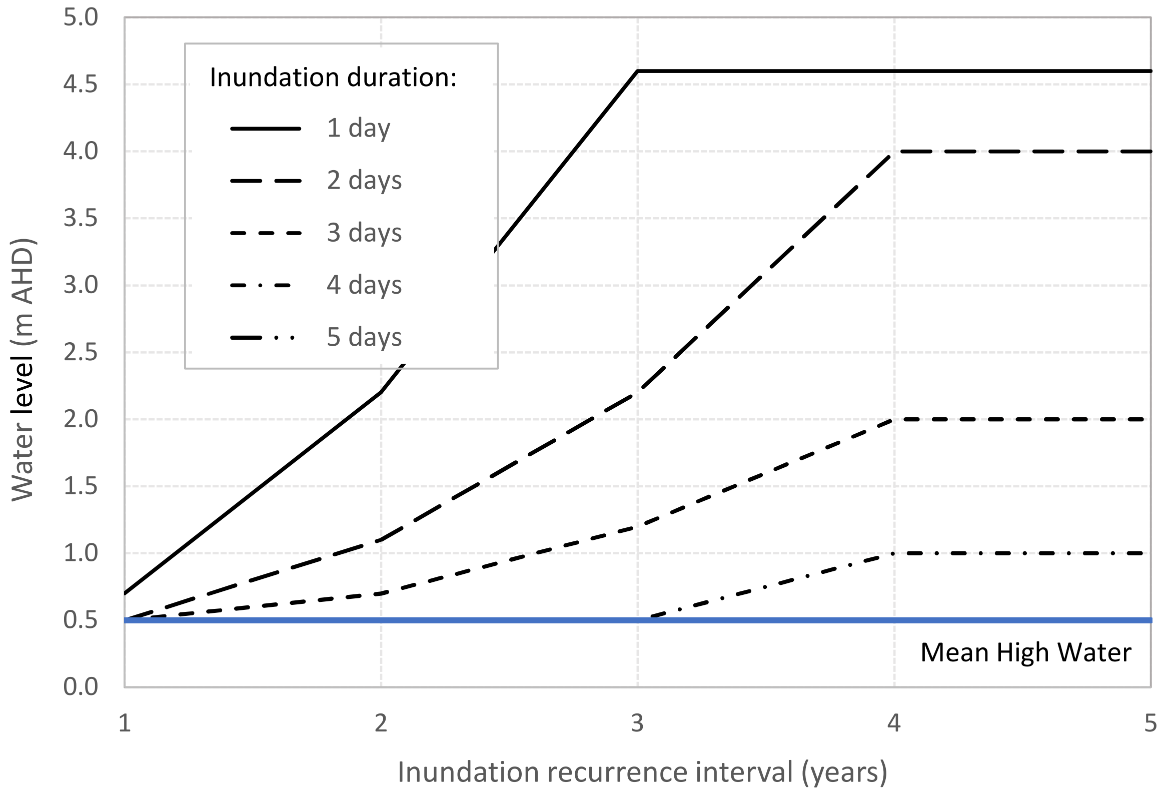

Figure S80. Water levels corresponding to inundation durations of 1 to 5 days with recurrence intervals of 1 to 5 years for Taree West (Station 208420)

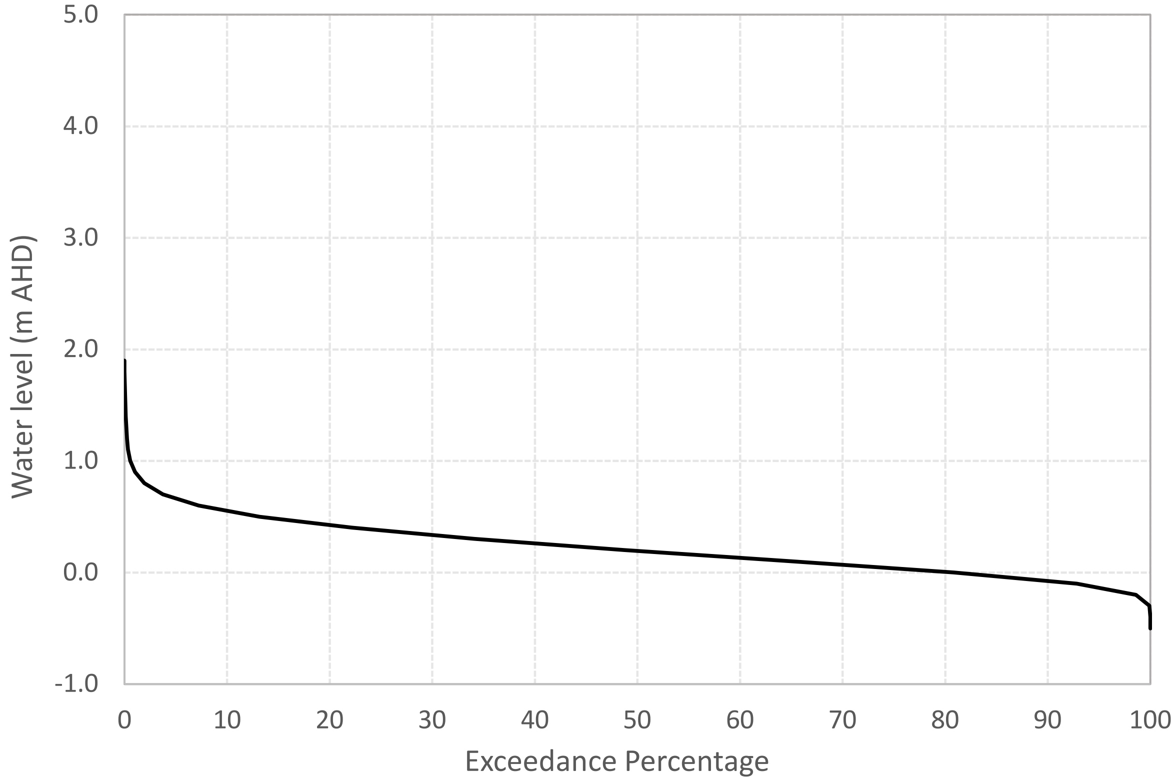

Figure S81. Frequency distribution of water levels at Farquhar Inlet (Station 208415)

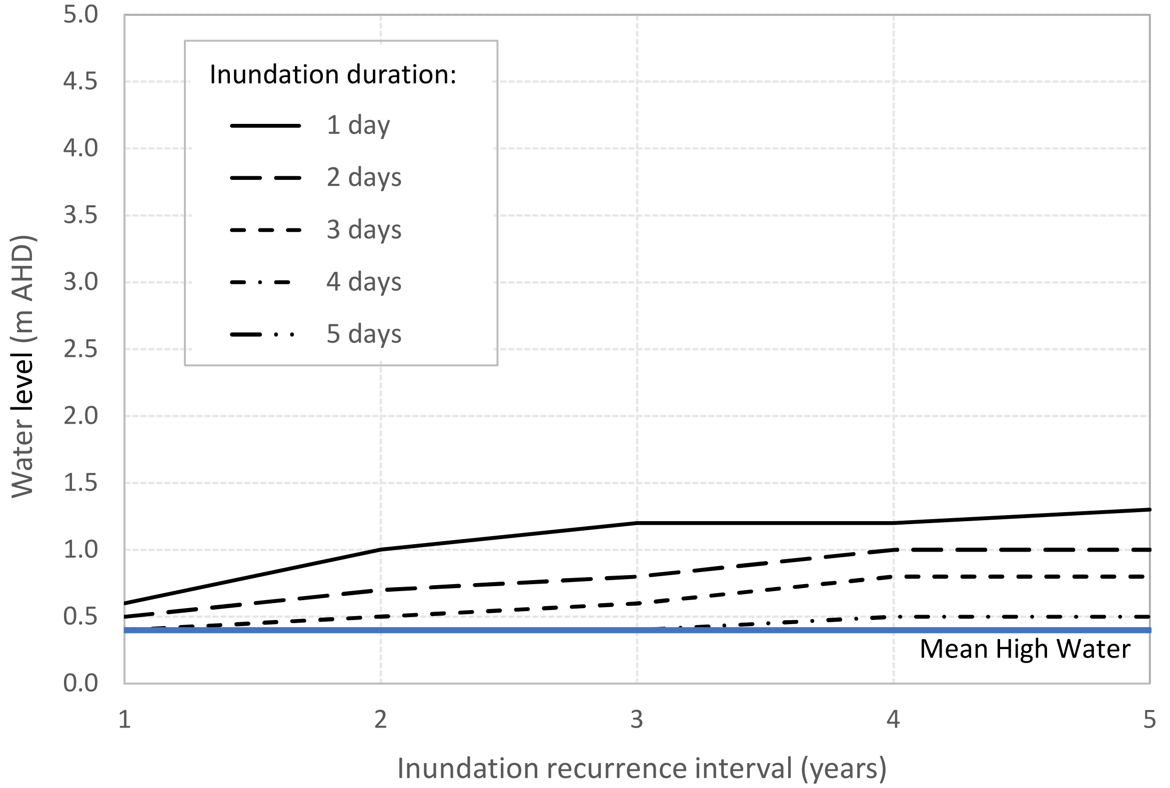

Figure S82. Water levels corresponding to inundation durations of 1 to 5 days with recurrence intervals of 1 to 5 years for Farquhar Inlet (Station 208415)

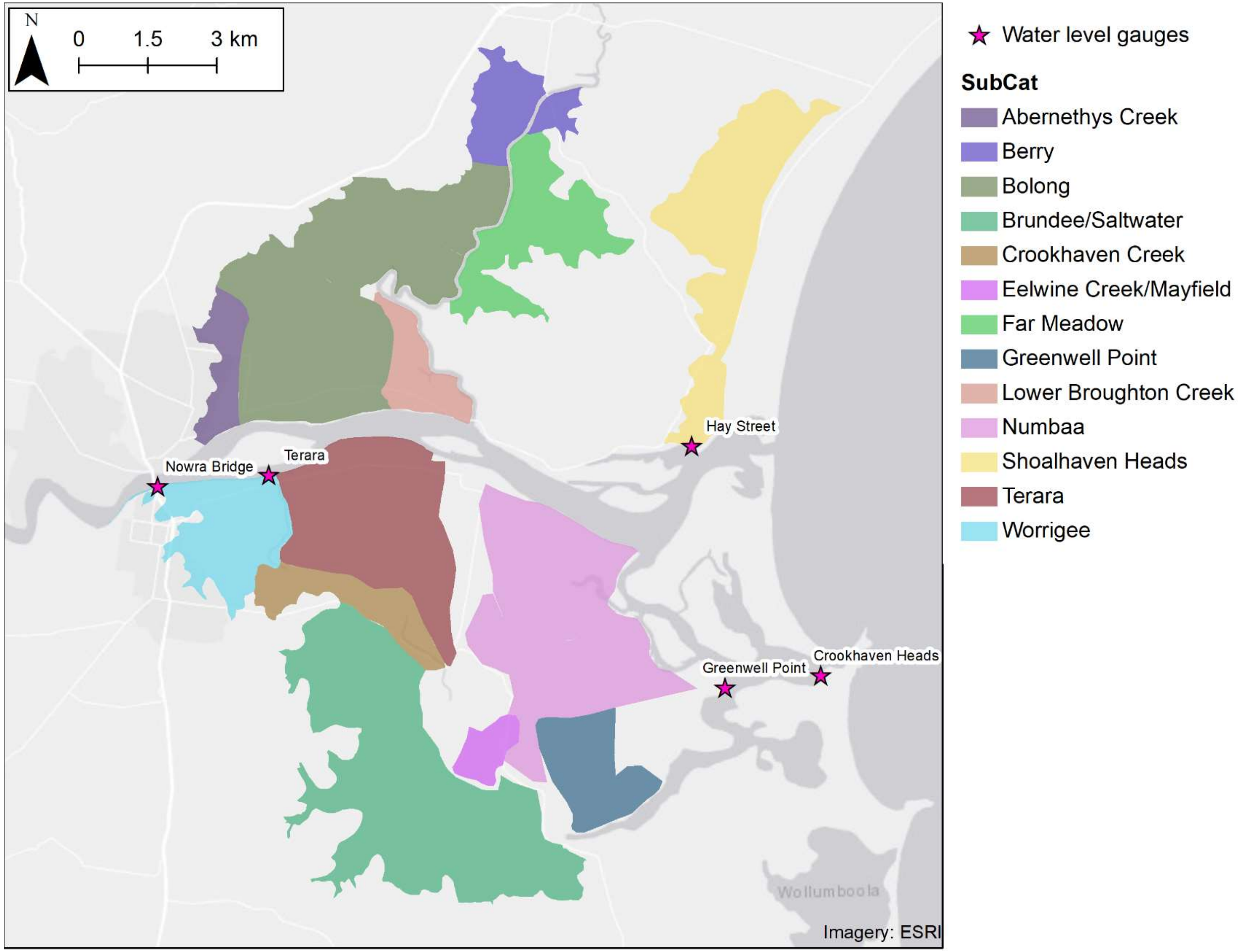

Figure S83. Water level gauge locations, Shoalhaven River

Table S14. Details of water level gauges, Shoalhaven River

Station	Length of record** (years)	Mean High Water level (m AHD)	Blackwater inundation level (m AHD)	
			Median	Maximum
Crookhaven Heads (215408)	27.4	0.4	0.5	0.5
Hay Street (215415)	17.3	0.4	0.4*	1.2
Greenwell Point (215417)	29.2	0.4	0.4*	0.5
Terara (215420)	17.4	0.4	0.4*	2.6
Nowra Bridge (215411)	28.8	0.4	0.4*	2.9

* Mean High Water adopted as minimum blackwater inundation level

** Excluding data gaps in excess of 6 hours

Table S15. Distribution of water level gauges to catchments, Shoalhaven River

Catchment	Water level station(s) adopted
Shoalhaven Heads	Hay Street
Coolangatta	Hay Street
Greenwell Point	Greenwell Point
Brundee-Saltwater*	Using Greenwell Point as a proxy
Eelwine Creek-Mayfield*	Using Greenwell Point as a proxy
Crookhaven Creek*	Using Greenwell Point as a proxy
Comerong Island*	Using Greenwell Point as a proxy
Numbaa	0.57 x Greenwell Point + 0.43 x Hay Street
Terara	0.43 x Hay Street + 0.57 x Terara
Lower Broughton Creek	0.40 x Hay Street + 0.60 x Terara
Bolong*	Using Lower Broughton Creek as a proxy
Far Meadow*	Using Lower Broughton Creek as a proxy
Berry*	Using Lower Broughton Creek as a proxy
Abernethys Creek	0.52 x Terara + 0.48 x Nowra Bridge
Worrigee	0.57 x Terara + 0.43 x Nowra Bridge

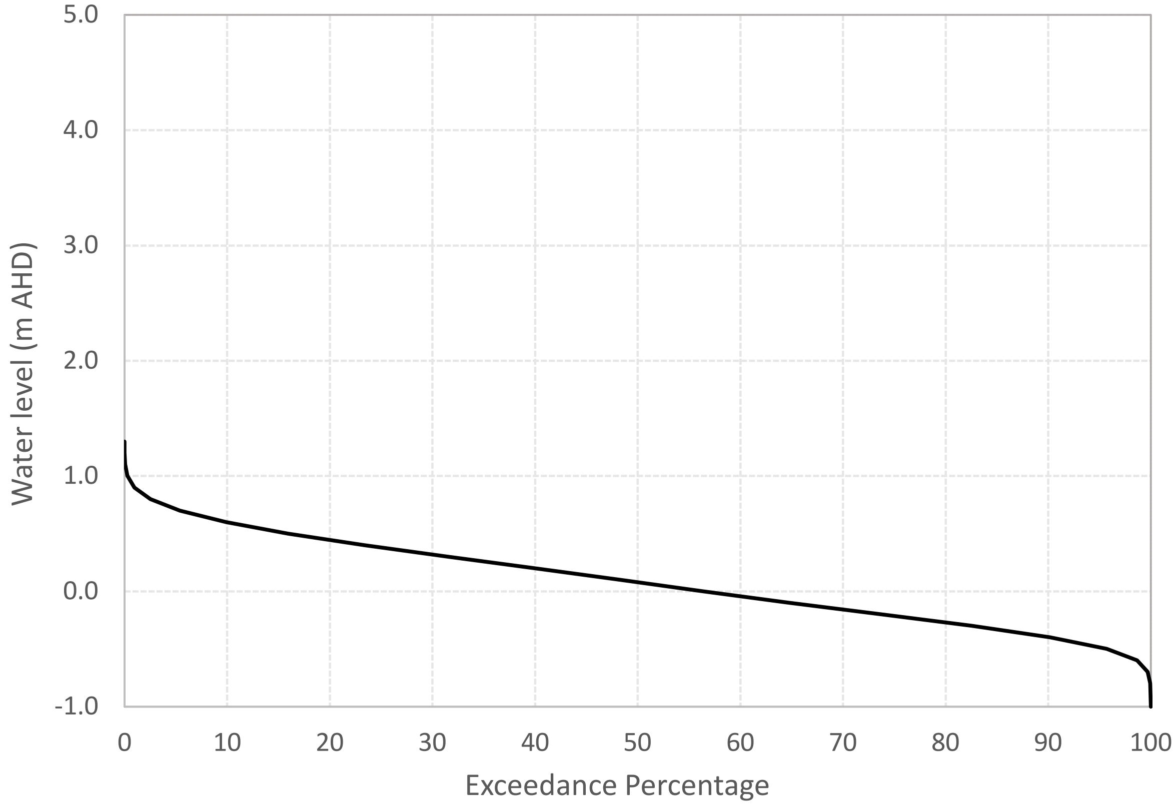

Figure S84. Frequency distribution of water levels at Crookhaven Heads (Station 215408)

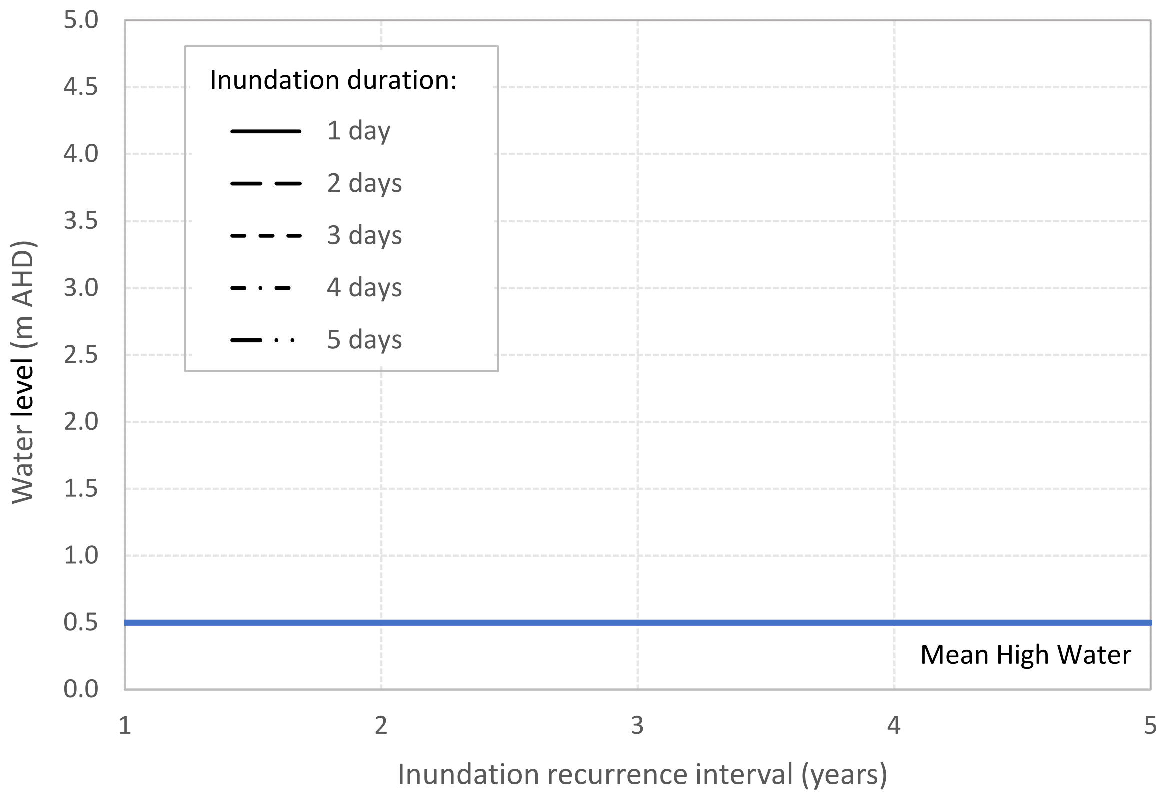

Figure S85. Water levels corresponding to inundation durations of 1 to 5 days with recurrence intervals of 1 to 5 years for Crookhaven Heads (Station 215408)

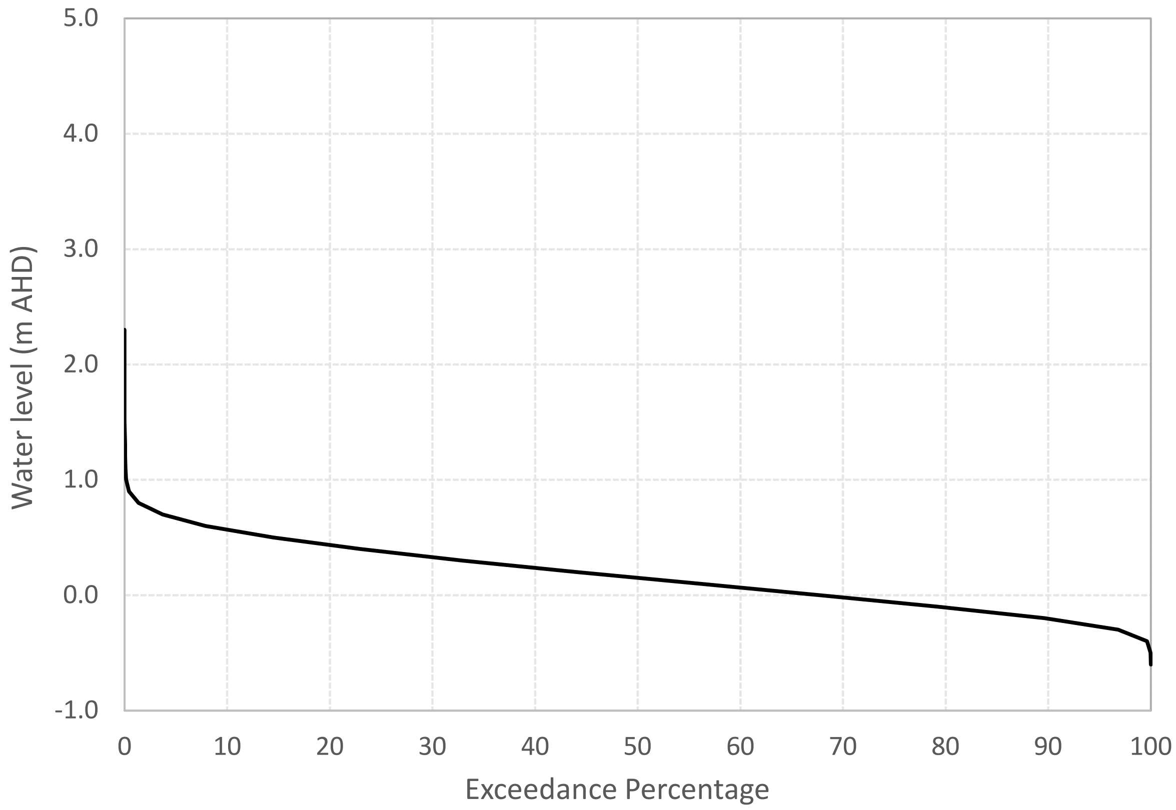

Figure S86. Frequency distribution of water levels at Hay Street (Station 215415)

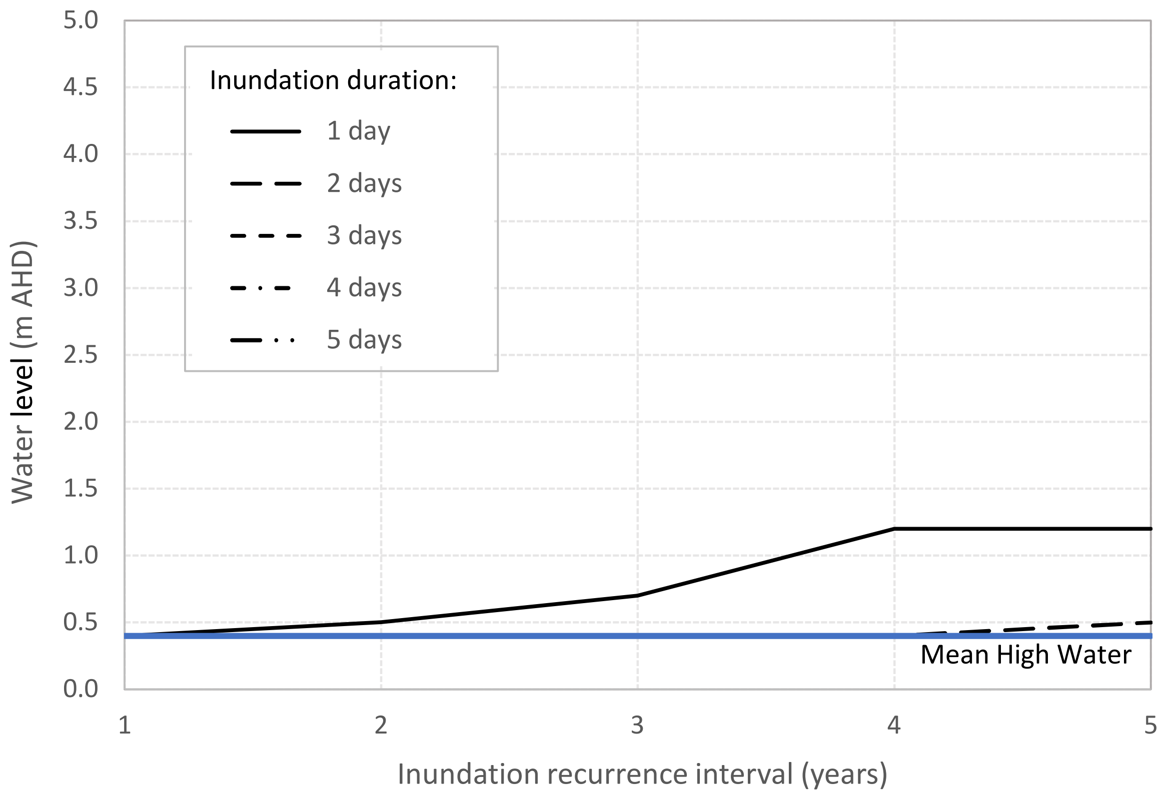

Figure S87. Water levels corresponding to inundation durations of 1 to 5 days with recurrence intervals of 1 to 5 years for Hay Street (Station 215415)

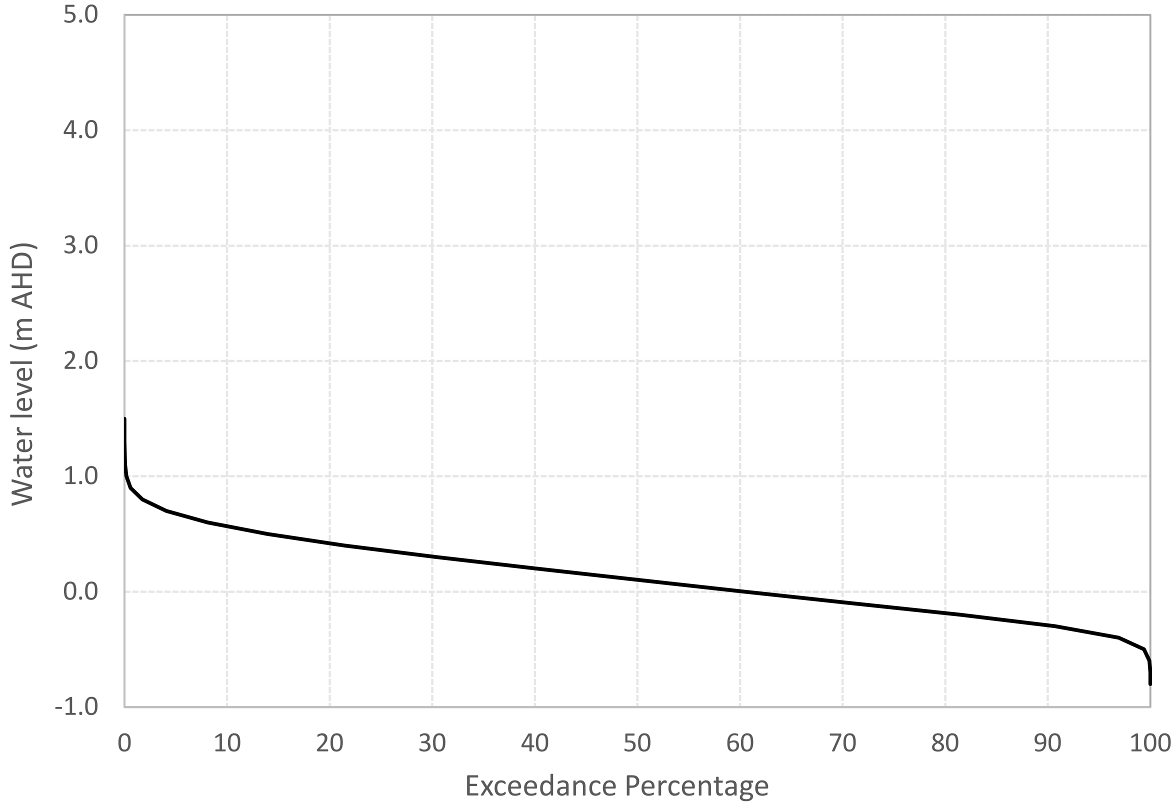

Figure S88. Frequency distribution of water levels at Greenwell Point (Station 215417)

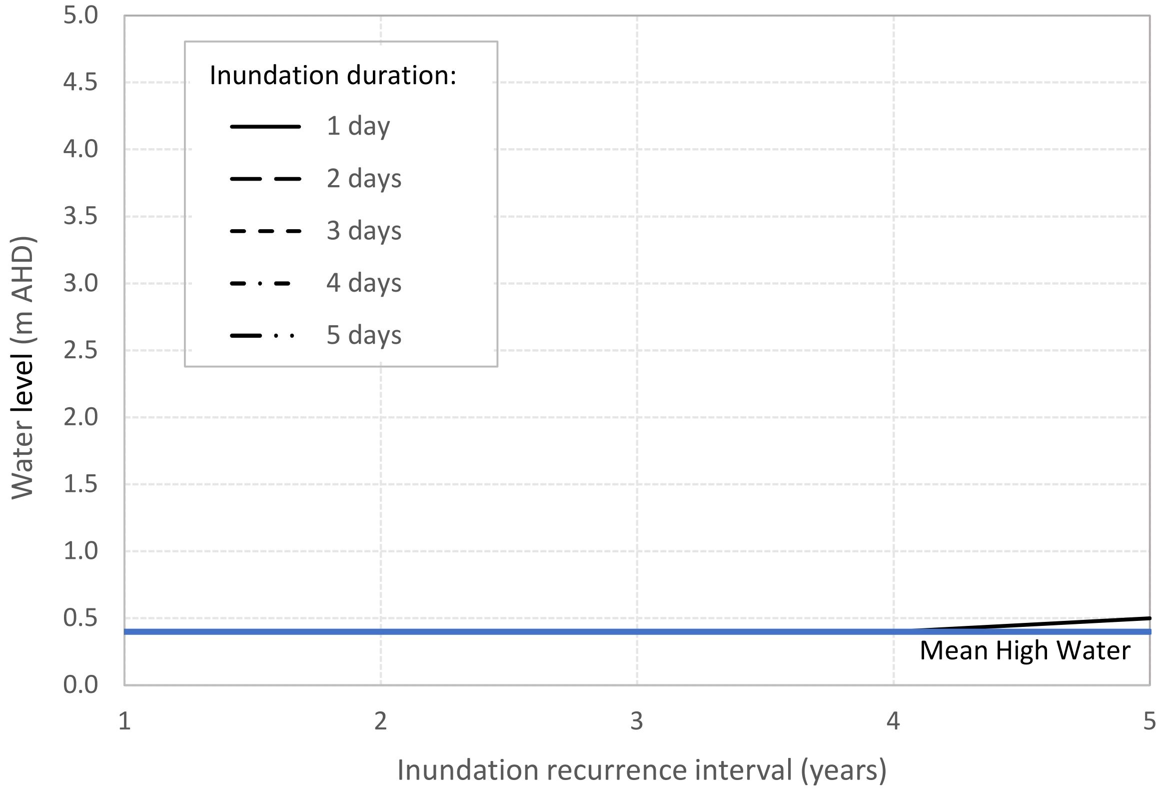

Figure S89. Water levels corresponding to inundation durations of 1 to 5 days with recurrence intervals of 1 to 5 years for Greenwell Point (Station 215417)

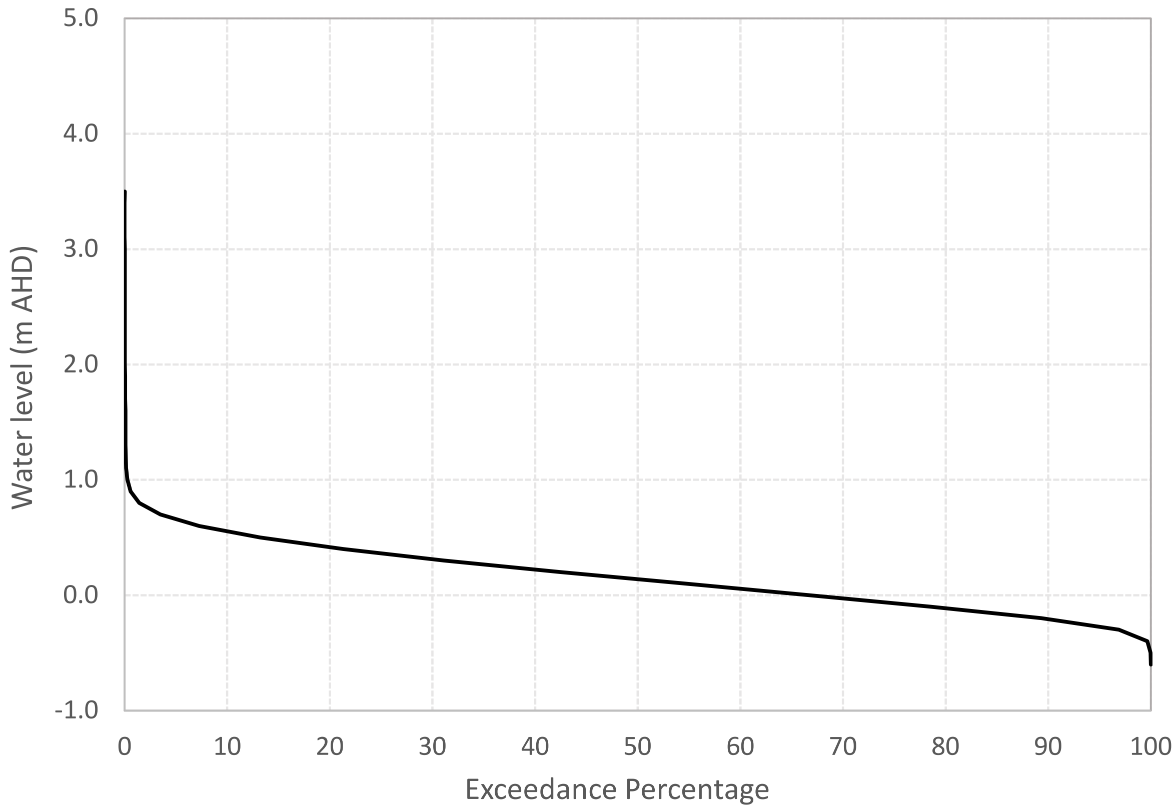

Figure S90. Frequency distribution of water levels at Terara (Station 215420)

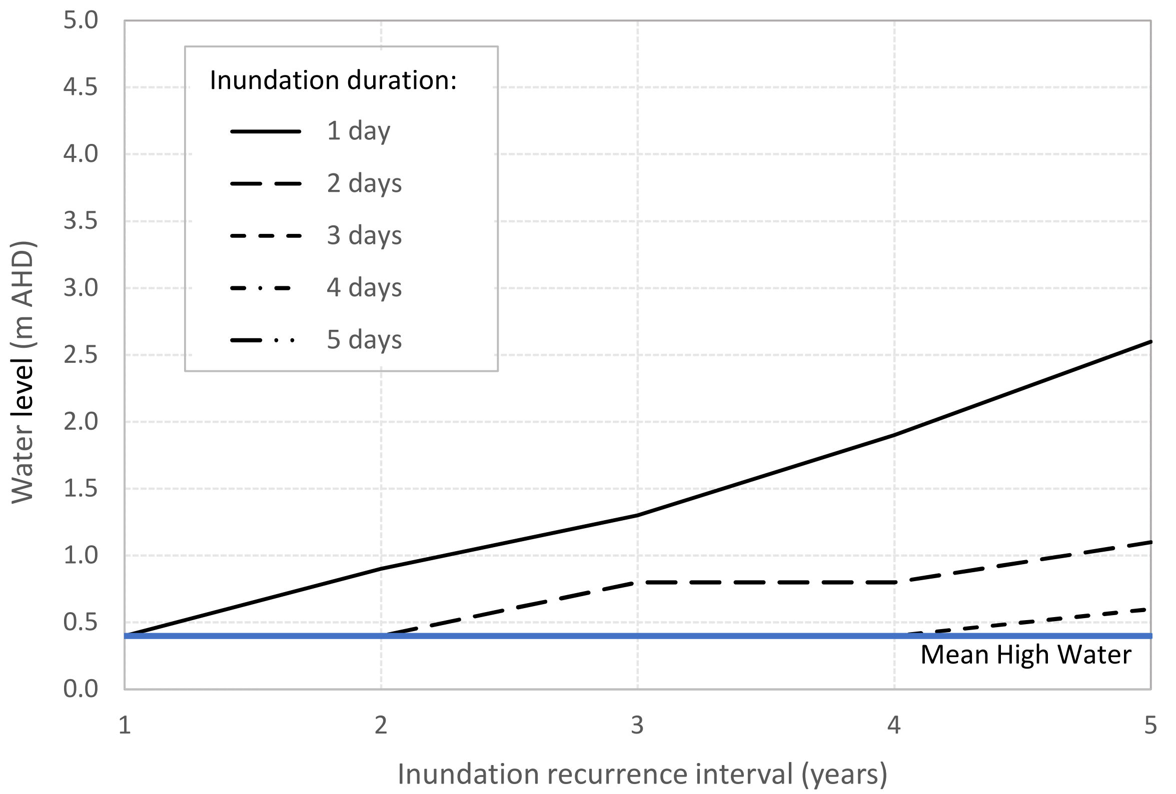

Figure S91. Water levels corresponding to inundation durations of 1 to 5 days with recurrence intervals of 1 to 5 years for Terara (Station 215420)

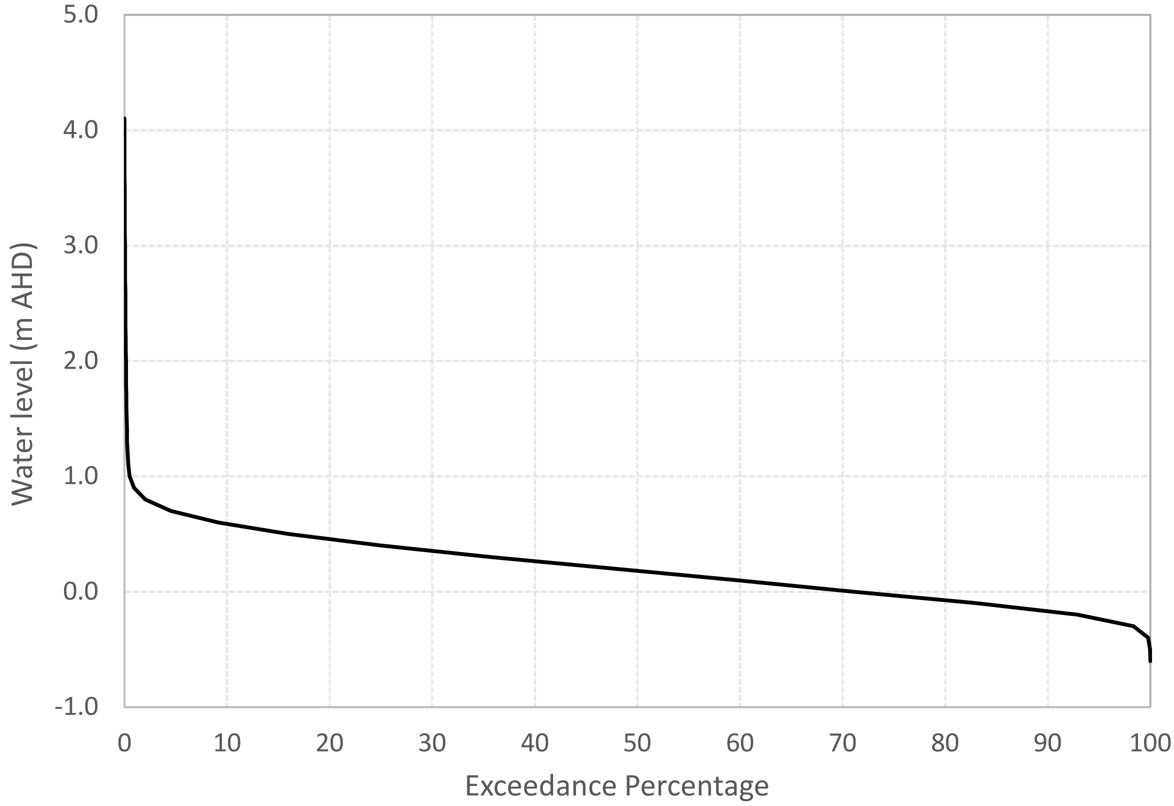

Figure S92. Frequency distribution of water levels at Nowra Bridge (Station 215411)

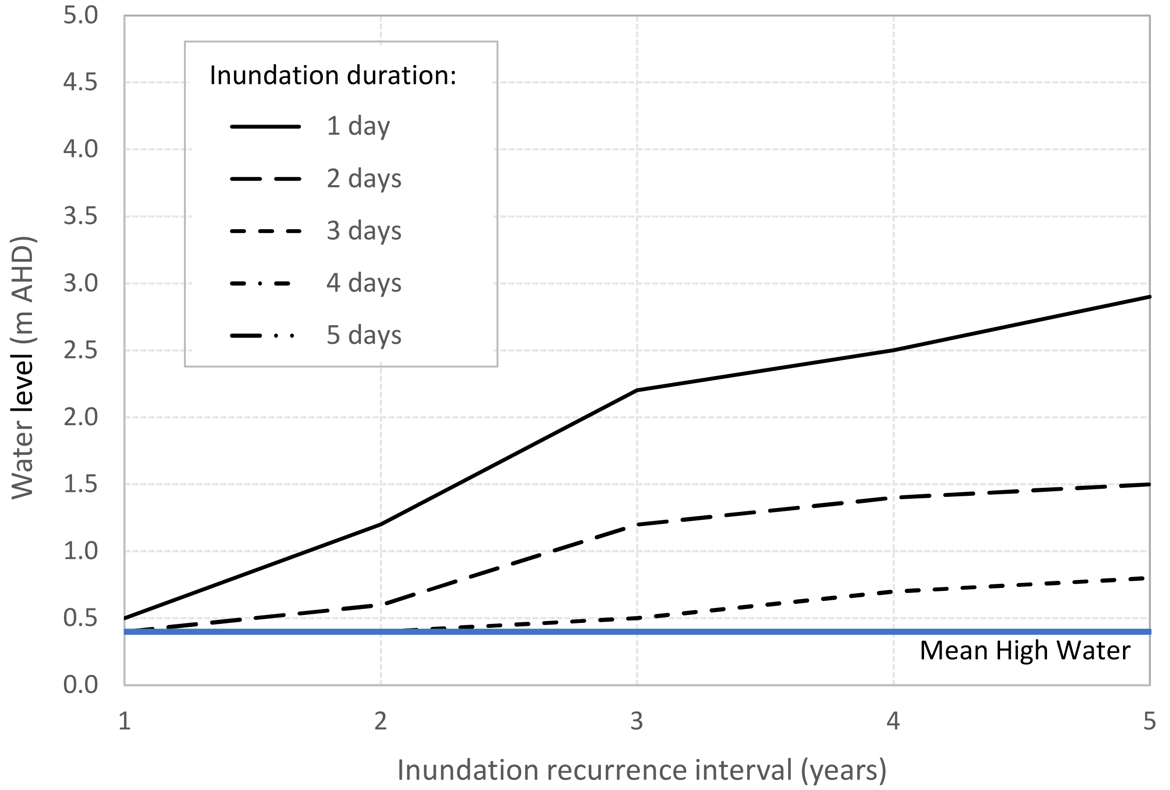

Figure S93. Water levels corresponding to inundation durations of 1 to 5 days with recurrence intervals of 1 to 5 years for Nowra Bridge (Station 215411)

Table S16. Median inundation level, blackwater contribution factor and ranking of catchments, Tweed River

Catchment	Median blackwater elevation (m AHD)	Blackwater contribution factor	Rank
Tumbulgum/Eviron	0.8	12.2	1
Tygalgah	1.0	12.1	2
Condong	0.8	7.5	3
Stotts Creek	0.7	6.9	4
North Tumbulgum	0.7	5.9	5
Dulguigan	1.0	5.8	6
West Chinderah	0.5	5.6	7
Kynnumboon	1.4	5.4	8
South Murwillumbah	0.7	1.6	9
Cobaki	0.4	1.2	10
Bilambil/Terranora	0.4	1.1	11
East Chinderah	0.4	0.9	12
Dunbible Creek	0.7	0.8	13
Commercial Road	0.7	0.4	14

* Mean High Water adopted as minimum blackwater inundation level

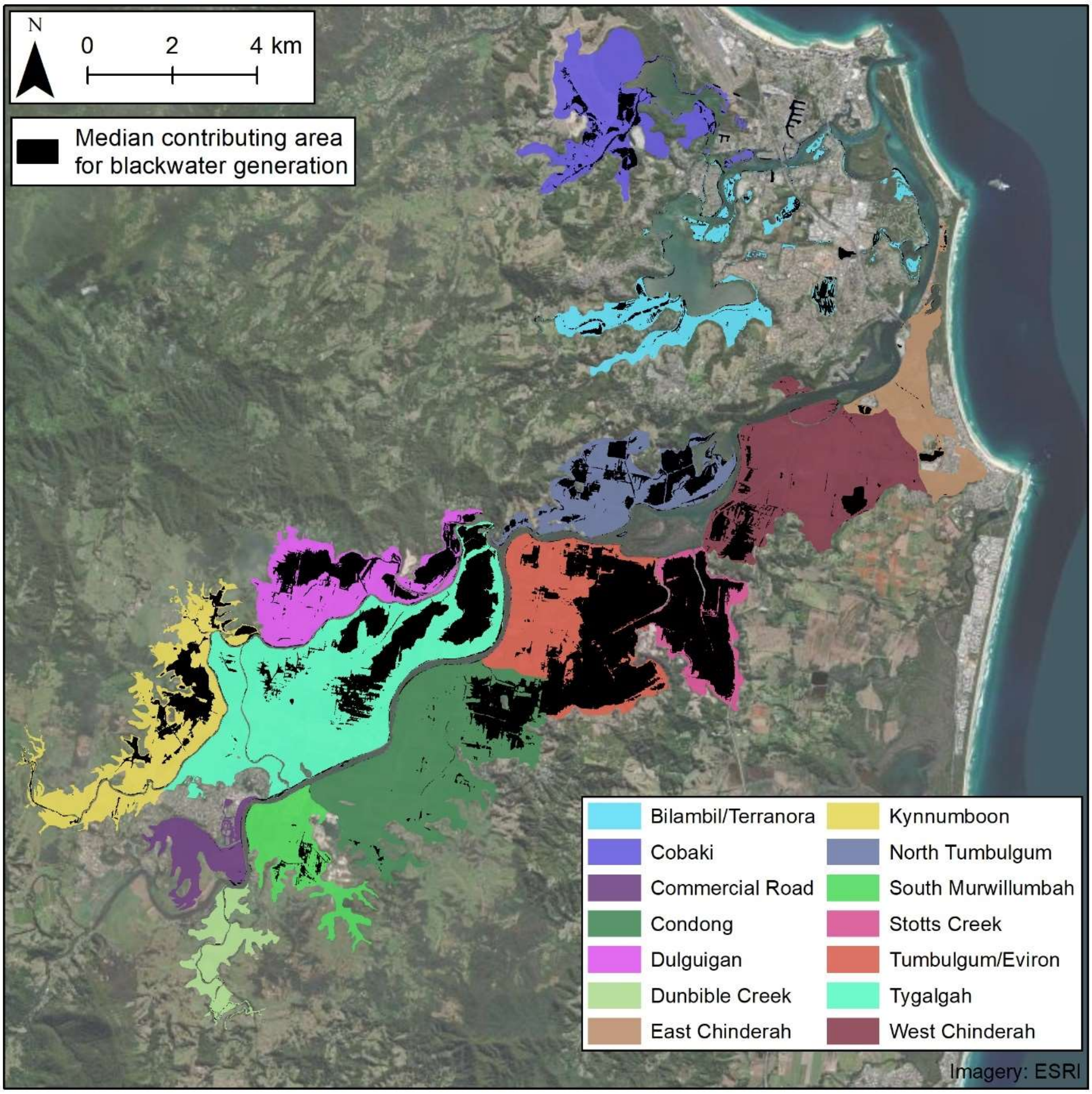

Figure S94. Extent of area contributing to blackwater generation under median inundation level, Tweed River

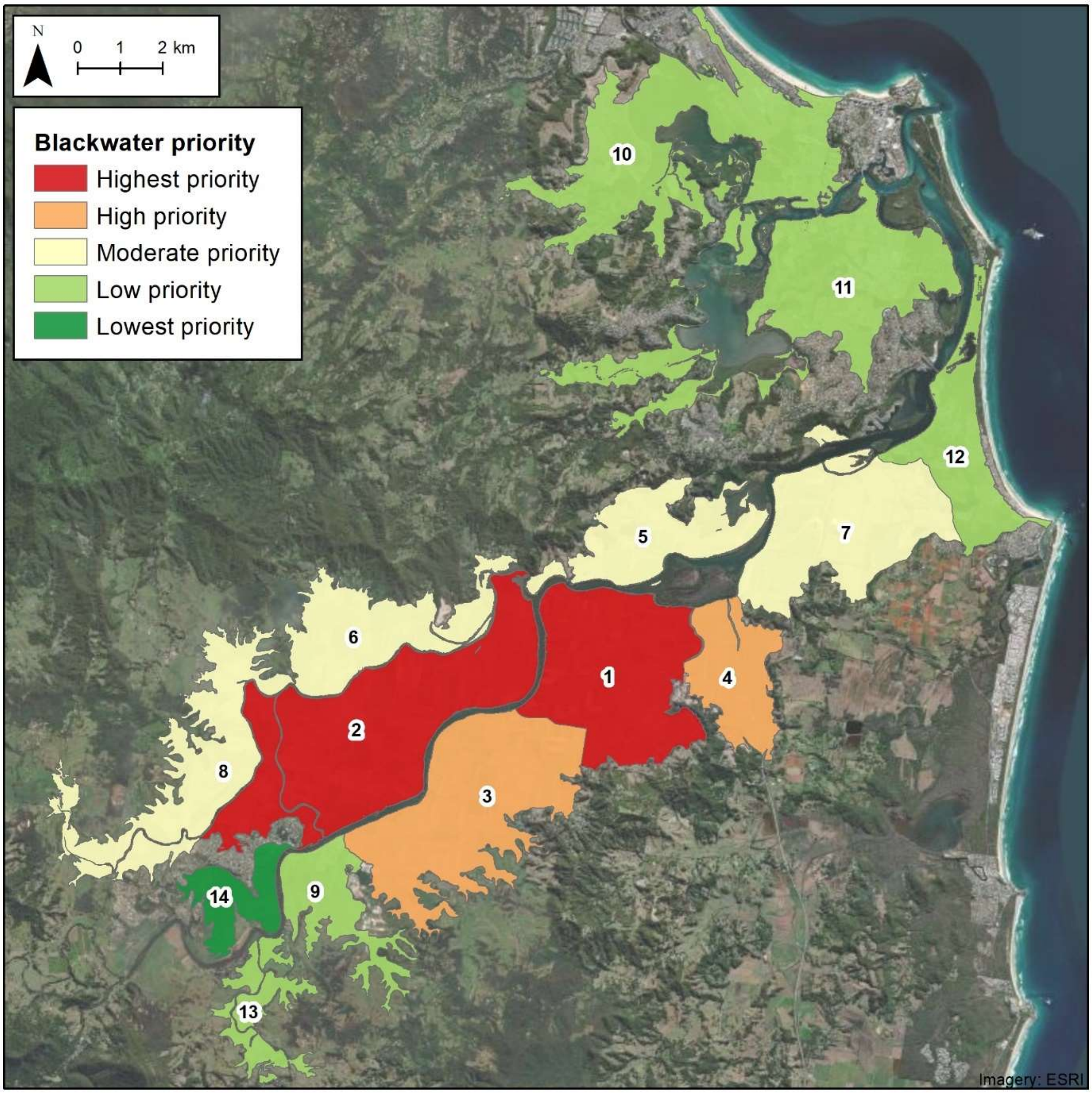

Figure S95. Ranking of catchments for blackwater risk, Tweed River

Table S17. Median inundation level, blackwater contribution factor and ranking of catchments, Richmond River

Catchment	Median blackwater elevation (m AHD)	Blackwater contribution factor	Rank
Bungawalbin Creek/Sandy Creek	2.9	135.4	1
Rocky Mouth Creek	1.5	44.0	2
Tuckean Swamp	1.0	37.4	3
East Coraki	2.5	33.4	4
Swan Bay	2.9	26.1	5
Kilgin/Buckendoon	1.5	25.6	6
Upper Richmond/Wilsons River	2.3	16.7	7
Rileys Hill	1.5	7.8	8
Emigrant Creek/Maguires Creek	0.4*	3.0	9
North Creek	0.5*	2.4	10
Empire Vale	0.5*	1.2	11
Back Channel	0.5*	0.9	12
South Ballina	0.5*	0.2	13

* Mean High Water adopted as minimum blackwater inundation level

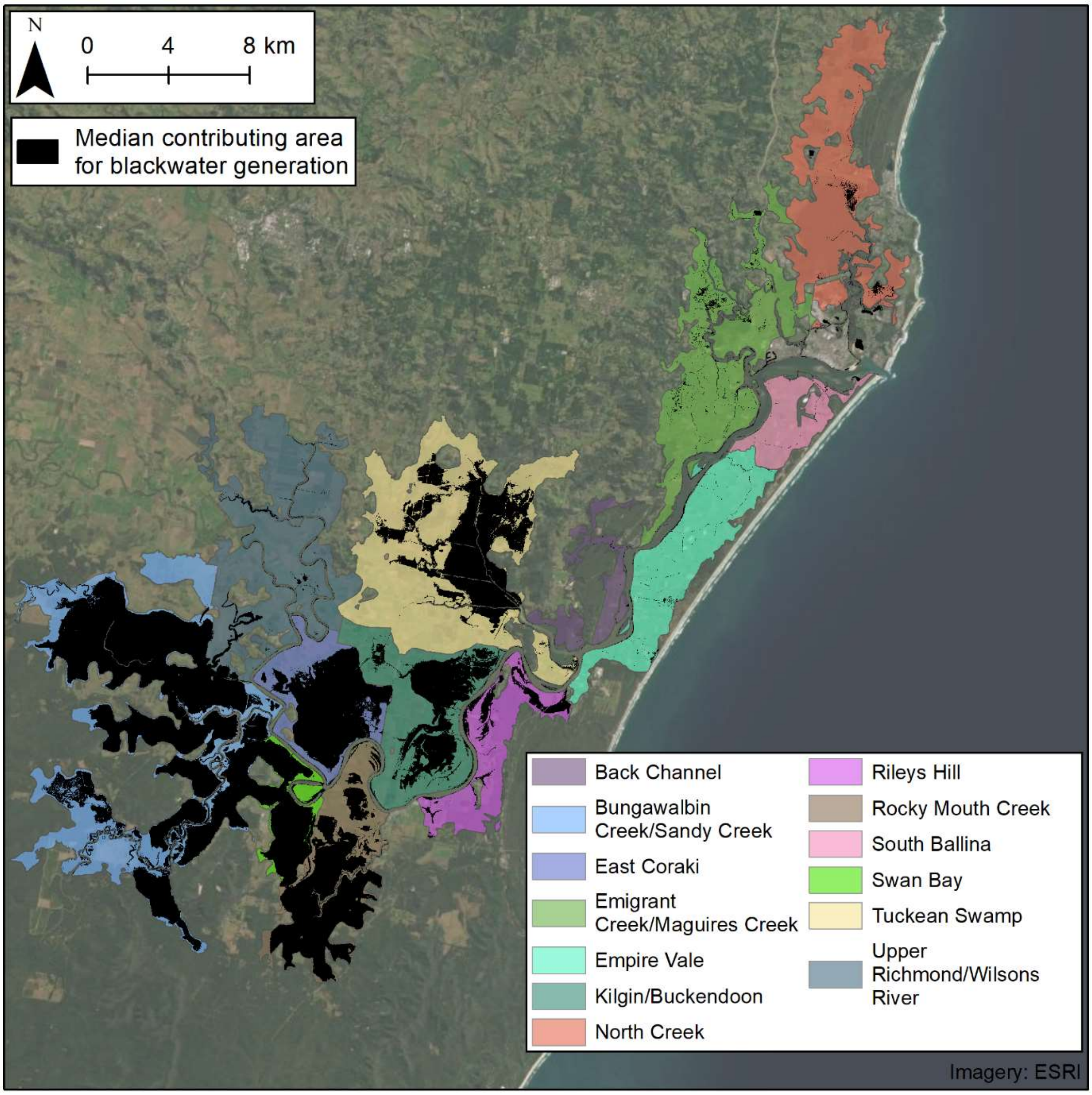

Figure S96. Extent of area contributing to blackwater generation under median inundation level, Richmond River

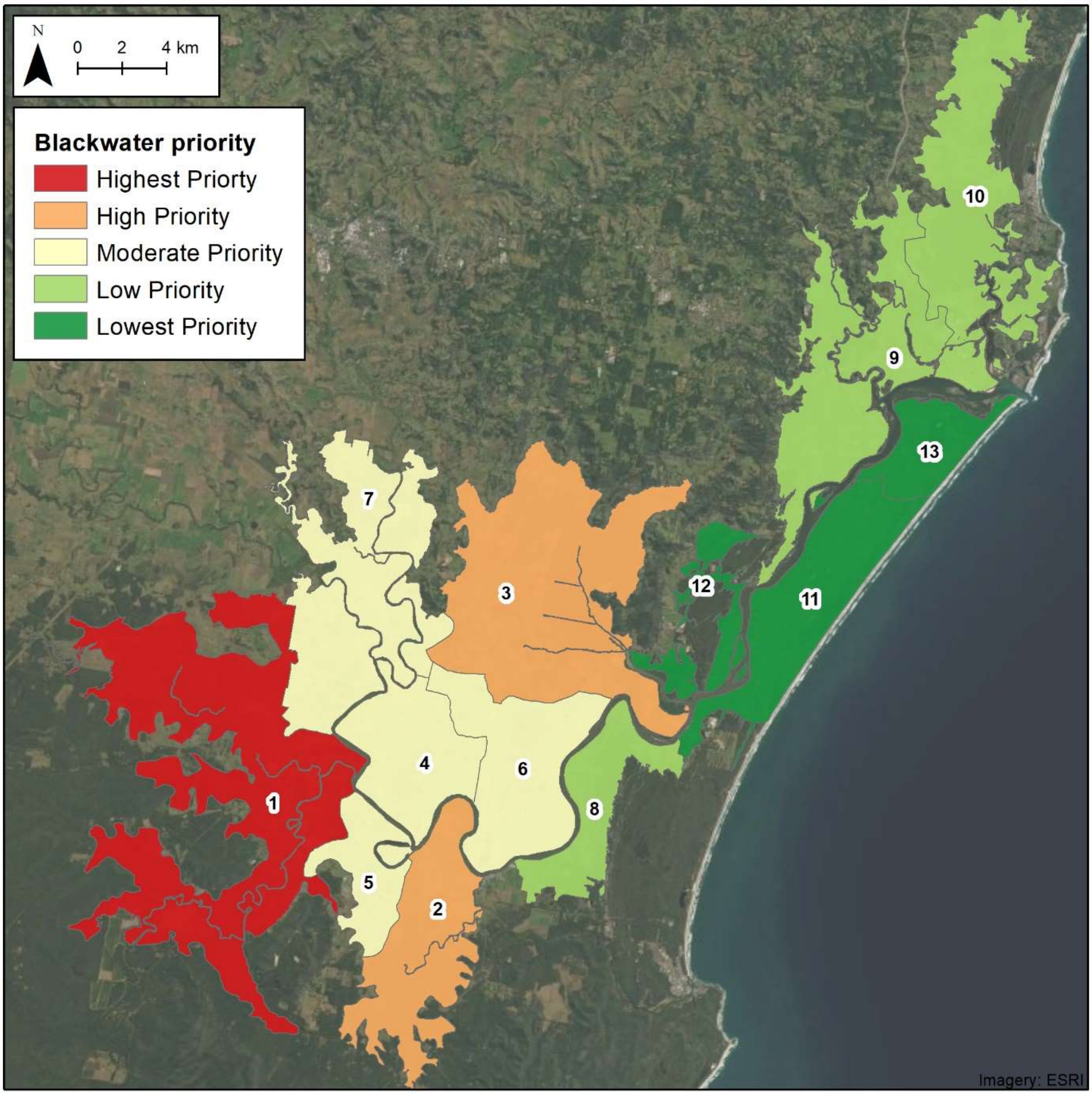

Figure S97. Ranking of catchments for blackwater risk, Richmond River

Table S18. Median inundation level, blackwater contribution factor and ranking of catchments, Clarence River

Catchment	Median blackwater elevation (m AHD)	Blackwater contribution factor	Rank
Coldstream River	1.9	153.5	1
Sportsmans Creek	1.9	99.3	2
Swan Creek	1.9	62.1	3
Taloumbi/Palmers Channel	0.9	52.2	4
Shark Creek	1.1	43.1	5
West Woodford Island	1.6	32.9	6
Alumy Creek	2.1	32.9	7
The Broadwater	1.3	25.3	8
Harwood/Chatsworth/ Goodwood/Warregah Islands	0.9	20.0	9
Gulmarrad/East Woodford Island	0.9	12.2	10
South Grafton	1.5	11.6	11
Southgate	1.8	10.7	12
Maclean	0.9	10.3	13
Palmers Island/Micalo Island/ Yamba	0.5*	9.2	14
Mororo/Ashby	0.9	8.4	15
The Freshwater	0.9	7.0	16

* Mean High Water adopted as minimum blackwater inundation level

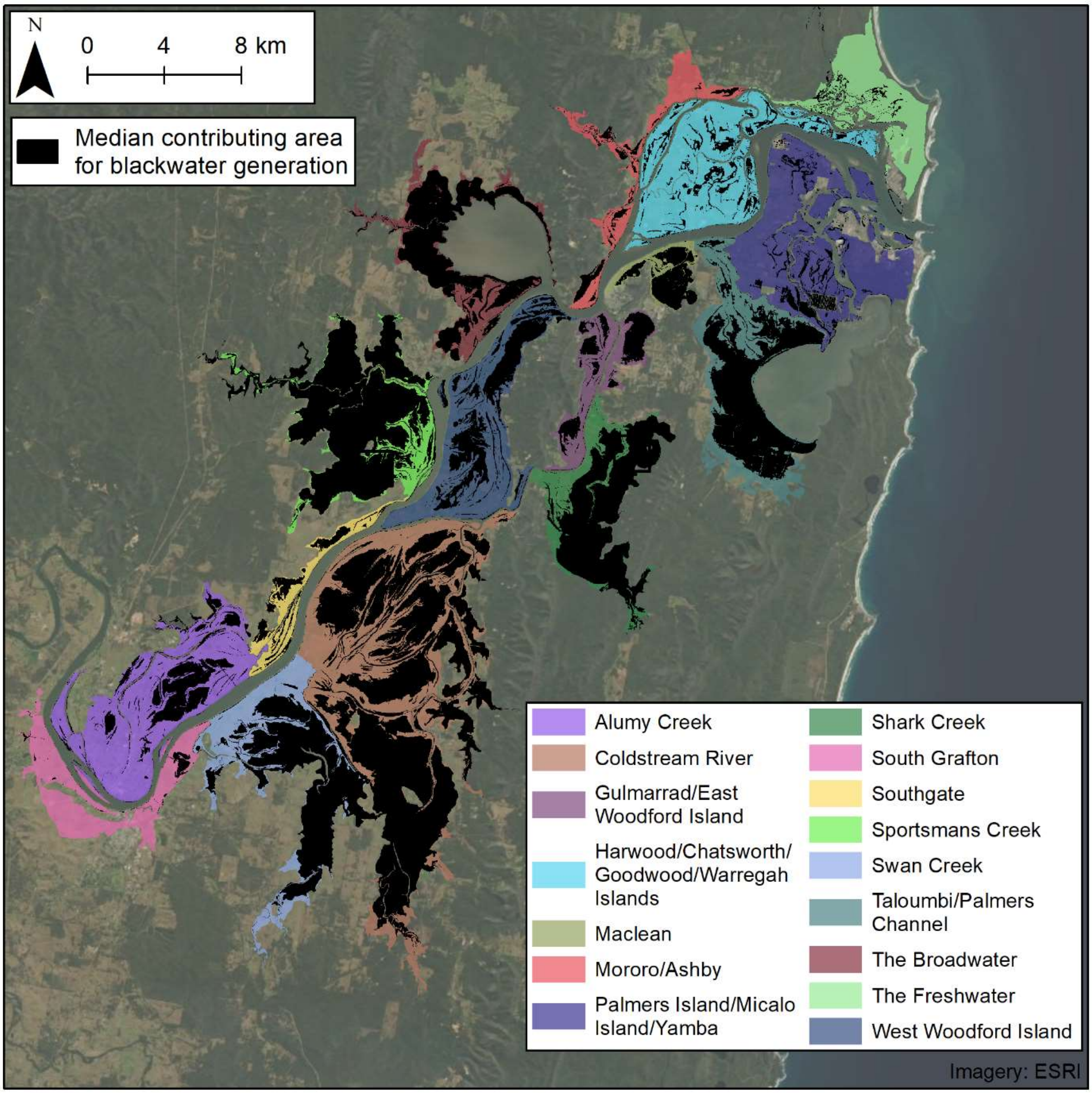

Figure S98. Extent of area contributing to blackwater generation under median inundation level, Clarence River

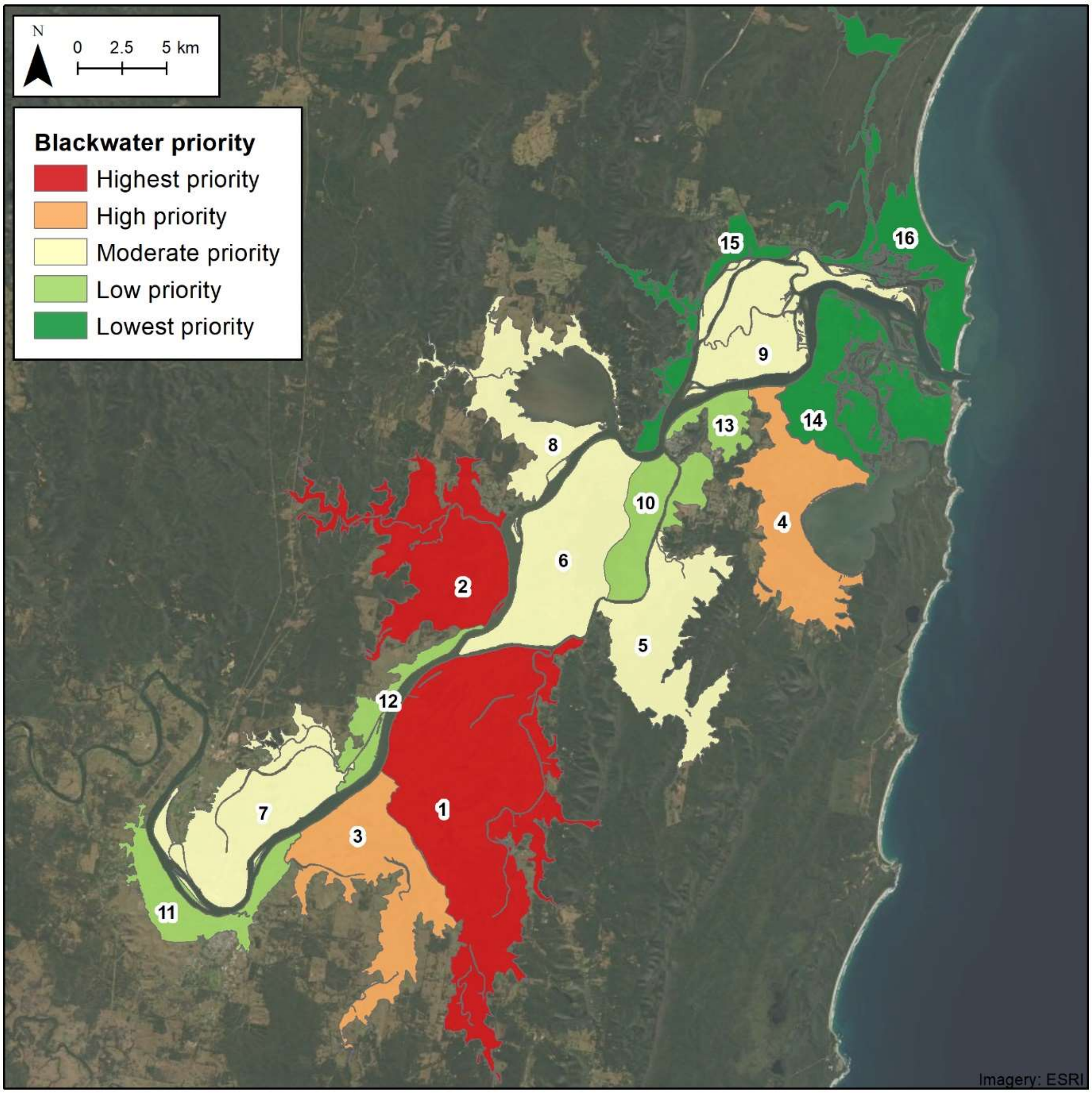

Figure S99. Ranking of catchments for blackwater risk, Clarence River

Table S19. Median inundation level, blackwater contribution factor and ranking of catchments, Macleay River

Catchment	Median blackwater elevation (m AHD)	Blackwater contribution factor	Rank
Kinchela Creek	1.0	87.0	1
Belmore Swamp	1.2	73.9	2
Collombatti-Clybucca	1.1	69.3	3
Frogmore/Austral Eden/Verges Swamp	1.2	48.6	4
Yarrahapinni	1.1	39.8	5
Raffertys/Saltwater Inlet	0.8	34.8	6
Summer Island	0.9	29.6	7
Christmas Creek	1.9	13.8	8
Rainbow Reach	0.6	9.8	9
Pola Creek	2.1	4.0	10
Euroka Creek	2.0	2.1	11

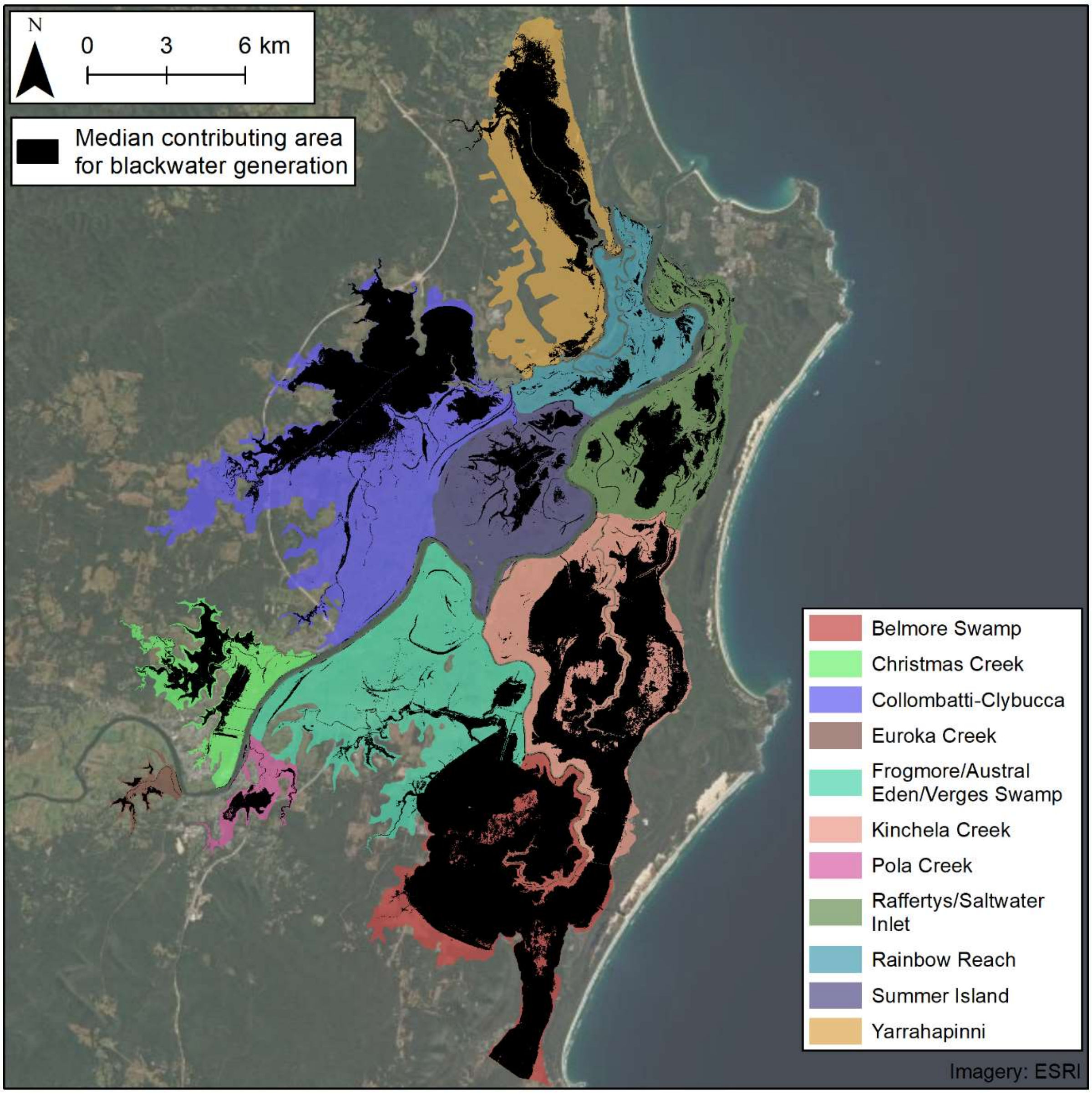

Figure S100. Extent of area contributing to blackwater generation under median inundation level, Macleay River

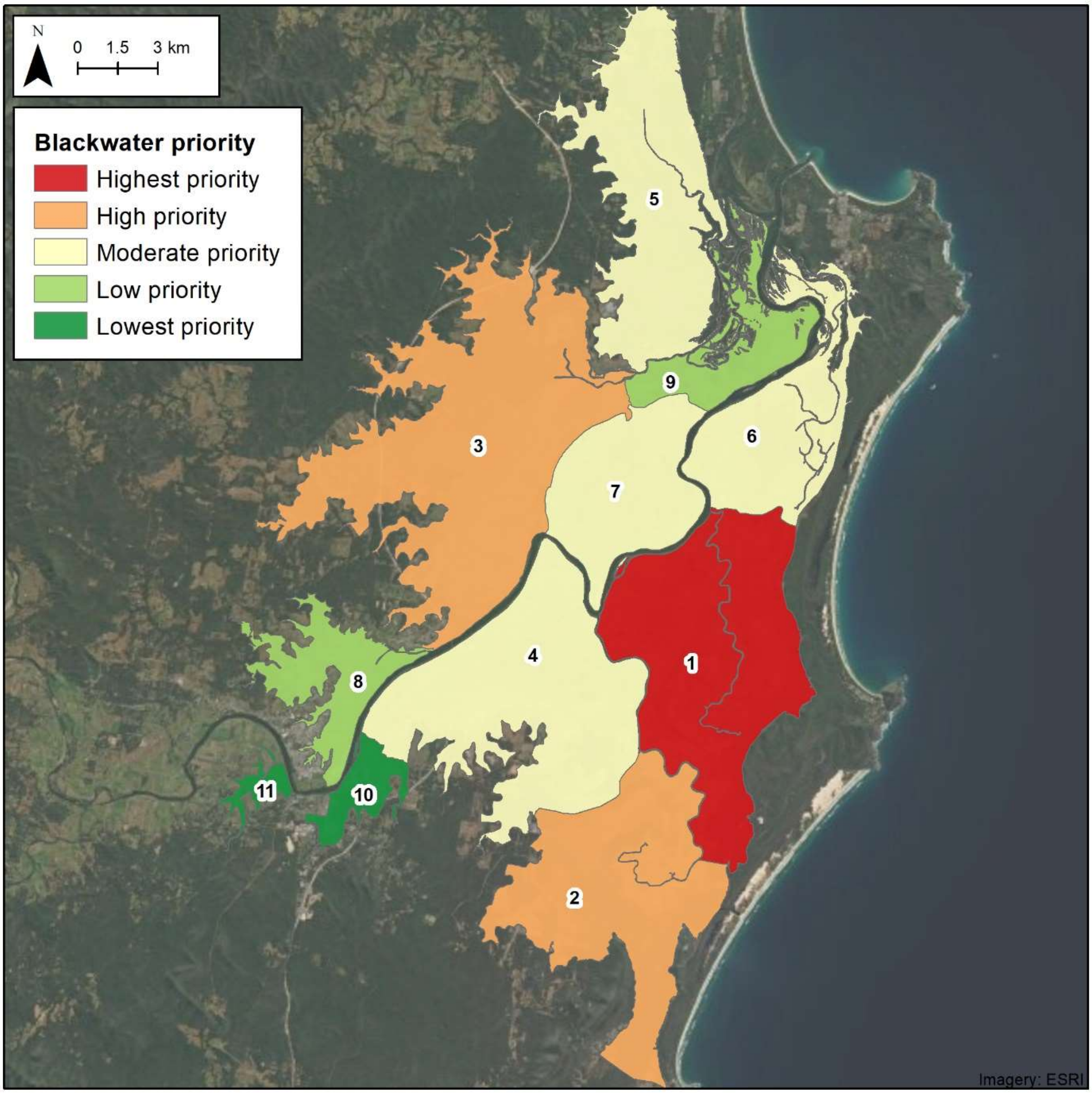

Figure S101. Ranking of catchments for blackwater risk, Macleay River

Table S20. Median inundation level, blackwater contribution factor and ranking of catchments, Hastings River

Catchment	Median blackwater elevation (m AHD)	Blackwater contribution factor	Rank
Connection Creek	1.0	66.8	1
Upper Maria River	1.0	66.5	2
Lower Maria River West	0.7	19.1	3
Lower Maria River East	0.7	11.4	4
Pembrooke	0.6	1.8	5
Fernbank Creek	0.5*	1.6	6
Limeburners Creek	0.4*	1.3	7
Rawdon Island	0.6	1.2	8
Kings Creek	0.7	1.1	9
Sarahs Creek/Sancrox	0.7	0.5	10
Redbank	0.7	0.5	11
Port Macquarie Airport	0.4*	0.1	12
Partridge Creek	0.5*	0.1	13

* Mean High Water adopted as minimum blackwater inundation level

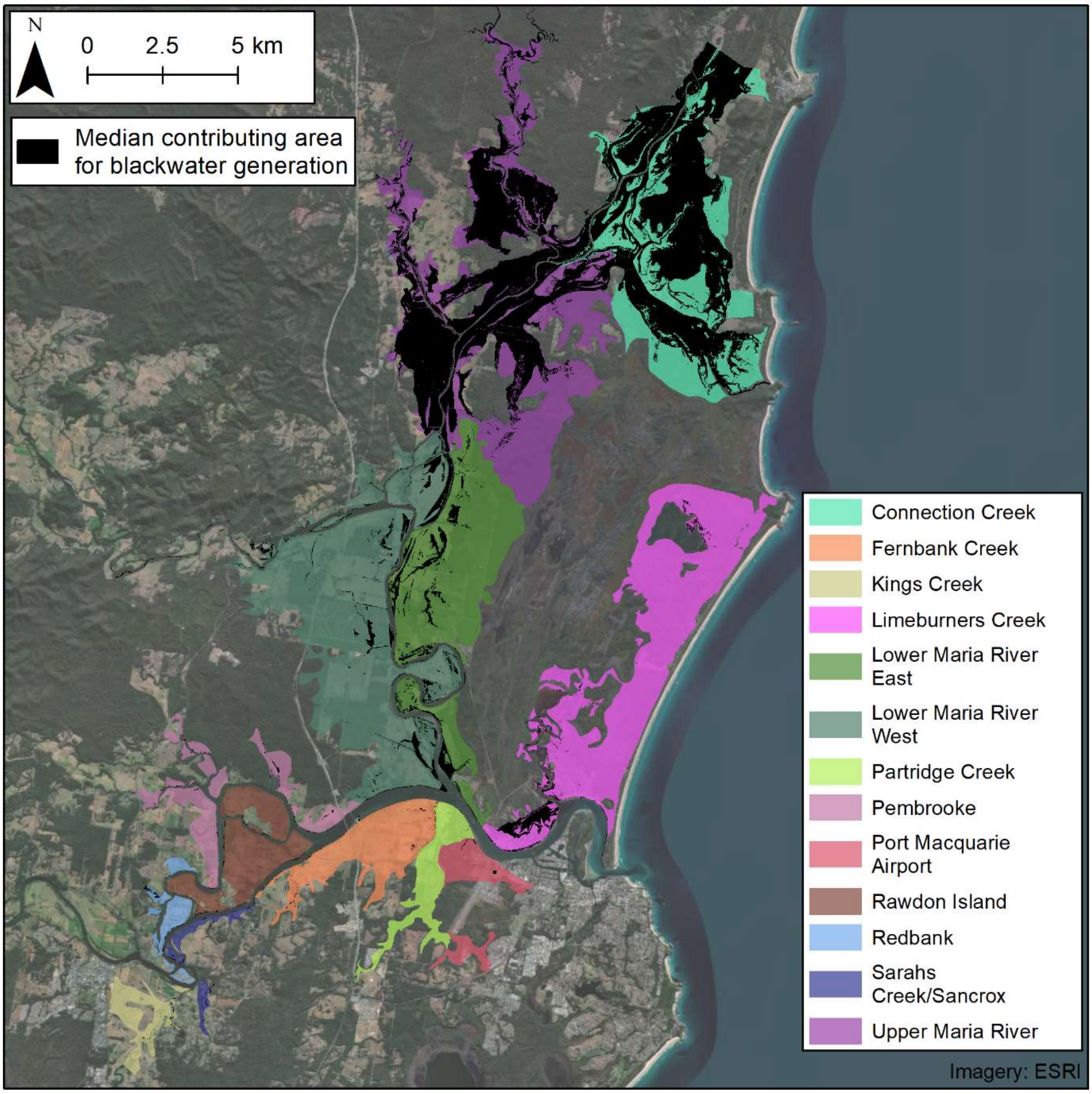

Figure S102. Extent of area contributing to blackwater generation under median inundation level, Hastings River

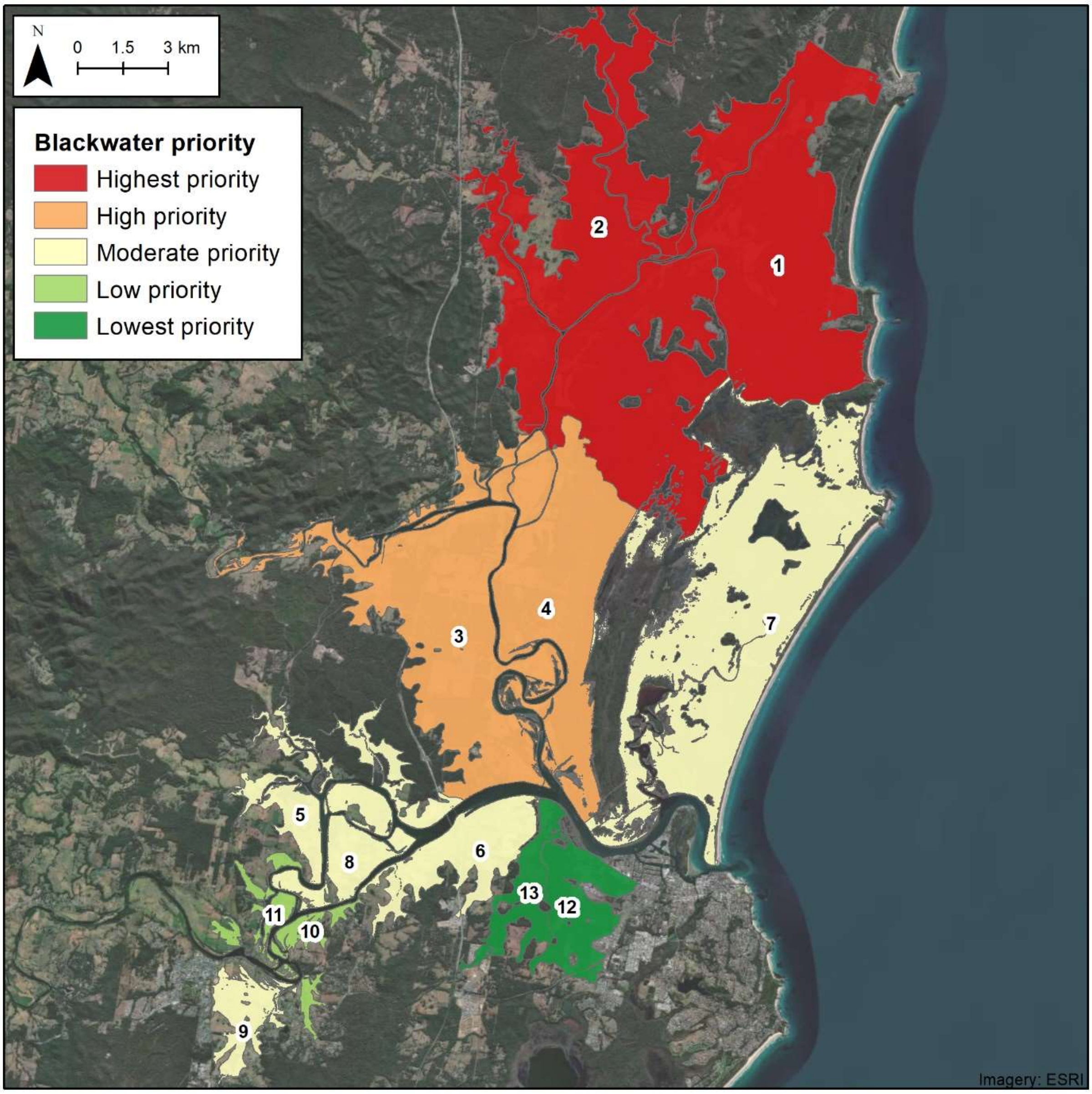

Figure S103. Ranking of catchments for blackwater risk, Hastings River

Table S21. Median inundation level, blackwater contribution factor and ranking of catchments, Manning River

Catchment	Median blackwater elevation (m AHD)	Blackwater contribution factor	Rank
Ghinni Ghinni	0.7	9.5	1
Moto	0.6	7.7	2
Big Swamp	0.5	6.4	3
Jones Island	0.6	5.4	4
Bukkan Bukkan Creek	0.6	4.5	5
Coopernook	0.6	4.1	6
Cattai Creek	0.5	3.1	7
Croakers Creek	0.5	2.8	8
Glenthorne	0.7	1.8	9
Dawson River	0.7	1.6	10
Dumaresq Island	0.7	1.4	11
Mambo Island	0.5	1.2	12
Pampoolah	0.6	1.1	13
Taree Estate	0.7	0.4	14
Mitchells Island	0.5	0.4	15
Old Bar	0.5	0.2	16
Harrington	0.4*	0.03	17

* Mean High Water adopted as minimum blackwater inundation level

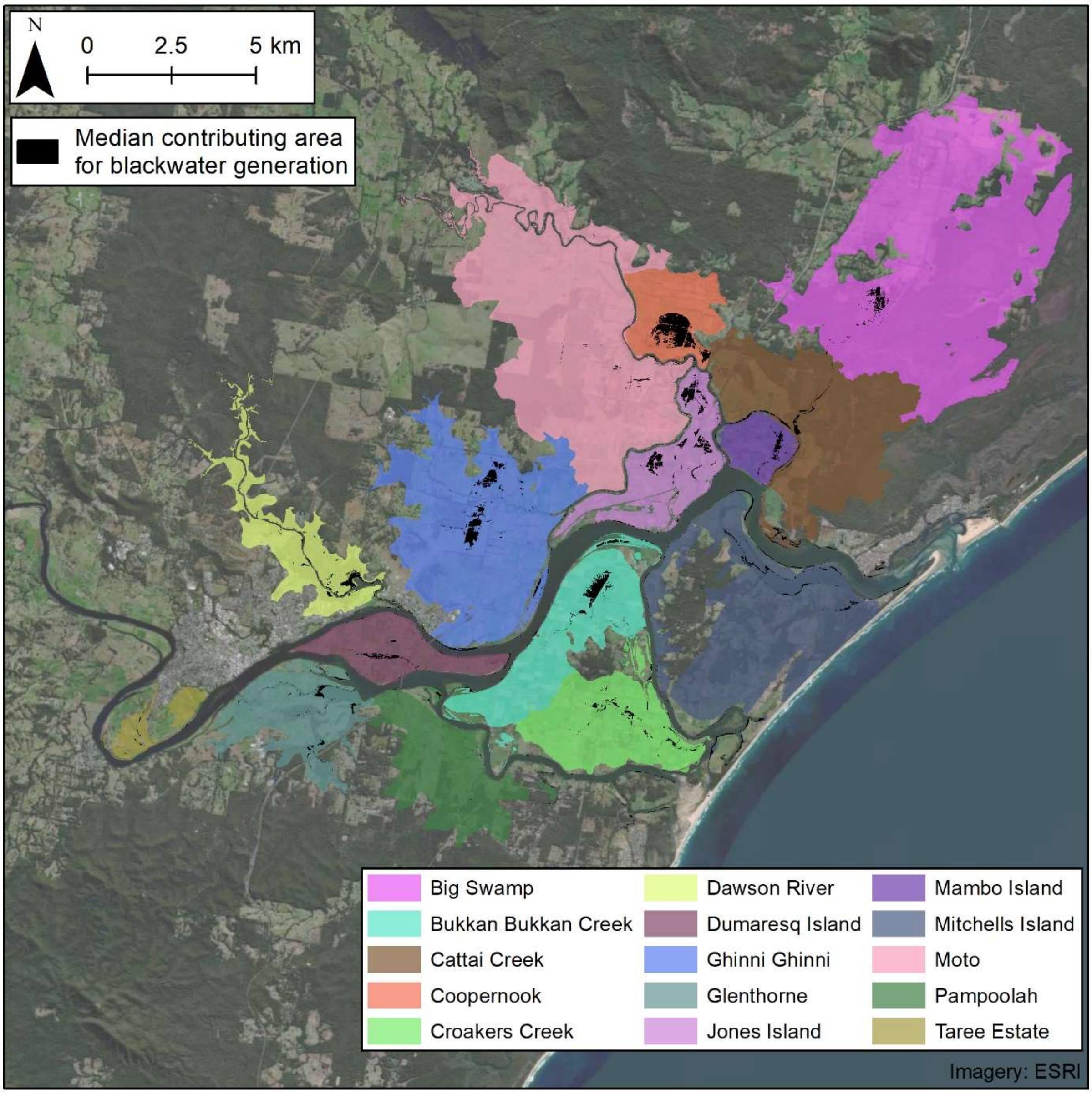

Figure S104. Extent of area contributing to blackwater generation under median inundation level, Manning River

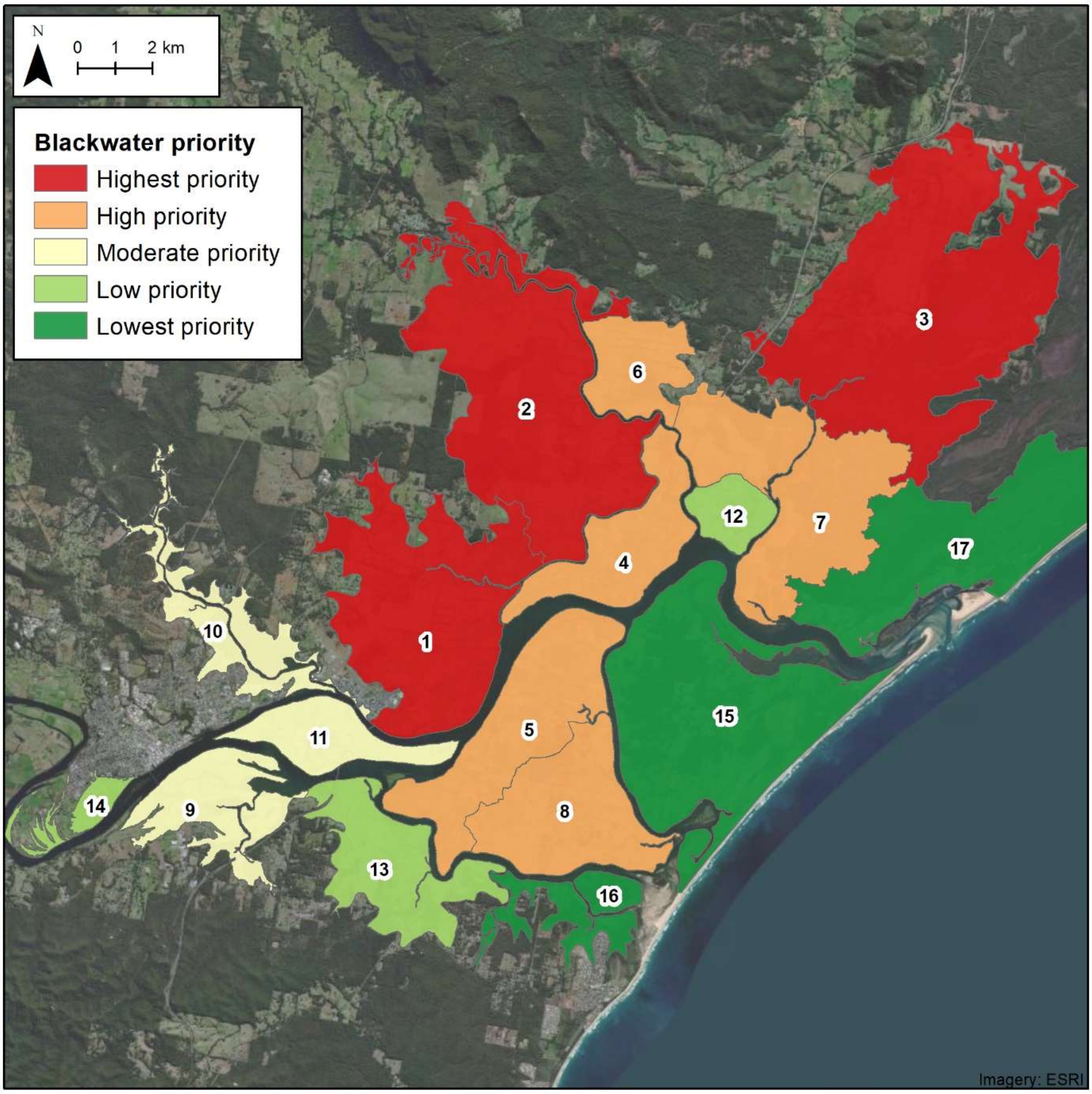

Figure S105. Ranking of catchments for blackwater risk, Manning River

Table S22. Median inundation level, blackwater contribution factor and ranking of catchments, Shoalhaven River

Catchment	Median blackwater elevation (m AHD)	Blackwater contribution factor	Rank
Brundee/Saltwater	0.4*	18.4	1
Terara	0.4*	8.0	2
Bolong	0.4*	5.8	3
Numbaa	0.4*	2.9	4
Far Meadow	0.4*	2.2	5
Worrigee	0.4*	0.8	6
Lower Broughton Creek	0.4*	0.8	7
Greenwell Point	0.4*	0.5	8
Berry	0.4*	0.5	9
Eelwine Creek/Mayfield	0.4*	0.3	10
Coolangatta	0.4*	0.2	11
Abernethys Creek	0.4*	0.2	12
Shoalhaven Heads	0.4*	0.1	13
Crookhaven Creek	0.4*	0.1	14
Comerong Island	0.4*	0.05	15

* Mean High Water adopted as minimum blackwater inundation level

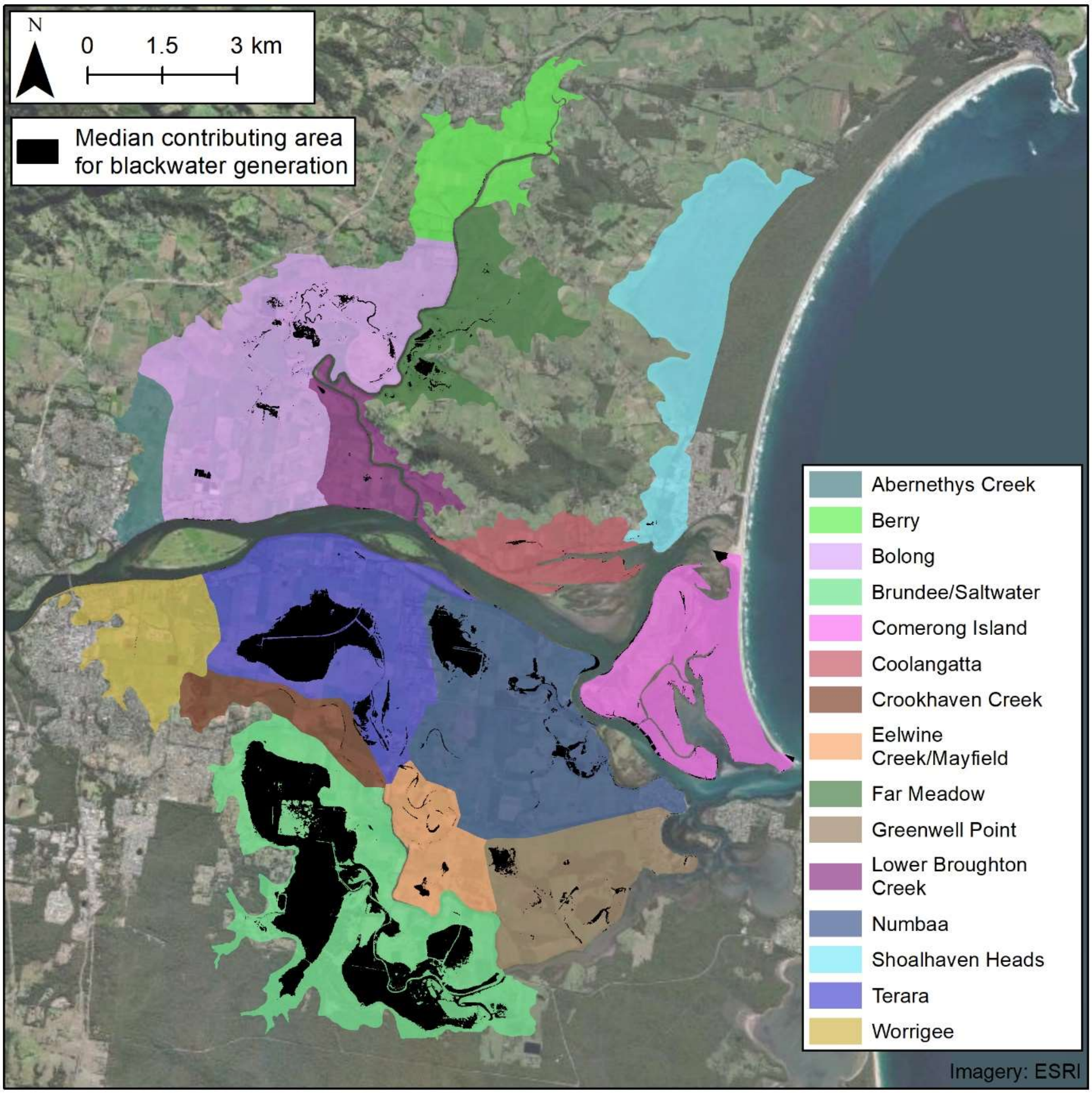

Figure S106. Extent of area contributing to blackwater generation under median inundation level, Shoalhaven River

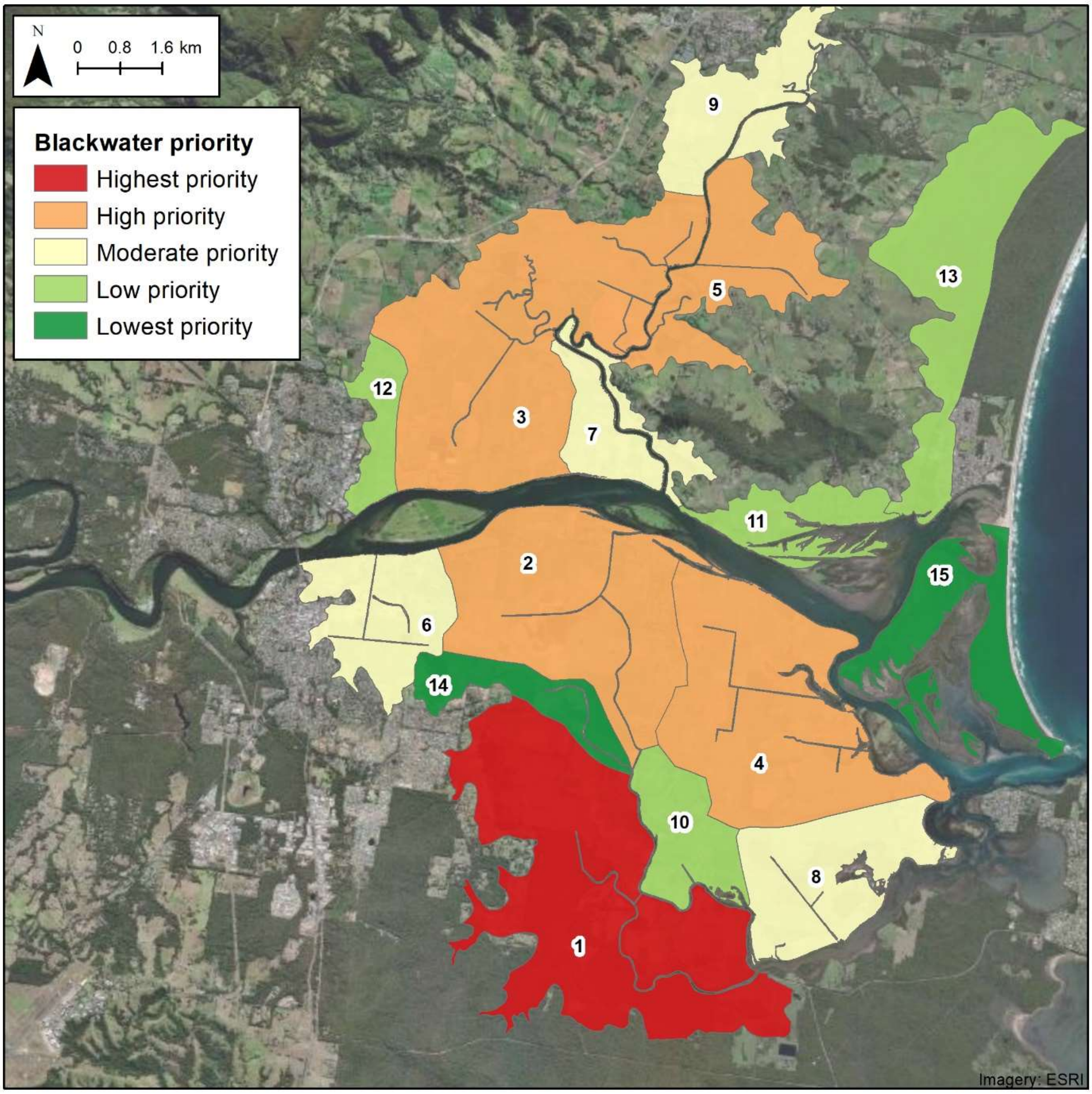

Figure S107. Ranking of catchments for blackwater risk, Shoalhaven River

Table S23. Sensitivity of inundation level and ranking of aggregated blackwater risk factor to changes in duration and flood frequency matrices

River system		**Tweed**	**Richmond**	**Clarence**	**Macleay**	**Hastings**	**Manning**	**Shoalhaven**
Base case:*								
	median inundation level	0.7	1.5	1.2	1.1	0.7	0.6	0.4
	max inundation level	3.8	4.1	6.2	5.9	3.6	3.0	2.7
Increased inundation duration:								
2 – 5 days	median inundation level	0.5	1.25	1.0	1.1	0.55	0.45	0.4
	max inundation level	2.8	4.1	4.5	4.9	1.7	2.2	1.3
	rank correlation of results	0.98	1.0	0.99	0.99	0.96	0.99	0.88
3 – 5 days	median inundation level	0.5	1.1	0.9	0.8	0.5	0.4	0.4
	max inundation level	2.4	3.6	4.0	3.7	1.5	1.3	0.7
	rank correlation of results	0.97	0.99	0.99	0.98	0.92	0.95	0.77
Reduced flood frequency:								
2 – 5 years	median inundation level	0.8	1.6	1.4	1.4	0.7	0.65	0.4
	max inundation level	3.8	4.1	6.2	5.9	3.6	3.0	2.7
	rank correlation of results	0.995	0.996	0.997	1.0	0.99	1.0	0.997
3 – 5 years	median inundation level	0.9	1.6	1.4	1.3	0.7	0.6	0.4
	max inundation level	3.8	4.1	6.2	5.9	3.6	3.0	2.7
	rank correlation of results	0.98	0.996	0.996	1.0	0.996	0.998	0.995

* Base case represents the results for the full matrix of 1 to 5 days inundation and 1 to 5 year event frequency

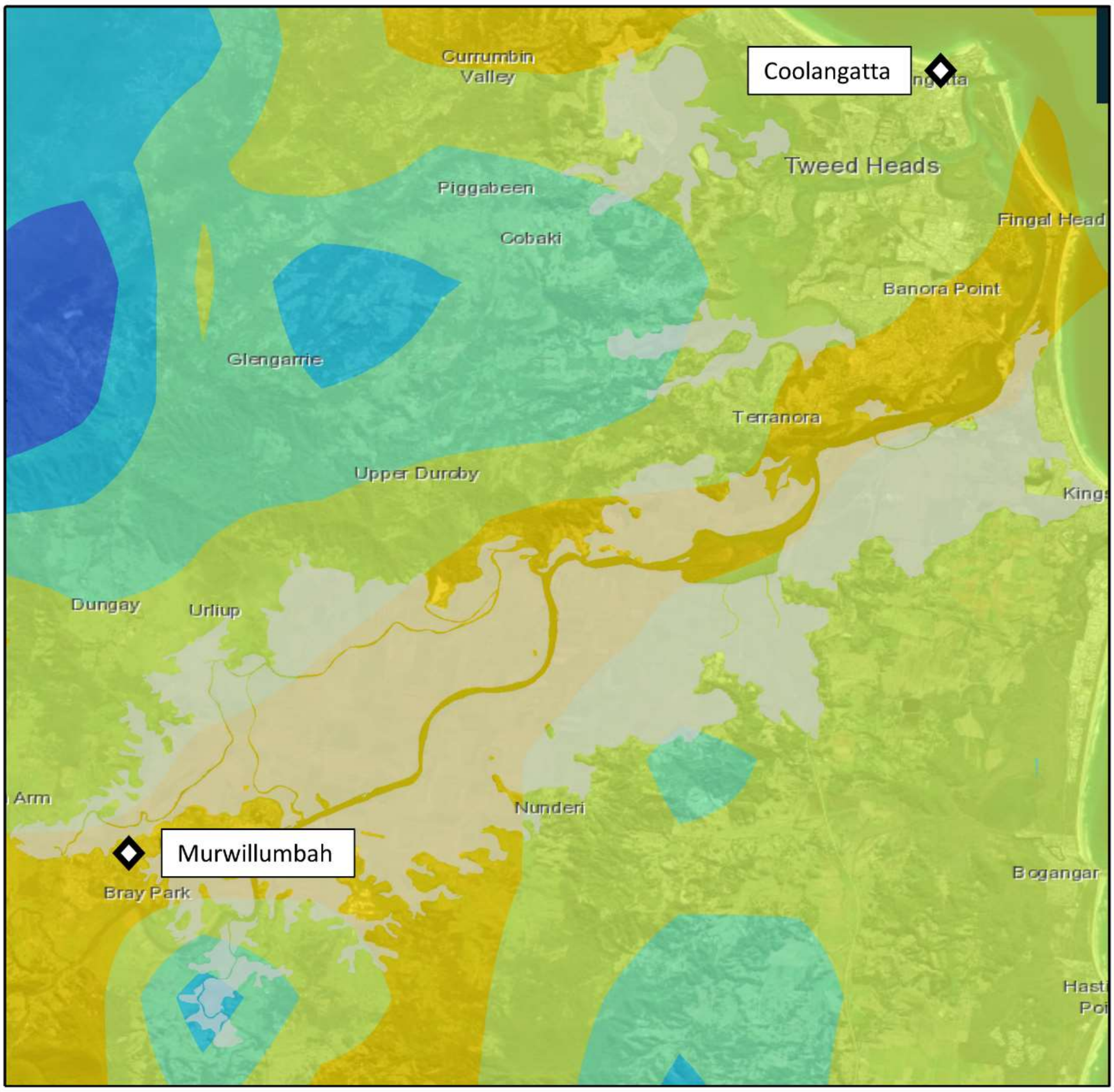

Legend:

◇ Temperature monitoring station

Extent of estuarine subcatchments subject to inundation and subsequent potential blackwater production

N

0 2 4 km

Temperature (°C)

- < 23
- 23 - 24
- 24 - 25
- 25 - 26
- 26 - 27
- 27 - 28
- 28 - 29
- 29 - 30

Figure S108. Average maximum temperature (October to April), Tweed River

Table S24. Average maximum temperatures within the Tweed River catchments

Station: Coolangatta (40717) **Elevation:** 4m AHD
Data period: November 1982 to June 2022

Month	Monthly maximum temperature			
	5%	50%	95%	Average
January	26.8	28.5	30.0	28.4
February	27.0	28.4	29.8	28.3
March	25.9	27.5	28.6	27.4
April	24.4	25.5	26.9	25.5
May	22.4	23.1	24.5	23.2
June	20.0	21.0	22.1	21.1
July	19.4	20.9	21.8	20.7
August	20.4	21.5	23.2	21.6
September	22.1	23.3	25.1	23.4
October	23.2	24.6	26.4	24.7
November	24.1	26.0	27.6	26.1
December	26.1	27.4	29.2	27.4

Station: Bray Park, Murwillumbah (58158) **Elevation:** 8m AHD
Data period: October 1972 to June 2022

Month	Monthly maximum temperature			
	5%	50%	95%	Average
January	27.9	29.5	31.2	29.6
February	27.5	28.9	30.8	29.0
March	26.6	28.2	29.4	28.1
April	24.9	26.0	27.6	26.2
May	22.5	23.4	25.2	23.6
June	20.4	21.3	22.4	21.3
July	19.9	21.2	22.4	21.1
August	21.3	22.6	24.1	22.6
September	23.4	24.8	27.8	25.1
October	24.5	26.2	28.0	26.4
November	25.8	27.8	29.4	27.8
December	27.0	29.0	31.6	29.1

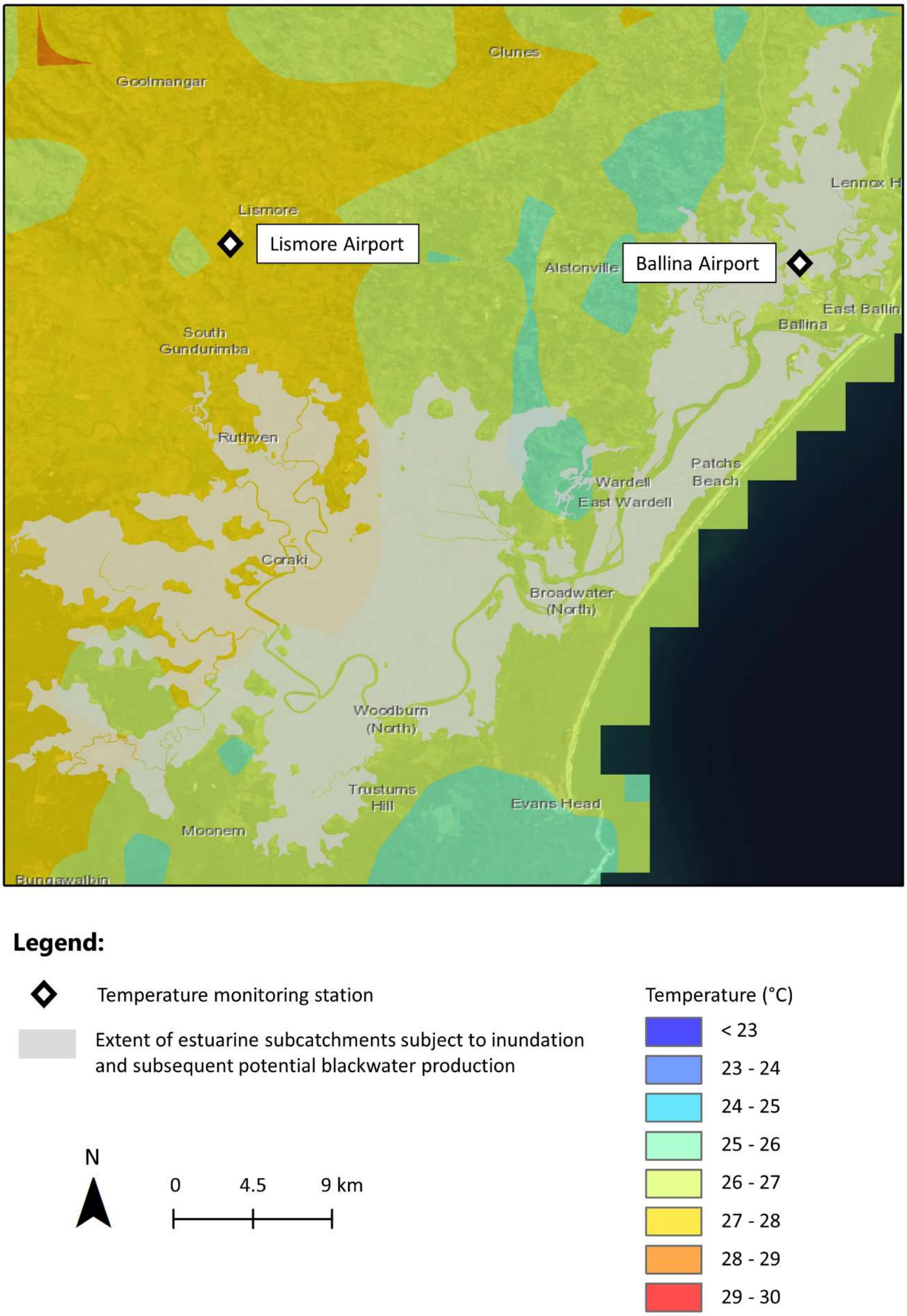

Figure S109. Average maximum temperature (October to April), Richmond River

Table S25. Average maximum temperatures within the Richmond River catchments

Station: Ballina Airport AWS (58198) **Elevation:** 1m AHD
Data period: November 1992 to June 2022

Month	Monthly maximum temperature			
	5%	50%	95%	Average
January	26.7	28.2	30.2	28.4
February	26.8	28.0	29.6	28.1
March	25.8	27.1	28.6	27.1
April	23.7	25.0	26.3	25.0
May	21.7	22.4	23.7	22.5
June	19.5	20.4	21.2	20.3
July	19.3	20.1	21.2	20.1
August	20.2	21.3	23.1	21.4
September	22.2	23.4	25.7	23.6
October	23.6	24.9	26.2	24.9
November	24.4	26.4	28.6	26.3
December	25.5	27.5	29.5	27.6

Station: Lismore Airport AWS (58214) **Elevation:** 9m AHD
Data period: March 2002 to June 2022

Month	Monthly maximum temperature			
	5%	50%	95%	Average
January	28.2	30.0	32.5	30.2
February	27.9	29.5	21.7	29.5
March	27.0	28.0	29.9	28.2
April	24.4	26.0	27.3	25.9
May	22.3	23.2	25.3	23.4
June	19.8	20.9	21.9	20.8
July	19.7	20.9	22.1	20.9
August	21.4	22.6	24.2	22.8
September	23.9	25.2	28.1	25.7
October	24.8	27.6	28.7	27.3
November	26.1	29.0	31.1	28.8
December	27.0	29.9	32.2	29.6

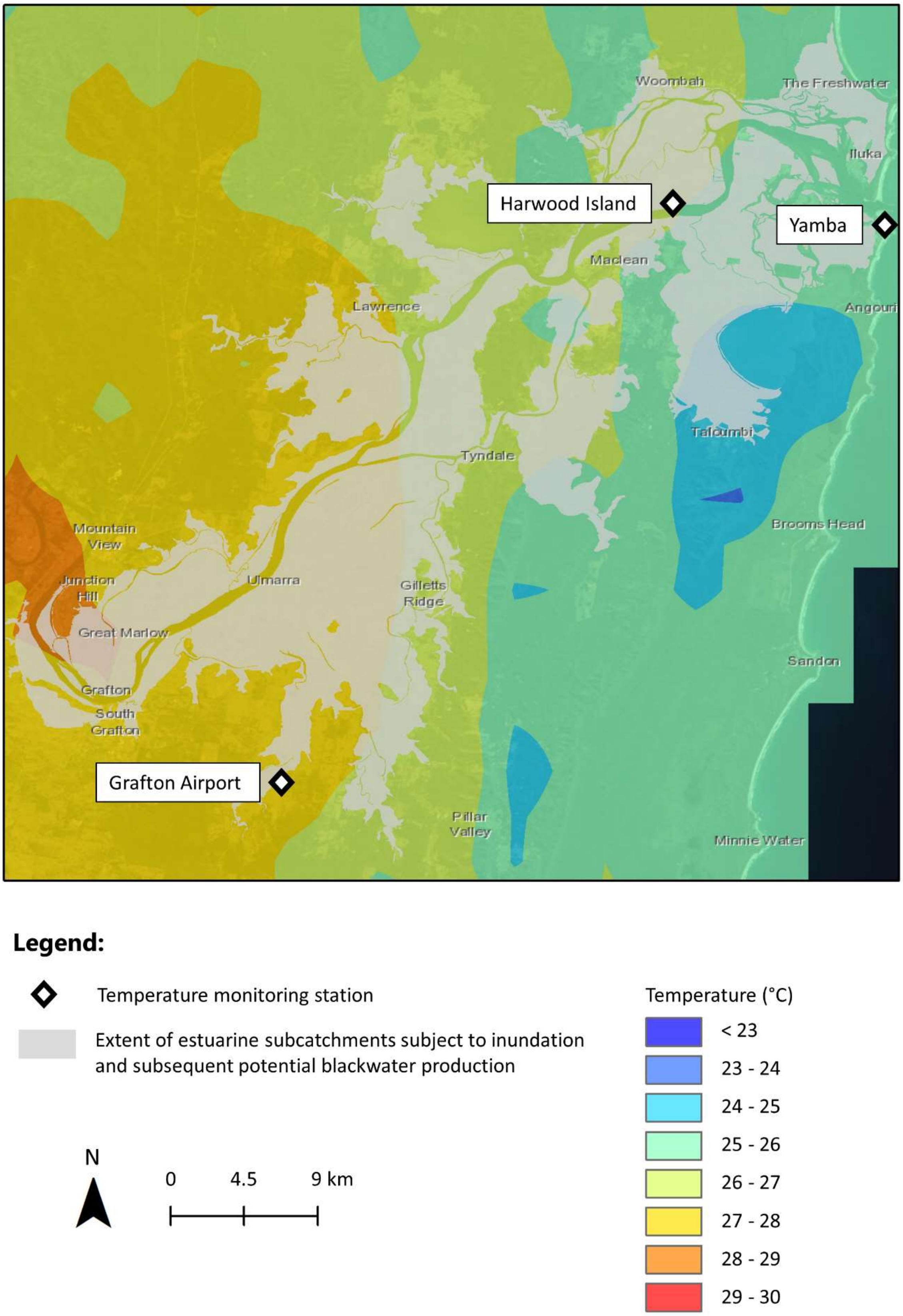

Figure S110. Average maximum temperature (October to April), Clarence River

Table S26. Average maximum temperatures within the Clarence River catchments

Station: Yamba Pilot Station (58012) **Elevation:** 27m AHD

Data period: June 1887 to June 2022

Month	Monthly maximum temperature			
	5%	50%	95%	Average
January	25.1	26.5	28.9	26.8
February	25.3	26.6	28.9	26.8
March	24.5	25.9	28.2	26.1
April	22.9	24.2	26.4	24.3
May	20.5	21.7	23.6	21.8
June	18.4	19.6	21.2	19.7
July	17.8	19.1	20.8	19.1
August	18.5	20.2	21.9	20.2
September	20.3	21.8	24.2	22.1
October	21.6	23.1	25.8	23.4
November	23.0	24.5	27.3	24.7
December	24.3	25.7	28.5	26.0

Station: Harwood Island Sugar Mill (58027) **Elevation:** 2m AHD

Data period: January 1915 to November 1972

Month	Monthly maximum temperature			
	5%	50%	95%	Average
January	26.4	29.3	31.3	29.0
February	26.5	28.7	30.9	28.7
March	25.9	27.8	29.7	27.7
April	23.8	25.9	28.2	26.0
May	21.8	23.1	25.8	23.3
June	19.4	21.1	23.0	21.1
July	19.1	20.5	23.1	20.8
August	19.8	21.6	23.8	21.8
September	21.9	23.8	27.0	24.0
October	23.8	26.0	28.0	26.0
November	25.3	27.8	30.6	27.8
December	26.8	28.6	31.7	28.8

Table S26 (cont'd). Average maximum temperatures within the Clarence River catchments

Station: Grafton Airport AWS (58161) **Elevation:** 25m AHD

Data period: April 2006 to June 2022

Month	Monthly maximum temperature			
	5%	50%	95%	Average
January	28.0	30.0	32.5	30.2
February	27.6	29.5	32.0	29.6
March	27.0	27.9	29.6	28.1
April	24.6	25.5	27.0	25.7
May	22.1	22.8	25.0	23.2
June	19.7	20.4	21.9	20.6
July	19.7	20.5	21.9	20.6
August	21.3	22.7	23.9	22.5
September	23.5	24.6	27.1	24.9
October	24.2	26.8	28.8	26.8
November	26.0	29.0	30.06	28.5
December	26.8	29.6	31.6	29.2

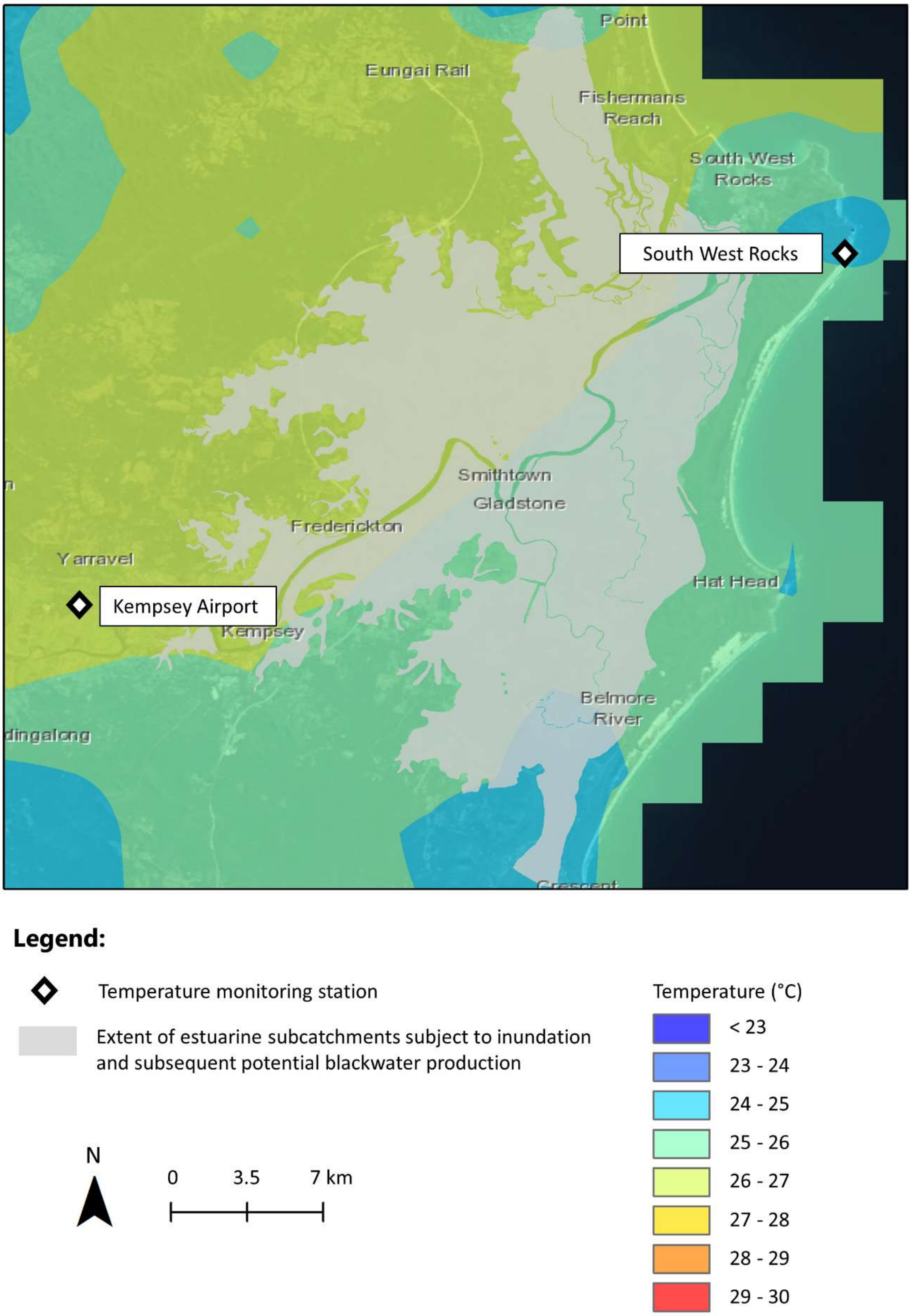

Figure S111. Average maximum temperature (October to April), Macleay River

Table S27. Average maximum temperatures within the Macleay River catchments

Station: Smoky Cape Lighthouse, South West Rocks (59030) **Elevation:** 117m AHD
Data period: January 1939 to June 2022

Month	Monthly maximum temperature			
	5%	50%	95%	Average
January	25.4	26.9	28.9	27.0
February	25.6	26.9	29.2	27.1
March	24.9	26.3	27.7	26.3
April	22.7	24.0	25.8	24.2
May	20.4	21.4	23.5	21.6
June	18.2	19.2	20.8	19.3
July	17.7	18.8	20.3	18.8
August	18.6	19.9	22.1	20.0
September	20.3	21.8	24.3	21.9
October	21.7	23.3	25.3	23.4
November	22.9	24.7	26.3	24.7
December	24.5	25.9	28.1	26.1

Station: Kempsey Airport AWS (59007) **Elevation:** 13m AHD
Data period: February 2001 to June 2022

Month	Monthly maximum temperature			
	5%	50%	95%	Average
January	27.8	29.0	32.4	29.5
February	27.0	28.6	30.8	28.8
March	26.1	27.1	28.8	27.3
April	24.3	25.4	26.8	25.4
May	21.2	22.3	24.3	22.5
June	19.1	20.0	21.3	20.1
July	18.9	20.0	21.0	20.1
August	20.6	21.9	23.4	21.7
September	23.0	24.1	26.6	24.5
October	23.7	25.9	27.7	25.8
November	25.4	27.2	29.1	27.0
December	26.8	28.3	30.6	28.4

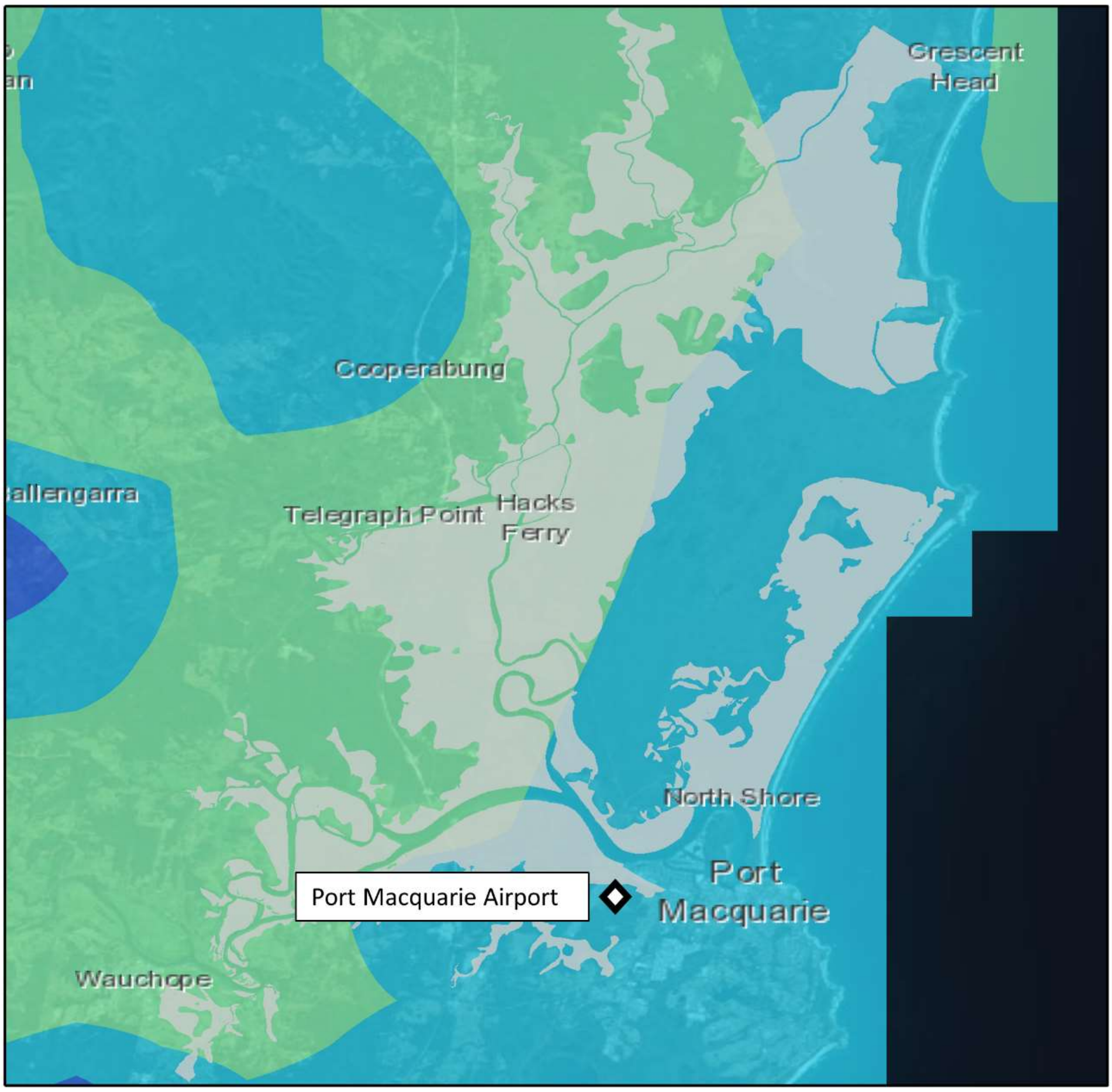

Legend:

Temperature monitoring station

Extent of estuarine subcatchments subject to inundation and subsequent potential blackwater production

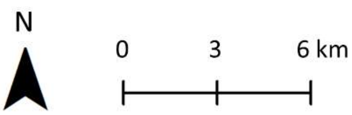

Temperature (°C)

- < 23
- 23 - 24
- 24 - 25
- 25 - 26
- 26 - 27
- 27 - 28
- 28 - 29
- 29 - 30

Figure S112. Average maximum temperature (October to April), Hastings River

Table S28. Average maximum temperatures within the Hastings River catchments

Station: Port Macquarie Airport AWS (60168) **Elevation:** 4m AHD
Data period: October 2020 to June 2022

Month	Monthly maximum temperature Lowest	Monthly maximum temperature Highest
January	27.3	27.5
February	26.4	26.6
March	25.7	25.9
April	24.0	24.3
May	21.5	21.6
June	19.0	19.3
July	19.3	19.3
August	21.4	21.4
September	22.8	22.8
October	24.5	25.1
November	25.0	26.2
December	26.6	26.6

Station: Eloura Street, Laurieton (60022) **Elevation:** 12m AHD
Data period: January 1907 to September 1930

Month	Monthly maximum temperature 5%	50%	95%	Average
January	23.8	25.6	27.9	25.8
February	22.7	26.0	28.6	25.8
March	21.9	24.8	26.3	24.6
April	19.1	23.4	25.4	22.8
May	15.9	20.7	21.4	19.6
June	14.1	17.9	19.3	17.3
July	12.8	17.8	18.8	16.6
August	14.3	19.0	20.9	18.0
September	16.6	20.8	22.9	20.1
October	19.7	22.2	25.0	22.3
November	21.1	24.0	25.9	23.9
December	23.3	25.0	27.4	25.2

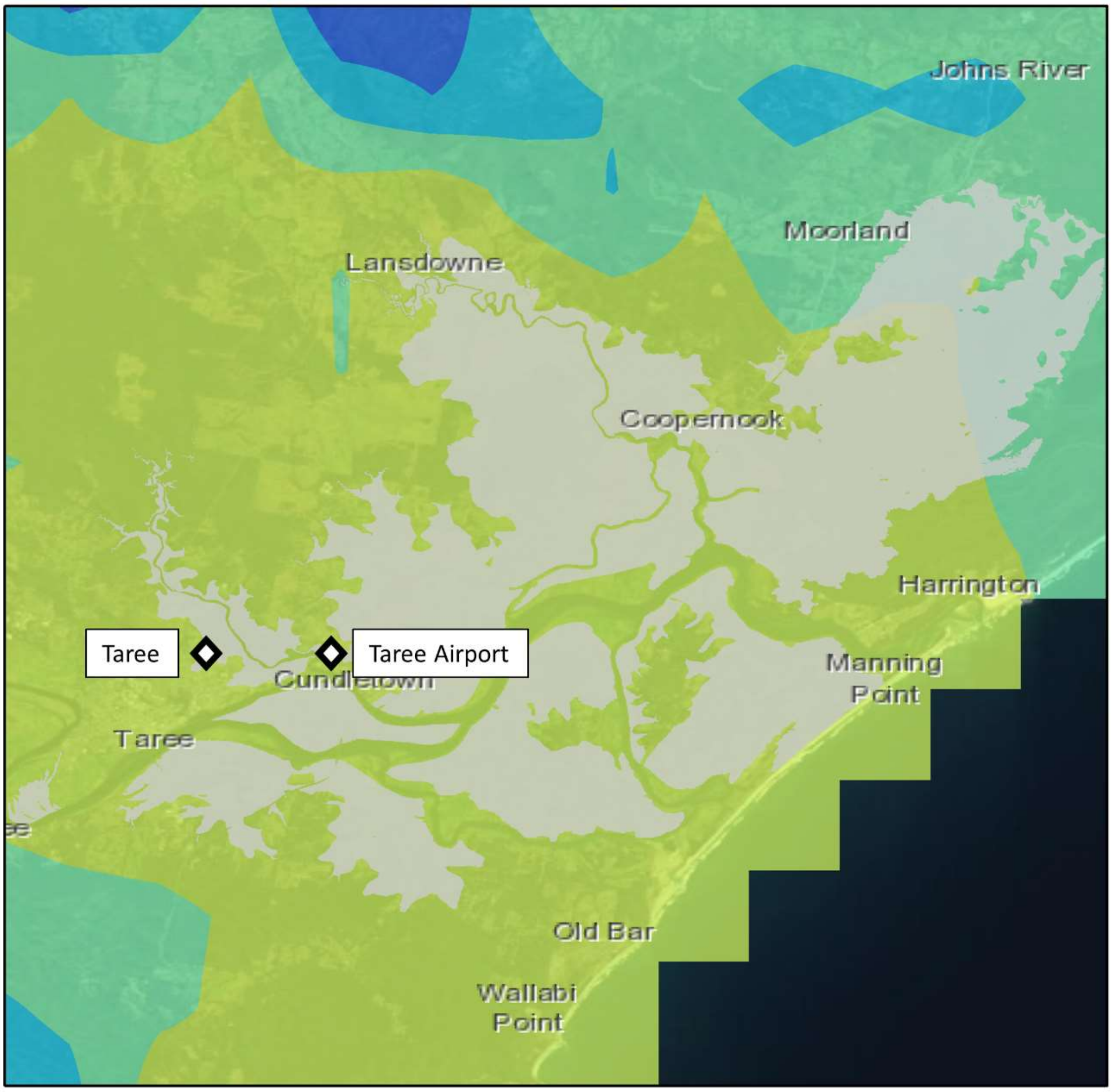

Legend:

Temperature monitoring station

Extent of estuarine subcatchments subject to inundation and subsequent potential blackwater production

N

0 3 6 km

Temperature (°C)

- < 23
- 23 - 24
- 24 - 25
- 25 - 26
- 26 - 27
- 27 - 28
- 28 - 29
- 29 - 30

Figure S113. Average maximum temperature (October to April), Manning River

Table S29. Average maximum temperatures within the Manning River catchments

Station: Taree Airport (60141)			**Elevation:** 8m AHD	
Data period: July 1997 to June 2022				
Month	**Monthly maximum temperature**			
	5%	**50%**	**95%**	**Average**
January	27.2	29.1	30.8	29.0
February	26.3	28.2	30.2	28.3
March	25.5	26.7	28.1	26.8
April	22.4	24.3	25.9	24.4
May	20.3	21.3	23.0	21.5
June	17.9	18.9	20.2	18.9
July	17.8	18.5	19.9	18.7
August	18.7	20.1	21.7	20.2
September	21.4	22.9	25.3	23.1
October	22.8	24.9	26.8	24.8
November	23.6	26.2	28.3	26.1
December	25.7	27.8	29.8	27.8
Station: Patanga Close, Taree (60030)			**Elevation:** 14m AHD	
Data period: January 1907 to March 2005				
Month	**Monthly maximum temperature**			
	5%	**50%**	**95%**	**Average**
January	26.4	28.7	31.7	29.0
February	26.4	28.5	31.2	28.6
March	25.3	27.2	29.2	27.3
April	22.9	24.8	26.7	24.7
May	19.4	21.7	23.0	21.5
June	17.6	19.1	21.0	19.1
July	16.2	18.6	20.4	18.5
August	16.5	20.2	22.1	19.9
September	19.9	22.8	25.2	22.7
October	22.5	24.9	27.1	24.9
November	23.8	26.9	29.6	26.7
December	26.1	28.3	31.0	28.4

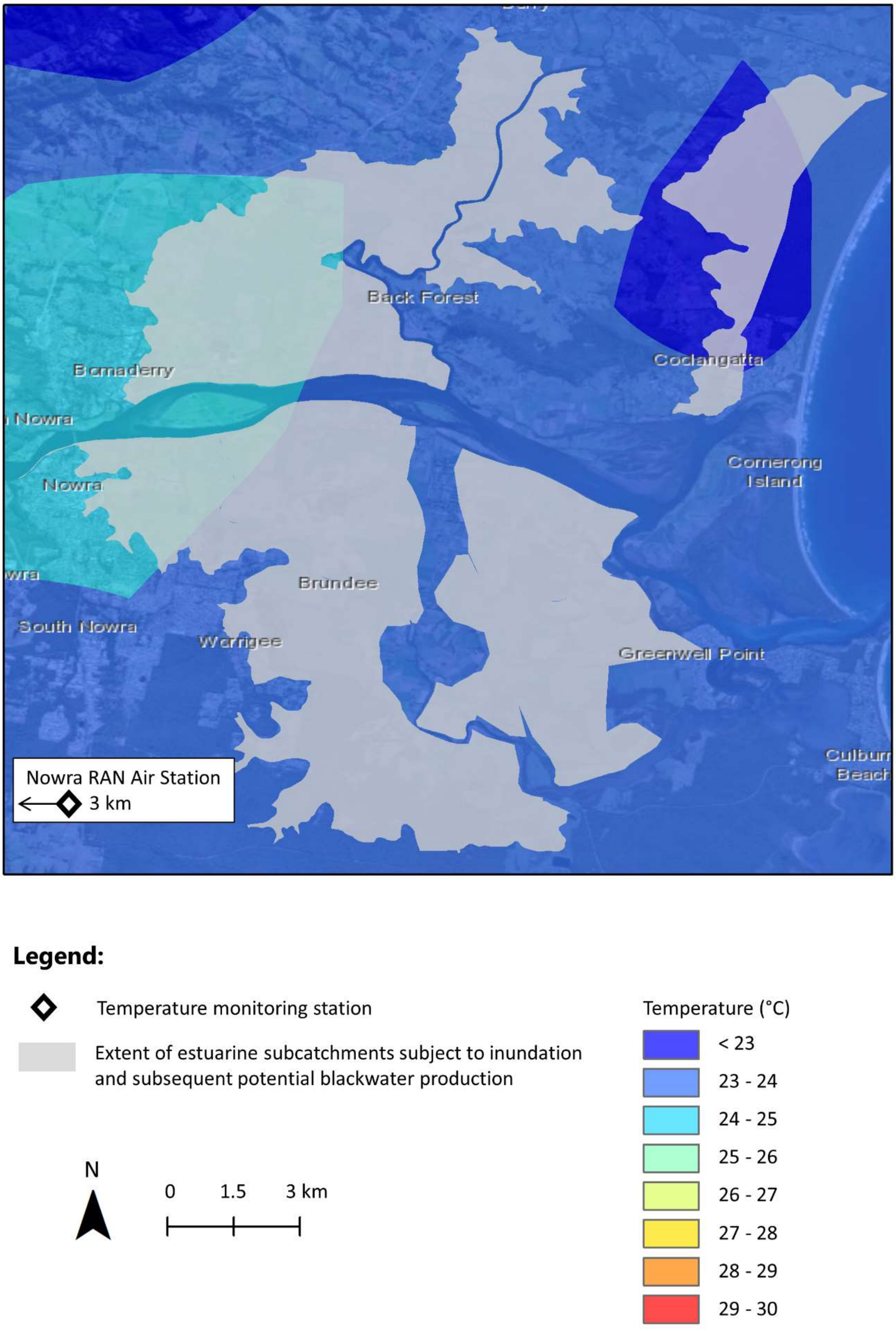

Figure S114. Average maximum temperature (October to April), Shoalhaven River

Table S30. Average maximum temperatures within the Shoalhaven River catchments

Station: Nowra RAN Air Station AWS (68072) **Elevation:** 109m AHD

Data period: November 2000 to June 2022

Month	Monthly maximum temperature			
	5%	50%	95%	Average
January	26.5	27.5	29.6	27.7
February	24.2	26.5	27.7	26.4
March	23.2	25.1	26.4	25.1
April	21.4	22.9	24.7	22.9
May	18.3	19.5	21.4	19.7
June	15.3	17.0	18.0	16.9
July	15.7	16.8	17.9	16.8
August	16.9	18.2	19.3	18.2
September	19.7	20.9	22.5	21.1
October	21.0	23.3	25.5	23.2
November	22.5	24.9	27.5	24.8
December	24.2	25.9	28.4	26.1

References

Couriel, E., Alley, K., & Modra, B. (2012). OEH NSW Tidal Planes Analysis 1990–2010 Harmonic Analysis (Report MHL2053). *Sydney, Australia*.

DPIE. (2020). NSW Landuse 2017 Version 1.2. Retrieved from https://datasets.seed.nsw.gov.au/dataset/nsw-landuse-2017-v1p2-f0ed

Mallin, M. A., Posey, M. H., McIver, M. R., Parsons, D. C., Ensign, S. H., & Alphin, T. D. (2002). Impacts and Recovery from Multiple Hurricanes in a Piedmont–Coastal Plain River System: Human development of floodplains greatly compounds the impacts of hurricanes on water quality and aquatic life. *BioScience, 52*(11), 999-1010. https://doi.org/10.1641/0006-3568(2002)052[0999:IARFMH]2.0.CO;2

USEPA. (2001). *PLOAD version 3.0. An ArcView GIS Tool to Calculate Non-Point Sources of Pollution in Watershed and Stormwater Project: Users Manual.* Retrieved from https://permanent.fdlp.gov/lps49376/PLOAD_v3.pdf.

Vithana, C. L., Sullivan, L. A., & Shepherd, T. (2019). Role of temperature on the development of hypoxia in blackwater from grass. *Science of The Total Environment, 667*, 152-159.

Wong, V., Walsh, S., & Morris, S. (2018). Climate affects fish-kill events in subtropical estuaries of eastern Australia. *Marine and Freshwater Research, 69*(11), 1641-1648.